AD-A061 589 SYRACUSE UNIV N Y F/G 12/2
PARAMETRIC IDENTIFICATION OF SYSTEMS VIA LINEAR OPERATORS.(U)
SEP 78 J NEBAT F30602-75-C-0121
UNCLASSIFIED RADC-TR-78-199 NL

1 OF 3
ADA
061589




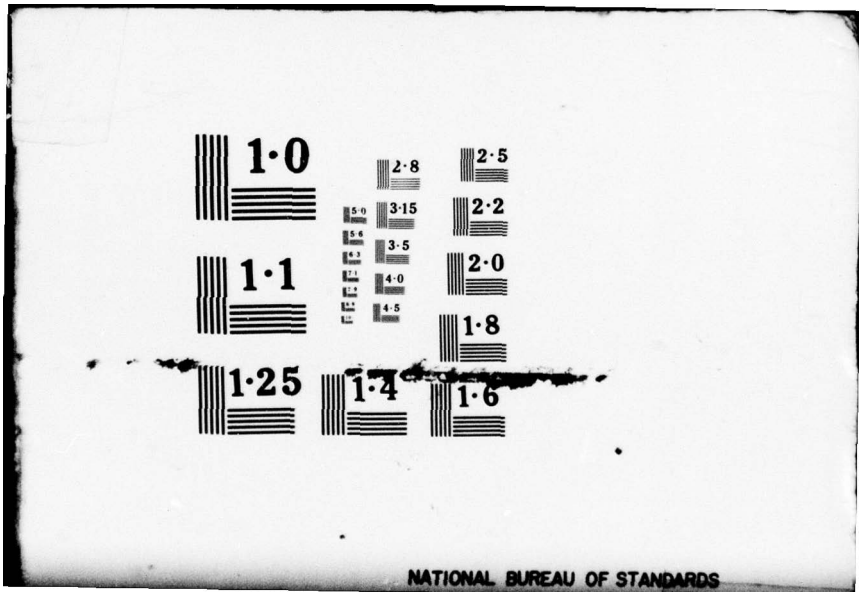
1·0
1·1
1·25
1·4
1·6
1·8
2·0
2·2
2·5
2·8
3·15
3·5
4·0
4·5
NATIONAL BUREAU OF STANDARDS

LEVEL II

12

(18) (19)
RADC-TR-78-199
(9) Interim Technical Report. Jun 77 - Jul 78,
September 1978

(6) PARAMETRIC IDENTIFICATION OF SYSTEMS VIA LINEAR OPERATORS,

(10) Joshua Nebat
Syracuse University

(11) Sep 78 (12) 203 p.

(15) F3062-75-C-0121

(16) 2338 (17) 03

Approved for public release; distribution unlimited.

ROME AIR DEVELOPMENT CENTER
Air Force Systems Command
Griffiss Air Force Base, New York 13441

This report has been reviewed by the RADC Information Office (OI) and is releasable to the National Technical Information Service (NTIS). At NTIS it will be releasable to the general public, including foreign nations.

RADC-TR-78-199 has been reviewed and is approved for publication.

APPROVED:

JOHN F. SPINA
Project Engineer

APPROVED:

JOSEPH J. NARESKY
Chief, Reliability & Compatibility Division

FOR THE COMMANDER:

JOHN P. HUSS
Acting Chief, Plans Office

If your address has changed or if you wish to be removed from the RADC mailing list, or if the addressee is no longer employed by your organization, please notify RADC (RBCT) Griffiss AFB NY 13441. This will assist us in maintaining a current mailing list.

Do not return this copy. Retain or destroy.

UNCLASSIFIED

SECURITY CLASSIFICATION OF THIS PAGE *(When Data Entered)*

REPORT DOCUMENTATION PAGE		READ INSTRUCTIONS BEFORE COMPLETING FORM
1. REPORT NUMBER RADC-TR-78-199	2. GOVT ACCESSION NO.	3. RECIPIENT'S CATALOG NUMBER
4. TITLE *(and Subtitle)* PARAMETRIC IDENTIFICATION OF SYSTEMS VIA LINEAR OPERATORS		5. TYPE OF REPORT & PERIOD COVERED Interim Technical Report Jun 77 - Jul 78
		6. PERFORMING ORG. REPORT NUMBER N/A
7. AUTHOR(s) Joshua Nebat		8. CONTRACT OR GRANT NUMBER(s) F30602-75-C-0121
9. PERFORMING ORGANIZATION NAME AND ADDRESS Syracuse University Syracuse NY 13201		10. PROGRAM ELEMENT, PROJECT, TASK AREA & WORK UNIT NUMBERS 62702F 23380321
11. CONTROLLING OFFICE NAME AND ADDRESS Rome Air Development Center (RBCT) Griffiss AFB NY 13441		12. REPORT DATE September 1978
		13. NUMBER OF PAGES 195
14. MONITORING AGENCY NAME & ADDRESS*(if different from Controlling Office)* Same		15. SECURITY CLASS. *(of this report)* UNCLASSIFIED
		15a. DECLASSIFICATION/DOWNGRADING SCHEDULE N/A

16. DISTRIBUTION STATEMENT *(of this Report)*

Approved for public release; distribution unlimited.

17. DISTRIBUTION STATEMENT *(of the abstract entered in Block 20, if different from Report)*

Same

18. SUPPLEMENTARY NOTES

RADC Project Engineer: John F. Spina (RBCT)

19. KEY WORDS *(Continue on reverse side if necessary and identify by block number)*

electromagnetic compatibility	basic functions
black box identification	linear operators
linear time	system approximation model
invarient systems	error criterion
rational transfer functions	

20. ABSTRACT *(Continue on reverse side if necessary and identify by block number)*

A general parametric identification/approximation model is developed for the black box identification of linear time invariant systems in terms of rational transfer functions. The identification procedure is shown to consist of two basic parts: 1) the generation of a set of basic functions through a linear operation upon the input and output signals of the system, and 2) the choice of an error criterion and its associated approximation scheme, which, when used along with the basis set, generate the numerator and denominator parameters of the transfer function.

DD FORM 1 JAN 73 1473 EDITION OF 1 NOV 65 IS OBSOLETE

UNCLASSIFIED

SECURITY CLASSIFICATION OF THIS PAGE *(When Data Entered)*

20. Abstract (Cont'd)

It is demonstrated that some known parametric identification techniques derive from the general model as special cases associated with a particular linear operator. Some possible operators are discussed on the grounds of their performance in an identification procedure. It is shown that certain operators are inherently ill-posed and generate a set of basis functions that is practically linearly dependent. In general, the performance of a linear operator will depend upon the data provided.

The extensions of the technique to slowly time-varying systems and weakly nonlinear systems are discussed and demonstrated through examples.

Poles belonging to successive approximations of increasing order form so-called "growing tree" patterns in the S-plane. The potential benefit of the "growing tree" in time domain synthesis and in system identification is pointed out.

LEVEL II

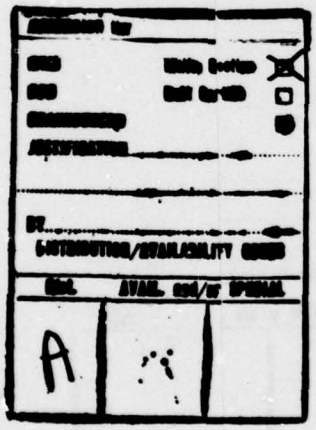

PREFACE

This effort was conducted by Syracuse University under the sponsorship of the Rome Air Development Center Post-Doctoral Program for Rome Air Development Center. Mr. John F. Spina RADC/RBCT was the task project engineer and provided overall technical direction and guidance.

The RADC Post-Doctoral Program is a cooperative venture between RADC and some sixty-five universities eligible to participate in the program. Syracuse University (Department of Electrical Engineering), Purdue University (School of Electrical Engineering), Georgia Institute of Technology (School of Electrical Engineering). and State University of New York at Buffalo (Department of Electrical Engineering) act as prime contractor schools with other schools participating via sub-contracts with the prime schools. The U.S. Air Force Academy (Department of Electrical Engineering), and the Institute of Technology (Department of Electrical Engineering), and the Naval Post Graduate School (Department of Electrical Engineering) also participate in the program.

The Post-Doctoral Program provides an opportunity for faculty at participating universities to spend up to one year full time on exploratory development and problem-solving efforts with the post-doctorals splitting their time between the customer location and their educational institutions. The program is totally customer-funded with current projects being undertaken for Rome Air Development Center (RADC), Space and Missile Systems Organization (SAMSO, Aeronautical System Division (ASD), Electronics Systems Division (ESD), Air Force Avionics Laboratory (AFAL), Foreign Technology Division (FTD), Air Force Weapons Laboratory (AFWL), Armanment Development and Test Center (ADTC), Air Force Communications Service (AFSC), Aerospace Defense Command (ADC), HQ USAF, Defense Communications Agency (DCA), Navy, Army, Aerospace Medical Division (AMD), and Federal Aviation Administration (FAA).

Further information about the RADC Post-Doctoral Program can be obtained from Mr. Jacob Scherer, RADC/RBC, Griffiss AFB NY 13441, telephone Autovon 587-2543, Commercial (315) 330-2543.

ACKNOWLEDGMENT

I wish to express my sincere gratitude to my advisor Dr. Donald D. Weiner. His constant interest in my work and his supportive guidance during this effort as well as the many hours he has spent in consultation with me and reviewing written material are deeply appreciated. I would also like to thank the many other faculty members of Syracuse University who have participated in my pursuit of this degree. Special thanks are due to Dr. Stephen T. Kowel, the reader of this dissertation, whose constructive comments are deeply appreciated.

To my dear friend and colleague A. Udaya Shankar, I am thankful for the help given in the final preparation of this dissertation and for the many hours he spent with me in constructive discussions.

During my entire stay at Syracuse University, financial support was provided by John Spina of the Compatibility Division at the Rome Air Development Center, Griffiss AFB, N.Y, through the RADC Post-Doctoral Program, directed by Jacob Scherer. This support, without which I could not have conducted my studies, is gratefully acknowledged.

A special acknowledgement is due to Louise Naylor, Mary T. Dufel, and Pamela Bielby for the excellent typing of the manuscript.

Finally, I express my gratitude to my wife, Ruth, and my sons, Michael and Yoav, who I will be glad to see again.

TABLE OF CONTENTS

Chapter 1

INTRODUCTION

The problems of linear system synthesis and identification are closely related. In system synthesis, one tries to synthesize an input-output relation that will yield a specified behavior. The first step usually consists of determining either the impulse response or transfer function of the system. The impulse response is then approximated by a sum of exponentials while the transfer function is approximated by a realizable rational function. Since the physical system does not exist during the synthesis phase, system synthesis is characterized by the feature that one deals with idealized analytical functions.

This is not the case with system identification. Here the system actually exists and the identification process is based upon measured data at the system input and output ports. This data is usually contaminated by measurement errors, thermal noise, and spurious signals. In addition, the record lengths are, by necessity, finite.

In system identification, as in system synthesis, complex exponential functions provide a natural basis for the impulse response. However, in some cases the impulse response cannot be exactly represented as a sum of exponentials. The identification problem then becomes an approximation problem.

The intrinsic difference between synthesis and identification is that the former seeks a system, not yet in existence, to approximate an operator which relates idealized inputs and outputs, while the latter attempts to describe an existing unknown system through measured input-output records. Since both problems emphasize the input-output behavior of an unknown system, the strategies involved with their solution are similar. However, they are distinguished on the basis of the type of data provided. Whereas a synthesis problem is characterized by synthetic data, an identification problem is characterized by measured data records.

The goal of this dissertation is to develop a general parametric approximation/identification technique for linear time-invariant systems. The technique models the system impulse response as a sum of exponentials. It is shown that this technique can be extended to slowly time-variant and weakly nonlinear systems.

Chapter 1 presents some useful definitions and discusses system classification with respect to input-output relations. Beginning with the general class of systems, attention is first focussed on linear time-invariant systems and then specialized further to the subset of rational systems within this class. The suitability of the exponential family of functions for modeling an impulse response is examined. The chapter closes with a literature review and an outline of the dissertation.

1.1 System Classification and Definitions

Before addressing the system identification problem, a brief discussion about the classification of systems, their pertinent qualitative properties, and some definitions are presented.

In general, characterization of the input-output properties of a system implies an operator H that operates on a class of signals (functions) {x} and results in another class of signals {y}. A system is relaxed (or at rest) at time $t = t_o$ if inputs are not applied over $-\infty \leq t \leq t_o$ and/or the output signal depends solely upon the operation of H on the input signal over $t_o < t < \infty$. In the most general case, an operator H might involve memory and be nonlinear, time-variant, anticipative, and ambiguous.

The above properties are defined as follows [1]:

(a) A system is said to involve memory if the output at time t depends upon values of the input prior to time t.

(b) A relaxed system is linear if and only if

$$H \sum_{i=1}^{n} \alpha_i x_i = \sum_{i=1}^{n} \alpha_i (Hx_i) \qquad (1\text{-}1\text{-}1)$$

for any input signals x_i, and for any real numbers α_i $i = 1,2,\ldots,n$. Otherwise the relaxed system is nonlinear.

(c) Let Q_α denote the time-shift operator with shift α. A relaxed system is time invariant (stationary or fixed) if and only if

$$HQ_\alpha x = Q_\alpha Hx \qquad (1\text{-}1\text{-}2)$$

for any input signal x, and for any real number α. Otherwise the system is time-variant.

(d) A system is causal (nonanticipatory) if and only if the output signal y(t) depends solely upon the operation of H on the present and past of the incoming signal x(t). If y(t) also depends upon future values of x(t), the system is anticipatory.

(e) A system is said to be unique if and only if there exists a single output signal y(t) for any input signal x(t). Otherwise, the system is ambiguous.

In this dissertation only physical systems which are causal, unique, slowly time - variant, and weakly nonlinear with memory are considered. In general, the input-output relationship for a weakly nonlinear system can be characterized in terms of the Volterra representation which is expressed as [2]

$$y(t) = \sum_{i=1}^{\infty} \underbrace{\int_{-\infty}^{\infty} \cdots \int_{-\infty}^{\infty}}_{i} h_i(\tau_1,\ldots,\tau_i) \prod_{j=1}^{i} x(t,\tau_j)d\tau_j \,. \qquad (1\text{-}1\text{-}3)$$

This representation was first utilized by Norbert Wiener [3] in the analysis of nonlinear systems. For physical systems which are initially relaxed at time t_o, the input-output relation can be written as

$$y(t) = \sum_{i=1}^{\infty} \underbrace{\int_0^{t-t_o} \cdots \int_0^{t-t_o}}_{i} h_i(\tau_1,\ldots,\tau_i) \prod_{j=1}^{i} x(t,\tau_j)d\tau_j, \quad t \geq t_o. \tag{1-1-4}$$

In addition, the infinite sum in (1-1-4) can be adequately approximated by a finite number of terms for systems which are weakly nonlinear. Also, for systems which are time-invariant, (1-1-4) becomes

$$y(t) \simeq \sum_{i=1}^{N} \underbrace{\int_0^{t-t_o} \cdots \int_0^{t-t_o}}_{i} h_i(\tau_1,\ldots,\tau_i) \prod_{j=1}^{i} x(t-\tau_j)d\tau_j, \quad t \geq t_o. \tag{1-1-5}$$

Alternatively, (1-1-5) can be written as

$$y(t) \simeq \sum_{i=1}^{N} \underbrace{\int_{t_o}^{t} \cdots \int_{t_o}^{t}}_{i} h_i(t-\tau_1,\ldots,t-\tau_i) \prod_{j=1}^{i} x(\tau_j)d\tau_j, \quad t \geq t_o. \tag{1-1-6}$$

In practice, there exists a broad class of electronic circuits which are weakly nonlinear. Values of N from 3 to 5 are commonly used when modeling amplifiers in communications receivers [4]. For N=1, (1-1-6) describes the input-output relationship of a linear, time-invariant, causal system with memory which is relaxed at time t_o.

1.2 Input-output Stability for Linear Systems

One of the important characteristics of a physical system is its stability. Since an identification process utilizes information provided by the input and output signals of the system, it is convenient to describe a system's stability in terms of its impulse response.

The following useful theorems [1] are referred to in the later development:

Theorem 1-2-1

A relaxed system at $t = t_o$ is bounded-input bounded output stable (BIBO) if and only if there exists a finite number K such that

$$\int_{t_o}^{t} |h(t,\tau)| d\tau \leq K < \infty \qquad (1\text{-}2\text{-}1)$$

for all $t_o \leq t \leq \infty$.

For the time-invariant case, the theorem becomes stronger.

Theorem 1-2-2

Consider a linear time-invariant system relaxed at $t = t_o$, which is described by the following relation

$$y(t) = \int_{t_o}^{t} h(t-\tau)x(\tau)d\tau \,. \qquad (1\text{-}2\text{-}2)$$

If

$$\int_{t_o}^{\infty} |h(t)| dt \leq K < \infty \qquad (1\text{-}2\text{-}3)$$

for some constant K, then we have the following:

(a) If x is a periodic function with period T for all $t \geq t_o$, then the output y tends to a periodic function with the same period (not necessarily of the same waveform).

(b) If x is bounded and tends to a constant, then the output y is bounded and tends to a constant.

(c) If x is of finite energy, that is,

$$\left(\int_{t_o}^{\infty} |x(t)|^2 dt\right)^{1/2} \leq K_1 < \infty , \tag{1-2-4}$$

then the output is also of finite energy; that is, there exists a finite K_2 that depends on K_1 such that

$$\left(\int_{t_o}^{\infty} |y(t)|^2 dt\right)^{1/2} \leq K_2 < \infty . \tag{1-2-5}$$

(d) The system is BIBO stable (This is a corollary of Theorem 1-2-1).

For systems described by proper rational transfer functions the following theorem applies.

Theorem 1-2-3

A system relaxed at $t = t_o$ that is described by a proper rational function H(S) (or equivalently, an impulse response h(t) which is a sum of complex exponentials) is BIBO stable if and only if all the poles of H(S) are in the open left half S-plane (i.e., excluding the imaginary axis). All the poles of H(S) then have negative real parts.

The only requirement imposed on the kernel $h(\cdot)$ in theorems 1-2-1 and 1-2-2 is that it should be absolutely integrable. This fact does not imply boundedness or that h(t) approaches zero as $t \to \infty$. On the other hand, the impulse response of theorem 1-2-3 is bounded and approaches zero as $t \to \infty$. We may write for this case

$$h(t) = \begin{cases} \sum_{i=1}^{k} \sum_{j=1}^{m_i} A_{ij} t^{j-1} e^{S_i t} ; & t \geq 0 \\ 0 ; & 0 > t \end{cases} \tag{1-2-6}$$

where $A_{im_i} \neq 0$, $\sigma_i = \text{Real}\,[s_i] < 0$, $s_{i_1} \neq s_{i_2}$ for $i_1 \neq i_2$. m_i denotes the order of the pole at s_i. The total number of poles in h(t) is given by $\sum_{i=1}^{k} m_i = n$. Using (1-2-6) we write

$$|h(t)| = \left| \sum_{i=1}^{k} \sum_{j=1}^{m_i} A_{ij} t^{j-1} e^{s_i t} \right| \leq \sum_{i=1}^{k} \sum_{j=1}^{m_i} |A_{ij}| t^{j-1} e^{\sigma_i t}$$

$$\leq \sum_{i=1}^{k} \max \begin{cases} \sum_{j=1}^{m_i} |A_{ij}| \left(\frac{1-j}{\sigma_i}\right)^{j-1} e^{1-j} \\ |A_{i1}| \end{cases} . \qquad (1\text{-}2\text{-}7)$$

Inequality (1-2-7) shows the boundedness of h(t). It is clear that $\lim_{t \to \infty} h(t) = 0$ since $\sigma_i < 0$.

As a matter of fact, (1-2-6) not only belongs to $L^1[0,\infty]$ space (i.e., is absolutely integrable over $[0,\infty]$), but also belongs to $L^P[0,\infty]$ where $P \geq 1$, since

$$\int_0^{\infty} \left| \sum_{i=1}^{k} \sum_{j=1}^{m_i} A_{ij} t^{j-1} e^{s_i t} \right|^P dt < \infty . \qquad (1\text{-}2\text{-}8)$$

In $L^2[0,\infty]$ (Hilbert space) the infinite sum

$$\sum_{i=1}^{\infty} \sum_{j=1}^{m_i} A_{ij} t^{j-1} e^{s_i t} \qquad (1\text{-}2\text{-}9)$$

provides a complete representation for piecewise continuous square integrable functions, assuming proper choices of the poles $\{s_i\}$. As a matter of fact, many choices of $\{s_i\}$ exist. From Szasz's form of Muntz's theorem [5], all that is required for the set $\{t^{j-1} e^{s_i t}\}$ to be complete in $L^2[0,\infty]$ is that

$$\sum_{i=1}^{\infty} - \frac{\text{Real } [s_i]}{1 + |s_i + \frac{1}{2}|^2} \to \infty \ . \qquad (1\text{-}2\text{-}10)$$

For example, possible complete sets are

(a) $\{e^{-t}, e^{-2t}, \ldots, e^{-it} \ldots\}$

(b) $\{e^{-(1\pm\sqrt{-1})t}, e^{-2(1\pm\sqrt{-1})t}, \ldots, e^{-i(1\pm\sqrt{-1})t}, \ldots\}^{\substack{m_i = j = 1 \\ i = 1,2,\ldots}}$.

In practice, when approximating a waveform by (1-2-9), a finite set is used and an error is involved in the representation which one tries to minimize by a proper choice of $\{s_i\}$. Hence, representations in the form of (1-2-6) result.

It can be shown [6] that a function which both belongs to $L^1[0,\infty]$ and is bounded also belongs to $L^2[0,\infty]$. In other words, the boundedness constraint added to an L^1 function is sufficient to guarantee membership in L^2. (In fact, membership is also guaranteed in L^P, $P \geq 1$).

In physical systems, the boundedness requirement is not a severe constraint (i.e., physical stable systems are inherently bounded.) It is true that theorem 1-2-1 does allow $h(\cdot)$ to contain a countable linear combination of impulses provided their coefficients constitute an absolutely converging series. However, as is well known, there is no real system for which the impulse response is an ideal impulse. Therefore, all transfer functions belonging to physical systems have a zero at ∞. However, transfer functions cannot be identically zero over any nonzero frequency interval. The Paley-Wiener criterion [7] allows at most a countable number of zeros to exist on the imaginary axis in the s plane for any transfer function related to a causal

impulse response.

1.3 The Rational Linear System

A general rational linear system is described in the time domain by its impulse response as given in (1-2-6). The Laplace transform of (1-2-6) yields the rational transfer function

$$H(S) = \sum_{i=1}^{k} \sum_{j=1}^{m_i} A_{ij} \frac{(j-1)!}{(S - S_i)^j} = \frac{\sum_{i=0}^{m} N_i S^i}{\sum_{j=0}^{n} D_j S^j} \qquad (1\text{-}3\text{-}1)$$

where $m < n$. This is a frequency-domain description. Clearly, (1-3-1) has a countable number of finite zeros (exactly m) and a zero at infinity.

One way to describe the input-output relations for such a system is through the convolution integral. Using (1-2-6) in (1-2-2), there results

$$y(t) = \sum_{i=1}^{k} \sum_{j=1}^{m_i} A_{ij} \int_0^t (t-\tau)^{j-1} e^{S_i(t-\tau)} x(\tau) d\tau \qquad (1\text{-}3\text{-}2)$$

where the system is assumed to be relaxed at $t = 0$. Taking the Laplace transform of (1-3-2), we obtain

$$Y(S) = H(S)X(S) = \frac{\sum_{i=0}^{m} N_i S^i}{\sum_{j=0}^{n} D_j S^j} X(S) . \qquad (1\text{-}3\text{-}3)$$

Premultiplying (1-3-3) by the denominator polynomial yields

$$\sum_{j=0}^{n} D_j S^j Y(S) = \sum_{i=0}^{m} N_i S^i X(S) . \qquad (1\text{-}3\text{-}4)$$

The inverse Laplace transform of (1-3-4) is

$$\sum_{j=0}^{n} D_j y^{(j)}(t) = \sum_{i=0}^{m} N_i x^{(i)}(t) \qquad (1\text{-}3\text{-}5)$$

where the initial conditions are given by $y^{(k)}(0) = 0$, $k = 0,1,2,\ldots,n-1$ $x^{(\ell)}(0) = 0$, $\ell = 0,1,2,\ldots,m-1$.

Observe that $y^{(j)}(t)$ is the jth derivative of $y(t)$ and $x^{(i)}(t)$ is the ith derivative of $x(t)$. Thus, (1-3-5) is a differential equation which represents the input-output relation of a causal, time-invariant, linear system. For the more general situation in which the initial conditions are nonzero (i.e., $y^{(k)}(0) \neq 0$, $k = 0,1,\ldots,n-1$ and $x^{(\ell)}(0) \neq 0$, $\ell = 0,1,2,\ldots,m-1$), the Laplace transform of (1-3-5) is

$$Y(S) = X(S)\,\frac{\sum_{i=0}^{m} N_i S^i}{\sum_{j=0}^{n} D_j S^j} + \frac{\sum_{q=0}^{n-1} C_q S^q}{\sum_{j=0}^{n} D_j S^j}, \qquad (1\text{-}3\text{-}6)$$

where

$$\sum_{q=0}^{n-1} C_q S^q = \sum_{j=1}^{n} \sum_{k=0}^{j-1} D_j S^k y^{(j-k-1)}(0) - \sum_{i=1}^{m} \sum_{\ell=0}^{i-1} N_i S^\ell x^{(i-\ell-1)}(0),$$

and

$$C_q = \sum_{j=q+1}^{n} D_j y^{(j-q-1)}(0) - \sum_{i=q+1}^{m} N_i x^{(i-q-1)}(0).$$

If (1-3-1) is irreducible, then (1-3-6) is said to represent the Laplace transform of the differential equation of an observable and controllable system [1],[8]. Only irreducible transfer functions are considered in this dissertation.

1.4 Literature Review and Problem Statement

Many investigators have been involved with various aspects of the system identification problem since the late 1940's. The proposed techniques can be partitioned between those that utilize parametric versus nonparametric models. Nonparametric models are characterized by the fact that the linear impulse response and/or transfer function is presented in either tabular or graphical form. On the other hand, parametric models result in a numerical set of values for parameters associated with a set of basis functions used to model the impulse response and/or transfer function. This dissertation is devoted to the parametric approach in which the basis functions for the impulse response are chosen to be a set of complex exponential time functions where the coefficients and exponents are the parameters to be determined.

Historically, the first attempts at the identification problem were linked to system synthesis where exponential approximations were generated to represent a prescribed impulse response. The simplest solutions were obtained by first specifying the exponents a priori and then solving a linear set of equations for the coefficients based upon either linear interpolation, the least-square approach, or minimization of the integrated squared error [9]. By specifying the exponents a priori, the difficult part of the problem was avoided. However, even when the exponents are not specified a priori, the coefficients may be determined as mentioned above. Appendix A provides a tutorial review for the case in which the set of basis functions is chosen in advance.

Other approximations for the impulse response involved known orthonormal sets of exponential basis functions [10], [11], [12].

Since an a priori choice of exponents is uneconomical (i.e., the number of exponents needed for an adequate approximation may be unnecessarily large), attention was focused on the nonlinear problem of obtaining the "best" exponents according to some criterion. One procedure was suggested by Prony [13] as early as 1795. This method uses a set of 2N equidistant data points to generate 2N nonlinear equations in the N unknown exponents and their corresponding N unknown coefficients. In an effort to obtain increased accuracy and noise immunity, Prony's method was extended to make use of more than 2N data points in the search for the N exponentials [14]. Other forms of the overdetermined Prony method were used in the areas of speech analysis [15] and electromagnetic fields [16], [17], [18]. All of the above techniques result in an estimate of the system characteristic equation which is solved for the unknown exponents.

Other methods, arising from the system synthesis problem, involve iterative schemes to determine the exponents and residues [19], [20], [21], [22]. These methods attempt to fit a closed form expression for the impulse response by a sum of exponentials. The procedure is optimized by minimizing either the integrated-squared error or least-squares error.

Whereas Prony's method uses delay operators to obtain the characteristic equation of a difference equation, other techniques have used either differential or integral operators to obtain the characteristic equation of a differential equation [23], [24], [25], [26].

As before, the exponents are determined from the characteristic equation.

All of the previous techniques can be used in the identification problem only when the waveform being approximated is the impulse response of the system. This implies that the input is restricted to be an impulse. However, other investigators have shown that the identification problem can be solved, given the input and output signals, even when the input has some arbitrary waveform. Gradient iterative techniques using general inputs are discussed in [27] and [28]. An extension of Prony's method for arbitrary inputs is presented in [8]. Finally, the approaches given in [25] and [26] are generalized for general input signals in [29], [30], and [31].

As is evident from the survey, many different approaches have been proposed for the linear system identification problem. Each approach has certain advantages and disadvantages. In addition, the various techniques have been proposed without insight into how they are related. In this dissertation, a generalized parametric model is presented which unifies those techniques that generate the system characteristic equation. Each of these techniques results by choosing the appropriate operator in the general model. These techniques all rely upon the inversion of a Hilbert type of inner-product matrix which is basically ill-posed. One advantage of the generalized model is that it enables the flexibility in a specific problem to select an operator which tends to diagonalize the matrix. This is of considerable help when inverting the matrix. The generalized model also enables the choice of operators for the purpose of increasing noise immunity. Some of the techniques

proposed in the literature required the availability of data over a semi-infinite interval. In practical applications the data is truncated. This results in a truncation error. One of the by-products of the general model is the ability to deal with portions of a data record without incurring truncation errors. In addition, most of the iterative schemes proposed in the literature suffer from either convergence problems or the lack of a proof of convergence. The generalized model may be used in conjunction with an iterative scheme by providing a good first guess at the solution. This eases the convergence problem. Finally, the generalized model is readily extended to handle complex data as opposed to real data.

1.5 Dissertation Outline

Chapter 2 is devoted to the development of the general parametric model for identification. Since the exponential family of functions plays a major role in the suggested model, we examine in Section 2.1 the behavior of this family when subjected to linear operators. Also, in 2.2, their correlation properties are investigated. In 2.3 the general parametric model is actually developed, and in 2.4 the identification procedure is demonstrated through examples where a variety of operators are used and their properties examined.

Chapter 3 introduces some supplemental tools. First the concept of the S-plane "growing tree" is introduced, its properties and structure discussed, and potential benefits when applied to synthesis and identification problems pointed out.

The need for a good initial guess in iterative techniques makes the model discussed in chapter 2 an attractive candidate as a generator

of such a guess. The use of such a scheme to obtain the initial guess is demonstrated through an example.

Chapter 4 treats the identification of a weakly nonlinear system. The system is modeled through a Volterra series representation. An identification procedure for the higher order impulse responses is outlined and demonstrated through an example.

A summary of the significant results and conclusions are presented in chapter 5.

Appendix A presents some tutorial material about possible approximation schemes.

Chapter 2

PARAMETRIC IDENTIFICATION SCHEMES VIA LINEAR OPERATORS

The general parametric identification model is developed in this chapter. In this model it is assumed that the data available consists of input and output records solely (i.e., black box identification). The model requires that those records be processed by linear operators. The exponential family of functions, being a natural candidate, is the one chosen to model the identified system. The behavior of that family, when subjected to linear operations, is first investigated. Also, the correlation properties of this family of functions is examined.

It is shown that the group of operators that can be used for identification purposes is large. The ease of use of a certain operator depends upon the ease of obtaining the parameter transformation associated with the particular operator. Different operators will affect differently a given identification situation. In general, one should choose an operator that is "tailored" for the identification problem at hand. Some operators are inherently ill-posed when used in any identification scheme outlined by the general model.

Several examples are presented using a variety of operators and different approximation schemes from Appendix A.

2.1 Effect of Linear Operator on the Exponential Basis

In general, an n^{th}-order complex exponential basis, with negative real parts for the complex frequencies, is presented by

$$\{t^{j-1}e^{S_i t}\}; \qquad \begin{array}{l} i = 1,2,\ldots,k \\ j = 1,2,\ldots,m_i \\ \text{real } [S_i] < 0 \\ t \geq 0. \end{array} \qquad \sum_{i=1}^{k} m_i = n \tag{2-1-1}$$

A linear combination representing either a function which belongs to the space spanned by this basis or the projection onto the space of a function which does not belong to the space is given by

$$g(t) = \sum_{i=1}^{k} \sum_{j=1}^{m_i} A_{ij} t^{j-1} e^{S_i t} \quad ; \quad t \geq 0 \, . \tag{2-1-2}$$

In this section the behavior of such representations when subjected to certain operators is investigated. The first operator to be considered is the differential operator. Operating upon (2-1-2) with a differentiator (for $t \geq 0$), there results

$$g^{(1)}(t) = \frac{dg(t)}{dt} = \sum_{i=1}^{k} \sum_{j=1}^{m_i} A_{1ij} t^{j-1} e^{S_i t} \tag{2-1-3}$$

where

$$A_{1ij} = S_i A_{ij} + j A_{i(j+1)}$$

$$A_{1im_i} = S_i A_{im_i} \quad ; \quad j = 1,2,\ldots,(m_i - 1) \, .$$

Subjecting (2-1-3) to a second differentiator, we obtain

$$g^{(2)}(t) = \frac{dg_1(t)}{dt} = \sum_{i=1}^{k} \sum_{j=1}^{m_i} A_{2ij} t^{j-1} e^{S_i t}; \quad t \geq 0 \qquad (2\text{-}1\text{-}4)$$

where $A_{2ij} = S_i A_{1ij} + jA_{1i(j+1)}$

$A_{2im_i} = S_i A_{1im_i}$; $j=1,2,\ldots,(m_i-1)$.

In general, after (2-1-2) has been subjected to ℓ differentiations,

$$g^{(\ell)}(t) = \frac{dg^{(\ell-1)}(t)}{dt} = \sum_{i=1}^{k} \sum_{j=1}^{m_i} A_{\ell ij} t^{j-1} e^{S_i t}; \quad t \geq 0 \qquad (2\text{-}1\text{-}5)$$

where $A_{\ell ij} = S_i A_{(\ell-1)ij} + jA_{(\ell-1)i(j+1)}$

$A_{\ell im_i} = S_i A_{(\ell-1)im_i}$; $j=1,2,\ldots,(m_i-1)$.

Looking at (2-1-5), we observe:

(a) Equation (2-1-2) is infinitely differentiable for all $t \geq 0$.

(b) $g^{(\ell)}(t)$ is a linear combination using the original basis (2-1-1) for any ℓ (i.e., space invariance is experienced under repeated operation of the differential operator on functions in the space spanned by (2-1-1)).

(c) For any integer value of ℓ_1, the basis set

$$\{ \sum_{i=1}^{k} \sum_{j=1}^{m_i} A_{\ell ij} t^{j-1} e^{S_i t} \}; \quad \ell = \ell_1, (\ell_1+1), \ldots, (\ell_1+n-1) \qquad (2\text{-}1\text{-}6)$$

spans exactly the same space as does the set (2-1-1).

(d) Any n+1 set (i.e., $\ell = \ell_1, (\ell_1+1), \ldots, (\ell_1+n)$) represented by (2-1-6) is linearly dependent.

It is concluded that the complex exponential n-space spanned by (2-1-1) is invariant under the differential operator.

The waveform (2-1-2) is now operated upon by the integral operator. First, an ℓ-fold reverse time integration over $[t,\infty)$ is performed where $t \geq 0$. Specifically, it is readily shown that

$$g_{(\ell)}(t) = \int_{\infty}^{t}\int_{\infty}^{t_\ell}\cdots\int_{\infty}^{t_2}\sum_{i=1}^{k}\sum_{j=1}^{m_i} A_{ij}t_1^{j-1}e^{S_i t_1}\prod_{q=1}^{\ell} dt_q \tag{2-1-7}$$

$$= \sum_{i=1}^{k}\sum_{j=1}^{m_i}\frac{A_{ij}}{(\ell-1)!}\underbrace{\int_{\infty}^{t}(t-\tau)^{\ell-1}\tau^{j-1}e^{S_i\tau}d\tau}_{I_1(t)}$$

where the subscript on g denotes an ℓ-fold integration. Concentrating on $I_1(t)$ and making use of the binomial expansion,

$$I_1(t) = \sum_{p=0}^{\ell-1}(-1)^p\binom{\ell-1}{p}t^{\ell-p-1}\underbrace{\int_{\infty}^{t}\tau^{j+p-1}e^{S_i\tau}d\tau}_{I_2(t)}. \tag{2-1-8}$$

Integrating $I_2(t)$ by parts successively j+p times yields,

$$I_1(t) = \sum_{p=0}^{\ell-1}(-1)^p\binom{\ell-1}{p}t^{\ell-p-1}\left[\sum_{q=0}^{j+p-1}(-1)^q q!\binom{j+p-1}{q}\frac{t^{j+p-q-1}}{S_i^{q+1}}e^{S_i t}\right] \tag{2-1-9}$$

$$= \sum_{p=0}^{\ell-1}\sum_{q=0}^{j+p-1}(-1)^{p+q}q!\binom{\ell-1}{p}\binom{j+p-1}{q}\frac{t^{j+\ell-q-2}}{S_i^{q+1}}e^{S_i t}.$$

Direct integration of the left-hand side of (2-1-7) reveals that it is not possible for (2-1-9) to contain functions in t involving powers

greater than (j-1). With reference to the expression in (2-1-9), this implies for integer values of q less than (ℓ-1) that

$$\sum_{p=0}^{\ell-1} (-1)^{p+q} q! \binom{\ell-1}{p} \binom{j+q-1}{q} = 0 . \qquad (2\text{-}1\text{-}10)$$

The net result is that (2-2-9) can be rewritten as

$$I_1(t) = \sum_{p=0}^{\ell-1} \sum_{q=\ell-1}^{j+p-1} (-1)^{p+q} q! \binom{\ell-1}{p} \binom{j+p-1}{q} \frac{t^{j+\ell-q-2}}{S_i^{q+1}} e^{S_i t} . \qquad (2\text{-}1\text{-}11)$$

Performing a change in the dummy variable q, such that $q = \nu + (\ell-1)$,

$$I_1(t) = \sum_{p=0}^{\ell-1} \sum_{\nu=0}^{j+p-\ell} (-1)^{p+\nu+\ell-1} (\nu+\ell-1)! \binom{\ell-1}{p} \binom{j+p-1}{\nu+\ell-1} \frac{t^{j-\nu-1}}{S_i^{\nu+\ell}} e^{S_i t} . \qquad (2\text{-}1\text{-}12)$$

Finally, substituting (2-1-12) into (2-1-7) yields

$$g_{(\ell)}(t) = \sum_{i=1}^{k} \sum_{j=1}^{m_i} \frac{A_{ij}}{(\ell-1)!} \sum_{p=0}^{\ell-1} \binom{\ell-1}{p} \sum_{\nu=0}^{j+p-\ell} (-1)^{p+\nu+\ell-1} (\nu+\ell-1)! \binom{j+p-1}{\nu+\ell-1} \frac{t^{j-\nu-1}}{S_i^{\nu+\ell}} e^{S_i t} . \qquad (2\text{-}1\text{-}13)$$

From (2-1-13), it is concluded that:

(a) Equation (2-1-2) is infinitely integrable over $(\infty,0]$.

(b) $g_{(\ell)}(t)$ is a linear combination using the original basis in (2-1-1) for any ℓ (i.e., space invariance).

(c) For any integer value of ℓ_1, $\{g_{(\ell)}(t)\}, \ell = \ell_1, (\ell_1+1), \ldots, (\ell_1+n-1)$, spans exactly the same space as does the set (2-1-1).

(d) Any n+1 set (i.e., $\ell = \ell_1, (\ell_1+1, \ldots, (\ell_1+n))$ represented by (2-1-13) is linearly dependent.

It is concluded that the complex exponential n-space spanned by (2-1-1) is invariant under the integral operator over $[0,\infty)$ (i.e., the results

for operations over $[0,\infty)$ and $(\infty,0]$ are related through the sign operator $(-1)^{\ell}$ for an ℓ-fold integration).

The limits of the integral operation are now chosen to obtain a finite arbitrary interval of integration. Let this interval be $[t_o,t]$. $g_{(\ell)}(t)$ in (2-1-7) becomes

$$g_{(\ell)}(t;t_o) = \int_{t_o}^{t}\int_{t_o}^{t_\ell}\cdots\int_{t_o}^{t_2}\sum_{i=1}^{k}\sum_{j=1}^{m_i} A_{ij}\, t_1^{j-1} e^{S_i t_1} \prod_{q=1}^{\ell} dt_q \tag{2-1-14}$$

$$= \sum_{i=1}^{k}\sum_{j=1}^{m_i} \frac{A_{ij}}{(\ell-1)!} \underbrace{\int_{t_o}^{t} (t-\tau)^{\ell-1}\tau^{j-1} e^{S_i\tau} d\tau}_{I_3(t)}.$$

Use of the binomial expansion on $I_3(t)$ results in

$$I_3(t) = \sum_{p=0}^{\ell-1} (-1)^p \binom{\ell-1}{p} t^{\ell-p-1}[I_2(t) - I_2(t_o)]. \tag{2-1-15}$$

It follows that

$$I_3(t) = \sum_{p=0}^{\ell-1} (-1)^p \binom{\ell-1}{p} t^{\ell-p-1} \left[\sum_{q=0}^{j+p-1} (-1)^q q! \binom{j+p-1}{q} \frac{t^{j+p-q-1}e^{S_i t} - t_o^{j+p-q-1}e^{S_i t_o}}{S_i^{q+1}}\right]$$

$$= \sum_{p=0}^{\ell-1}\sum_{q=0}^{j+p-1} (-1)^{p+q} q! \binom{\ell-1}{p}\binom{j+p-1}{q}\left\{\frac{t^{j+\ell-q-2}}{S_i^{q+1}} e^{S_i t} - \right. \tag{2-1-16}$$

$$\left.\left[\frac{\tau_o^{j+p-q-1} e^{S_i t_o}}{S_i^{q+1}}\right] t^{\ell-p-1}\right\}.$$

Notice that the finite limits of integration have introduced into (2-1-16) a polynomial in t of order $\ell-1$. Again, as for (2-1-9), the coefficients for $q < \ell-1$ are identically zero. Hence, following the

steps taken in the development of (2-1-13), (2-1-14) becomes

$$g_{(\ell)}(t;t_o)= \sum_{i=1}^{k} \sum_{j=1}^{m_i} \frac{A_{ij}}{(\ell-1)!} \sum_{p=0}^{\ell-1} \binom{\ell-1}{p} \sum_{\nu=0}^{j+p-\ell} (-1)^{p+\nu+\ell-1} (\nu+\ell-1)! \binom{j+p-1}{\nu+\ell-1}$$

$$\left\{ \frac{t^{j-\nu-1}}{S_i^{\nu+\ell}} e^{S_i t} - \left[\frac{t_o^{j+p-\ell-\nu} e^{S_i t_o}}{S_i^{\nu+\ell}}\right] t^{\ell-p-1} \right\} . \qquad (2\text{-}1\text{-}17)$$

Examination of (2-1-17) reveals:

(a) $g_{(\ell)}(t;t_o)$ is a linear combination of the functions in the $m+\ell$ basis $\{t^{j-1} e^{S_i t}, 1, \ldots, t^{\ell-1}\}$ for any ℓ where $i = 1,2,\ldots,k$; $j = 1,2,\ldots,m_i$;

$$\sum_{i=1}^{k} m_i = n. \qquad (2\text{-}1\text{-}18)$$

(b) The new space consists of the subspace spanned by (2-1-1) plus the subspace spanned by $\{1,\ldots,t^{\ell-1}\}$.

We next consider the operation of passing the waveform g(t), as given by (2-1-2), through ℓ cascaded identical low-pass filters. Let the impulse response of each filter be given by

$$h(t) = \begin{cases} e^{\lambda t} & ; \quad t \geq 0 \\ 0 & ; \quad t < 0 \end{cases} \qquad (2\text{-}1\text{-}19)$$

where λ is a negative real number. The impulse response of the ℓ cascaded low-pass filters is

$$h_\ell(t) = \begin{cases} \frac{t^{\ell-1} e^{\lambda t}}{(\ell-1)!} & ; \quad t \geq 0 \\ 0 & ; \quad t < 0 \end{cases} . \qquad (2\text{-}1\text{-}20)$$

Passing g(t) through the cascade, assuming the filtering begins at

$t = t_o$, results in

$$g_{(\ell)}(t;t_o,\lambda) = \sum_{i=1}^{k} \sum_{j=1}^{m_i} \frac{A_{ij}}{(\ell-1)!} e^{\lambda t} \int_{t_o}^{t} (t-\tau)^{\ell-i} \tau^{j-1} e^{(S_i-\lambda)\tau} d\tau. \quad (2\text{-}1\text{-}21)$$

By direct comparison of (2-1-21) with (2-1-14), it follows from (2-1-17) that

$$g_{(\ell)}(t;t_o,\lambda) = \sum_{i=1}^{k} \sum_{j=1}^{m_i} \frac{A_{ij}}{(\ell-1)!} \sum_{p=0}^{\ell-1} \binom{\ell-1}{p} \sum_{\nu=0}^{j+p-\ell} (-1)^{p+\nu+\ell-1} (\nu+\ell-1)! \binom{j+p-1}{\nu+\ell-1}$$

$$\left\{ \frac{t^{j-\nu-1}}{(S_i-\lambda)^{\nu+\ell}} e^{S_i t} - \left[\frac{t_o^{j+p-\ell-\nu} e^{(S_i-\lambda)t_o}}{(S_i-\lambda)^{\nu+\ell}} \right] e^{\lambda t} t^{\ell-p-1} \right\} \quad (2\text{-}1\text{-}22)$$

Notice that $g_{(\ell)}(t;t_o,\lambda)$ is a linear combination of the functions in the $n+\ell$ basis

$$\{t^{j-1} e^{S_i t}, \; t^{\ell_1-1} e^{\lambda t}\}, \qquad \begin{matrix} i = 1,2,\ldots,k \\ j = 1,2,\ldots,m_i \\ \ell_1 = 1,2,\ldots,\ell \end{matrix} \qquad \sum_{i=1}^{k} m_i = n. \quad (2\text{-}1\text{-}23)$$

For $\lambda = 0$, this basis reduces to that of (2-1-18).

The next operation to be considered is that of passing g(t) as given by (2-1-2), through ℓ cascaded identical filters having simple poles. Let the linear transfer function of each filter be given by

$$H(S) = \frac{P(S)}{Q(S)} = \frac{\prod_{j=1}^{n_1-1} (S - z_j)}{\prod_{j=1}^{n_1} (S - \lambda_j)}. \quad (2\text{-}1\text{-}24)$$

It is assumed that the real part of each pole is negative and that complex poles appear in conjugate pairs. The transfer function of

the ℓ cascaded filters is

$$H_\ell(S) = [H(S)]^\ell = \frac{\prod_{j=1}^{n_1-1} (S - z_j)^\ell}{\prod_{j=1}^{n_1} (S - \lambda_j)^\ell} . \qquad (2\text{-}1\text{-}25)$$

Note that each of the n_1 poles of $H_\ell(S)$ is of ℓ^{th}-order. Taking the inverse Laplace transform of $H_\ell(S)$, the impulse response of the ℓ cascaded filters is

$$h_\ell(t) = \sum_{r=1}^{n_1} \frac{1}{(\ell-1)!} \frac{d^{\ell-1}}{dS^{\ell-1}} [(S-\lambda_r)^\ell H_\ell(S) e^{St}]\Big|_{S=\lambda_r} \qquad (2\text{-}1\text{-}26)$$

$$= \sum_{r=1}^{n_1} \frac{1}{(\ell-1)!} \sum_{\ell_1=1}^{\ell} \binom{\ell-1}{\ell_1-1} R_r^{(\ell-\ell_1)}(\lambda_r) t^{\ell_1-1} e^{\lambda_r t}$$

where

$$R_r(S) = (S - \lambda_r)^\ell H_\ell(S) \qquad (2\text{-}1\text{-}27)$$

and $R_r^{(\ell-\ell_1)}(\lambda_r)$ denotes the $(\ell-\ell_1)^{th}$ derivative of $R_r(S)$ evaluated for $S = \lambda_r$. Passing g(t) through the cascade, assuming the filtering begins at $t = t_o$, results in

$$g_{(\ell)}(t;t_o,\lambda_1,\ldots,\lambda_{n_1}) = \sum_{i=1}^{k} \sum_{j=1}^{m_i} \sum_{r=1}^{n_1} \frac{A_{ij}}{(\ell-1)!} \sum_{\ell_1=1}^{\ell} \binom{\ell-1}{\ell_1-1} R_r^{(\ell-\ell_1)}(\lambda_r) \qquad (2\text{-}1\text{-}28)$$

$$\int_{t_o}^{t} (t-\tau)^{\ell_1-1} \tau^{j-1} e^{\lambda_r(t-\tau)} e^{S_i\tau} d\tau .$$

To carry out the integration in (2-1-28) we may use the results in (2-1-22) which arose from (2-1-21) since the kernels of both integrals

have the same form. The result is

$$g_{(\ell)}(t;t_o,\lambda_1,\ldots,\lambda_{n_1}) = \sum_{i=1}^{k}\sum_{j=1}^{m_i}\sum_{r=1}^{n_1}\frac{A_{ij}}{(\ell-1)!}\sum_{\ell_1=1}^{\ell}\binom{\ell-1}{\ell_1-1}R_r^{(\ell-\ell_1)}(\lambda_r)$$

$$\sum_{p=0}^{\ell_1-1}\binom{\ell_1-1}{p}\sum_{\nu=0}^{j+p-\ell_1}(-1)^{p+\nu+\ell_1-1}(\nu+\ell_1-1)!\binom{j+p-1}{\nu+\ell_1-1} \qquad (2\text{-}1\text{-}29)$$

$$\{\frac{t^{j-\nu-1}}{(S_i-\lambda_r)^{\nu+\ell_1}}e^{S_it} - \underbrace{[\frac{t_o^{j+p-\ell_1-\nu}\,e^{(S_i-\lambda_r)t_o}}{(S_i-\lambda_r)^{\nu+\ell_1}}]}_{C_{jp\ell_1\nu ri}}e^{\lambda_r t}t^{\ell_1-p-1}\}.$$

The basis representing (2-1-29) is given by

$$\{t^{j-1}e^{S_it}, t^{\ell_1-1}e^{\lambda_1 t}, \ldots, t^{\ell_1-1}e^{\lambda_{n_1}t}\} \qquad (2\text{-}1\text{-}30)$$

where $i = 1,2,\ldots,k$; $j = 1,2,\ldots,m_i$; $\sum_{i=1}^{k} m_i = n$; $\ell_1 = 1,2,\ldots,\ell$.

The new space formed through the ℓ-fold operation is $n+n_1\ell$ dimensional and includes the subspace (2-1-1). If we let $t_o \to \infty$ under the condition Real $[S_i - \lambda_r] < 0$ for all possible values of i and r, then all of the coefficients $C_{jp\ell_1\nu ri}$ are identically zero and the ℓ-fold reverse time operation is space invariant.

Another operator that preserves space invariance is the pure delay operator. If we operate repeatedly on (2-1-2) ℓ times with a delay operator of Δ seconds, there results

$$g(t;\ell\Delta) = \sum_{i=1}^{k} \sum_{j=1}^{m_i} A_{ij} \int_0^t \delta(t-\ell\Delta-\tau)\tau^{j-1}e^{-S_i\tau}\,d\tau \qquad (2\text{-}1\text{-}31)$$

$$= \sum_{i=1}^{k} \sum_{j=1}^{m_i} A_{ij}(t-\ell\Delta)^{j-1}e^{-S_i(t-\ell\Delta)}$$

$$= \sum_{i=1}^{k} \sum_{j=1}^{m_i} A_{ij} \sum_{q=0}^{j-1} (-1)^q \binom{j-1}{q} (\ell\Delta)^q e^{S_i\ell\Delta} t^{j-q-1} e^{-S_i t}, \quad t \geq \ell\Delta \geq 0 .$$

Equation (2-1-31) verifies the space invariance under the repeated delay operation.

2.2 Correlation Considerations Involving Complex Exponentials

In general, identification of the complex exponential components of a signal involves solution of a simultaneous set of equations. As the correlation between the components is increased, the equations become more ill conditioned. Consequently, the correlation coefficient between the two complex exponentials is a measure of the difficulty by which the two components may be resolved. By way of illustration, two signals with unit correlation result in a singular set of equations whereas two signals with zero correlation yield an uncoupled set.

Consider two simple complex exponentials given by

$$\{e^{S_i t}\}\ ; \quad i = 1,2, \quad 0 \leq t < \infty \qquad (2\text{-}2\text{-}1)$$

where $S_i = \sigma_i + j\omega_i$, $S_i^* = \sigma_i - j\omega_i$, $\sigma_i < 0$ and $j = \sqrt{-1}$. The correlation

coefficient between exp $[S_1 t]$ and exp $[S_2 t]$ over the time interval $[T_1, T_1+\Delta]$ is defined to be

$$\rho_{12}(T_1,T_1+\Delta) = \frac{\int_{T_1}^{T_1+\Delta} e^{S_1 t} e^{S_2^* t}\, dt}{\left[\int_{T_1}^{T_1+\Delta} e^{S_1 t} e^{S_1^* t}\, dt \int_{T_1}^{T_1+\Delta} e^{S_2 t} e^{S_2^* t}\, dt\right]^{1/2}} \qquad (2\text{-}2\text{-}2)$$

Performing the integrations and rearranging terms yields

$$\rho_{12}(T_1,T_1+\Delta) = \frac{\sqrt{4\sigma_1\sigma_2}}{\sigma_1+\sigma_2+j(\omega_1-\omega_2)} \frac{e^{(\sigma_1+\sigma_2)\Delta} e^{j(\omega_1-\omega_2)\Delta} - 1}{\sqrt{(1-e^{2T_1\Delta})(1-e^{2\sigma_2\Delta})}} e^{j(\omega_1-\omega_2)T_1} . \qquad (2\text{-}2\text{-}3)$$

In general, the correlation coefficient is a complex quantity. The initial time instant T_1 simply adds a constant to the phase. Since we are primarily interested in the magnitude, there is no loss in generality by assuming $T_1 = 0$. For this special case, the coefficient is denoted by $\rho_{12}(\Delta)$.

Of particular interest is the sinusoidal case for which $\sigma_i = 0$, $i = 1,2$. Taking the limit as σ_i approaches zero with $T_1 = 0$, (2-2-3) becomes

$$\rho_{12}(\Delta)\Big|_{\sigma_1,\sigma_2=0} = \frac{e^{j(\omega_1-\omega_2)\Delta} - 1}{j(\omega_1-\omega_2)\Delta} = \frac{\sin\left(\frac{\omega_1-\omega_2}{2}\Delta\right)}{\frac{\omega_1-\omega_2}{2}\Delta} \angle \frac{\omega_1-\omega_2}{2}\Delta . \qquad (2\text{-}2\text{-}4)$$

The phase and magnitude of the correlation coefficient are plotted in Figure (2-2-1) where it is assumed that $\omega_1 \geq \omega_2$. Observe that the

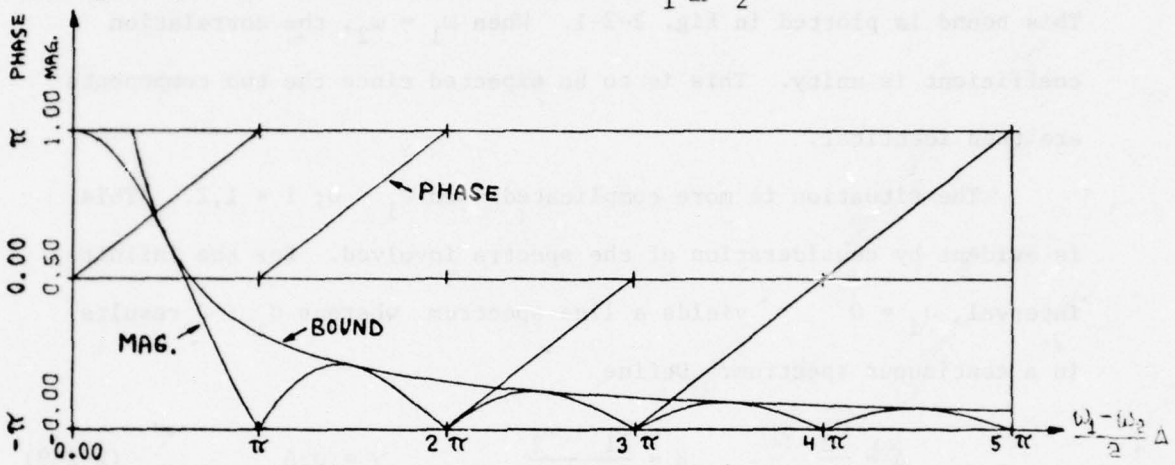

Fig. 2-2-1. Phase and magnitude of $\rho_{12}(\Delta)\big|_{\sigma_1\sigma_2=0}$.

coefficient is zero for

$$\frac{\omega_1 - \omega_2}{2}\Delta = \frac{2\pi(f_1 - f_2)}{2}\Delta = n\pi \; ; \quad n = 1,2,.... \qquad (2\text{-}2\text{-}5)$$

Hence, for an observation interval of length Δ, the two components are uncorrelated for

$$f_1 - f_2 = \frac{n}{\Delta} \; ; \qquad n = 1,2, \ldots \qquad (2\text{-}2\text{-}6)$$

with n = 1, we obtain the conventional condition for resolution of two frequency components which is given by

$$f_1 - f_2 = \frac{1}{\Delta} \; . \qquad (2\text{-}2\text{-}7)$$

For other values of $f_1 - f_2$, the magnitude of the correlation coefficient is bounded by

$$|\rho_{12}(\Delta)|_{\sigma_1,\sigma_2=0} \leq \frac{1}{(f_1 - f_2)\Delta} . \qquad (2\text{-}2\text{-}8)$$

This bound is plotted in Fig. 2-2-1. When $\omega_1 = \omega_2$, the correlation coefficient is unity. This is to be expected since the two components are then identical.

The situation is more complicated when $\sigma_i < 0$; $i = 1,2$. This is evident by consideration of the spectra involved. For the infinite interval, $\sigma_i = 0$ yields a line spectrum whereas $\sigma_i < 0$ results in a continuous spectrum. Define

$$\alpha = \frac{\sigma_2}{\sigma_1} \qquad \beta = \frac{\omega_1 - \omega_2}{\sigma_1} \qquad \gamma = \sigma_1\Delta \qquad (2\text{-}2\text{-}9)$$

where, for convenience, it is assumed $\sigma_2 \leq \sigma_1 < 0$. Substitution of (2-2-9) into (2-2-3), with $T_1 = 0$, the co relation coefficient is expressed as

$$\rho_{12}(\Delta) = \frac{\sqrt{4\alpha}}{1 + \alpha + j\beta} \frac{e^{(1+\alpha)\gamma} e^{j\beta\gamma} - 1}{\sqrt{[1 - e^{2\gamma}][1 - e^{2\alpha\gamma}]}} . \qquad (2\text{-}2\text{-}10)$$

For the infinite observation interval, $\Delta = \infty$ and $\gamma = -\infty$. This yields

$$\rho_{12}(\infty) = - \frac{\sqrt{4\alpha}}{1 + \alpha + j\beta} . \qquad (2\text{-}2\text{-}11)$$

Observe that

$$\rho_{12}(\Delta) = -\rho_{12}(\infty) \left[\frac{e^{(1+\alpha)\gamma} e^{j\beta\gamma} - 1}{\sqrt{[1 - e^{2\gamma}][1 - e^{2\alpha\gamma}]}}\right] . \qquad (2\text{-}2\text{-}12)$$

The second factor in (2-2-12) can be interpreted as a "windowing" factor due to the finite observation interval.

The magnitude and phase of (2-2-10) are given by

$$|\rho_{12}(\Delta)| = \sqrt{\frac{4\alpha}{(1+\alpha)^2 + \beta^2}} \sqrt{\frac{1 - 2e^{(1+\alpha)\gamma}\cos\beta\gamma + e^{2(1+\alpha)\gamma}}{1 - (e^{2\gamma}+e^{2\alpha\gamma}) + e^{2(1+\alpha)\gamma}}} \tag{2-2-13}$$

$$\angle\rho_{12}(\Delta) = \tan^{-1}\left[\frac{(1+\alpha)\sin\beta\gamma - \beta(\cos\beta\gamma - e^{-(1+\alpha)\gamma})}{\beta\sin\beta\gamma + (1+\alpha)(\cos\beta\gamma - e^{-(1+\alpha)\gamma})}\right] .$$

Because this is a rather complicated expression, attention is first devoted to the case of the infinite observation interval. The effect of windowing (i.e., finite observation interval) is discussed later. As is evident, either from (2-2-11) or (2-2-13), the magnitude and phase of the correlation coefficient for $\Delta = \infty$ are

$$|\rho_{12}(\infty)| = \sqrt{\frac{4\alpha}{(1+\alpha)^2 + \beta^2}} \tag{2-2-14}$$

$$\angle\rho_{12}(\infty) = \tan^{-1}\left[-\frac{\beta}{1+\alpha}\right] .$$

For a fixed value of β, the maximum value of $|\rho_{12}(\infty)|$ occurs for

$$\alpha_M = \sqrt{1 + \beta^2} . \tag{2-2-15}$$

The peak value of $|\rho_{12}(\infty)|$ is then given by

$$|\rho_{12}(\infty)|\big|_{\alpha=\alpha_M} = \sqrt{\frac{2}{1 + \sqrt{1 + \beta^2}}} . \tag{2-2-16}$$

It is interesting to note that (2-2-10) is unchanged by interchanging the subscripts 1 and 2 in the definitions of (2-2-9). For this reason,

it is necessary to consider only values of α greater than or equal to unity. The value of $\alpha = 1$ is, therefore, of special interest because it serves as the "origin" in our plots. Interestingly enough, for both large and small values of $|\beta|$, the peak value in (2-2-16) is approximately related to the value of the correlation coefficient for $\alpha = 1$. Specifically,

$$|\rho_{12}(\infty)|_{\alpha=1} = \sqrt{\frac{4}{4 + \beta^2}} \quad . \tag{2-2-17}$$

For $|\beta| >> 1$,

$$|\rho_{12}(\infty)|_{\alpha=1} \simeq \frac{2}{|\beta|} \simeq [|\rho_{12}(\infty)|_{\alpha=\alpha_M}]^2. \tag{2-2-18}$$

On the other hand, for $|\beta| << 1$,

$$|\rho_{12}(\infty)|_{\alpha=1} \simeq 1 \simeq |\rho_{12}(\infty)|_{\alpha=\alpha_M} . \tag{2-2-19}$$

Also, for $\alpha >> 1$ and $\alpha >> |\beta|$, observe from (2-2-14) that

$$|\rho_{12}(\infty)| \simeq \frac{2}{\sqrt{\alpha}} \quad . \tag{2-2-20}$$

Hence, for a fixed value of $|\beta|$, the correlation coefficient approaches zero in the limit as α approaches infinity.

Equation (2-2-14) is now investigated as a function of β. For a fixed value of α, the maximum value of $|\rho_{12}(\infty)|$ occurs for

$$\beta_M = 0. \tag{2-2-21}$$

It is interesting to note that the correlation coefficient peaks when $\omega_1 = \omega_2$ but does not necessarily peak when $\sigma_1 = \sigma_2$ (i.e., $\alpha = 1$). For $\beta_M = 0$, the peak value of the correlation coefficient is

$$|\rho_{12}(\infty)|\,|_{\beta=\beta_M=0} = \frac{2\sqrt{\alpha}}{1+\alpha} \quad . \tag{2-2-22}$$

For $\alpha >> 1$, the peak becomes

$$|\rho_{12}(\infty)|\,|_{\beta=\beta_M=0} \simeq \frac{2}{\sqrt{\alpha}} \quad . \tag{2-2-23}$$

Assymptotically, for $|\beta| >> \alpha$, (2-2-14) reduces to

$$|\rho_{12}(\infty)| \simeq \frac{2\sqrt{\alpha}}{|\beta|} \quad . \tag{2-2-24}$$

Therefore, for a fixed value of α, the correlation coefficient approaches zero in the limit as $|\beta|$ approaches infinity. By comparison of (2-2-20) with (2-2-24), it is seen that the correlation coefficient asymptotically approaches zero at a faster rate with respect to $|\beta|$ as opposed to α.

A plot of $|\rho_{12}(\infty)|$ versus $|\beta|$, with α as a parameter is shown in Fig. 2-2-2. Recall that the larger is the correlation between signal components, the more ill-conditioned are the equations which arise in the identification problem. Figure 2-2-2 points out that the problem of resolution is eased under situations of either small α's and large β's or vice versa. Recognizing that α is constrained to be greater than unity, small α implies $\sigma_1 \simeq \sigma_2$. Then a large value of $|\beta|$ is desirable so that the difference in ω_1 and ω_2 will aid in discriminating between the two components. On the other hand, if $|\beta|$ is small, a large value of α is desirable. It is interesting to note that, for large α, the correlation coefficient is relatively insensitive to $|\beta|$ (e.g., see curve with $\alpha = 100$). This is reasonable since a large value of α implies that one component decays much more rapidly than the other.

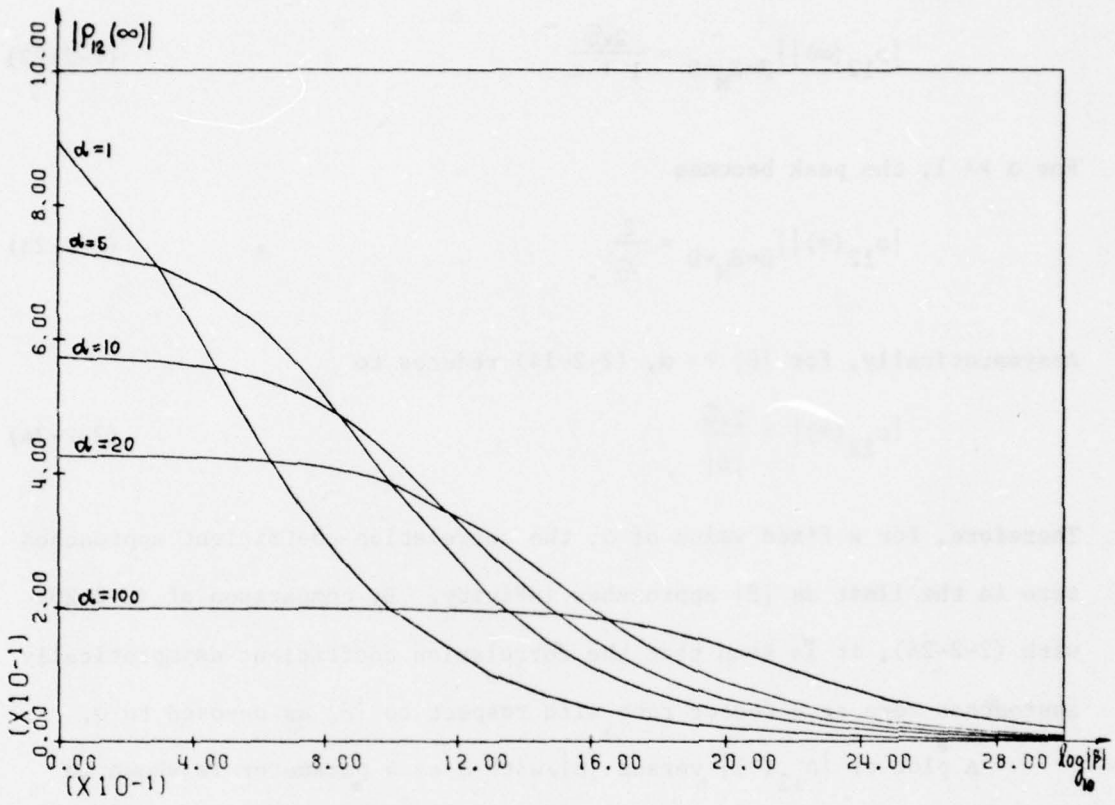

Fig. 2-2-2. $|\rho_{12}(\infty)|$ as a function of $|\beta|$.

Hence, the correlation coefficient is more influenced by the relative decays as opposed to the relative oscillations. In the identification problem α and β are specified and the observation interval is finite. Since an infinite observation interval was assumed in obtaining the curves in Fig. 2-2-2, they serve as a lower bound on the correlation coefficient for the finite interval.

A second way of viewing $|\rho_{12}(\infty)|$ is presented in Fig. 2-2-3 where the magnitude is plotted as a function of α with $|\beta|$ as a parameter. The conclusions arrived at from the previous figure are still valid.

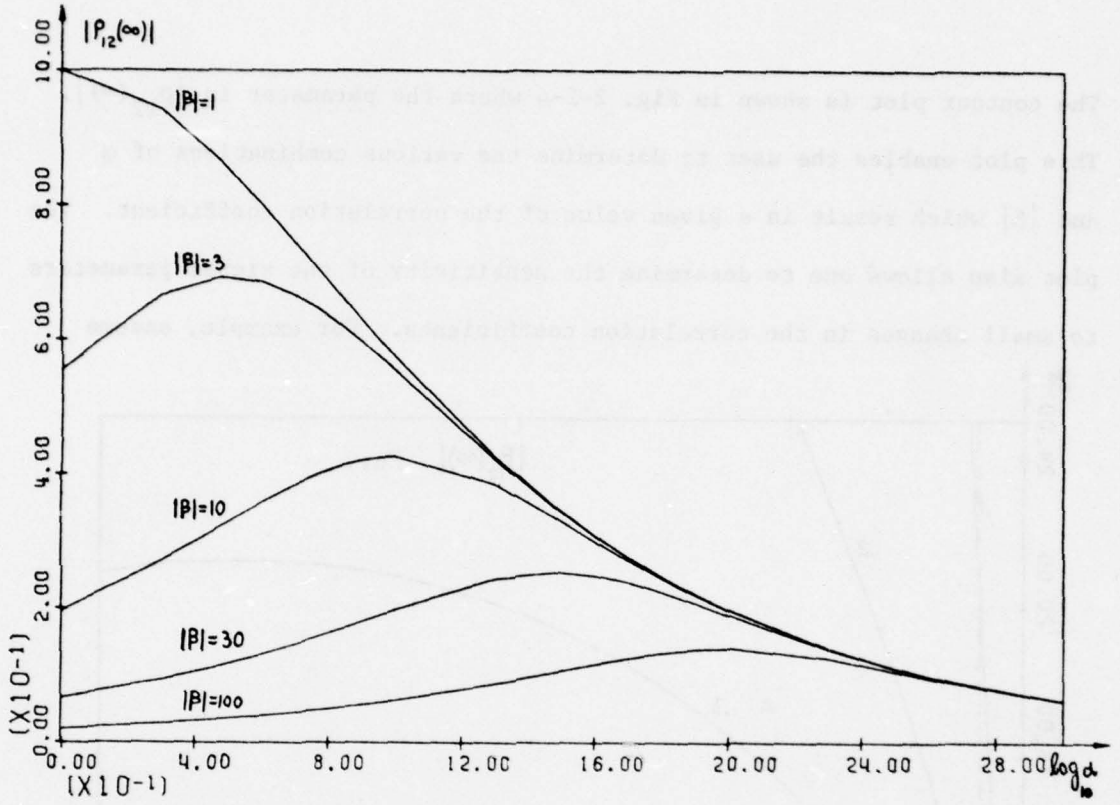

Fig. 2-2-3. $|\rho_{12}(\alpha)|$ as a function of α.

However, Fig. 2-2-3 clearly shows that large values for both α and $|\beta|$ are preferable. Also, note the sequence of peaks at values of α_M predicted by (2-2-15). For large values of $|\beta|$, α_M [illegible]. The maximum value of the correlation coefficient then arises when $|\sigma_2| \simeq |\omega_1 - \omega_2|$ where it is assumed $|\sigma_2| > |\sigma_1|$.

Still another way of presenting the results is to construct equal correlation magnitude contours as a function of α and $|\beta|$. Solution of (2-2-14) for $|\beta|$ results in

$$|\beta| = \sqrt{2\alpha \left(\frac{2}{|\rho_{12}(\infty)|^2} - 1\right) - (1 + \alpha^2)}. \qquad (2\text{-}2\text{-}25)$$

The contour plot is shown in Fig. 2-2-4 where the parameter is $|\rho_{12}(\infty)|$. This plot enables the user to determine the various combinations of α and $|\beta|$ which result in a given value of the correlation coefficient. The plot also allows one to determine the sensitivity of the signal parameters to small changes in the correlation coefficients. For example, assume

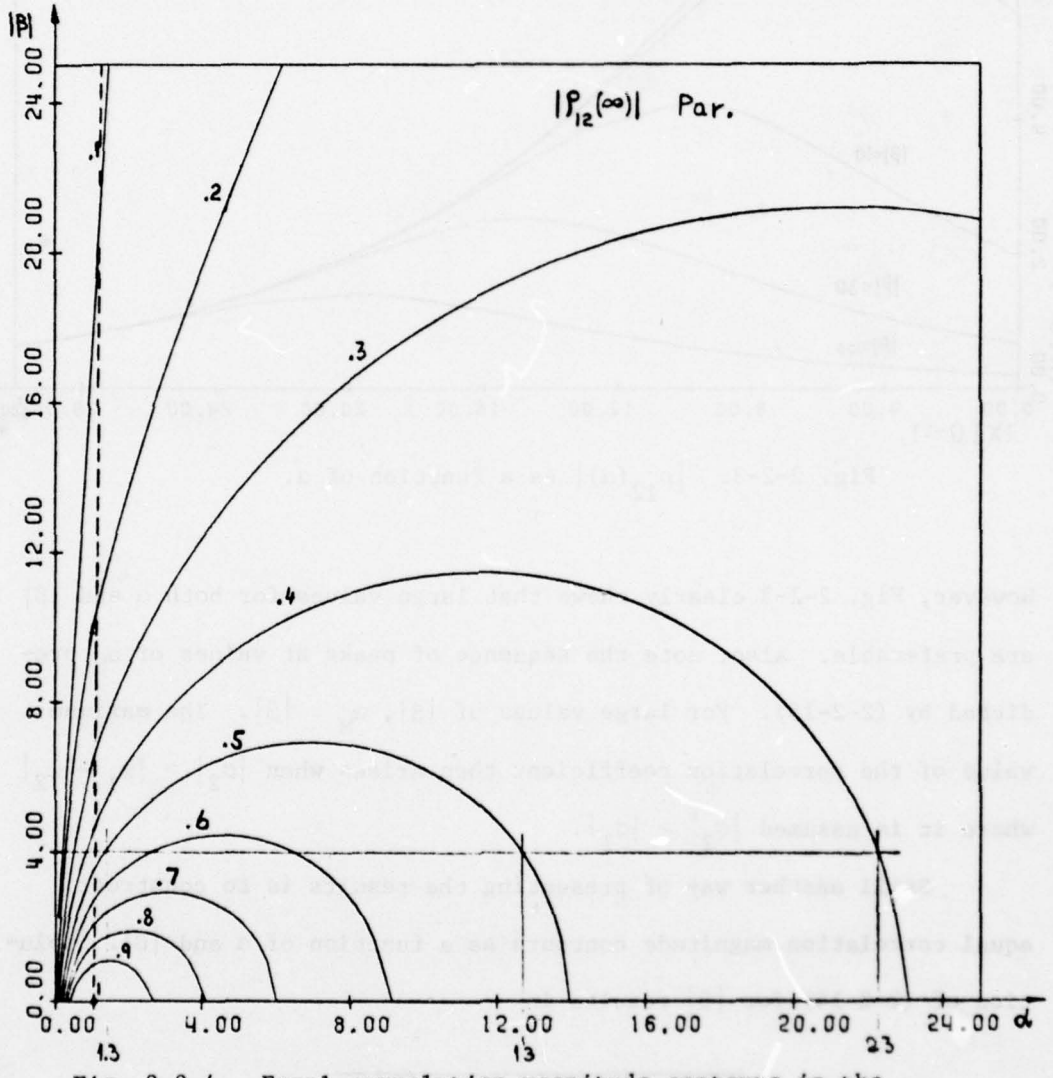

Fig. 2-2-4. Equal correlation magnitude contours in the α, $|\beta|$ plane. $\alpha > 1$ is assumed in the text.

$\sigma_1 = -3$ and $|\beta| = 4$. For $|\rho_{12}(\infty)| = 0.4$, the allowable value of α is approximately 23, as read from Fig. 2-2-4. The corresponding value of σ_2 is -69. When $|\rho_{12}(\infty)| = 0.5$, the allowable values for α are 1.3 and 13. This yields values for σ_2 of -3.9 and -39, respectively. In this case, the value of σ_2 is seen to be highly sensitive to changes in the correlation coefficient.

Our discussion, thus far, has dealt with the infinite interval. We now consider the effect of a finite observation. The windowing effect is accounted for in (2-2-13) by the second factor which is

$$w(\alpha,\beta,\gamma) = \sqrt{\frac{1 - 2e^{(1+\alpha)\gamma}\cos\beta\gamma + e^{2(1+\alpha)\gamma}}{1 - (e^{2\gamma} + e^{2\alpha\gamma}) + e^{2(1+\alpha)\gamma}}} \quad . \qquad (2\text{-}2\text{-}26)$$

$w(\alpha,\beta,\gamma)$ can be shown to approach unity for all possible choices of α and β, as $|\gamma| \to \infty$. Obviously, the effect of windowing is negligible when $w(\alpha,\beta,\gamma) \simeq 1$. Since $\alpha \geq 1$ and $\gamma < 0$, $w(\alpha,\beta,\gamma)$ is bounded by

$$1 - e^{2\gamma} < w(\alpha,\beta,\gamma) < (1 - 2e^{2\gamma})^{-1} . \qquad (2\text{-}2\text{-}27)$$

Observe that the bounds are independent of α and β. The inequality in (2-2-27) can be used to obtain an estimate for the minimum length of the observation interval in order that the correlation between the two components be approximately the same as for the infinite interval. (In general, windowing tends to increase the correlation). From (2-2-27) the following table is obtained:

Table 2-2-1. Lower and Upper Bounds on $w(\alpha,\beta,\gamma)$.

γ	$1 - e^{2\gamma}$	$(1 - 2e^{2\gamma})^{-1}$
-1	.864	1.372
-2	.982	1.038
-3	.997	1.005

It is concluded from Table 2-2-1 that the record length can be assumed to be infinite, as far as $w(\alpha,\beta,\gamma)$ is concerned, provided $\gamma < -2$. In other words, when the length of the observation interval is such that

$$\Delta \geq -\frac{2}{\sigma_1} \quad \text{where } \sigma_i < \sigma_1 < 0;\ i = 2,3, \ldots, \tag{2-2-28}$$

then $|\rho_{12}(\Delta)| \simeq |\rho_{12}(\infty)|$. Since a finite interval tends to increase the correlation coefficient, it is desirable that the inequality in (2-2-28) be satisfied.

The behavior of $|\rho_{12}(\Delta)|$ as a function of $|\gamma|$ is illustrated in Figures 2-2-5 and 2-2-6. In Figure 2-2-5 α is constrained to be unity as the parameter $|\beta|$ is varied from 1 to 100. Note that the curves have settled down to their asymptotic behavior for $|\gamma| > 2$. It is interesting to compare the damped case (i.e., $\sigma_i \neq 0$) to the sinusoidal case (i.e., $\sigma_i = 0$). For $\sigma_1 = -1$, $|\beta| = |\omega_1 - \omega_2|$. The dashed line in Fig. 2-2-5 corresponds to the sinusoidal case where $|\omega_1 - \omega_2| = 10$. This serves as a reference for the damped case where $|\beta| = 10$ and $\sigma_1 = -1$. In Figure 2-2-6 $|\beta|$ is constrained to equal the value 3 as the parameter α is varied from 1 to 100. Again asymptotic values have been "reached" for $|\gamma| > 2$. The dashed curve in Fig. 2-2-6 represents

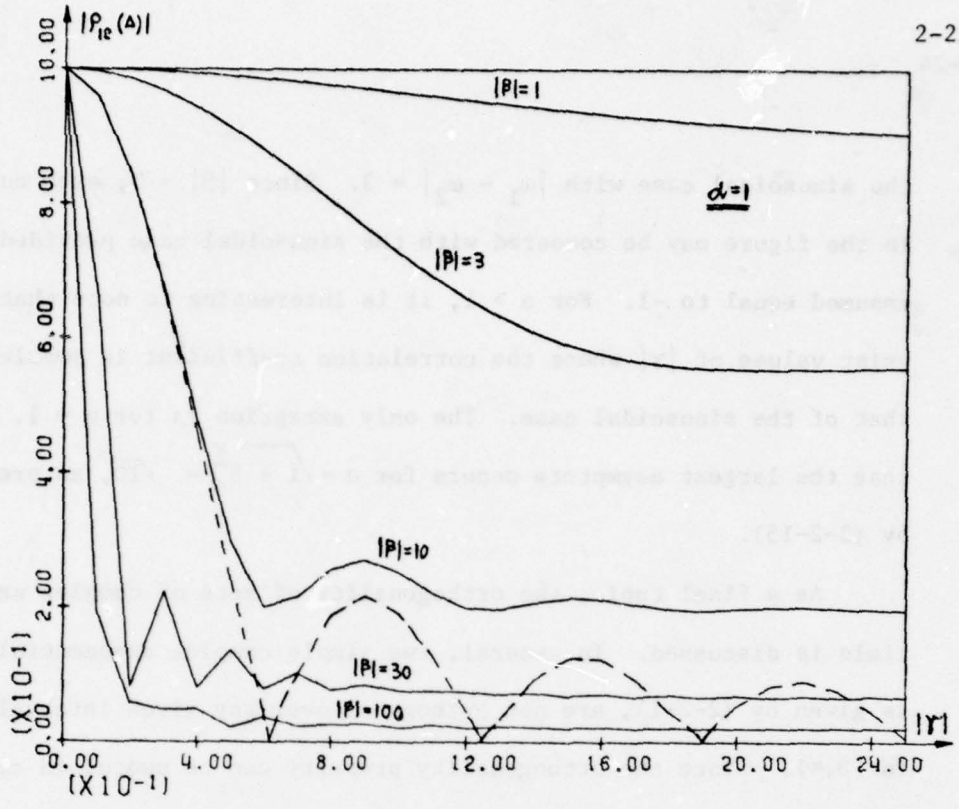

Fig. 2-2-5. $|\rho_{12}(\Delta)|$ vs. $|\gamma|$ with $\alpha = 1$ and $|\beta|$ as a parameter.

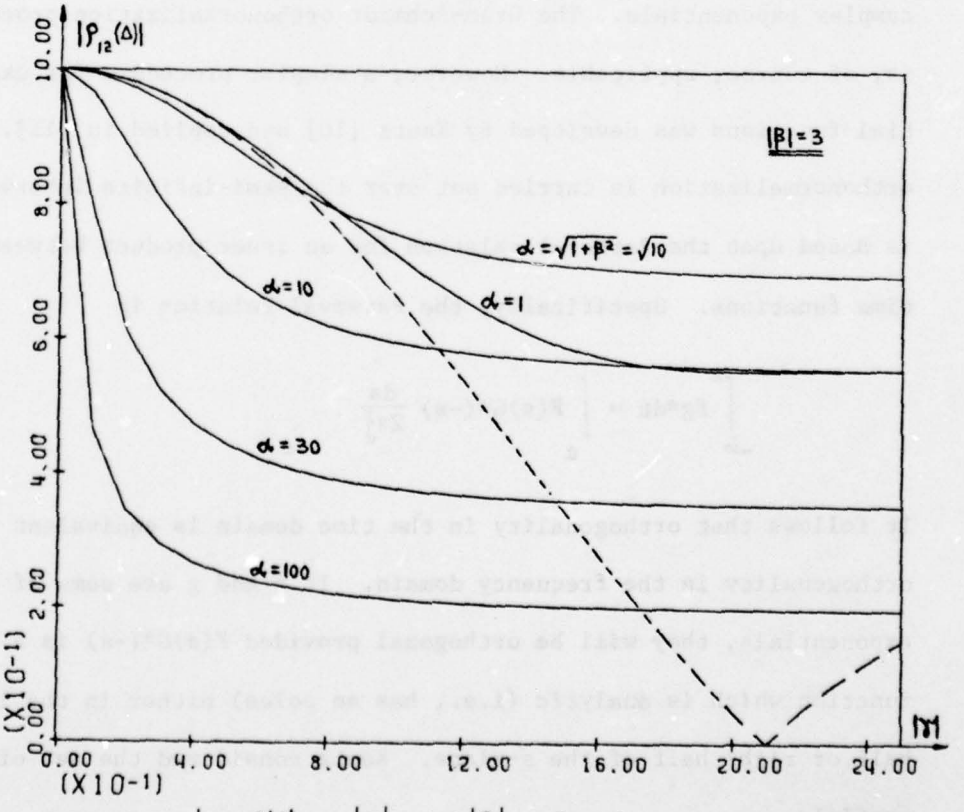

Fig. 2-2-6 $|\rho_{12}(\Delta)|$ vs. $|\gamma|$ with $|\beta| = 3$ and α as a parameter.

the sinusoidal case with $|\omega_1 - \omega_2| = 3$. Since $|\beta| = 3$, each curve in the figure may be compared with the sinusoidal case provided σ_1 is assumed equal to -1. For $\alpha > 1$, it is interesting to note that there exist values of $|\gamma|$ where the correlation coefficient is smaller than that of the sinusoidal case. The only exception is for $\alpha = 1$. Notice that the largest asymptote occurs for $\alpha = \sqrt{1 + \beta^2} = \sqrt{10}$, as predicted by (2-2-15).

As a final topic, the orthogonality of sets of complex exponentials is discussed. In general, two simple complex exponentials, as given by (2-2-1), are not orthogonal over any given interval within $[0,\infty)$. Since the orthogonality property can be useful in certain situations, it is desirable to be able to orthogonalize a set of complex exponentials. The Gram-Schmidt orthonormalization procedure is, of course, applicable. However, a simpler procedure for exponential functions was developed by Kautz [10] and applied in [11]. The orthonormalization is carried out over the semi-infinite interval and is based upon the Parseval relation for an inner product between two time functions. Specifically, the Parseval relation is

$$\int_{-\infty}^{\infty} fg^* dt = \int_c F(s)G^*(-s)\,\frac{ds}{2\pi j}\,. \qquad (2\text{-}2\text{-}29)$$

It follows that orthogonality in the time domain is equivalent to orthogonality in the frequency domain. If f and g are sums of complex exponentials, they will be orthogonal provided F(s)G*(-s) is a rational function which is analytic (i.e., has no poles) either in the left half or right half of the s-plane. Kautz considered the set of exponentials

$$\{e^{S_i t}\}, \quad i = 1,2,\ldots,n,\ldots,m, \quad t \geq 0, \ \sigma_i < 0 \tag{2-2-30}$$

and constructed an orthonormal set where the n^{th} orthonormal basis function is given by

$$\Psi_n(S) = \sqrt{-S_n - S_n^*}\ \frac{\prod_{k=1}^{n-1}(S + S_k^*)}{\prod_{i=1}^{n}(S - S_i)} = \frac{\sqrt{-2\sigma_n}}{S - S_n} \prod_{i=1}^{n-1} \frac{S + S_i^*}{S - S_i} . \tag{2-2-31}$$

To verify that (2-2-31) is the n^{th} representative of an orthonormal basis, we show that

$$\int_{-j\infty}^{j\infty} \Psi_\ell(S)\, \Psi_q^*(-S)\, \frac{dS}{2\pi j} = \begin{cases} 1 & \ell = q \\ 0 & \ell \neq q \end{cases} . \tag{2-2-32}$$

For $\ell < q$, the integral in (2-2-32) becomes

$$\frac{\sqrt{-S_\ell - S_\ell^*}\sqrt{-S_q - S_q^*}}{2\pi j} \int_{-j\infty}^{j\infty} \frac{\prod_{k_1=1}^{\ell-1}(S+S_{k_1}^*) \prod_{k_2=1}^{\ell}(S-S_{k_2}) \prod_{k_3=\ell+1}^{q-1}(S-S_{k_3})(-1)^{q-1}}{\prod_{i_1=1}^{\ell}(S-S_{i_1}) \prod_{i_2=1}^{q}(S+S_{i_2}^*)(-1)^q} ds . \tag{2-2-33}$$

Note that the integrand is analytic in the left-half plane and on the imaginary axis. Therefore, closing the contour to the left, the resulting integral is zero. For $\ell > q$, the integral is analytic in the right-half plane and on the imaginary axis. By closing the contour to the right, the resulting integral is again zero. For $\ell = q$, (2-2-33) reduces to

$$\frac{\sqrt{-S_\ell - S_\ell^*}\sqrt{-S_q - S_q^*}}{2\pi j}\int_{-j\infty}^{j\infty}\frac{-1}{(S-S_\ell)(S+S_\ell^*)}\,dS = \frac{(-1)(-S_k-S_k^*)}{S_k+S_k^*} = 1 \qquad (2\text{-}2\text{-}34)$$

where the contour can be closed either to the right or left without affecting the result. Equation (2-2-31) can be interpreted in terms of passing the n^{th} exponential time function through an all-pass filter structured from the previous n-1 exponents. The all-pass filter interpretation points out that it is the phase which is responsible for the orthogonality.

Thus far, orthogonality has been considered over a semi-infinite interval. Provided a finite interval is suitably long, orthogonality can still be approximated by the Kautz procedure. From (2-2-31), note that

$$\psi_n(t) = \mathcal{L}^{-1}\{\Psi_n(S)\} = \sum_{i=1}^{n} A_i e^{S_i t}. \qquad (2\text{-}2\text{-}35)$$

In the time domain orthonormality requires

$$\int_0^\infty \psi_\ell(t)\psi_q^*(t)\,dt = \begin{cases} 1 & ; \quad \ell = q \\ 0 & ; \quad \ell \neq q \end{cases}. \qquad (2\text{-}2\text{-}36)$$

Substitution of (2-2-35) into (2-2-36) yields

$$\int_0^\infty \psi_\ell(t)\psi_q^*(t)dt = \sum_{i=1}^{\ell}\sum_{k=1}^{q} A_i A_k^* \int_0^\infty e^{(S_i+S_k^*)t}\,dt$$

$$= \sum_{i=1}^{\ell}\sum_{k=1}^{q} -\frac{A_i A_k^*}{S_i + S_k^*} = \begin{cases} 1 & ; \quad \ell = q \\ 0 & ; \quad \ell \neq q \end{cases}. \qquad (2\text{-}2\text{-}37)$$

For a finite interval of length Δ, consider

$$\int_0^{\Delta} \psi_{\ell}(t)\psi_q^*(t)dt = \sum_{i=1}^{\ell} \sum_{k=1}^{q} A_i A_k^* \frac{e^{(S_i+S_k^*)\Delta} - 1}{S_i + S_k^*} \tag{2-2-38}$$

Clearly, (2-2-38) reduces to (2-2-37) provided

$$\left| e^{(S_i+S_k^*)\Delta} \right| << 1. \tag{2-2-39}$$

Assume $|\sigma_1| < |\sigma_i|$ for i = 2,3,...,n. Since

$$\left| e^{(S_i+S_k^*)\Delta} \right| \leq e^{2\sigma_1\Delta}, \tag{2-2-40}$$

(2-2-39) can be replaced by the similar inequality

$$e^{2\sigma_1\Delta} = e^{2\gamma} << 1. \tag{2-2-41}$$

Provided the interval length is chosen such that (2-2-41) is satisfied, the orthonormal basis generated by (2-2-31) is very close to being orthonormal over the finite interval. Interestingly enough, $|\gamma| \geq 2$, which was the condition for $|\rho_{12}(\Delta)| \simeq |\rho_{12}(\infty)|$, also satisfies the orthogonality condition of (2-2-41). In this dissertation,

$$|\gamma| \geq 2 \tag{2-2-42}$$

is the condition to be satisfied if a finite interval is to be considered as though it were an infinite interval.

2.3 A General Parametric Identification Approach

Consider a linear system with input x(t) and output y(t) as shown in Fig. 2-3-1. Assuming the system is described by a proper rational transfer function, the impulse response h(t) may be expressed as

$$h(t) = \begin{cases} \sum_{i=1}^{k} \sum_{j=1}^{m_i} A_{ij} t^{j-1} e^{S_i t} & ; \quad t \geq 0 \\ 0 & ; \quad t < 0. \end{cases} \tag{2-3-1}$$

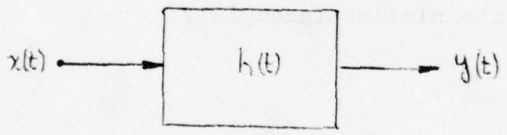

Fig. 2-3-1. Linear system.

In Section 1.3 it was shown that an irreducible representation for this system is the input-output relation given by the differential equation

$$\sum_{j=0}^{n} D_j y^{(j)}(t) = \sum_{i=0}^{m} N_i x^{(i)}(t). \tag{2-3-2}$$

For a complete specification of the equation the initial conditions at some arbitrary instant of time t_0

$$y^{(k)}(t_o); \quad k = 0,1,2,\ldots,n-1$$
$$x^{(\ell)}(t_o); \quad \ell = 0,1,2,\ldots,m,$$

must also be specified.

Notice that (2-3-2) can be rewritten as

$$\sum_{j=0}^{n} D_j y^{(j)}(t) - \sum_{i=0}^{m} N_i x^{(i)}(t) = 0 \quad . \tag{2-3-3}$$

Equation (2-3-3) represents a linear combination of the input and output signals and their derivatives up to the orders m and n, respectively. This implies that the set of functions

$$\{y^{(j)}, x^{(i)}\} \quad ; \quad \begin{matrix} j = 0,1,2,\ldots,n \\ i = 0,1,2,\ldots,m \end{matrix} \tag{2-3-4}$$

is linearly dependent. Assuming none of the coefficients in (2-3-3) is zero, all of the (n+m+2) functions in (2-3-4) are needed to satisfy the differential equation. Linear independence results when one of the functions is removed from the set (2-3-4) since it is no longer possible to express any one function as a linear combination of the others. This suggests that (2-3-3) is defined on a space having dimension (n+m+1).

The general solution of the differential equation given by (2-3-2) is $y^{(0)}(t) = y(t)$ and consists of the homogeneous solution $y_h(t)$ plus the particular solution $y_p(t)$. The impulse response h(t) can be determined from the homogeneous solution alone. Hence, it is desirable that any identification procedure be able to separate $y_h(t)$ and $y_p(t)$ from y(t) conceptually, if not in practice.

Since a proper rational transfer function is assumed, m in (2-3-2) is strictly smaller than n. In the identification problem both m and n are unknown. It is possible to simplify determination of the values for m and n by first assuming that m equals n. The value of n is then found. The value of m follows from the fact that the coefficients

N_i; $i = m+1,\ldots,n$ are then found to be zero. To accomplish this procedure we consider the set

$$\{y^{(j)},x^{(i)}\} \quad ; \quad \begin{matrix} j = 1,2,\ldots,n \\ i = 0,1,2,\ldots,m,\ldots,n. \end{matrix} \tag{2-3-5}$$

Note that $y^{(0)}$ has been removed from (2-3-4), as mentioned previously, this results in linear independence of the set

$$\{y^{(j)},x^{(i)}\} \quad ; \quad \begin{matrix} j = 1,2,\ldots,n \\ i = 0,1,2,\ldots,m. \end{matrix} \tag{2-3-6}$$

Also, observe that the set (2-3-5) contains the function $x^{(m+1)},\ldots,x^{(n)}$ which were not originally contained in (2-3-4). The set (2-3-5) will also be linearly independent provided none of the functions $x^{(m+1)},\ldots,$ $x^{(n)}$ can be expressed as a linear combination of the functions in (2-3-6). The functions in (2-3-5) can then serve as a basis to span a (2n+1) dimensional space. For those cases where (2-3-5) constitutes a linearly independent set, the value of n can be determined as explained next.

For purpose of illustration, we consider an idealized identification problem. Assume for all $t \geq 0$, that analytical representations are available for the system input and output. Consider the (2n+2) functions

$$x^{(0)}, \ldots, x^{(n)}, y^{(0)}, \ldots, y^{(n)}$$

which are generated as shown in Fig. 2-3-2. Assume (2-3-5) constitutes a linearly independent set. The object is to determine n and then to identify the system.

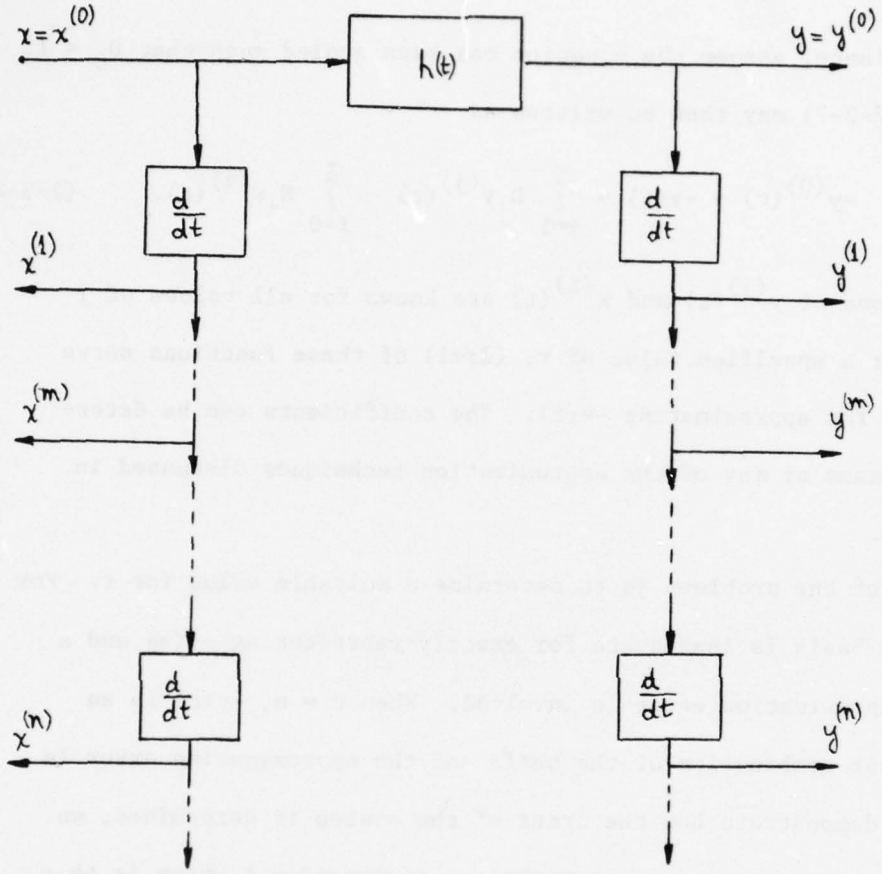

Fig. 2-3-2. Reconstruction of the differential equation describing the system h.

Because known analytical expressions are assumed for x(t) and y(t), this example represents a highly simplified situation. Nevertheless, it serves to illustrate the point. The procedure begins by assuming the system differential equation is given by

$$\sum_{j=0}^{r} D_j y^{(j)}(t) - \sum_{i=0}^{r} N_i x^{(i)}(t) = 0 \qquad (2\text{-}3\text{-}7)$$

Clearly, (2-3-7) remains unchanged when multiplied by a constant.

For convenience, assume the equation has been scaled such that $D_0 = 1$. Equation (2-3-7) may then be written as

$$-y^{(0)}(t) = -y(t) = \sum_{j=1}^{r} D_j y^{(j)}(t) - \sum_{i=0}^{r} N_i x^{(i)}(t). \qquad (2\text{-}3\text{-}8)$$

The functions of $y^{(j)}(t)$ and $x^{(i)}(t)$ are known for all values of j and i. For a specified value of r, (2r+1) of these functions serve as a basis for approximating -y(t). The coefficients can be determined by means of any of the approximation techniques discussed in Appendix A.

One of the problems is to determine a suitable value for r. For $r < n$, the basis is inadequate for exactly representing -y(t) and a nonzero approximation error is involved. When $r = n$, -y(t) is an exact linear combination of the basis and the approximation error is zero. To demonstrate how the order of the system is determined, we use the simplest approximation technique in Appendix A which is that of interpolation.

Consider the (2r+1) equations obtained by evaluating (2-3-8) at (2r+1) different time instants. This results in

$$-y^{(0)}(t_k) = \sum_{j=1}^{r} D_j y^{(j)}(t_k) - \sum_{i=0}^{r} N_i x^{(i)}(t_k); \qquad (2\text{-}3\text{-}9)$$

$$k = 1,\ldots,2r+1 .$$

Equation (2-3-9) can be expressed in matrix form as

$$\begin{bmatrix} y^{(1)}(t_1) & \cdots & y^{(r)}(t_1) \\ y^{(1)}(t_2) & \cdots & y^{(r)}(t_2) \\ \vdots & & \vdots \\ y^{(1)}(t_{2r+1}) & \cdots & y^{(r)}(t_{2r+1}) \end{bmatrix} \begin{bmatrix} x^{(0)}(t_1) & x^{(1)}(t_1) & \cdots & x^{(r)}(t_1) \\ x^{(0)}(t_2) & x^{(1)}(t_2) & \cdots & x^{(r)}(t_2) \\ \vdots & \vdots & & \vdots \\ x^{(0)}(t_{2r+1}) & x^{(1)}(t_{2r+1}) & \cdots & x^{(r)}(t_{2r+1}) \end{bmatrix} \begin{bmatrix} D_1 \\ D_2 \\ \vdots \\ D_r \\ \hline -N_0 \\ -N_1 \\ \vdots \\ -N_r \end{bmatrix} = - \begin{bmatrix} y^{(0)}(t_1) \\ y^{(0)}(t_2) \\ \vdots \\ y^{(t)}(t_{2r+1}) \end{bmatrix} \tag{2-3-10}$$

The square matrix is nonsingular provided $r \leq n$. Consequently, n can be determined by successively increasing the value of r by unity until the matrix becomes singular. This will first occur when r = n+1. (The matrix is then of size 2n+3). Having determined the value of n, (2-3-10) is solved for the coefficients D_j and N_i where r is chosen equal to n. Under the assumption that (2-3-5) is a linearly independent set the coefficients N_i for i = (m+1), ..., n will be found to be identically zero since the original differential equation (2-3-2) is a linear combination of the basis in (2-3-6) which spans a subspace of the space spanned by (2-3-5).

The assumption of linear independence for $x^{(i)}$, where $(m+1) \leq i \leq n$, is now relaxed. The simultaneous set of equations in (2-3-10) are generated as before. However, in addition to checking the singularity of the square (2r+1) x (2r+1) matrix, the singularity of the submatrix

$$\begin{bmatrix} x^{(0)}(t_1) & x^{(1)}(t_1) & \cdots & x^{(r)}(t_1) \\ x^{(0)}(t_2) & x^{(1)}(t_2) & \cdots & x^{(r)}(t_2) \\ \vdots & \vdots & & \vdots \\ x^{(0)}(t_{r+1}) & x^{(1)}(t_{r+1}) & \cdots & x^{(r)}(t_{r+1}) \end{bmatrix}$$

is also checked. As long as the submatrix remains nonsingular, while the value of r is successively increased by unity, the procedure remains the same as before. The procedure is changed should the submatrix become singular. Suppose this occurs for the value of r equal to r_1. Then both the $(2r_1+1)^{th}$ column and row are removed from the square matrix in (2-3-10). The reduced matrix is checked for singularity. If this matrix is singular, the order of the reduced matrix is (2n+2) and the value of n has been found. If the reduced matrix is nonsingular, the procedure proceeds by adding to the reduced matrix an additional column to the $[y^{(j)}]$ submatrix while adding an additional row to the whole matrix as shown below.

$$\begin{bmatrix} y^{(1)}(t_1) & \cdots & y^{(r_1)}(t_1) & y^{(r_1+1)}(t_1) & \| & x^{(0)}(t_1) & \cdots & x^{(r_1-1)}(t_1) \\ y^{(1)}(t_2) & \cdots & y^{(r_1)}(t_2) & y^{(r_1+1)}(t_2) & \| & x^{(0)}(t_2) & \cdots & x^{(r_1-1)}(t_2) \\ \vdots & & \vdots & \vdots & \| & \vdots & & \vdots \\ y^{(1)}(t_{2r_1+1}) & \cdots & y^{(r_1)}(t_{2r_1+1}) & y^{(r_1+1)}(t_{2r_1+1}) & \| & x^{(0)}(t_{2r_1+1}) & \cdots & x^{(r_1-1)}(t_{2r_1+1}) \end{bmatrix} \begin{bmatrix} D_1 \\ D_2 \\ \vdots \\ D_{r_1+1} \\ -N_0 \\ -N_1 \\ \vdots \\ -N_{r_1-1} \end{bmatrix} = - \begin{bmatrix} y^{(0)}(t_1) \\ y^{(0)}(t_2) \\ \vdots \\ y^{(0)}(t_{2r_1+1}) \end{bmatrix}$$

This process is continued p times until the resulting $(2r_1+p) \times (2r_1+p)$ matrix is singular. The order of this matrix is $r_1 + n + 1$ from which n can be determined. The coefficients are found by solving the set of equations which result when the $(r_1+p)^{th}$ column and $(2r_1+p)^{th}$ row are removed from (2-3-11). This procedure also yields the value of m since the coefficients $N_{m+1}, \ldots, N_{r_1-1}$ will be identically zero.

The previous discussion utilized a differential equation description of the system. This was not necessary. Many other representations exist for a dynamical system. Provided each representation is equivalent, any given input will result in the same output irrespective of the representation used. Equivalency between the convolution integral and differential equation representations was demonstrated in Chapter 1.

A variety of equivalent representations can be generated from (2-3-3) by operating on the differential equation with various linear operators. Assume a particular linear operator is denoted by g_k. Applying this operator to (2-3-3), there results

$$g_k\{\sum_{j=0}^{n} D_j y^{(j)}(t) - \sum_{i=0}^{m} N_i x^{(i)}(t)\} = 0 . \qquad (2\text{-}3\text{-}12)$$

Making use of linearity, as defined in (1-1-1), (2-3-12) can be written as

$$\sum_{j=0}^{n} D_j[g_k y^{(j)}(t)] - \sum_{i=0}^{m} N_i[g_k x^{(i)}(t)] = 0 . \qquad (2\text{-}3\text{-}13)$$

This procedure can be extended to a cascade of ℓ such operators.

Let $g_k(t)$ denote the impulse response obtained when the unit impulse is applied to the operator g_k. The Laplace transform of $g_k(t)$ is denoted by $G_k(S)$. Since convolution in the time domain corresponds to multiplication in the frequency domain, the process of operating on (2-3-3) by the sequence of operators $g_1, g_2, \ldots, g_\ell$ can be described by

$$\sum_{j=0}^{n} D_j \int_0^{t-t_o} f_\ell(\tau) y^{(j)}(t-\tau)d\tau - \sum_{i=0}^{m} \int_0^{t-t_o} f_\ell(\tau) x^{(i)}(t-\tau)d\tau = 0 \; ; \; t \geq t_o \quad (2\text{-}3\text{-}14)$$

where

$$f_\ell(t) = \mathcal{L}^{-1}\left[\prod_{k=1}^{\ell} G_k(S)\right]. \quad (2\text{-}3\text{-}15)$$

For convenience, define

$$\tilde{y}_j(t;\ell) = \int_0^{t-t_o} f_\ell(\tau) y^{(j)}(t-\tau)d\tau$$

$$\tilde{x}_i(t;\ell) = \int_0^{t-t_o} f_\ell(\tau) x^{(i)}(t-\tau)d\tau. \quad (2\text{-}3\text{-}16)$$

Equation (2-3-14) can be rewritten then as

$$\sum_{j=0}^{n} D_j \tilde{y}_j(t;\ell) - \sum_{i=0}^{m} N_i \tilde{x}_i(t;\ell) = 0 \quad (2\text{-}3\text{-}17)$$

where it is understood that the system is initially relaxed at time t_o. The representation in (2-3-17) is in terms of the new set of functions

$$\{\tilde{y}_j(t;\ell);\ \tilde{x}_i(t;\ell)\} \quad ; \quad \begin{matrix} j = 0,1,\ldots,n \\ i = 0,1,\ldots,m. \end{matrix} \qquad (2\text{-}3\text{-}18)$$

Provided these functions span an $n + m + 1$ dimensional space, the representation in (2-3-17) is equivalent to that in (2-3-7). Note that the coefficients D_j and N_i are identical in the two representations.

Equation (2-3-17) has significant implications as far as the identification problem is concerned. In general, only finite records of the input and output are available. The differentiation scheme shown in Fig. 2-3-2 for generating a set of $n + m + 2$ functions to be used in the identification is, in general, impractical. Differentiation tends to enhance the noise and measurement errors inherent in experimental data. Alternative schemes are suggested by (2-3-17) which incorporate the $n + m + 2$ functions of (2-3-18). In other words, operators other than differentiators can be utilized to generate a suitable set of $n + m + 2$ functions from the input-output data.

A practical difficulty yet remains with use of (2-3-17). The functions in (2-3-16) are generated from derivatives of the input and output. In practice, only the input, $x^{(0)}$, and output, $y^{(0)}$, are given. The question then arises, "Is it possible to generate an equation similar to (2-3-17), where the coefficients D_j and N_i are preserved, but the functions involved are generated only from the given input and output?"

To answer this question, consider the frequency-domain input-output relation for a nonrelaxed, linear, time-invariant, causal system

which is given by (1-3-6). Recall that the coefficients C_q arise from the nonzero initial conditions at time t = 0. Rewriting (1-3-6), there results

$$\sum_{j=0}^{n} D_j S^j Y(S) - \sum_{i=0}^{m} N_i S^i X(S) - \sum_{q=0}^{n-1} C_q S^q = 0 . \qquad (2\text{-}3\text{-}19)$$

Let the transfer function of a linear cascade of ℓ filters be denoted by

$$F_\ell(S) = [\prod_{k=1}^{\ell} G_k(S)]. \qquad (2\text{-}3\text{-}20)$$

Multiplication of (2-3-19) by $F_\ell(S)$ yields

$$\sum_{j=0}^{n} D_j S^j F_\ell(S) Y(S) - \sum_{i=0}^{m} N_i S^i F_\ell(S) X(S) - \sum_{q=0}^{n-1} C_q S^q F_\ell(S) = 0. \qquad (2\text{-}3\text{-}21)$$

The inverse Laplace transform of $F_\ell(S)$, as pointed out in (2-3-15), is $f_\ell(t)$. Hence,

$$\mathcal{L}^{-1}\{S^p F_\ell(S)\} = \frac{d^p}{dt^p}\{f_\ell(t)\} = f_\ell^{(p)}(t). \qquad (2\text{-}3\text{-}22)$$

Converting (2-3-21) to the time domain, we obtain

$$\sum_{j=0}^{n} D_j \int_0^t y(\tau) f_\ell^{(j)}(t-\tau)\,d\tau - \sum_{i=0}^{m} N_i \int_0^t x(\tau) f_\ell^{(i)}(t-\tau)\,d\tau - \sum_{q=0}^{n-1} C_q f_\ell^{(q)}(t) = 0 \qquad (2\text{-}3\text{-}23)$$

where it is understood that differentiation is with respect to the variable t. For convenience, define the functions

$$y_j(t;\ell) = \int_0^t y(\tau) f_\ell^{(j)}(t-\tau)\,d\tau$$

$$x_i(t;\ell) = \int_0^t x(\tau) f_\ell^{(i)}(t-\tau)\,d\tau \,. \qquad (2\text{-}3\text{-}24)$$

Notice the reversed roles of the functions in (2-3-16) and (2-3-24). Equation (2-3-23) now becomes

$$\sum_{j=0}^{n} D_j y_j(t;\ell) - \sum_{i=0}^{m} N_i x_i(t;\ell) - \sum_{q=0}^{n-1} C_q f_\ell^{(q)}(t) = 0. \qquad (2\text{-}3\text{-}25)$$

For the relaxed case the coefficients C_q are identically zero and (2-3-25) is identical in form to (2-3-17). For the system representation in (2-3-25) to be equivalent to the original differential equation, $f_\ell(t)$ should be n differentiable and the set

$$\{f_\ell^{(p)}(t)\} \quad ; \quad p = 0,1,\ldots, n \qquad (2\text{-}3\text{-}26)$$

should span an (n+1)-dimensional function space. A block diagram of (2-3-25) is given in Figure 2-3-3.

In general, arbitrary inputs and nonzero initial conditions must be considered. For simplicity, a relaxed system whose input is a unit impulse is first discussed. For a system with impulse response given by (2-3-1), the output is

$$y(t) = \begin{cases} \sum_{i=1}^{k} \sum_{j=1}^{m_i} A_{ij} t^{j-1} e^{S_i t} & ; \quad t \geq 0 \\ 0 & ; \quad t < 0 \,. \end{cases} \qquad (2\text{-}3\text{-}27)$$

Notice that y(t) is a linear combination of the n basis functions in

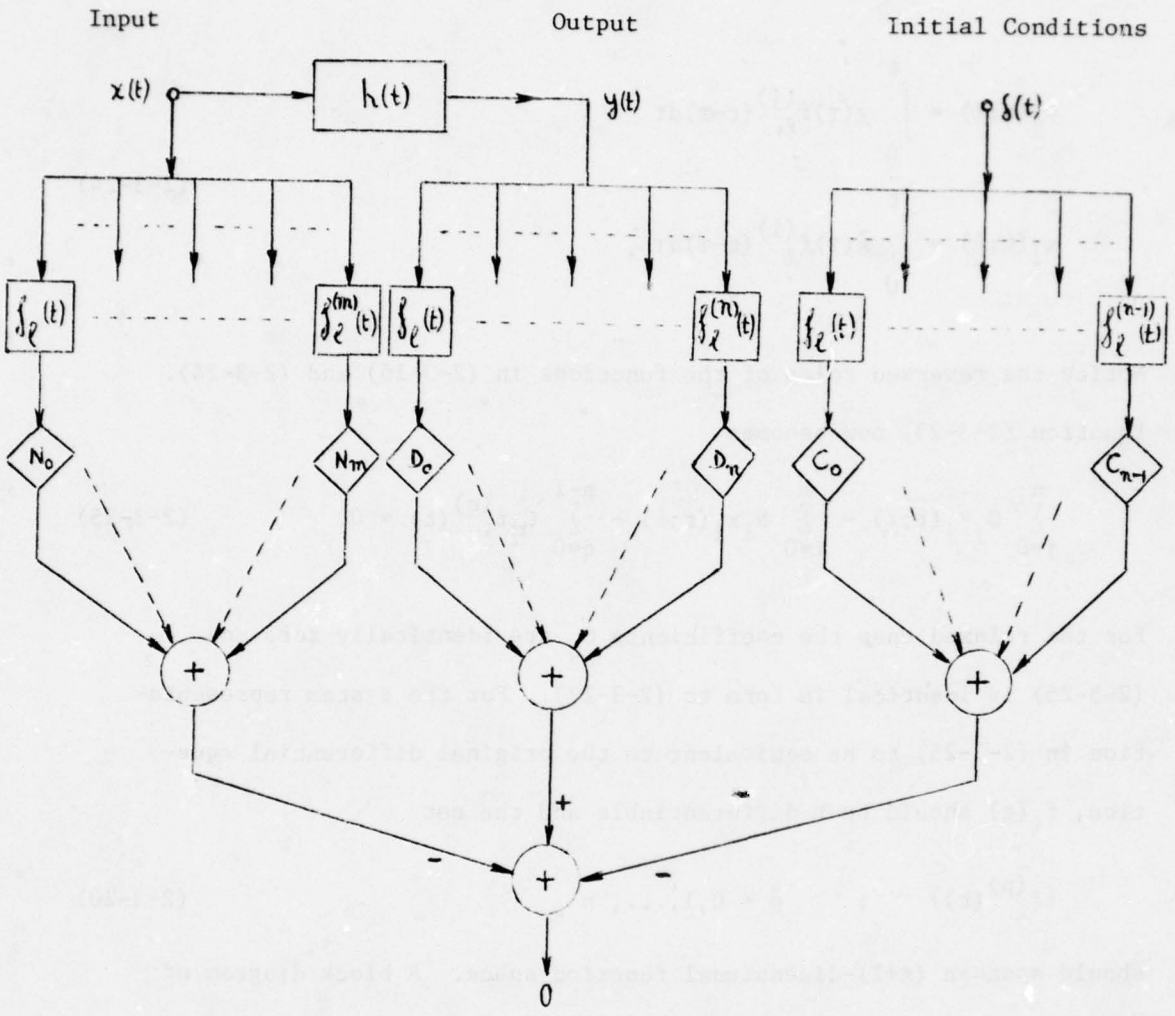

Fig. 2-3-3. Block diagram of (2-3-25).

(2-1-1). Because the output is the impulse response, we are dealing with the homogeneous case. Hence, it is necessary to treat only the output signal. Any space-invariant linear operators which generate a suitable function $f_\ell(t)$ may be used. The coefficients D_j can be determined by using one of the techniques in Appendix A to construct from the (r+1)-basis set

$$\{y_j(t;\ell)\} \qquad j = 0, \ldots, r$$

a set of (r+1) homogeneous linear equations in the unknowns D_j. The next step is to determine the value of n, as discussed earlier in this section. The linear equations can then be reduced to n non-homogeneous equations by selecting D_o equal to unity. The coefficients D_j are used to write the characteristic equation of the system from which the poles are extracted. The resulting n complex exponential time functions are then used to fit the output record y(t) to determine the residues A_{ij} in (2-3-27). Knowledge of the residues and poles is sufficient to determine the coefficients N_i.

Previous techniques described in the literature can be interpreted in this context. For example, the differential operator is used in [23], [24]. This procedure is usually applied to idealized synthesis problems and is impractical for the identification case where measured records are involved. References [25], [26] make use of the time-reverse integral operator given in (2-1-7). For finite records truncation errors are incurred. This error can be reduced by using a suitably long interval, as shown in Section 2.2.

A nonrelaxed system with a general input x(t) is now considered. The time response is the inverse Laplace transform of (1-3-6). This results in

$$y(t) = \sum_{i=1}^{k} \sum_{j=1}^{m_i} B_{ij} t^{j-1} e^{S_i t} + \int_0^t x(t-\tau)\left[\sum_{i=1}^{k} \sum_{j=1}^{m_i} A_{ij} \tau^{j-1} e^{S_i \tau}\right] d\tau \qquad (2\text{-}3\text{-}28)$$

where the coefficients B_{ij} are functions of the coefficients C_q, which are, in turn, functions of the initial conditions and the coefficients D_j and N_i. From the point of view of (2-3-19), it is of interest to

identify the 2n + m + 1 parameters

$$\{D_j; N_i; C_q\} \quad ; \quad \begin{matrix} j = 1,\ldots, n \\ i = 0,\ldots, m \\ q = 0,\ldots, n-1 \end{matrix} . \tag{2-3-29}$$

The response in (2-3-28) can be interpreted as the sum of two responses. Let

$$h_I(t) = \begin{cases} \sum_{i=1}^{k} \sum_{j=1}^{m_i} B_{ij} t^{j-1} e^{S_i t} & ; \quad t \geq 0 \\ 0 & ; \quad t < 0. \end{cases} \tag{2-3-30}$$

Hence, one of the responses is the response of a relaxed system with impulse response $h_I(t)$ to a unit impulse. The second response is the response of a relaxed system with impulse response h(t), as given in (2-3-1), to the input x(t). This interpretation is illustrated in Fig. 2-3-4. Notice that both $h_I(t)$ and h(t) utilize the same basis functions given in (2-1-1).

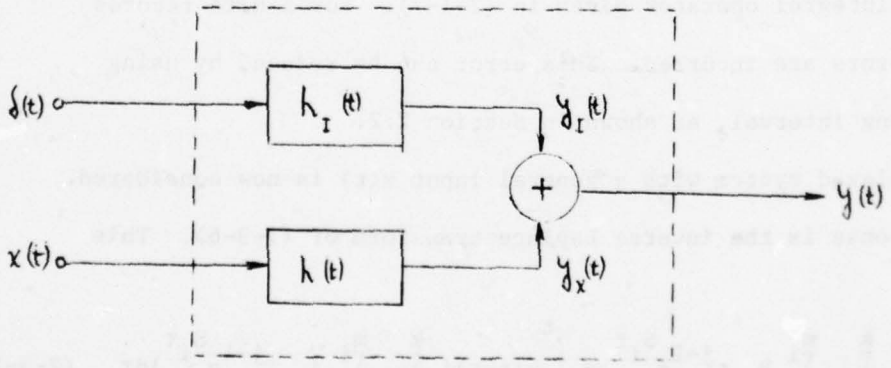

Fig. 2-3-4. Interpretation of (2-3-28).

Identification of the system requires generation of the set of functions

$$\{f_{\ell}^{(q)}(t);\ y_j(t;\ell);\ x_i(t;\ell)\} \quad ; \quad \begin{matrix} q = 0, \ldots, r \\ j = 0, \ldots, r \\ i = 0, \ldots, r. \end{matrix} \qquad (2\text{-}3\text{-}31)$$

The coefficients in (2-3-29) can be determined by using one of the techniques in Appendix A to construct from the (3r+3)-basis set of (2-3-31) a set of (3r + 3) homogeneous linear equations in the unknown coefficients. The next step is to determine the value of n, as discussed earlier in this section. It is unnecessary to check the functions $f_{\ell}^{(q)}(t)$ for linear independence because they are chosen to be linearly independent, as explained in conjunction with (2-3-26). In general, the coefficients C_q are not of interest because they depend on initial conditions which are input dependent. If desirable, the (3r + 3) equations can be reduced to a set of (2r + 2) equations by means of a systematic elimination. The remaining equations can then be solved for the coefficients D_j and N_i.

Thus far, the identification approach has utilized operators which preserve the numerator and denominator polynomial coefficients of the linear system rational transfer function (i.e., the coefficients D_j and N_i of the differential equation). This is not necessary. Operators which do not preserve these coefficients can be used provided a transformation can be determined which enables the original differential equation coefficients to be obtained from the new coefficients. This results in a much larger class of operators than those previously discussed.

In analogy with Fig. 2-3-3, consider the block diagram of Fig. 2-3-5. The impulse response of the filters in the filter banks of Fig. 2-3-5 are no longer required to be successive derivatives of each other as was the case in Fig. 2-3-3. In fact, it is not even required that $f_k(t)$; $k = 0, \ldots, n$ be differentiable. The coefficients

$$\{\hat{D}_j;\ \hat{N}_i;\ \hat{C}_q\}\ ; \qquad \begin{matrix} j = 0, \ldots, n \\ i = 0, \ldots, m \\ q = 0, \ldots, n-1 \end{matrix} \tag{2-3-32}$$

are chosen to satisfy the constraint

$$\sum_{j=0}^{n} \hat{D}_j F_j(S)Y(S) - \sum_{i=0}^{m} \hat{N}_i F_i(S)X(S) - \sum_{q=0}^{n-1} \hat{C}_q F_q(S) = 0 \tag{2-3-33}$$

where $F_k(S)$ is the Laplace transform of $f_k(t)$. The system identification can be based upon (2-3-33) provided a transformation can be developed between the "hatted" coefficients of (2-3-32) and the "unhatted" coefficients of (2-3-29). Of course, the block diagram of Fig. 2-3-5 reduces to that in Fig. 2-3-3 when $f_k(t) = f_\ell^{(k)}(t)$.

For this purpose, consider the mapping of variables

$$F_k(S) = \nu^k \text{ where } S = F_k^{-1}(\nu^k) \tag{2-3-34}$$

and a unique inverse is assumed to exist. (Multiple-valued inverses are permitted provided a meaningful unique inverse can be defined.) Use of (2-3-34) in (2-3-33) results in

$$\sum_{j=0}^{n} \hat{D}_j \nu^j Y[F_j^{-1}(\nu^j)] - \sum_{i=0}^{m} \hat{N}_i \nu^i X[F_i^{-1}(\nu^i)] - \sum_{q=0}^{n-1} \hat{C}_q \nu^q = 0. \tag{2-3-34}$$

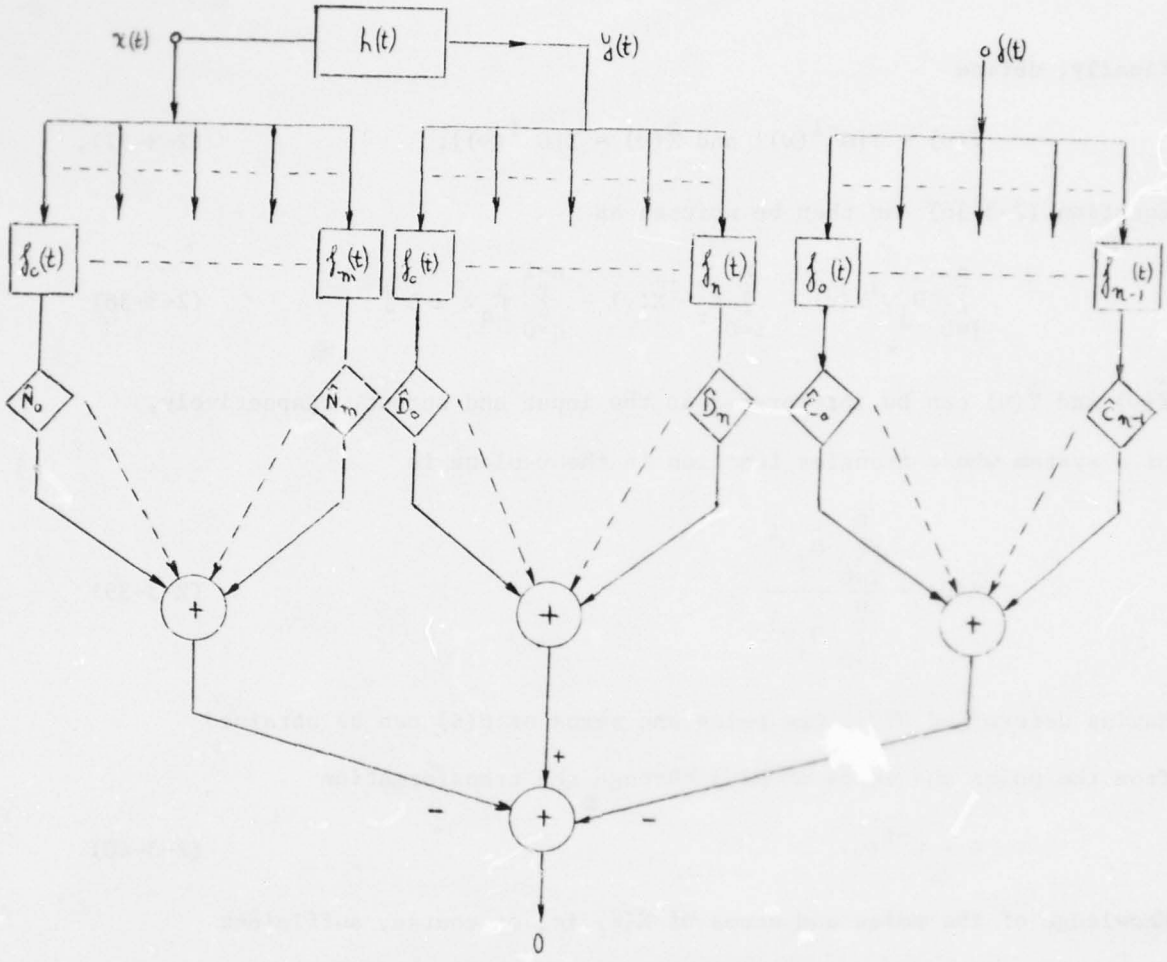

Fig. 2-3-5. Block diagram of (2-3-33) where $F_k(S)$ is the Laplace transform of $f_k(t)$.

In general, the desired transformation between the coefficients is difficult to obtain. The situation is simplified for the particular class of mappings

$$F_k(S) = [G(S)]^k = \nu^k \quad \text{where } S = G^{-1}(\nu). \tag{2-3-35}$$

Substitution of (2-3-35) into (2-3-33) yields

$$\sum_{j=0}^{n} \hat{D}_j \nu^j Y[G^{-1}(\nu)] - \sum_{i=0}^{m} \hat{N}_i \nu^i X[G^{-1}(\nu)] - \sum_{q=0}^{n-1} \hat{C}_q \nu^q = 0 . \tag{2-3-36}$$

Finally, define

$$\hat{Y}(\nu) = Y[G^{-1}(\nu)] \text{ and } \hat{X}(\nu) = X[G^{-1}(\nu)]. \qquad (2\text{-}3\text{-}37).$$

Equation (2-3-36) can then be written as

$$\sum_{j=0}^{n} \hat{D}_j \nu^j \hat{Y}(\nu) - \sum_{i=0}^{m} \hat{N}_i \nu^i \hat{X}(\nu) - \sum_{q=0}^{n-1} \hat{C}_q \nu^q = 0 . \qquad (2\text{-}3\text{-}38)$$

$\hat{X}(\nu)$ and $\hat{Y}(\nu)$ can be interpreted as the input and output, respectively, of a system whose transfer function in the ν-plane is

$$\hat{H}(\nu) = \frac{\sum_{i=0}^{m} \hat{N}_i \nu^i}{\sum_{j=0}^{n} \hat{D}_j \nu^j} . \qquad (2\text{-}3\text{-}39)$$

Having determined $\hat{H}(\nu)$, the poles and zeros of H(S) can be obtained from the poles and zeros of $\hat{H}(\nu)$ through the transformation

$$S = G^{-1}(\nu). \qquad (2\text{-}3\text{-}40)$$

Knowledge of the poles and zeros of H(S) is, of course, sufficient to construct the numerator and denominator polynomials and, therefore, the coefficients N_i and D_j.

As a final point, the mapping of (2-3-35) suggests that the block diagram realization of (2-3-33) is more efficiently realized through the cascade connections shown in Fig. 2-3-6.

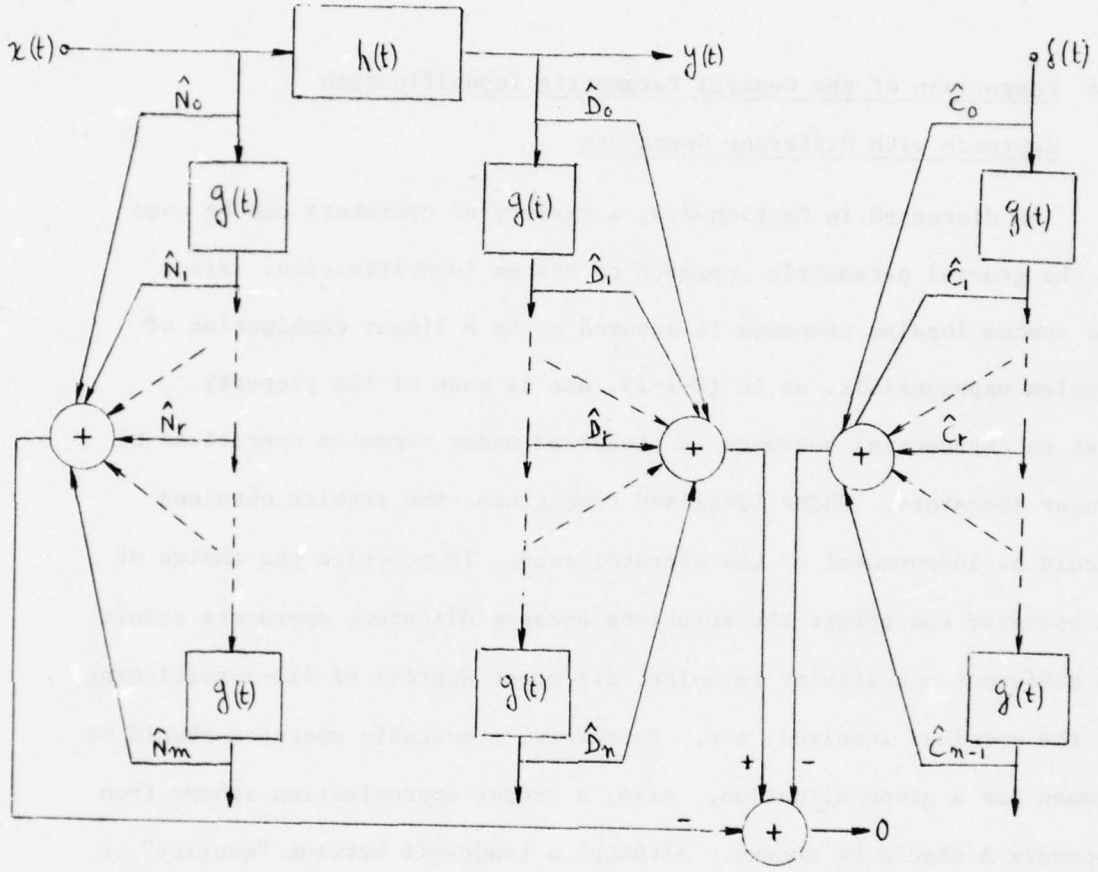

Fig. 2-3-6. Preferred block diagram of (2-3-33) when $F_k(S) = [G(S)]^k$.

2.4 Comparison of the General Parametric Identification Approach with Different Operators

As discussed in Section 2.3, a variety of operators can be used in the general parametric approach to system identification. Since the system impulse response is assumed to be a linear combination of complex exponentials, as in (2-1-1), use is made of the property that an exponential subspace is preserved under repeated operations of linear operators. Under idealized conditions, the results obtained should be independent of the operator used. In practice the choice of an operator can affect the solutions because different operators result in different sensitivity to noise, different degrees of ill-conditioning of the matrices involved, etc. Therefore, a suitable operator should be chosen for a given situation. Also, a proper approximation scheme from Appendix A should be chosen. Although a trade-off between "quality" of the identification and ease of implementation of the approximation scheme usually exists, in general, an increase in computational complexity does not guarantee an increase in quality.

We start by first introducing a noiseless ideal example where the operations are performed analytically. The system is assumed to be nonrelaxed (i.e., an unknown excitation is assumed to exist before the identification procedure begins). In the initial problem the input is assumed to be exponential. Later, an input of a non-exponential type is employed. Also, noise is introduced at which time the identification is carried out entirely numerically.

Example 2-4-1

The system to be identified is shown in Fig. 2-4-1. Let its impulse response be given by

$$h(t) = \begin{cases} 2e^{-t}\cos t; & t \geq 0 \\ 0 \quad ; & t < 0 \end{cases} = \begin{cases} e^{(-1+j)t} + e^{(-1-j)t} \; ; & t \geq 0 \\ 0 \quad ; & t < 0 \end{cases} \tag{2-4-1}$$

The probing signal for the identification is chosen to be

$$x(t) = \begin{cases} e^{-2t} \; ; \; t \geq 0 \\ 0 \quad ; \; t < 0 \end{cases} \tag{2-4-2}$$

If the system had been relaxed at $t = 0$, the output would be

$$y_x(t) = \begin{cases} e^{-t}(\cos t + \sin t) - e^{-2t} \; ; & t \geq 0 \\ 0 \quad ; & t < 0 \end{cases}$$

$$= \begin{cases} \frac{1}{2}\left[(1-j)e^{(-1+j)t} + (1+j)e^{(-1-j)t}\right] - e^{-2t}; & t \geq 0 \\ 0 \quad ; & t < 0 \end{cases} \tag{2-4-3}$$

However, the system is assumed to be non-relaxed at $t = 0$. Assume its response due to the non-zero initial conditions results in

$$y_I(t) = \begin{cases} e^{-t}(\cos t - \sin t) \; ; & t \geq 0 \\ ? \quad ; & t < 0 \end{cases}$$

$$= \begin{cases} \frac{1}{2}\left[(1+j)e^{(-1+j)t} + (1-j)e^{(-1-j)t}\right]; & t \geq 0 \\ ? \quad ; & t < 0 \end{cases} \tag{2-4-4}$$

Hence, the overall output as a result of the response to $x(t)$ and the

initial conditions is given by

$$y(t) = y_x(t) + y_I(t) = \begin{cases} 2e^{-t}\cos t - e^{-2t} & ; \ t \geq 0 \\ ? & t < 0 \end{cases} \tag{2-4-5}$$

$$\text{unknown input for } t<0 = \begin{cases} e^{(-1+j)t} + e^{(-1-j)t} - e^{-2t} & ; \ t \geq 0 \\ ? & ; \ t < 0. \end{cases}$$

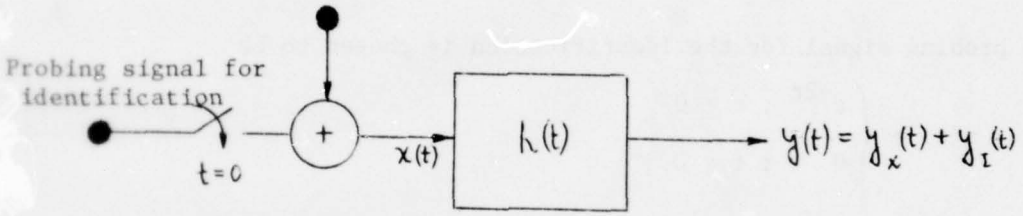

Fig. 2-4-1. A non-relaxed system to be identified.

Several different operators are used to solve this example. In each case the input and output are given as in (2-4-2) and (2-4-5), respectively. With the information provided, the problem is to identify the system.

For purpose of illustration, we begin by taking advantage of the fact that x(t) is exponential. Hence, it can be included within a modified system which is excited by an impulse as presented in Fig. 2-4-2. The object now is to determine the modified impulse response $h_m(t)$ from which h(t) can be developed. The solution is checked by noting that $h_m(t)$ should be identical to y(t).

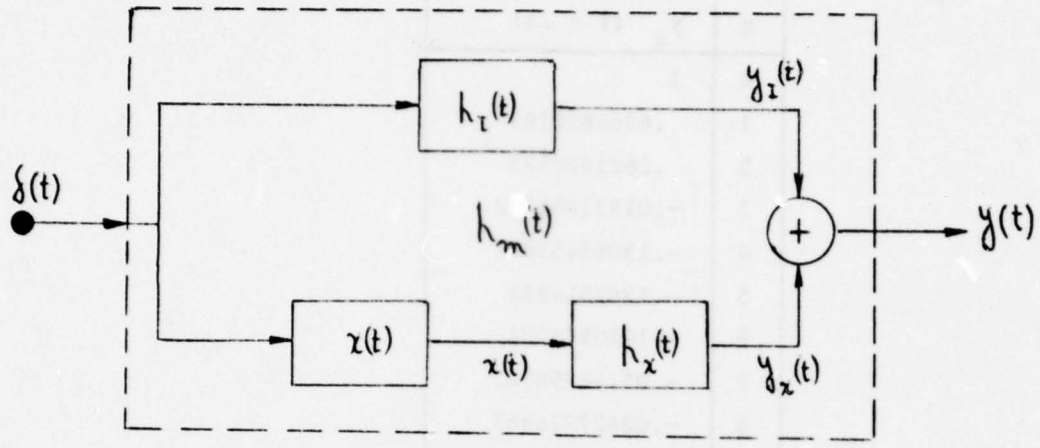

Fig. 2-4-2. The modified system $h_m(t)$.

Case 1 - The original Prony method

First we evaluate the signal at several points as given in Table 2-4-1. This implies that a sampled version of the given data is used. The sampling increment T has been chosen properly to omit the occurrence of multiple Riemann surfaces. The sampled version of the general linear combination of exponentials, as given in (2-1-2), is

$$y_q = y(t_q) = \sum_{i=1}^{k} \sum_{\ell=1}^{m_i} A_{i\ell} (Tq)^{\ell-1} e^{S_i Tq} = \sum_{i=1}^{k} \sum_{\ell=1}^{m_i} B_{i\ell} q^{\ell-1} z_i^q \qquad (2\text{-}4\text{-}6)$$

where $q = 0, 1, 2, \ldots$

$$B_{i\ell} = A_{i\ell} T^{\ell-1} \qquad (2\text{-}4\text{-}7)$$

$$z_i = e^{S_i T} .$$

q	y_q (T = .5)
0	1
1	.6966820193
2	.2621969375
3	-.01821986209
4	-.1309543389
5	-.1382616922
6	-.1010564004
7	-.05746896525
8	-.02427926367
9	-.004806869416
10	.003777201613

Table 2-4-1

With reference to (2-3-33) and (2-3-35), a cascade of shift operators in the sampled data is equivalent to the mapping

$$G(S) = e^{ST} \quad \text{and} \quad F_k(S) = [e^{ST}]^k = z^k \tag{2-4-8}$$

(the variable z is used in place of ν, to conform with the usual notation for this particular mapping.) The equivalent system of Fig. 2-4-2 is then characterized by the homogeneous equation

$$\sum_{j=0}^{n} D_j e^{STj} Y(S) = 0. \tag{2-4-9}$$

However,

$$\mathcal{L}^{-1}\{e^{STj} Y(S)\} = y(t + jT) \quad .$$

This results in the time-domain equation

$$\sum_{j=0}^{n} \hat{D}_j \, y(t + jT) = 0. \tag{2-4-10}$$

Let $y(jT) = y_j$. For t=0, the above equation becomes

$$\sum_{j=0}^{n} \hat{D}_j y_j = 0. \tag{2-4-11}$$

Equation (2-4-11) may be rewritten as

$$\sum_{j=1}^{n} \hat{D}_j y_j = -y_0 \quad \text{where } \hat{D}_0 = 1. \tag{2-4-12}$$

It is interesting to note that

$$y_n = -\sum_{j=0}^{n-1} \hat{D}_j y_j \qquad \text{where } \hat{D}_n = 1 \tag{2-4-13}$$

serves as an extrapolation scheme.

The first step is to determine the value of n. To start we set r = 1 and check the singularity of

$$M_1 = \begin{bmatrix} y_0 & y_1 \\ y_1 & y_2 \end{bmatrix} = \begin{bmatrix} 1 & .6966820193 \\ .6966820193 & .2621969375 \end{bmatrix}. \tag{2-4-14}$$

The computed value of the determinant is

$$\det. M_1 = -.2231688985. \tag{2-4-15}$$

Since M_1 is nonsingular, we set r = 2. The corresponding matrix is

$$M_2 = \left[\begin{array}{cc:c} y_0 & y_1 & y_2 \\ y_1 & y_2 & y_3 \\ \hdashline y_2 & y_3 & y_4 \end{array}\right] = \begin{bmatrix} 1 & .6966820193 & .2621969375 \\ .6966820193 & .2621969375 & -.01821986209 \\ .2621969375 & -.01821986209 & -.1309543389 \end{bmatrix}. \tag{2-4-16}$$

Checking the singularity of M_2, it is found that

$$\det. M_2 = .004211290373. \tag{2-4-17}$$

M_2 is also non-singular. Hence M_3 is checked for singularity. This time

$$\det.\ M_3 = \det. \left[\begin{array}{c|c|c|c} y_0 & y_1 & y_2 & y_3 \\ \hline y_1 & y_2 & y_3 & y_4 \\ \hline y_2 & y_3 & y_4 & y_5 \\ \hline y_3 & y_4 & y_5 & y_6 \end{array}\right] = 0 . \qquad (2\text{-}4\text{-}18)$$

Having determined that M_3 is singular, the order of the system is established at n = 3. We now set $\hat{D}_0$ equal to unity and solve for $\hat{D}_1$, $\hat{D}_2$, $\hat{D}_3$ using the following set of equations:

$$\begin{bmatrix} y_1 & y_2 & y_3 \\ y_2 & y_3 & y_4 \\ y_3 & y_4 & y_5 \end{bmatrix} \begin{bmatrix} \hat{D}_1 \\ \hat{D}_2 \\ \hat{D}_3 \end{bmatrix} = - \begin{bmatrix} y_0 \\ y_1 \\ y_2 \end{bmatrix} . \qquad (2\text{-}4\text{-}19)$$

The solution to (2-4-19) is

$$\begin{bmatrix} \hat{D}_1 \\ \hat{D}_2 \\ \hat{D}_3 \end{bmatrix} = \begin{bmatrix} -5.612059902 \\ 10.58438618 \\ -7.389056099 \end{bmatrix} . \qquad (2\text{-}4\text{-}20)$$

Knowledge of the coefficients is adequate to obtain the characteristic equation of the difference equation in (2-4-11). In particular, the characteristic equation is

$$\hat{D}_0 + \hat{D}_1 z + \hat{D}_2 z^2 + \hat{D}_3 z^3 = 0 . \qquad (2\text{-}4\text{-}21)$$

The roots of the characteristic equation in the z-phase are

$$\begin{bmatrix} z_1 \\ z_2 \\ z_3 \end{bmatrix} = \begin{bmatrix} .3678794412 + j.0 \\ .5322807302 + j.2907862882 \\ .5322807302 - j.2907862882 \end{bmatrix}. \tag{2-4-22}$$

Using the inverse of the mapping in (2-4-8), we have

$$S = G^{-1}(z) = \frac{1}{T} \ln z. \tag{2-4-23}$$

Hence, the poles of the system in the S-plane are

$$\begin{bmatrix} S_1 \\ S_2 \\ S_3 \end{bmatrix} = \frac{1}{T} \ln \begin{bmatrix} z_1 \\ z_2 \\ z_3 \end{bmatrix} = \begin{bmatrix} -2 + j0 \\ -1 + j1 \\ -1 - j1 \end{bmatrix}. \tag{2-4-24}$$

The natural frequencies in (2-4-24) are identical to those in $y(t) = h_m(t)$ given by (2-4-5). Observe that $(2n+1) = 7$ samples were needed (i.e., y_0 through y_6) in order to establish the order of the system at $n = 3$. On the other hand, $2n = 6$ samples were needed (i.e., y_0 through y_5) in order to determine the coefficients $\hat{D}_1$, $\hat{D}_2$, $\hat{D}_3$ from which the system poles were computed.

In connection with Prony's method, two questions arise: (1) What should be the sampling rate?, (2) How long a data record is needed? The following observations are pertinent:

a) Closely spaced samples give rise to highly dependent sets of linear equations. A measure of the dependence is the magnitude of the determinant of the set of equations. For this example, the

magnitudes of the determinants corresponding to r = 1 and 2 are plotted in Fig. 2-4-3 as a function of the sampling interval T. Note the small magnitudes which occur for small values of T . This is reasonable because the variation in the signal is small for closely spaced samples. A column dependence occurs even if one is willing to use $(n+1)^2$ different samples in the form

$$\begin{bmatrix} y_0 & y_1 & y_2 & \cdots & y_n \\ y_{n_1} & y_{n_1+1} & y_{n_1+2} & \cdots & y_{n_1+n} \\ y_{n_2} & y_{n_2+1} & y_{n_2+2} & & y_{n_2+n} \\ & & & & \\ y_{n_n} & y_{n_n+1} & y_{n_n+2} & \cdots & y_{n_n+n} \end{bmatrix} ; \quad n_n > \cdots > n_2 > n_1 > n.$$

b) Widely spaced samples also give rise to highly ill-conditioned sets of linear equations. Note the small magnitudes which occur for large values of T in Fig. 2-4-3. This arises when dealing with transient waveforms due to the large dynamic range associated with the initial and final samples of the signal. Hence, the final rows and columns are numerically small with the result that the magnitude of the determinant is also small.

c) An optimum sampling interval exists. For example, the curves in Fig. 2-4-3 peak for T ≃ 0.7. By maximizing $|\det. M_1|$ with respect to T, an estimate of the optimum value of the sampling interval can be obtained. Knowledge of this value can also be used to obtain a rough estimate of the system order n. From Section 2.2 it is known

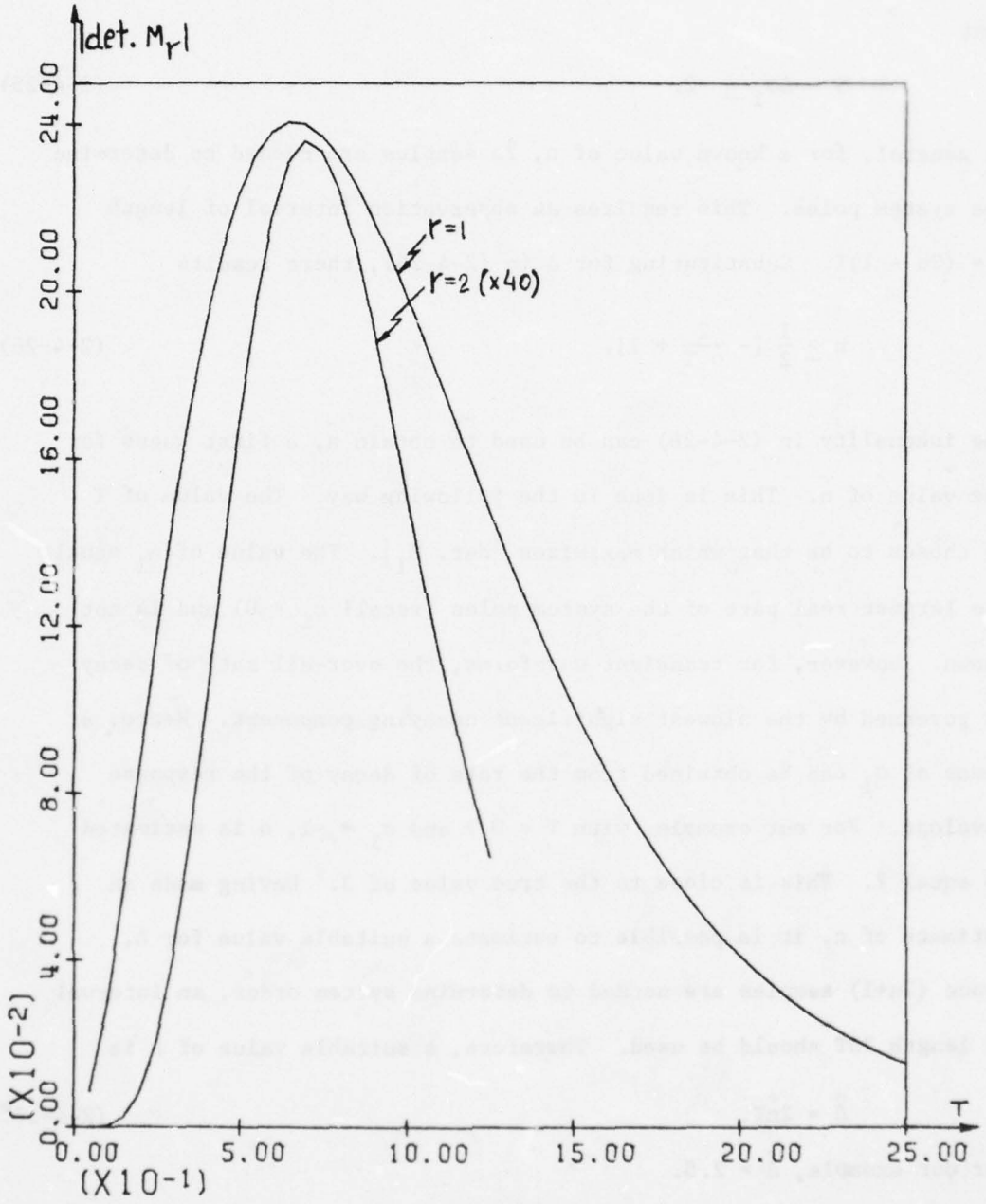

Fig. 2-4-3. Magnitude of the determinants corresponding to r = 1 and 2 as a function of the sampling interval T. The scale for $|\det M_2|$ is 40 times that for $|\det. M_1|$.

that the length of the observation interval, Δ, should be chosen such that

$$\gamma = \Delta\sigma_1 \leq -2. \tag{2-4-25}$$

In general, for a known value of n, 2n samples are needed to determine the system poles. This requires an observation interval of length $\Delta = (2n - 1)T$. Substituting for Δ in (2-4-25), there results

$$n \geq \frac{1}{2}\left[-\frac{2}{\sigma_1 T} + 1\right]. \tag{2-4-26}$$

The inequality in (2-4-26) can be used to obtain $\hat{n}$, a first guess for the value of n. This is done in the following way. The value of T is chosen to be that which maximizes $|\det. M_1|$. The value of σ_1 equals the largest real part of the system poles (recall $\sigma_i < 0$) and is not known. However, for transient waveforms, the over-all rate of decay is governed by the slowest significant decaying component. Hence, a guess of σ_1 can be obtained from the rate of decay of the response envelope. For our example, with $T = 0.7$ and $\sigma_1 = -1$, n is estimated to equal 2. This is close to the true value of 3. Having made an estimate of n, it is possible to estimate a suitable value for Δ. Since (2n+1) samples are needed to determine system order, an interval of length 2nT should be used. Therefore, a suitable value of Δ is

$$\hat{\Delta} = 2\hat{n}T. \tag{2-4-27}$$

For our example, $\hat{\Delta} = 2.8$.

Case 2 - The Overdetermined Prony Method

The basic difference between the overdetermined Prony method [16], [17], [18] and the original Prony method [13] is in the type of approximation scheme utilized. While the former utilizes a pseudo-inverse technique, which is equivalent to the least-square technique, the latter uses an interpolation scheme. (See Appendix A). Let n_1 be greater than n, the order of the system. With reference to (2-4-11), an overdetermined set of equations is given by

$$\begin{bmatrix} y_0 & y_1 & y_2 & \cdots & y_n \\ y_1 & y_2 & y_3 & & y_{n+1} \\ \vdots & & & & \\ y_{n_1} & y_{n_1+1} & y_{n_1+2} & \cdots & y_{n_1+n} \end{bmatrix} \begin{bmatrix} \hat{D}_0 \\ \hat{D}_1 \\ \hat{D}_2 \\ \vdots \\ \hat{D}_n \end{bmatrix} = \begin{bmatrix} 0 \\ 0 \\ \\ \\ \vdots \\ \\ 0 \end{bmatrix} \qquad (2\text{-}4\text{-}28)$$

where $(n_1 + n + 1)$ different samples are used. To solve for the $\hat{D}_i$'s, we premultiply (2-4-28) by the transpose of the rectangular matrix. This yields

$$\begin{bmatrix} \sum_{i=0}^{n-1} y_i^2 & \sum_{i=0}^{n-1} y_i y_{i+1} & \sum_{i=0}^{n-1} y_i y_{i+2} & \cdots \sum_{i=0}^{n-1} y_i y_{i+n} \\ \sum_{i=0}^{n-1} y_{i+1} y_i & \sum_{i=0}^{n-1} y_{i+1}^2 & \sum_{i=0}^{n-1} y_{i+1} y_{i+2} & \cdots \sum_{i=0}^{n-1} y_{i+1} y_{i+n} \\ \vdots & & & \\ \sum_{i=0}^{n-1} y_{i+n} y_i & \sum_{i=0}^{n-1} y_{i+n} y_{i+1} & \sum_{i=0}^{n-1} y_{i+n} y_{i+2} & \cdots \sum_{i=0}^{n-1} y_{i+n}^2 \end{bmatrix} \begin{bmatrix} \hat{D}_0 \\ \hat{D}_1 \\ \hat{D}_2 \\ \vdots \\ \hat{D}_n \end{bmatrix} = \begin{bmatrix} 0 \\ 0 \\ 0 \\ \vdots \\ 0 \end{bmatrix} \quad (2\text{-}4\text{-}29)$$

Equation (2-4-29) can be rewritten as

$$\sum_{i=0}^{n-1} \sum_{\ell=0}^{n} y_{i+k} y_{\ell+i} \hat{D}_\ell = 0 \quad ; \quad k = 0,1,2, \ldots,n. \qquad (2\text{-}4\text{-}30)$$

With $\hat{D}_0$ arbitrarily set to unity, (2-4-30) can be rewritten as

$$\sum_{i=0}^{n-1-1} \sum_{\ell=1}^{n} y_{i+k} y_{\ell+i} \hat{D}_\ell = - \sum_{i=0}^{n-1-1} y_{i+k} y_i \qquad k = 0,1,2,\ldots, n-1. \qquad (2\text{-}4\text{-}31)$$

This is of the same form as the least-squares equation (A-1-7). As with the original Prony method, the square matrix in (2-4-29) has a very small determinant for closely spaced samples (i.e., a highly linearly dependent set of equations results). For instance, a record of y(t) of length 5 with T = .05 (i.e., 101 samples) yields the following determinant for r = 2:

$$\det. \begin{bmatrix} \sum_{i=0}^{98} y_i^2 & \sum_{i=0}^{98} y_i y_{i+1} & \sum_{i=0}^{98} y_i y_{i+2} \\ \sum_{i=0}^{98} y_{i+1} y_i & \sum_{i=0}^{98} y_{i+1}^2 & \sum_{i=0}^{98} y_{i+1} y_{i+2} \\ \sum_{i=0}^{98} y_{i+2} y_i & \sum_{i=0}^{98} y_{i+2} y_{i+1} & \sum_{i=0}^{98} y_{i+2}^2 \end{bmatrix}$$

$$= \det. \begin{bmatrix} 11.49921692 & 10.97923768 & 10.42420972 \\ 10.97923768 & 10.4992277 & 9.984006238 \\ 10.42420972 & 9.984006238 & 9.508731645 \end{bmatrix}$$

$$= 2.029682836 \cdot 10^{-6}. \qquad (2\text{-}4\text{-}32)$$

This is an extremely small value. In general, oversampling results in small determinant values.

Oversampling does not offer any advantage even with more widely spaced samples. In the original Prony method, previously discussed, it was pointed out that a sampling interval of T = 0.7 is desirable. For a modest oversampling ratio of $R = n_1/(r + 1) = 5$, $n_1 = 15$ when $r = 2$. The corresponding record length is $\Delta = 2n_1T = 21$. As pointed out in Section 2.2, a record length of 2 is adequate for $\sigma_1 = -1$. Hence, the record length of 5 used in conjunction with (2-4-32) already represented a very long record. The record length of 21 offers negligibly more information than was contained in the record length of 5 due to the exponential nature of the signal (i.e., $e^{21\sigma_1} << e^{5\sigma_1} << e^{0}$). Hence, negligible improvement results from overdetermining the problem in this way. Since the lower rows in the rectangular matrix of (2-4-28)

are extremely small, they contribute negligibly to the inner products in (2-4-29). Thus, the inner products obtained for the oversampled case are approximately the same as those obtained by using the least-squares technique with the square matrix of the original Prony method. In effect, the usual overdetermined Prony does not offer any advantage over the original Prony method.

By introducing a delay, it is possible to achieve an advantage over the original Prony method. This newly proposed approach is discussed next.

Case 3 - The Delay Operator Method

Once again, let n_1 be greater than the system order n. Consider the overdetermined set of equations in (2-4-33).

$$\begin{bmatrix} y_0 & y_j & y_{2j} & \cdots & y_{nj} \\ y_1 & y_{j+1} & y_{2j+1} & \cdots & y_{nj+1} \\ y_2 & y_{j+2} & y_{2j+2} & \cdots & y_{nj+2} \\ \vdots & & & & \\ y_{n_1} & y_{j+n_1} & y_{2j+n_1} & \cdots & y_{nj+n_1} \end{bmatrix} \begin{bmatrix} \hat{D}_0 \\ \hat{D}_1 \\ \hat{D}_2 \\ \vdots \\ \hat{D}_n \end{bmatrix} = \begin{bmatrix} 0 \\ 0 \\ \vdots \\ 0 \end{bmatrix} . \qquad (2\text{-}4\text{-}33)$$

Observe that the original data record must be of length $\Delta = (n_1 + nj)T_d$ where T_d denotes the sampling interval. Each column of the rectangular matrix is composed of $(n_1 + 1)$ consecutive time samples. However, the significant difference from (2-4-28) is that consecutive columns in (2-4-33) are advanced by j time samples. When j = 1, (2-4-33) reduces to (2-4-28). Each column can be interpreted as a basis function. The

matrix equations can then be viewed as a linear combination of the basis functions. Whereas the basis functions in (2-4-28) do not change very much from one to the next, they are drastically different in (2-4-33). In this approach, T_d is chosen to be as small as desired. The value of j is then determined from the relation

$$jT_d = T \tag{2-4-34}$$

where T is the preferred sampling interval of the original Prony method. Note that $n_1 = (\Delta/T_d) - nj$.

As before, the $\hat{D}_i$'s are obtained by premultiplying (2-4-33) by the transpose of the rectangular matrix. With $\hat{D}_0 = 1$, we obtain the n equations

$$\sum_{i=0}^{n_1-1} \sum_{\ell=1}^{n} y_{i+k} y_{\ell j+i} \hat{D}_\ell = - \sum_{i=0}^{n_1-1} y_{i+k} y_i \quad ; \quad k = 0,1,2, \ldots, n-1. \tag{2-4-35}$$

We now illustrate the advantage of this approach. As in cases 1 and 2, let the record length be $\Delta = 5$. Let the sampling interval T_d equal .05 (this was also the sampling interval used in Case 2). Hence, 101 samples are available as in Case 2. From Case 1 it is known that the preferred value of T is 0.7. Hence, j = 14 and $n_1 = 58$. For r = 2, the following determinant is obtained when checking for the system order:

$$\det. \begin{bmatrix} \sum_{i=0}^{58} y_i^2 & \sum_{i=0}^{58} y_i y_{14+i} & \sum_{i=0}^{58} y_i y_{28+i} \\ \sum_{i=0}^{58} y_{14+i} y_i & \sum_{i=0}^{58} y_{14+i}^2 & \sum_{i=0}^{58} y_{14+i} y_{28+i} \\ \sum_{i=0}^{58} y_{28+i} y_i & \sum_{i=0}^{58} y_{28+i} y_{14+i} & \sum_{i=0}^{58} y_{28+i}^2 \end{bmatrix} = \tag{2-3-36}$$

$$\det. \begin{bmatrix} 11.40028809 & 3.418188405 & -1.116650923 \\ 3.418188405 & 1.731065907 & .1945935105 \\ -1.116650923 & .1945935105 & .5143890218 \end{bmatrix} = .06549016746 .$$

From Fig. 2-4-3, the value of the determinant for the original Prony method (r = 2) is calculated to be approximately .0039. From (2-4-32), the value for the overdetermined Prony method (r = 2) is approximately .000002. These values are one order of magnitude and four orders of magnitude smaller, respectively, than the value in (2-4-36). A definite improvement is noted for this case without having expended any more computational effort than in Case 2. A plot of the continuous basis functions (i.e., $y(t)$, $y(t + 0.7)$, $y(t + 1.4)$, and $y(t + 2.10)$ is given in Fig. 2-4-4 for $t > 0$. Note that these basis functions correspond to successive columns of the square matrix in (2-4-33) where $y_{kj+i} = y(t + (kj+i)T_d)$ is evaluated at $t = 0$. These basis functions involve the advance operator exp [ST] of (2-4-8).

Solution of (2-4-35) for the coefficients yields

$$\begin{bmatrix} \hat{D}_1 \\ \hat{D}_2 \\ \hat{D}_3 \end{bmatrix} = \begin{bmatrix} -7.135606018 \\ 16.54686248 \\ -16.44464677 \end{bmatrix} . \qquad (2\text{-}4\text{-}37)$$

The characteristic equation of the corresponding difference equation is

$$\hat{D}_0 + \hat{D}_1 z + \hat{D}_2 z^2 + \hat{D}_3 z^3 = 0.$$

Solving for the roots in the z-plane, performing the transformation to the S-plane results in

$$\begin{bmatrix} S_1 \\ S_2 \\ S_3 \end{bmatrix} = (jT_d)^{-1} \ln \begin{bmatrix} z_1 \\ z_2 \\ z_3 \end{bmatrix} = \begin{bmatrix} -2 + j0 \\ -1 + j1 \\ -1 - j1 \end{bmatrix} . \qquad (2\text{-}4\text{-}38)$$

Once again, the poles of H(S) have been found.

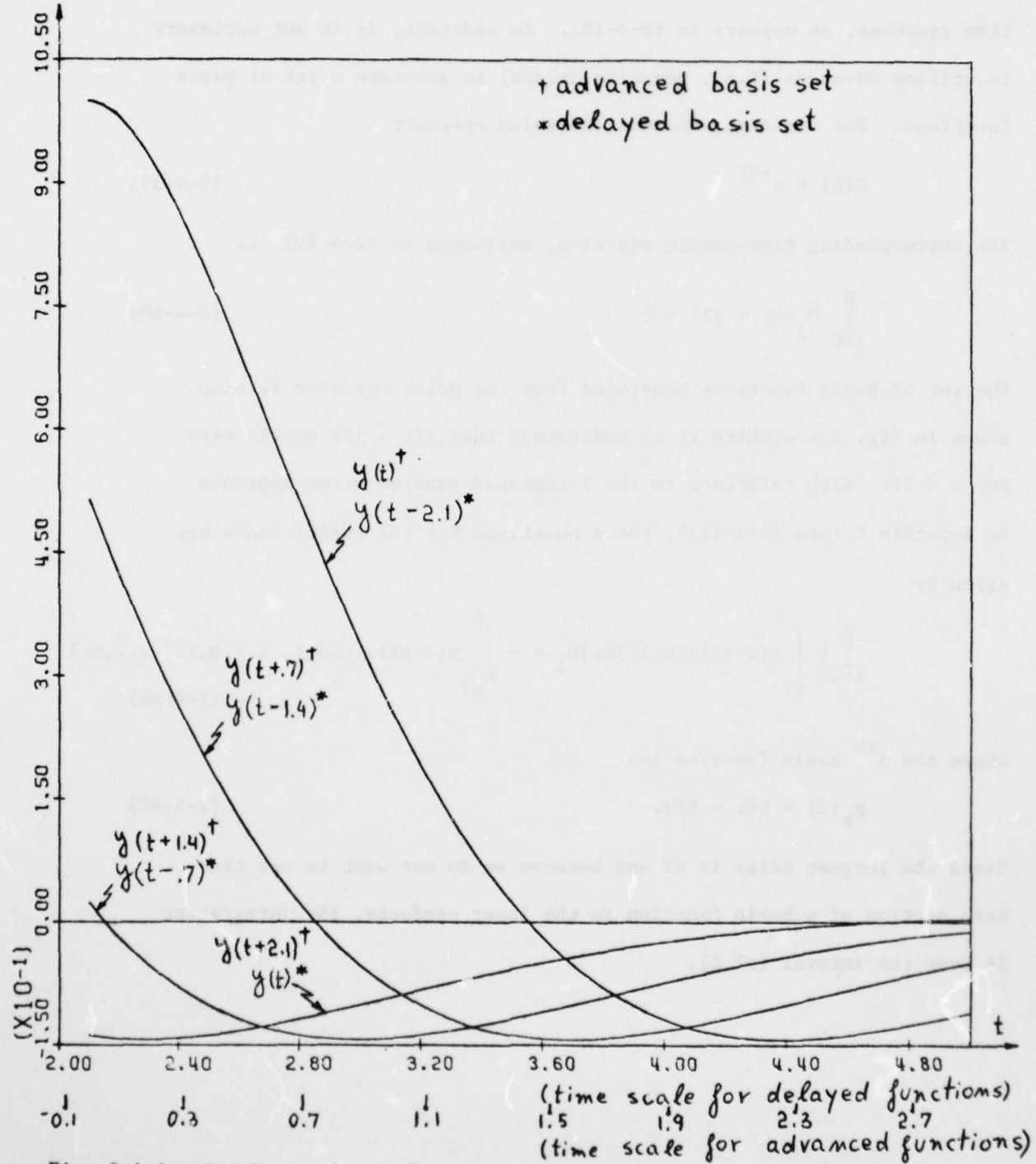

Fig. 2-4-4. Continuous basis functions structured through the delay operator.

Prony's method, and variations thereof, deal with samples of the observed waveform. One could just as well work with the continuous time response, as appears in (2-4-10). In addition, it is not necessary to utilize advances (i.e., negative delays) to generate a set of basis functions. For variety, consider the delay operator

$$G(S) = e^{-ST}. \tag{2-4-39}$$

The corresponding time-domain equation, analogous to (2-4-10), is

$$\sum_{j=0}^{n} \hat{D}_j y(t - jT) = 0. \tag{2-4-40}$$

The set of basis functions generated from the delay operator is also shown in Fig. 2-4-4 where it is understood that $y(t - jT)$ equals zero for $t < jT$. With reference to the integrated-squared-error approach in Appendix A (see (A-1-11)), the n equations for the coefficients are given by

$$\sum_{i=1}^{n} \left[\int_{nT}^{\Delta} y(t-kT)y(t-iT)dt \right] \hat{D}_i = - \int_{nT}^{\Delta} y(t-kT)y(t)dt; \quad k = 0,1,2,\ldots,n-1 \tag{2-4-41}$$

where the k^{th} basis function is

$$g_k(t) = y(t - kT). \tag{2-4-42}$$

Since the largest delay is nT and because we do not want to use the zero portion of a basis function in the inner products, the integration is over the inteval (nT,Δ).

Case 4 - The Reverse Time Integral Operator

The parameters of $h_m(t)$ are now identified using the reverse time integral operator introduced in (2-1-7) to generate a set of basis functions. This operator was first utilized by Carr [25] and then by Jain [26] who developed their approaches from different points of view. The results of this dissertation, however, make clear that the two approaches are essentially the same.

The simplest development of the identification scheme with the reverse time integral operator proceeds from the time-domain version of (2-3-21). Let the operator $f_\ell\{\cdot\}$ consist of an n-fold reverse time integration from ∞ to t. In particular,

$$f_\ell\{\cdot\} = \int_\infty^t \int_\infty^{t_\ell} \cdots \int_\infty^{t_2} \{\cdot\} \prod_{q=1}^{\ell} dt_q$$
$$= \int_\infty^t \frac{(t-\tau)^{\ell-1}}{(\ell-1)!} \{\cdot\}\, d\tau \,. \qquad (2\text{-}4\text{-}43)$$

Carrying out an ℓ-fold integration, where $\ell \geq n$, the time-domain version of (2-3-21) is then given by

$$\sum_{j=0}^{n} D_j \int_\infty^t \frac{(t-\tau)^{\ell-1}}{(\ell-1)!}\, y^{(j)}(\tau)d\tau - \sum_{i=0}^{m} N_i \int_\infty^t \frac{(t-\tau)^{\ell-1}}{(\ell-1)!}\, x^{(i)}(\tau)d\tau$$
$$- \sum_{q=0}^{n-1} C_q \int_\infty^t \frac{(t-\tau)^{\ell-1}}{(\ell-1)!}\, \delta^{(q)}(\tau)d\tau = 0 \qquad (2\text{-}4\text{-}44)$$

where $\delta^{(q)}(t)$ is the singularity function which is the q^{th} derivative of the unit impulse, $\delta(t)$. Since the singularity functions occur at the origin, they are not within the interval of integration and each term

in the summation over the index q is identically zero. Let the ℓ-fold integrations of $y^{(j)}(t)$ and $x^{(i)}(t)$ from ∞ to t be deonted by $y^{(j-\ell)}(t)$ and $x^{(i-\ell)}(t)$, respectively. Equation (2-4-44) can then be written as

$$\sum_{j=0}^{n} D_j \, y^{(j-\ell)}(t) - \sum_{i=0}^{m} N_i \, x^{(i-\ell)}(t) = 0. \qquad (2\text{-}4\text{-}45)$$

Making a change of variables involving the indices, (2-4-45) becomes

$$\sum_{j=0}^{n} D_{n-j} y^{(n-\ell-j)}(t) - \sum_{i=0}^{m} N_{m-i} x^{(m-\ell-i)}(t) = 0. \qquad (2\text{-}4\text{-}46)$$

For ℓ=n, (2-4-46) yields

$$\sum_{j=0}^{n} D_{n-j} y^{(-j)}(t) - \sum_{i=0}^{m} N_{m-i} x^{(m-n-i)}(t) = 0. \qquad (2\text{-}4\text{-}47)$$

Hence, under the reverse time integral operation the coefficients of the differential equation description of the system are preserved in reversed order. Notice that, for a case where only exponential signals are involved, one could arrive at the same conclusion directly from properties (c) and (d) of (2-1-13).

For variety, the generalized integrated-squared-error approach is utilized as the approximation scheme for generating the simultaneous equations involving the coefficients (see Appendix A, (A-1-34)). The values of L and K are chosen to be 2 and 1 respectively (i.e., the coefficients D_j are computed such as to minimize the sum of integrated-squared-errors between the signal and its approximation and the first

time reverse integral of the signal and its approximation). Assuming a system of order r, we may write

$$\sum_{\ell=-1}^{0} \sum_{j=0}^{r} \left[\int_{t_1}^{t_2} y_k^{(\ell)}(t) y_j^{(\ell)}(t)dt \right] D_{r-j} = 0; \quad k=0,1,2,\ldots,r. \tag{2-4-48}$$

In matrix notation, (2-4-48) yields for r=1

$$\begin{bmatrix} \langle y_0^{(-1)}(t), y_0^{(-1)}(t)\rangle & \langle y_0^{(-1)}(t), y_1^{(-1)}(t)\rangle \\ \langle y_1^{(-1)}(t), y_0^{(-1)}(t)\rangle & \langle y_1^{(-1)}(t), y_1^{(-1)}(t)\rangle \end{bmatrix} \begin{bmatrix} D_1 \\ D_0 \end{bmatrix} + \begin{bmatrix} \langle y_0^{(0)}(t), y_0^{(0)}(t)\rangle & \langle y_0^{(0)}(t), y_1^{(0)}(t)\rangle \\ \langle y_1^{(0)}(t), y_0^{(0)}(t)\rangle & \langle y_1^{(0)}(t), y_1^{(0)}(t)\rangle \end{bmatrix} \begin{bmatrix} D_1 \\ D_0 \end{bmatrix} = \begin{bmatrix} 0 \\ 0 \end{bmatrix} \tag{2-4-49}$$

where

$$\langle y_k^{(\ell)}, y_j^{(\ell)} \rangle = \int_{t_1}^{t_2} y_k^{(\ell)}(t) y_j^{(\ell)}(t)dt$$

and

$$y_k^{(\ell)}(t) = y^{(\ell-k)}(t) = \int_{\infty}^{t} \frac{(t-\tau)^{k-\ell-1}}{(k-\ell-1)!} y_0^{(0)}(\tau)d\tau .$$

The function $y_0^{(0)}(t)$ is, of course, identical to y(t) of (2-4-5).

For r=1, the basis set needed is given by

$$\{y^{(0)}(t), y^{(-1)}(t), y^{(-2)}(t)\}. \tag{2-4-50}$$

Hence, applying a time reverse integral operator successively to y(t) in (2-4-5) yields the basis functions

$$y^{(0)}(t) = y(t) = \begin{cases} 2e^{-t}\cos t - e^{-2t}; & t\geq 0 \\ ? & ; \ t<0 \end{cases}$$

$$y^{(-1)}(t) = \int_{\infty}^{t} y^{(0)}(\tau)d\tau = \begin{cases} -e^{-t}(\cos t - \sin t) + \tfrac{1}{2}e^{-2t}; & t\geq 0 \\ ? & ; \ t<0 \end{cases} \tag{2-4-51}$$

$$y^{(-2)}(t) = \int_{\infty}^{t} y^{(-1)}(\tau)d\tau = \begin{cases} -e^{-t}\sin t - 1/4e^{-2t}; & t\geq 0 \\ ? & ; \ t<0 \end{cases}.$$

Let the approximation interval $[T_1, T_2]$ be $[0,5]$. Substituting (2-4-51) into (2-4-49) yields

$$M_1 \begin{bmatrix} D_1 \\ D_0 \end{bmatrix} = \left\{ \begin{bmatrix} .1126700914 & -.03122914547 \\ -.03122914547 & .1905598834 \end{bmatrix} + \begin{bmatrix} .5499617419 & -.1251736779 \\ -.1251736779 & .1126700914 \end{bmatrix} \right\} \begin{bmatrix} D_1 \\ D_0 \end{bmatrix} = \begin{bmatrix} 0 \\ 0 \end{bmatrix}. \quad (2\text{-}4\text{-}52)$$

Computing the deteminant of M_1 results in

$$\det. M_1 = .1764679909. \quad (2\text{-}4\text{-}53)$$

Hence, M_1 is nonsingular. For r=2, it is determined from (2-4-48) that the basis needed is given by

$$\{y^{(0)}, y^{(-1)}, y^{(-2)}, y^{(-3)}\}. \quad (2\text{-}4\text{-}54)$$

The new basis function is

$$y^{(-3)}(t) = \int_{\infty}^{t} y^{(-2)}(\tau)d\tau = \begin{cases} \frac{1}{2}e^{-t}(\cos t + \sin t) + \frac{1}{8}e^{-2t}; & t\geq 0 \\ ? & ; \ t<0. \end{cases} \quad (2\text{-}4\text{-}55)$$

For r=2, the determinant of M_2 is

$$\det. M_2 = \det. \left\{ \begin{bmatrix} \langle y_0^{(-1)}, y_0^{(-1)} \rangle & \langle y_0^{(-1)}, y_1^{(-1)} \rangle & \langle y_0^{(-1)}, y_2^{(-1)} \rangle \\ \langle y_1^{(-1)}, y_0^{(-1)} \rangle & \langle y_1^{(-1)}, y_1^{(-1)} \rangle & \langle y_1^{(-1)}, y_2^{(-1)} \rangle \\ \langle y_2^{(-1)}, y_0^{(-1)} \rangle & \langle y_2^{(-1)}, y_1^{(-1)} \rangle & \langle y_2^{(-1)}, y_2^{(-1)} \rangle \end{bmatrix} + \right.$$

$$\left. \begin{bmatrix} \langle y_0^{(0)}, y_0^{(0)} \rangle & \langle y_0^{(0)}, y_1^{(0)} \rangle & \langle y_0^{(0)}, y_2^{(0)} \rangle \\ \langle y_1^{(0)}, y_0^{(0)} \rangle & \langle y_1^{(0)}, y_1^{(0)} \rangle & \langle y_1^{(0)}, y_2^{(0)} \rangle \\ \langle y_2^{(0)}, y_0^{(0)} \rangle & \langle y_2^{(0)}, y_1^{(0)} \rangle & \langle y_2^{(0)}, y_2^{(0)} \rangle \end{bmatrix} \right\}$$

$$= \det. \left\{ \begin{bmatrix} .1126700914 & -.03122914547 & -.03453295368 \\ -.03122914547 & .1905598834 & -.1952578315 \\ -.03453295368 & -.1952578315 & .241469618 \end{bmatrix} \right. \quad (2\text{-}4\text{-}56)$$

$$\left. + \begin{bmatrix} .5499617419 & -.1251736779 & -.2374113928 \\ -.1251736779 & .1126700914 & -.03122914547 \\ -.2374113928 & -.03122914547 & .1905598834 \end{bmatrix} \right\} = .0005575168764.$$

Hence, M_2 is nonsingular. For r=3, $y^{(-4)}$ has to be added to the basis set. Applying the time reverse operator to $y^{(-3)}$ yields

$$y^{(-4)}(t) = \int_{\infty}^{t} y^{(-3)}(\tau)d\tau = \begin{cases} -\frac{1}{2}e^{-t}\cos t - \frac{1}{16}e^{-2t}; & t \geq 0 \\ ? & t<0. \end{cases} \quad (2\text{-}4\text{-}57)$$

The determinant of M_3 is computed to be det. $M_3 = 0$. Hence, the system order is established at n=3. The basis functions utilized for the GISE approximation are shown in Fig. 2-4-5 over the time interval [0,5].

It is of interest to compare the magnitudes of the determinants which arise in the three separate cases of 1) an ISE approximation to y(t), 2) an ISE approximation to $y^{(-1)}(t)$, and 3) a GISE approximation to both y(t) and $y^{(-1)}(t)$. In the context of the GISE formulation, these cases arise with 1) L=1, K=0, 2) L=1, K=1, and 3) L=2, K=1, respectively. The magnitudes of the determinants for r=1 and 2 are tabulated in Table 2-4-2 for these three cases. Note that case 3 results in larger values of the determinants for the nonsingular matrices and is, therefore, superior to cases 1 and 2.

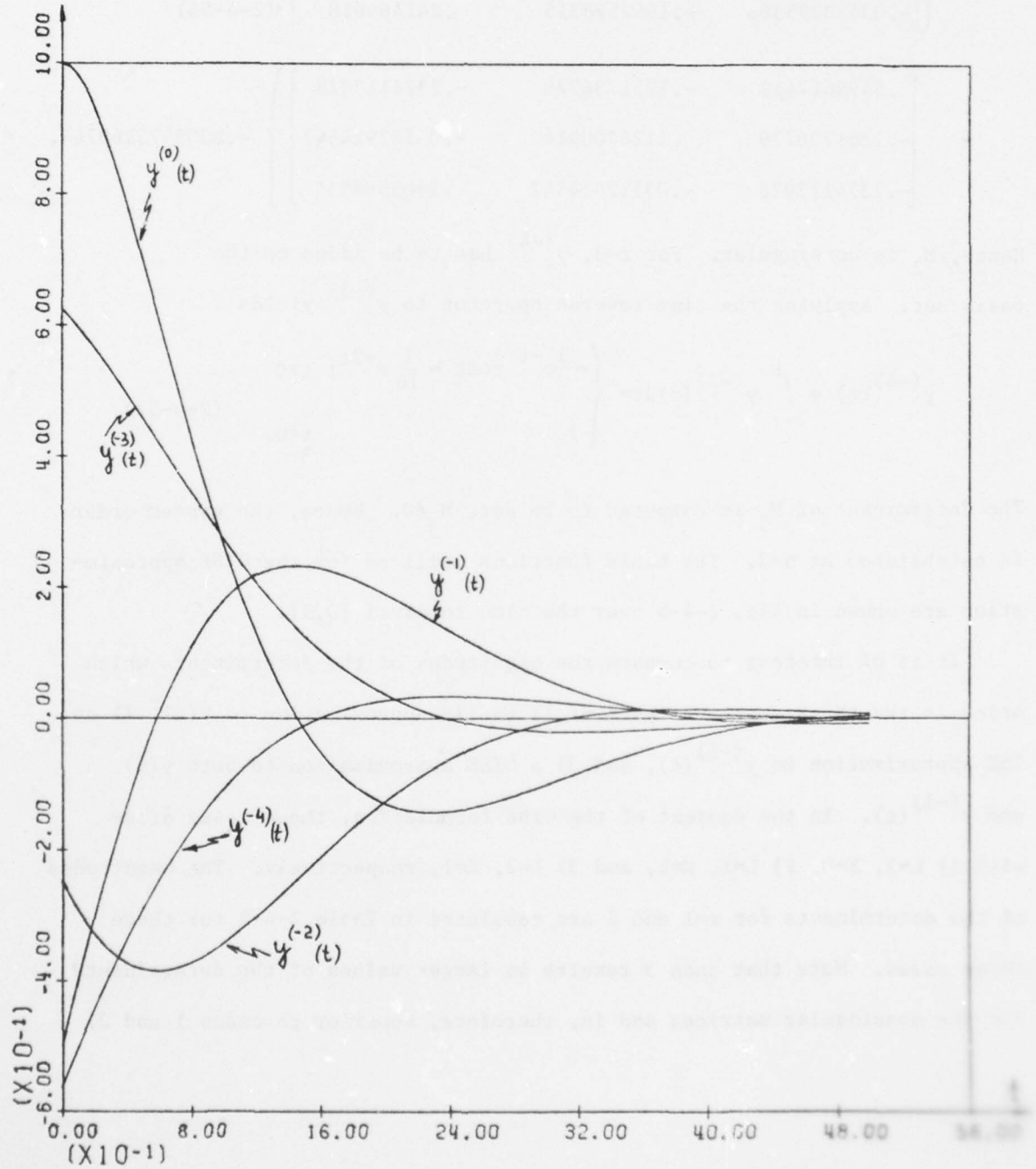

Fig. 2-4-5. Basis functions generated by the reverse time integral operator.

AD-A061 589 SYRACUSE UNIV N Y F/G 12/2
PARAMETRIC IDENTIFICATION OF SYSTEMS VIA LINEAR OPERATORS.(U)
SEP 78 J NEBAT F30602-75-C-0121
UNCLASSIFIED RADC-TR-78-199 NL

2 OF 3
ADA
061589

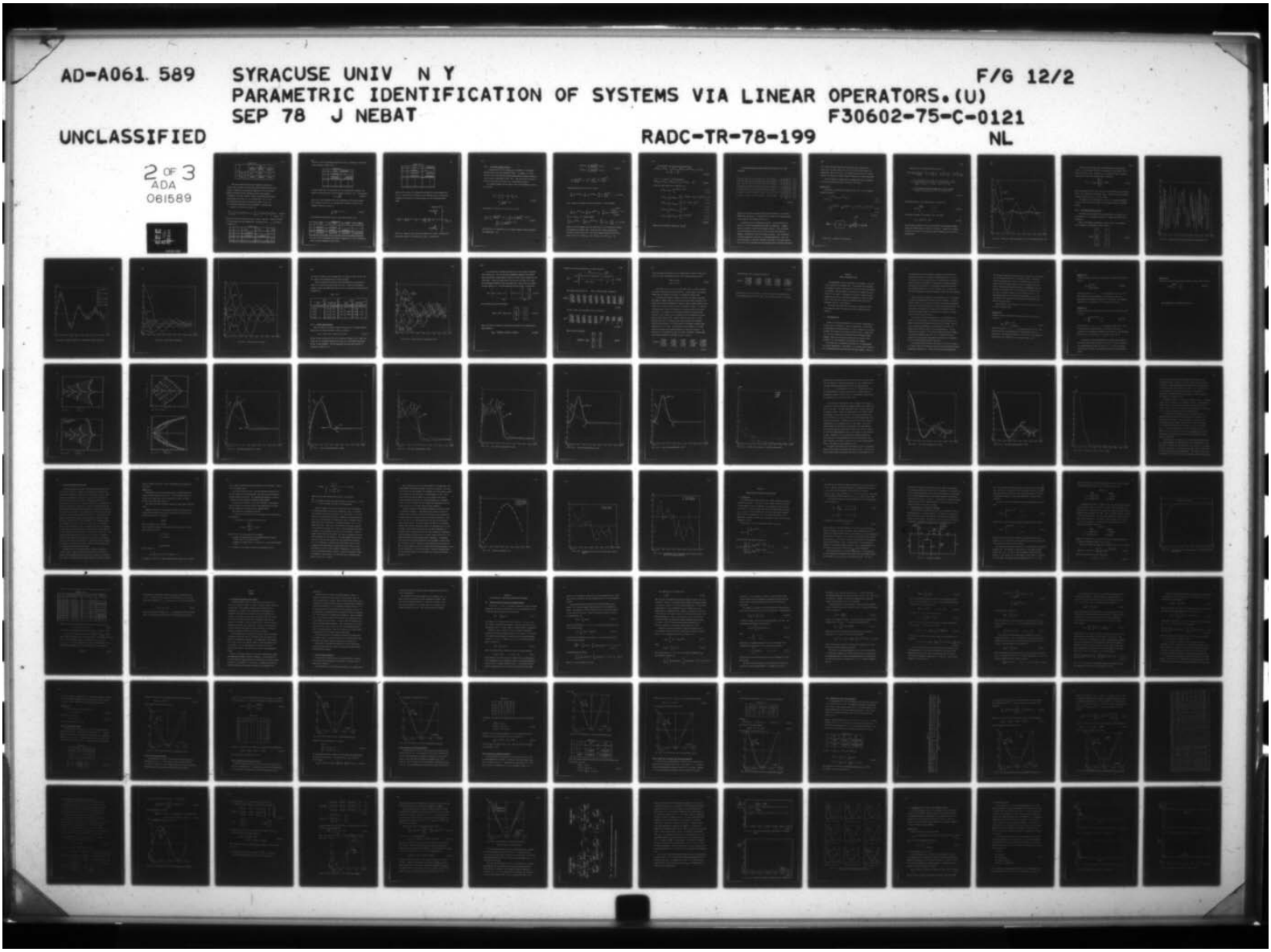

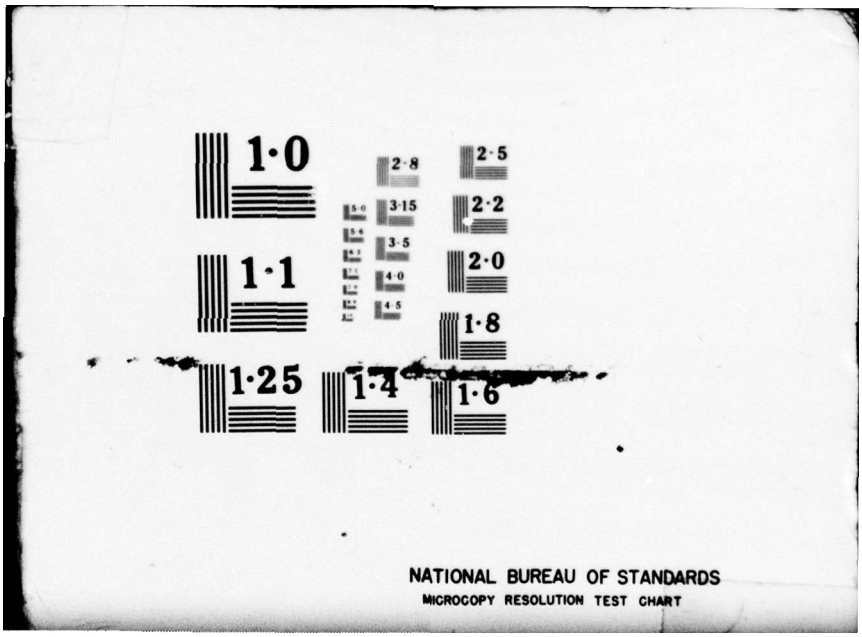
1·0
1·1
1·25
2·8
3·15
3·5
4·0
4·5
2·5
2·2
2·0
1·8
1·4
1·6
NATIONAL BUREAU OF STANDARDS
MICROCOPY RESOLUTION TEST CHART

Table 2-4-2

r		GISE		
		case 1 L=1, K=0	case 2 L=1, K=1	case 3 L=2, K=1
1	$\|\det. M_1\|$	.0463	.0205	.1765
2	$\|\det. M_2\|$	.0000791	.00000494	.000558

Both Carr's method [25] and Jain's method [26] employ the reverse time integrator to generate the basis functions and ISE approximation to generate the simultaneous equations for the coefficients. However, different solution methods are used on the equations. Consequently, the poles converge to their true values along different trajectories as the value of r is increased from 1 to 3. By way of illustration, the equations resulting for Case 3 (i.e., L=2, K=1) are solved using the two solution methods of Carr and Jain.

Equation (2-4-48) may be rewritten as

$$\sum_{\ell=-1}^{0}\sum_{j=1}^{r}\left[\int_0^5 y_k^{(\ell)}(t)y_j^{(\ell)}(t)dt\right]D_{r-j} = -\sum_{\ell=-1}^{0}\int_0^5 y_k^{(\ell)}(t)y_k^{(\ell)}(t)y_0^{(\ell)}(t)dt \qquad (2\text{-}4\text{-}58)$$

$$; k=0,2,\ldots,r-1$$

where D_r has arbitrarily been set equal to unity. With Carr's method, (2-4-58) is solved directly for the coefficients. The results for r = 1, 2, 3 are shown in Table 2-4-3.

Table 2-4-3

r	D_r	D_{r-1}	D_{r-2}	D_{r-3}
1	1	4.236699946		
2	1	1.496951865	1.633885061	
3	1	4	6	4

Solution of the corresponding equations for r=1,2,3, respectively yields the poles presented in Table 2-4-4.

Table 2-4-4

r	real	imaginary
1	-4.236699946	0
2	-.7484759325 -.7484759325	1.036179926 -1.036179926
3	-1 -1 -2	1 -1 0

In Jain's method the r+1 coefficients for the characteristic equations are given by the square roots of the r+1 diagonal co-factors of M_r. In particular,

$$D_{r-j} = \sqrt{\Delta_{jj}} \qquad (2\text{-}4\text{-}59)$$

where Δ_{jj} is the determinant of M_r after removing the j^{th} row and column. For a specified value of r, the characteristic equation in terms of the diagonal co-factors is given by

$$\sum_{j=0}^{r} \sqrt{\Delta_{jj}}\, s^{r-j} = 0 . \qquad (2\text{-}4\text{-}60)$$

The resulting coefficients for r=1,2,3 are found in Table 2-4-5.

Table 2-4-5

r	$D_r = \sqrt{\Delta_{00}}$	$D_{r-1} = \sqrt{\Delta_{11}}$	$D_{r-2} = \sqrt{\Delta_{22}}$	$D_{r-3} = \sqrt{\Delta_{33}}$
1	.5506632136	.8140220103		
2	.2823259536	.460784953	.4200809338	
3	.00590294882	.02361179528	.03541769292	.02361179528

Solution of the corresponding characteristic equations for r=1,2,3 respectively yields the poles presented in Table 2-4-6.

Table 2-4-6

r	real	imaginary
1	-1.47825473	0
2	-.8160513533	.9066361161
	-.8160513533	-.9066361161
3	-1	1
	-1	-1
	-2	0

Figure 2-4-6 presents the S-plane poles obtained for the two methods with r=1,2,3. The value of r for which the two different sets of trajectories converge to the same poles provides another way for determining system order.

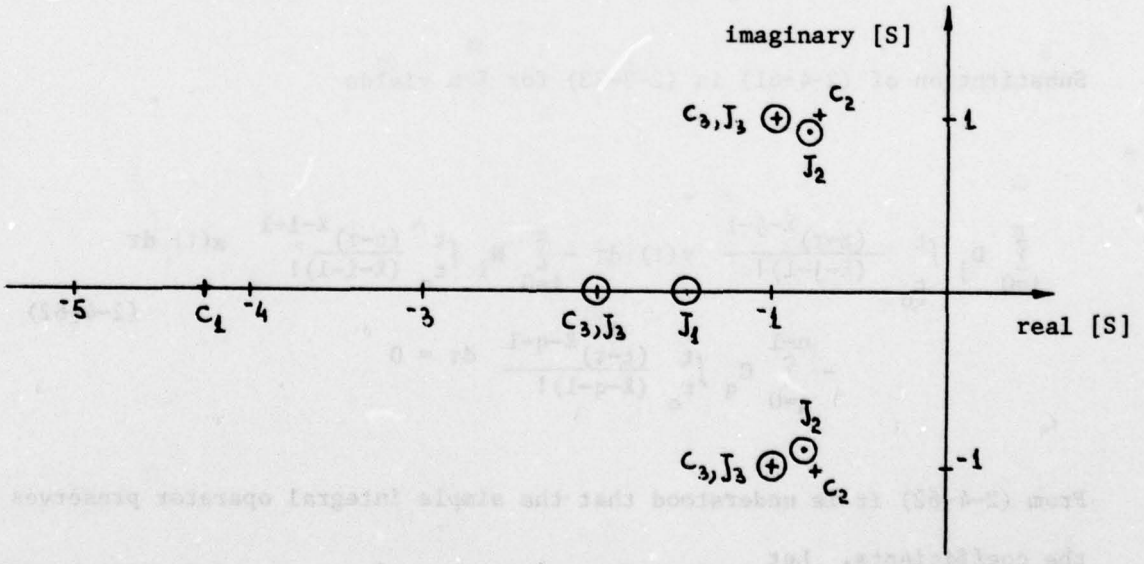

Fig. 2-4-6. Poles of Carr's and Jain's methods for r=1,2,3. The poles for a specified value of r are denoted by C_r and J_r, respectively.

Case 5 - The Simple Integral Operator

A representation of h(t) through $h_m(t)$ is possible, in the identification process, only for exponential inputs. In general, it is not required, and in this case the identification will be carried out directly on the system as represented in Fig. 2-4-1. This will serve as an introduction to the case of arbitrary (i.e., nonexponential) inputs.

The integral operator was utilized by [31] and introduced in (2-1-14). In particular

$$f_\ell\{\cdot\} = \int_{t_o}^{t} \int_{t_o}^{t_\ell} \cdots \int_{t_o}^{t_2} \{\cdot\} \prod_{q=1}^{\ell} dt_q$$

$$= \int_{t_o}^{t} \frac{(t-\tau)^{\ell-1}}{(\ell-1)!}\{\cdot\}\, d\tau. \qquad (2\text{-}4\text{-}61)$$

Substitution of (2-4-61) in (2-3-23) for $\ell > n$ yields

$$\sum_{j=0}^{n} D_j \int_{t_o}^{t} \frac{(t-\tau)^{\ell-j-1}}{(\ell-j-1)!}\, y(\tau)\, d\tau - \sum_{i=0}^{m} N_i \int_{t_o}^{t} \frac{(t-\tau)^{\ell-i-1}}{(\ell-i-1)!}\, x(\tau)\, d\tau$$

$$- \sum_{q=0}^{n-1} C_q \int_{t_o}^{t} \frac{(t-\tau)^{\ell-q-1}}{(\ell-q-1)!}\, d\tau = 0 \qquad (2\text{-}4\text{-}62)$$

From (2-4-62) it is understood that the simple integral operator preserves the coefficients. Let

$$y^{(j-\ell)}(t) = \int_{t_0}^{t} \frac{(t-\tau)^{\ell-j-1}}{(\ell-j-1)!}\, y(\tau)\, d\tau$$
$$x^{(i-\ell)}(t) = \int_{t_0}^{t} \frac{(t-\tau)^{\ell-i-1}}{(\ell-i-1)!}\, x(\tau)\, d\tau \qquad (2\text{-}4\text{-}63)$$

$$\int_{t_0}^{t} \frac{(t-\tau)^{\ell-q-1}}{(\ell-q-1)!}\, d\tau = \int_{0}^{t-t_0} \frac{u^{\ell-q-1}}{(\ell-q-1)!}\, du = \frac{(t-t_0)^{\ell-q}}{(\ell-q)!} .$$

Substituting (2-4-63) into (2-4-62) yields

$$\sum_{j=0}^{n} D_j\, y^{(j-\ell)}(t) - \sum_{i=0}^{m} N_i\, x^{(i-\ell)}(t) - \sum_{q=0}^{n-1} C_q\, \frac{(t-t_0)^{\ell-q}}{(\ell-q)!} = 0 . \qquad (2\text{-}4\text{-}64)$$

With a change of variables involving the indices, (2-4-64) becomes

$$\sum_{j=0}^{n} D_{n-j}\, y^{(n-\ell-j)}(t) - \sum_{i=0}^{m} N_{m-i}\, X^{(m-\ell-i)}(t) - \sum_{q=0}^{n-1} C_{n-q-1}\, \frac{(t-t_0)^{\ell+q+1-n}}{(\ell+q+1-n)!} = 0 . \qquad (2\text{-}4\text{-}65)$$

For $\ell = n$ and $t_0 = 0$, (2-4-65) yields

$$\sum_{j=0}^{n} D_{n-j}\, y^{(-j)}(t) - \sum_{i=0}^{m} N_{m-i}\, x^{(m-n-i)}(t) - \sum_{q=0}^{n-1} C_{n-q-1}\, \frac{t^{q+1}}{(q+1)!} = 0. \qquad (2\text{-}4\text{-}66)$$

Equation (2-4-66) suggests that the coefficients of the differential equation are preserved in reversed order. While the block diagram representing (2-4-62) is given in Fig. 2-3-3, the block diagram representing (2-4-66) is given in Fig. 2-3-6, where $D_{n-r} = \hat{D}_r$, and $N_{m-r} = \hat{N}_r$, and $C_{n-r-1} = \hat{C}_r$.

From (2-4-66), the basis functions involved are

$$\{y^{(0)}(t),\ y^{(-1)}(t),\ \ldots, y^{(-n)}(t),\ x^{(m-n)}(t),\ x^{(m-n-1)}(t), \ldots, x^{(-n)}(t),$$
$$\frac{t}{1!},\ \frac{t^2}{2!},\ \cdots\ \frac{t^n}{n!}\ \}\ . \qquad (2\text{-}4\text{-}67)$$

For $r = n = 2$ and $m = 1$, (2-4-67) becomes

$$\{y^{(0)}(t),\ y^{(-1)}(t),\ y^{(-2)}(t),\ x^{(-1)}(t),\ x^{(-2)}(t),\ t,\ \frac{t^2}{2}\ \} \qquad (2\text{-}4\text{-}68)$$

Then, the basis functions are computed to be

$$y^{(0)}(t) = y(t) = \begin{cases} 2e^{-t}\cos t - e^{-2t} & ;\ t \geq 0 \\ ? & ;\ t < 0 \end{cases}$$

$$y^{(-1)}(t) = \int_0^t y^{(0)}(\tau)d\tau = \begin{cases} \frac{1}{2} - e^{-t}(\cos t - \sin t) + \frac{1}{2}e^{-2t} & ;\ t \geq 0 \\ ? & ;\ t < 0 \end{cases}$$

$$y^{(-2)}(t) = \int_0^t y^{(-1)}(\tau)d\tau = \begin{cases} \frac{1}{2}t + \frac{1}{4} - e^{-t}\sin t - \frac{1}{4}e^{-2t} & ;\ t \geq 0 \\ ? & ;\ t < 0 \end{cases}$$

$$x^{(-1)}(t) = \int_0^t x^{(0)}(\tau)\,d\tau = \begin{cases} \frac{1}{2} - \frac{1}{2}e^{-2t} & ;\ t \geq 0 \\ 0 & ;\ t < 0 \end{cases}$$

$$x^{(-2)}(t) = \int_0^t x^{(-1)}(\tau)d\tau = \begin{cases} \frac{1}{2}t - \frac{1}{4} + \frac{1}{4}e^{-2t} & ;\ t \geq 0 \\ 0 & ;\ t < 0 \end{cases}$$

(2-4-69)

along with the polynomial components t and $\frac{t^2}{2}$.

The ISE approximation scheme yields the following set of linear equations:

$$\left[\begin{array}{ccccc|cc|c|cc}
\langle y^{(0)}, y^{(0)}\rangle & \langle y^{(0)}, y^{(-1)}\rangle & \langle y^{(0)}, y^{(-2)}\rangle & \langle y^{(0)}, x^{(-1)}\rangle & \langle y^{(0)}, x^{(-2)}\rangle & \langle y^{(0)}, t\rangle & \langle y^{(0)}, \frac{t^2}{2}\rangle & D_2 & 0 \\
\langle y^{(-1)}, y^{(0)}\rangle & \langle y^{(-1)}, y^{(-1)}\rangle & \langle y^{(-1)}, y^{(-2)}\rangle & \langle y^{(-1)}, x^{(-1)}\rangle & \langle y^{(-1)}, x^{(-2)}\rangle & \langle y^{(-1)}, t\rangle & \langle y^{(-1)}, \frac{t^2}{2}\rangle & D_1 & 0 \\
\langle y^{(-2)}, y^{(0)}\rangle & \langle y^{(-2)}, y^{(-1)}\rangle & \langle y^{(-2)}, y^{(-2)}\rangle & \langle y^{(-2)}, x^{(-1)}\rangle & \langle y^{(-2)}, x^{(-2)}\rangle & \langle y^{(-2)}, t\rangle & \langle y^{(-2)}, \frac{t^2}{2}\rangle & D_0 & 0 \\
\hline
\langle x^{(-1)}, y^{(0)}\rangle & \langle x^{(-1)}, y^{(-1)}\rangle & \langle x^{(-1)}, y^{(-2)}\rangle & \langle x^{(-1)}, x^{(-1)}\rangle & \langle x^{(-1)}, x^{(-2)}\rangle & \langle x^{(-1)}, t\rangle & \langle x^{(-1)}, \frac{t^2}{2}\rangle & N_1 & 0 \\
\langle x^{(-2)}, y^{(0)}\rangle & \langle x^{(-2)}, y^{(-1)}\rangle & \langle x^{(-2)}, y^{(-2)}\rangle & \langle x^{(-2)}, x^{(-1)}\rangle & \langle x^{(-2)}, x^{(-2)}\rangle & \langle x^{(-2)}, t\rangle & \langle x^{(-2)}, \frac{t^2}{2}\rangle & N_0 & 0 \\
\hline
\langle t, y^{(0)}\rangle & \langle t, y^{(-1)}\rangle & \langle t, y^{(-2)}\rangle & \langle t, x^{(-1)}\rangle & \langle t, x^{(-2)}\rangle & \langle t, t\rangle & \langle t, \frac{t^2}{2}\rangle & C_1 & 0 \\
\langle \frac{t^2}{2}, y(0)\rangle & \langle \frac{t^2}{2}, y^{(-1)}\rangle & \langle \frac{t^2}{2}, y^{(-2)}\rangle & \langle \frac{t^2}{2}, x^{(-1)}\rangle & \langle \frac{t^2}{2}, x^{(-2)}\rangle & \langle \frac{t^2}{2}, t\rangle & \langle \frac{t^2}{2}, \frac{t^2}{2}\rangle & C_0 & 0
\end{array}\right] = \left[\begin{array}{c} 0 \\ 0 \\ 0 \\ \hline 0 \\ 0 \\ \hline 0 \\ 0 \end{array}\right] \qquad (2\text{-}4\text{-}70)$$

Equation (2-4-70) can be solved directly by Jain's method. Or, by Carr's method after setting $D_2 = 1$, moving the first column to the right hand side of the equation, and removing the last row.

In general this is an insensitive operator. As was pointed out in section 2.1, and as is evident from (2-4-69), an additional polynomial space is structured via the simple integral operator. Since polynomials are ever-growing functions, even over short records they become the dominant contributors to the set of basis functions. This contribution is further magnified if the input is a decaying exponential. Thus, the main contribution of the basis functions of (2-4-69) to the inner products of (2-4-70) will be obtained from the polynomial part of the basis functions.

Since these particular basis functions include only a constant and a linear term, one should expect that the set (2-4-70) will be highly ill-conditioned. Hence, as in Case 2, the simple integral operator is another operator that generates a highly linearly dependent set of basis functions.

Next we consider an example where a nonexponential input is applied to the system and additive noise is present at the output.

Example 2-4-2

The system to be identified is shown in Fig. 2-4-7. Let its impulse response be given by

$$h(t) = \begin{cases} e^{-\frac{t}{2\pi}} \sin t + 2e^{-\frac{t}{\pi}} \cos .5t & ; t \geq 0 \\ 0 & ; t < 0 \end{cases}$$

$$= \begin{cases} \frac{1}{2j} e^{(-\frac{1}{2\pi}+j)t} - \frac{1}{2j} e^{(-\frac{1}{2\pi}-j)t} + e^{(-\frac{1}{\pi}+.5j)t} + e^{(-\frac{1}{\pi}-.5j)t} & ; t \geq 0 \\ 0 & ; t < 0 \end{cases} \quad (2\text{-}4\text{-}71)$$

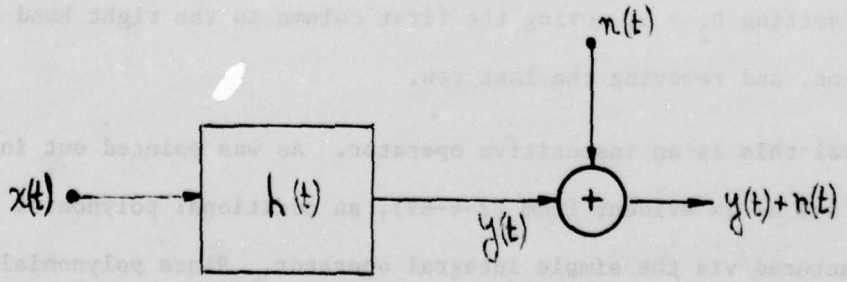

Fig. 2-4-7. A system to be identified.

From (2-4-71), the system's transfer function is

$$H(S) = \frac{1}{2j}\cdot\frac{1}{[S-(-\frac{1}{2\pi}+j)]} - \frac{1}{2j}\cdot\frac{1}{[S-(-\frac{1}{2\pi}-j)]} + \frac{1}{[S-(-\frac{1}{\pi}+.5j)]} + \frac{1}{[S-(-\frac{1}{\pi}-.5j)]}$$

$$=2\cdot\frac{S^3 + (\frac{1}{2}+\frac{2}{\pi})S^2 + (1+\frac{1}{\pi}+\frac{5}{4\pi^2})S + (\frac{1}{8}+\frac{1}{\pi}+\frac{1}{2\pi^2}+\frac{1}{4\pi^3})}{(S+\frac{1}{2\pi}-j)(S+\frac{1}{2\pi}+j)\ (S+\frac{1}{\pi}-.5j)\ (S+\frac{1}{\pi}+.5j)}$$

$$= 2\cdot\frac{(S+.4411)\ (S+.3478-j1.0086)\ (S+.3478+j1.0086)}{(S+\frac{1}{2\pi}-j)\ (S+\frac{1}{2\pi}+j)(S+\frac{1}{\pi}-.5j)\ (S+\frac{1}{\pi}+.5j)} \quad . \tag{2-4-72}$$

The probing signal for the identification is chosen to be

$$x(t) = \begin{cases} \dfrac{\sin t}{t} & ;\ t \geq 0 \\ 0 & ;\ t < 0 \end{cases} \quad . \tag{2-4-73}$$

The system is assumed to be relaxed at t=0. The output

$$y(t) = \int_0^t x(\tau)h(t-\tau)d\tau \tag{2-4-74}$$

was calculated numerically over the time interval $[0,6\pi]$ using 601 samples spaced $.01\pi$ seconds apart for each of x(t) and h(t). Figure 2-4-8 presents the input, the output, and the system's impulse response over the time interval $[0,6\pi]$.

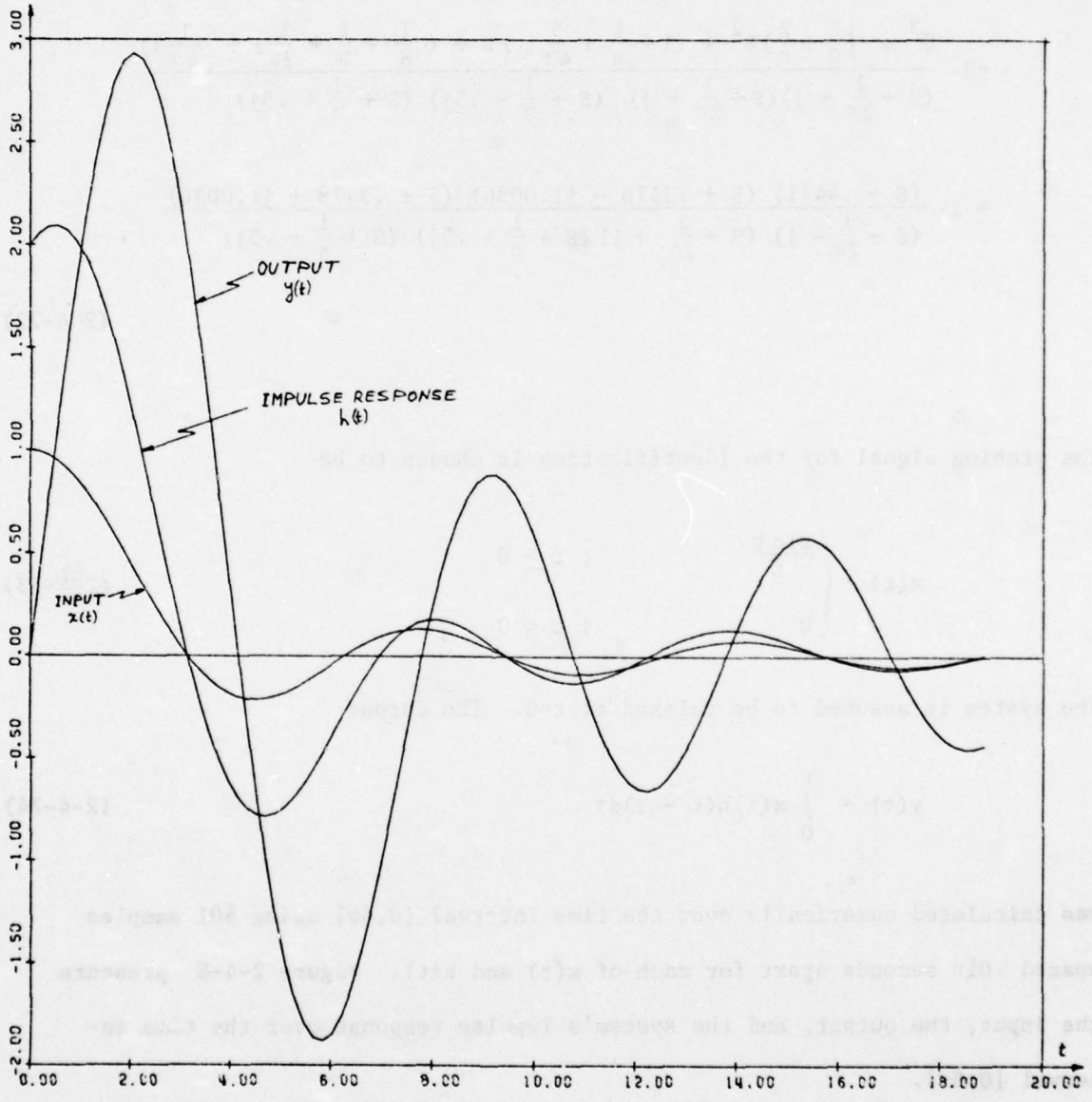

Fig. 2-4-8. Input x(t), impulse response h(t), and the resulting output y(t).

The noise n(t) is pseudo-random and uniformly distributed between -A and A. A noise sample function of 101 samples over the interval $[0,6\pi]$ is plotted in Fig. 2-4-9. The value of A is chosen such that the signal to noise ratio for the noise corrupted output is given by

$$S/N = 10 \log_{10} \frac{\sum_{i=1}^{101} y_i^2}{\sum_{i=1}^{101} n_i^2} = 10\,dB \quad , \tag{2-4-75}$$

where 101 samples of each of y(t) and n(t) were considered over the interval $[0,6\pi]$. The samples are $.06\pi$ seconds apart. Figure 2-2-10 shows the noise corrupted output, y(t) + n(t), for $S/N = 10\,dB$.

The system is first identified for n(t) = 0. The operator generating the set of basis functions is chosen to be the advance operator discussed earlier.

Case 1 - Zero Additive Noise (n(t) = 0)

The input and output basis functions generated for an advance of 10 time samples (i.e., $.6\pi$ seconds) are plotted in Figures 2-4-11 and 2-4-12 respectively.

When a least-squares approximation scheme is used, the homogeneous set of equations is represented in matrix form by

$$[M]^T[M] \begin{bmatrix} \hat{D}_0 \\ \vdots \\ \hat{D}_n \\ \hat{N}_0 \\ \vdots \\ \hat{N}_m \end{bmatrix} = \begin{bmatrix} 0 \\ \vdots \\ 0 \\ 0 \\ \vdots \\ 0 \end{bmatrix} \tag{2-4-76}$$

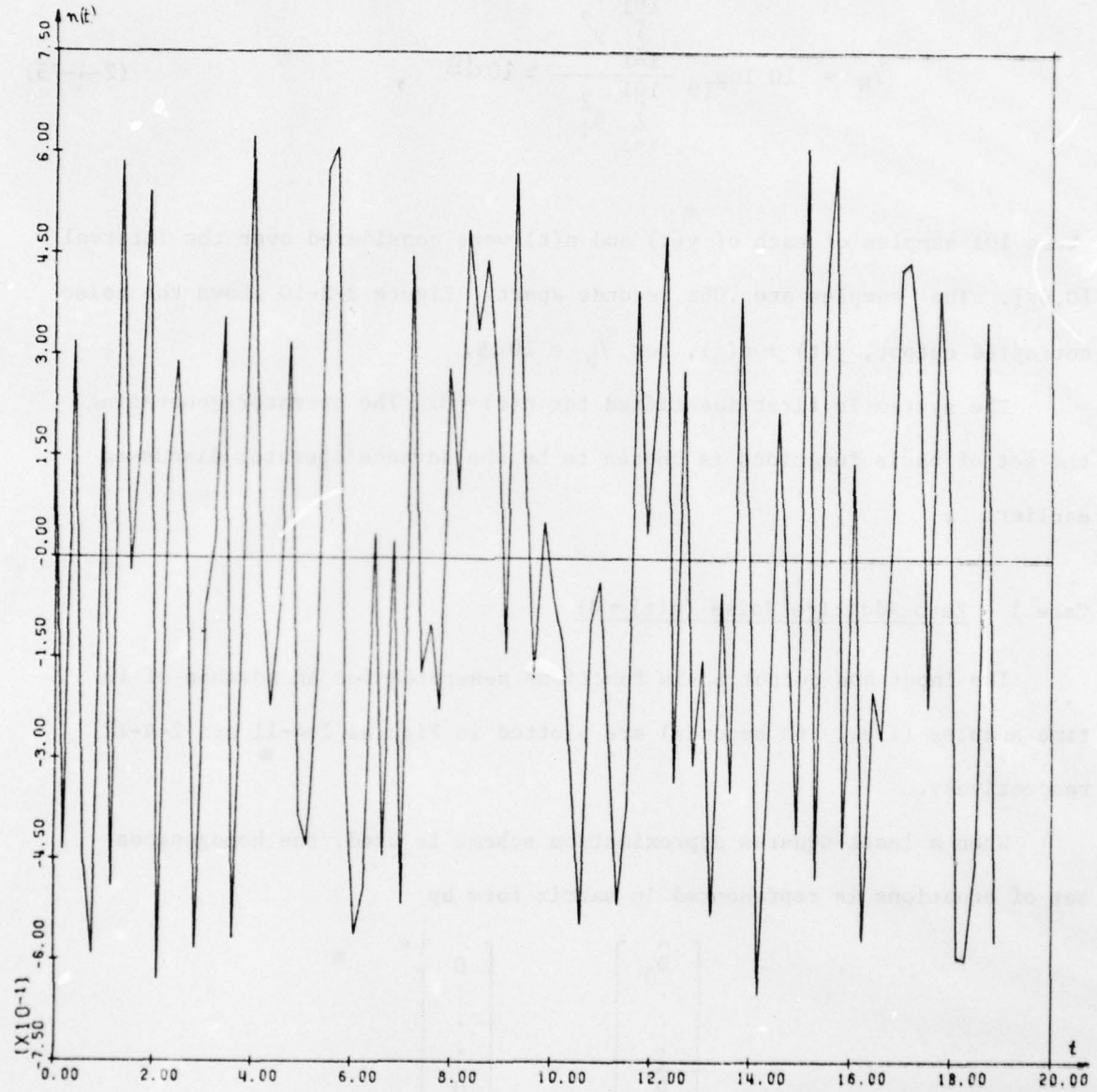

Fig. 2-4-9. Pseudo-random uniformly distributed noise sample, n(t).

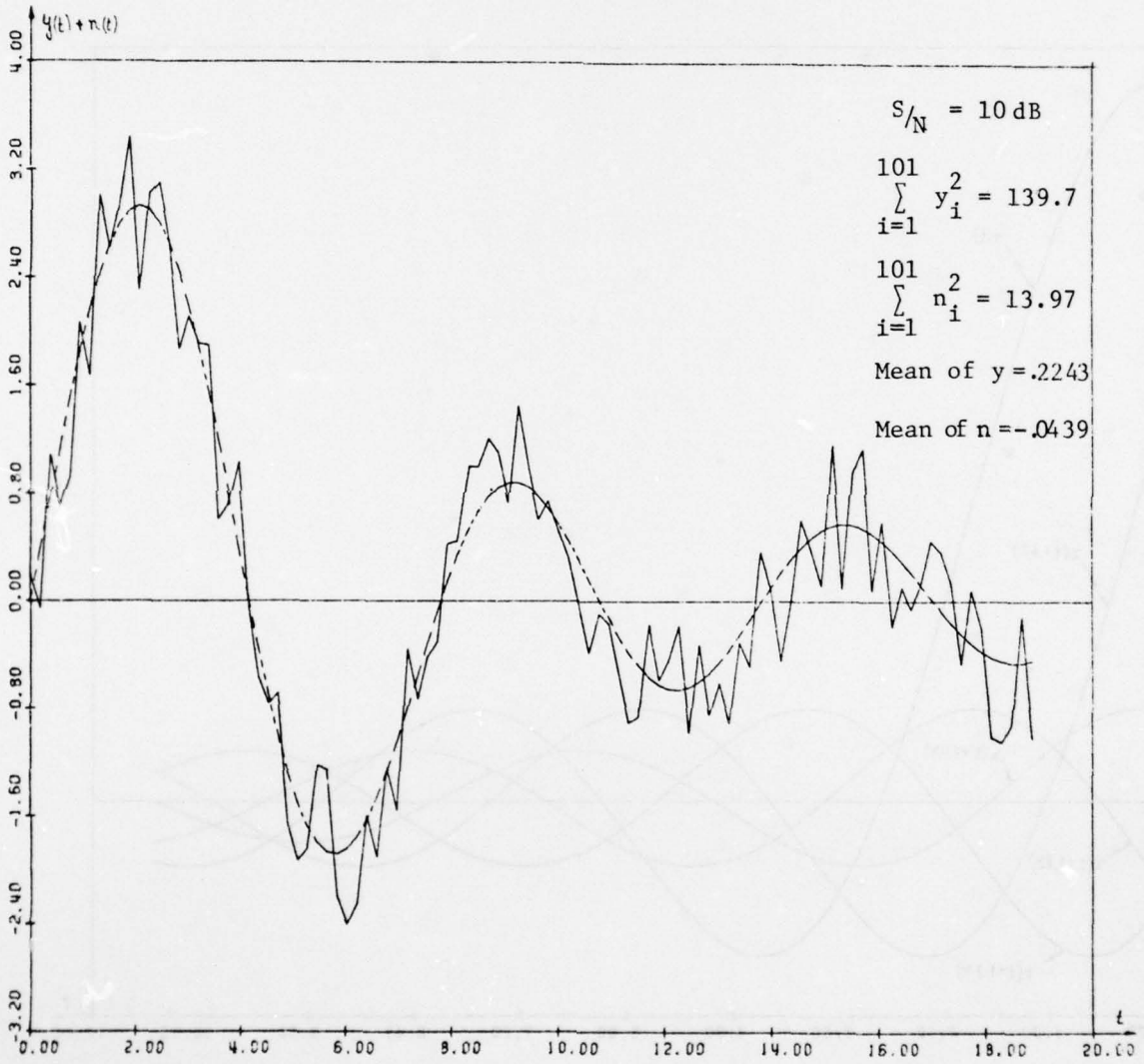

Fig. 2-4-10. System's output y(t), corrupted by additive noise n(t).

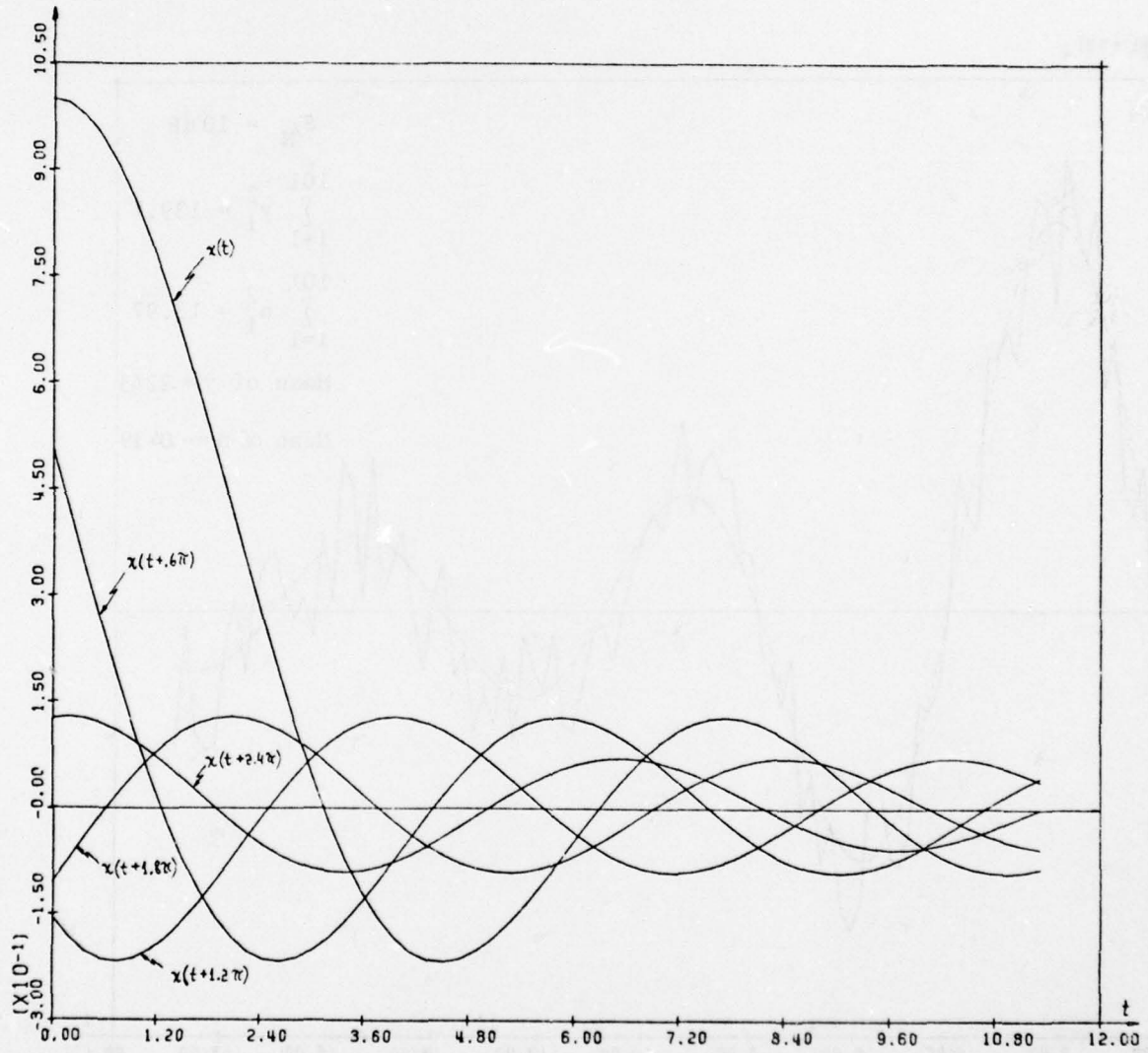

Fig. 2-4-11. Basis set for the input.

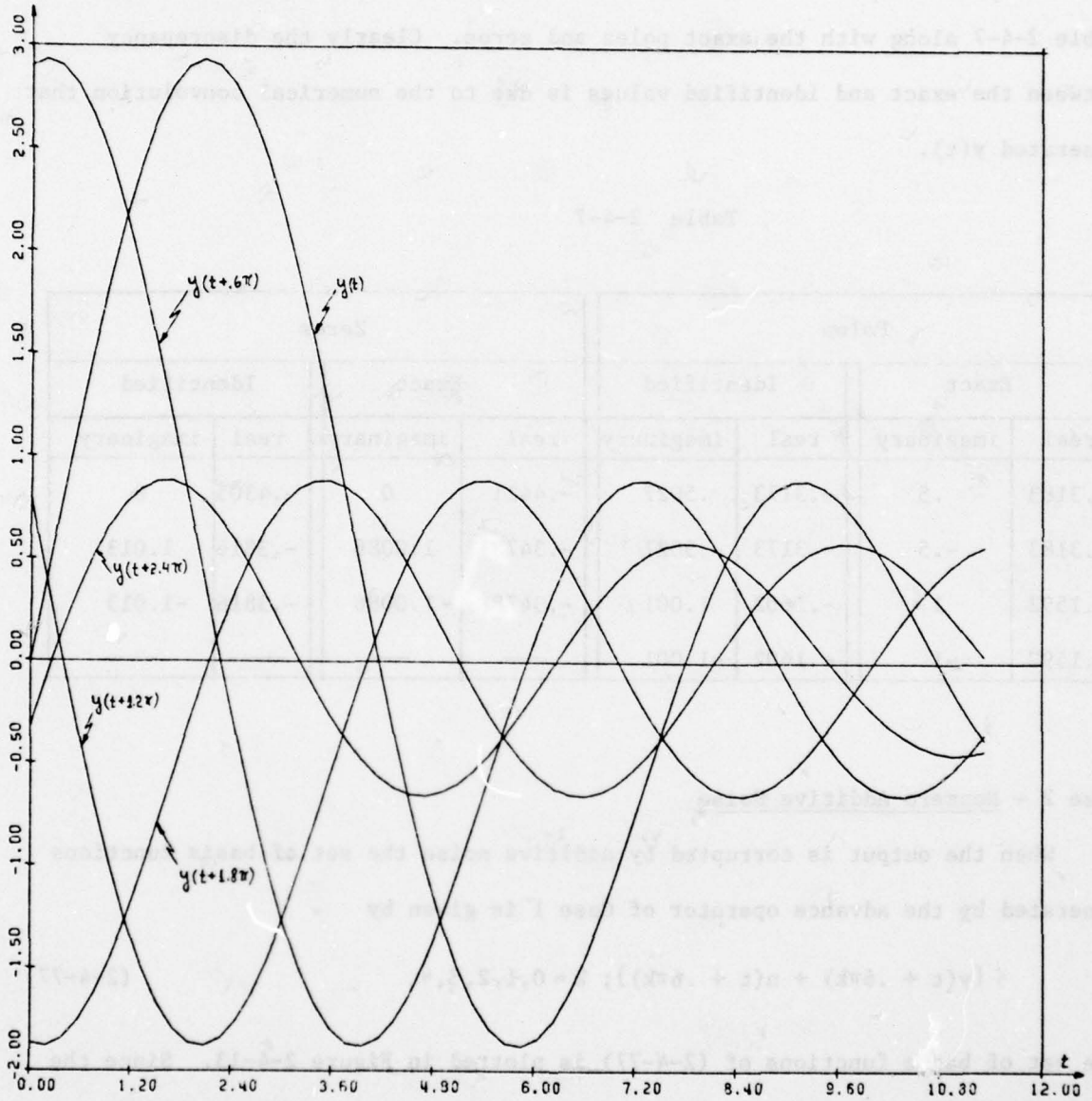

Fig. 2-4-12. Basis set for the output.

The first n+1 columns of [M] represent the y(.) basis functions, and the last m+1 columns of [M] represent the x(.) basis functions.

The poles and zeros resulting from the identification are presented in Table 2-4-7 along with the exact poles and zeros. Clearly the discrepancy between the exact and identified values is due to the numerical convolution that generated y(t).

Table 2-4-7

Poles				Zeros			
Exact		Identified		Exact		Identified	
real	imaginary	real	imaginary	real	imaginary	real	imaginary
-.3183	.5	-.3173	.5027	-.4411	0	-.4305	0
-.3183	-.5	-.3173	-.5027	-.3478	1.0086	-.3816	1.013
-.1592	1	-.1602	1.001	-.3478	-1.0086	-.3816	-1.013
-.1592	-1	-.1602	-1.001	——	——	——	——

Case 2 - Nonzero Additive Noise

When the output is corrupted by additive noise the set of basis functions generated by the advance operator of Case 1 is given by

$$\{y(t + .6\pi k) + n(t + .6\pi k)\};\ k = 0,1,2,3,4. \qquad (2\text{-}4\text{-}77)$$

The set of basis functions of (2-4-77) is plotted in Figure 2-4-13. Since the output y(t) is a decaying signal and the noise n(t) is uniformly distributed, the S/N is time dependent. The S/N associated with each basis function is presented in Figure 2-4-13.

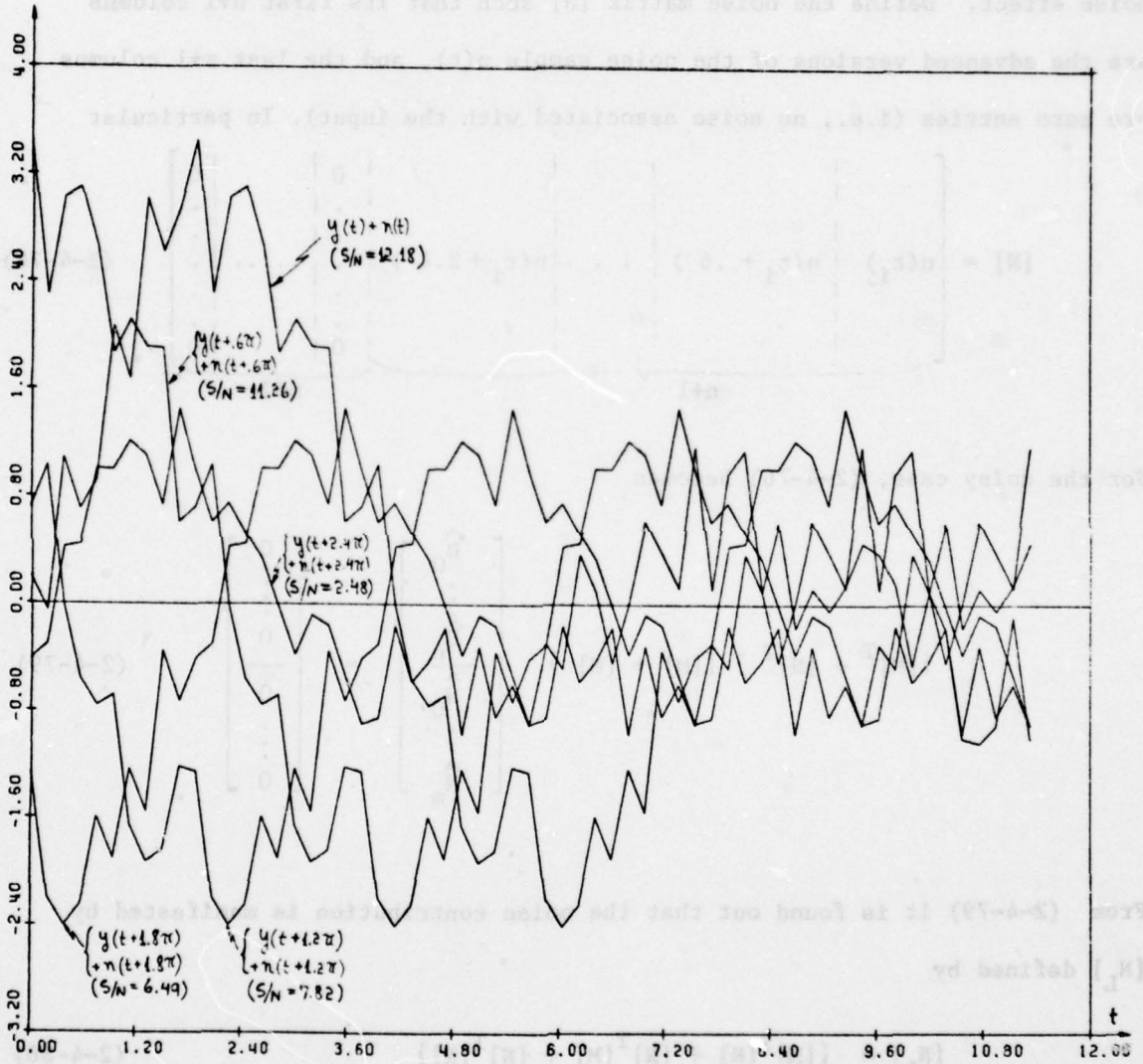

Fig. 2-4-13. Output basis set corrupted by noise.

It is clear that in practice the output $y(t)+n(t)$ cannot be separated into $y(t)$ and $n(t)$. But, for the given synthesized example we will define their contribution through separate matrices in order to gain insight into the noise effect. Define the noise matrix [N] such that its first n+1 columns are the advanced versions of the noise sample $n(t)$, and the last m+1 columns are zero entries (i.e., no noise associated with the input). In particular

$$[N] = \underbrace{\begin{bmatrix} n(t_i) & n(t_i+.6) & \cdots & n(t_i+2.4) \\ \vdots & \vdots & & \vdots \\ \vdots & \vdots & & \vdots \\ 0 & 0 & \cdots & 0 \end{bmatrix}}_{n+1} \quad \underbrace{\begin{bmatrix} 0 & \cdots & 0 \\ \vdots & & \vdots \\ \vdots & & \vdots \\ 0 & \cdots & 0 \end{bmatrix}}_{m+1} . \qquad (2\text{-}4\text{-}78)$$

For the noisy case, (2-4-76) becomes

$$\{[M]^T + [N]^T\}\{[M] + [N]\} \begin{bmatrix} \hat{D}_0 \\ \vdots \\ \hat{D}_n \\ \hline \hat{N}_0 \\ \vdots \\ \hat{N}_m \end{bmatrix} = \begin{bmatrix} 0 \\ \vdots \\ 0 \\ \hline 0 \\ \vdots \\ 0 \end{bmatrix} . \qquad (2\text{-}4\text{-}79)$$

From (2-4-79) it is found out that the noise contribution is manifested by $[N_L]$ defined by

$$[N_L] = \{[M]^T[N] + [N]^T[M] + [N]^T[N]\}. \qquad (2\text{-}4\text{-}80)$$

Carrying out the matrix operations in (2-4-80) results in

$$[N_L] = \begin{array}{c} \\ n+1 \\ \\ \\ m+1 \end{array} \overbrace{\left[\begin{array}{c|c} 2\langle n(.), y(.)\rangle + \langle n(.), n(.)\rangle & \langle n(.), x(.)\rangle \\ \hline \langle n(.), x(.)\rangle & 0 \end{array}\right]}^{n+1 \quad m+1} \cdot \qquad (2\text{-}4\text{-}81)$$

The inner product matrix for Case 1 (without noise) is given by

$$[M]^T[M] = \begin{bmatrix} 130.3 & 21.08 & -70.95 & 1.418 & 26.43 & 18.6 & -6.466 & -2.288 & 4.992 \\ 21.08 & 99.16 & -12.12 & -52.55 & 21.19 & 24.78 & 6.454 & -7.374 & 0.734 \\ -70.95 & -12.12 & 43.87 & -1.225 & -19.04 & -9.61 & 4.498 & 1.59 & -3.251 \\ 1.418 & -52.55 & -1.225 & 32.77 & -7.307 & -13.42 & -4.95 & 4.001 & 0.4388 \\ 26.43 & 21.19 & -19.04 & -7.307 & 12.62 & 6.506 & -1.087 & -1.902 & 1.542 \\ 18.6 & 24.78 & -9.61 & -13.42 & 6.506 & 8.553 & 1.254 & -1.963 & 0.5065 \\ -6.466 & 6.454 & 4.498 & -4.95 & -1.087 & 1.254 & 1.248 & -0.4067 & -0.4057 \\ -2.288 & -7.374 & 1.59 & 4.001 & -1.902 & -1.963 & -0.4067 & 0.5829 & -0.09747 \\ 4.992 & 0.734 & -3.251 & 0.4388 & 1.542 & 0.5065 & -0.4057 & -0.09747 & 0.2655 \end{bmatrix} \qquad (2\text{-}4\text{-}82)$$

For $S/N = 10\,dB$, the contribution due to the noise is

$$[N_L] = \begin{bmatrix} 13.72 & -8.078 & -5.345 & 4.132 & 3.719 & -0.3761 & -0.4894 & 0.1647 & 0.2172 \\ -8.078 & 13.13 & -2.664 & -5.829 & 4.886 & 0.1295 & 0.368 & -0.2664 & -0.09355 \\ -5.345 & -2.664 & 14.19 & -3.339 & -2.596 & -0.5919 & 0.4912 & 0.2192 & -0.3601 \\ 4.132 & -5.829 & -3.339 & 13.56 & -4.261 & -1.015 & -0.6522 & 0.4182 & 0.1588 \\ 3.719 & 4.886 & -2.596 & -4.261 & 8.553 & 1.516 & 0.2575 & -0.4491 & 0.07427 \\ -0.3761 & 0.1295 & -0.5919 & -1.015 & 1.516 & 0 & 0 & 0 & 0 \\ -0.4894 & 0.368 & 0.4912 & -0.6522 & 0.2575 & 0 & 0 & 0 & 0 \\ 0.1647 & -0.2664 & 0.2192 & 0.4182 & -0.4491 & 0 & 0 & 0 & 0 \\ 0.2172 & -0.09355 & -0.3601 & 0.1588 & 0.07427 & 0 & 0 & 0 & 0 \end{bmatrix} \qquad (2\text{-}4\text{-}83)$$

Then, solving the equation

$$\{[M]^T[M] + [N_L]\} \begin{bmatrix} \hat{D}_0 \\ \vdots \\ \hat{D}_n \\ \hat{N}_0 \\ \vdots \\ \hat{N}_m \end{bmatrix} = \begin{bmatrix} 0 \\ \vdots \\ 0 \\ 0 \\ \vdots \\ 0 \end{bmatrix} \qquad (2\text{-}4\text{-}84)$$

yields the hatted coefficients for the characteristic equation, whose roots, after the proper transformation result in the identified poles given by

$$-.0464 \pm j0.689$$
$$-.165 \pm j1.24 \ . \qquad (2\text{-}4\text{-}85)$$

From Figure 2-4-13, it is clear that there exists a trade-off between the amount of advance used and the given S/N. In this respect, the present example does not represent any effort to optimize the advance used.

To improve the solution obtained in (2-4-85), one should 1) increase the number of samples used over the given record (the basis functions of the example utilized just 61 samples), 2) properly choose a usable portion of the record, and 3) choose a 'good' value for the amount of advance. In addition, the approximation scheme can be improved by taking advantage of the noise properties. For instance, in a least-squares scheme we premultiply the equation by the transpose of the rectangular matrix representing the noisy basis functions (see(2-4-79)). Define the matrix operation Θ as first reversing the order of the matrix rows, and then taking the transpose. Utilizing this operator in (2-4-79) instead of the regular transpose might reduce the effect of noise. This operation takes advantage of the small correlation between noise samples separated by large time intervals. In particular, one contributer to $[N_L]$ in (2-4-80) is $[N]^T[N]$. Concentrating on the nonzero submatrix of $[N]^T[N]$ of Case 2, we have

$$[N]^T[N] = \begin{bmatrix} 3.266 & -1.566 & -1.832 & 2.401 & 0.6318 \\ -4.13 & 3.327 & 1.45 & -2.36 & 0.5546 \\ -4.924 & -1.989 & 4.062 & -0.06135 & -2.535 \\ 3.778 & -5.078 & -1.714 & 3.675 & -0.3168 \\ 2.959 & 6.018 & -1.159 & -3.034 & 1.264 \end{bmatrix} \qquad (2\text{-}4\text{-}86)$$

The same matrix with a Θ operation results in

$$[N]^{\Theta}[N] = \begin{bmatrix} -0.2258 & 0.1271 & 0.1849 & -0.1706 & 1.824 \\ 0.1271 & 0.4922 & -0.8318 & 0.9663 & -1.309 \\ 0.1849 & -0.8318 & -0.2702 & -2.058 & 0.02368 \\ -0.1706 & 0.9663 & -2.058 & 0.7081 & -0.2852 \\ 1.824 & -1.309 & 0.02368 & -0.2852 & -0.1529 \end{bmatrix}$$

(2-4-87)

Notice that 21 out of 25 entries of (2-4-87) are smaller in magnitude than the corresponding entries in (2-4-86). This reduces the effect of the noise.

Chapter 3

USEFUL SUPPLEMENTAL TOOLS

Two supplemental tools are discussed in this chapter. The first is the concept of the "growing tree." The "growing tree" describes the movement of poles in the S-plane as the order of the approximation is increased. The tree behaves in a distinct, but highly structured manner for each signal. Consequently, the tree is useful for extrapolating the poles of a lower-order approximation to those of higher order. Also, the tree is useful in separating signal poles from extraneous poles in a noisy problem.

The second topic deals with the problem of obtaining a "good" first guess for iterative schemes which utilize highly nonlinear equations.

3.1 The Growing Tree

Assume an r^{th}-order approximation is to be used to approximate a function which is composed of a sum of n exponentials. If the order of approximation is increased from r=1 to r=n, a trajectory of the pole locations can be drawn in the S-plane (see Fig. 2-4-6). Clearly, for r>n, the set of equations for determining the coefficients becomes singular. Hence, once the exact solution has been reached, corresponding to r=n, the "growth" of the trajectory is stopped.

Now assume that a nonexponential function is to be approximated by a sum of exponentials. From Chapter 1, it is known that an infinite set of exponential basis functions spans the space $L_2[0,\infty]$. Hence, if

the nonexponential function belongs to $L_2[0,\infty]$, the function can be approximated arbitrarily closely by the exponential basis. Since it is impractical to use an infinite set as a representation, an approximation of order r is utilized. A trajectory of the pole locations is structured in the S-plane as r is increased successively from unity. This "growing" trajectory is called a "growing" tree. Clearly, the tree of a nonexponential function continues to grow with ever-increasing r.

When discussing the behavior of the growing tree, it is convenient to divide the nonexponential functions into two subgroups. A natural division consists of 1) functions which have a faster than exponential decay, and 2) functions which have a slower than exponential decay. The first group is considered to be composed of time-limited functions (in some wide sense) while the second group is considered to be composed of nontime-limited functions.

On the basis of many worked examples, it is noticed that the growth of a tree belonging to a time-limited function expands in the general direction of the negative real axis of the S-plane. Also, if $r_2 > r_1$, the poles representing r_2 are positioned on a contour of greater extent than the contour of poles representing r_1. The two contours do not intersect. For real time signals, the tree is symmetrical about the negative real axis. As r is increased, the tree spreads out in the positive and negative directions of the imaginary axis as it grows along the negative real axis.

For nontime-limited functions, the base of the tree is localized in a narrow region of the negative real axis with the branches extending towards the imaginary axis. Since the functions being approximated

are assumed to decay with increasing time, the poles do not cross over into the right-half plane as r is increased in value. Instead the branches stop growing just short of the imaginary axis. For real signals the tree is again symmetrical about the negative real axis. However, because nontime-limited functions are bandlimited, the tree branches are confined within a finite region of the imaginary axis. For $r_2 > r_1$, the contour formed for r_2 grows inside that for r_1 by interleaving with all of the contours corresponding to $r < r_2$. Hence, the branches of the tree tend to bend inwards (as though they were heavily laden with fruit).

Some examples are now presented to illustrate the behavior of the two types of growing trees.

Example 3-1-1

Consider a strictly time-limited sine pulse, denoted by SINP, which is given by

$$\text{SINP} = \begin{cases} \sin \pi t \ ; \ 0 \le t \le 1 \\ 0 \ ; \ \text{elsewhere.} \end{cases} \qquad (3\text{-}1\text{-}1)$$

The SINP tree with r = 1, 2, . . ., 8 is presented in Fig. 3-1-1. The SINP function and its approximations for odd and even values of r, respectively, are presented in Figures 3-1-5 and 3-1-6. The integrated squared error, as a function of r, is plotted in Fig. 3-1-11.

Example 3-1-2

Consider a strictly time-limited square pulse, denoted by SQP, which is given by

$$SQP = \begin{cases} 1; & 0 \le t \le 1 \\ 0; & \text{elsewhere} . \end{cases} \qquad (3\text{-}1\text{-}2)$$

The SQP tree with r = 1, 2, . . ., 8 is presented in Fig. 3-1-2. The SQP function and its approximations for odd and even values of r, respectively, are presented in Figures 3-1-7 and 3-1-8. The integrated squared error, as a function of r, is plotted in Fig. 3-1-11.

Example 3-1-3

Consider a wide sense time-limited gaussian pulse, denoted by GP, which is given by

$$GP = \begin{cases} e^{-[4(t-1/2)]^2} & ; \ t \ge 0 \\ 0 & ; \ t < 0 . \end{cases} \qquad (3\text{-}1\text{-}3)$$

The GP tree with r = 1, 2, . . ., 8 is presented in Fig. 3-1-3. The GP function and its approximations for odd and even values of r, respectively, are presented in Figures 3-1-9 and 3-1-10. The integrated squared error, as a function of r, is plotted in Fig. 3-1-11.

In carrying out the approximations for the above three examples, the reverse time integral operator (see (2-4-43)) was used along with the ISE approximation scheme (see (A-1-11)). For the final example the differential operator is utilized along with the ISE approximation scheme.

Example 3-1-4

Consider the nontime-limited function, denoted by SINC, which is given by

$$\text{SINC} = \begin{cases} \dfrac{\sin t}{t} & ; \ t \geq 0 \\ 0 & ; \ t < 0 \ . \end{cases} \qquad (3\text{-}1\text{-}4)$$

TEXT CONTINUED FOR THIS EXAMPLE ON PAGE 3-15.

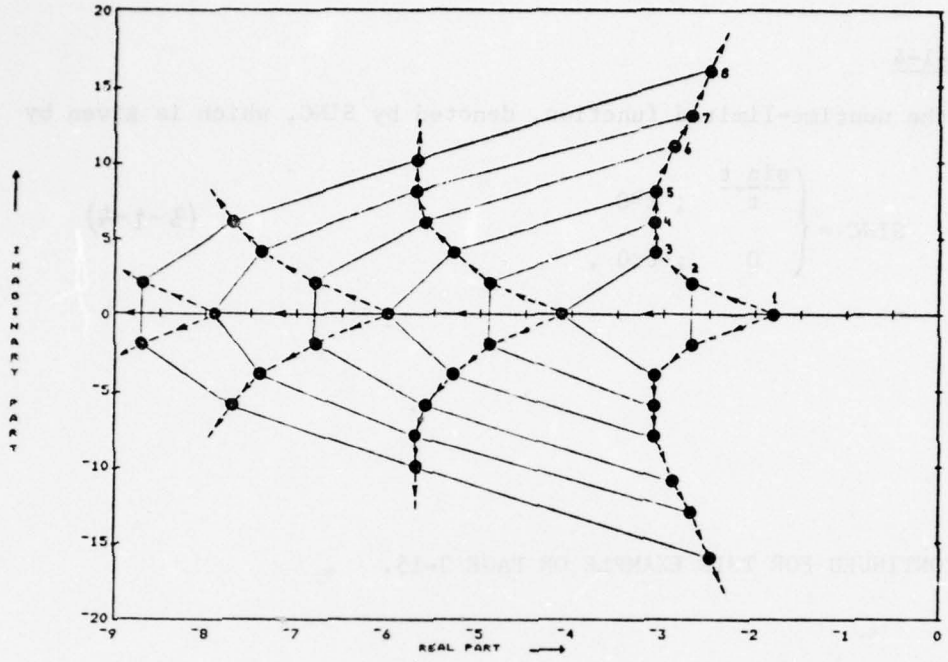

Fig. 3-1-1. SINP tree.

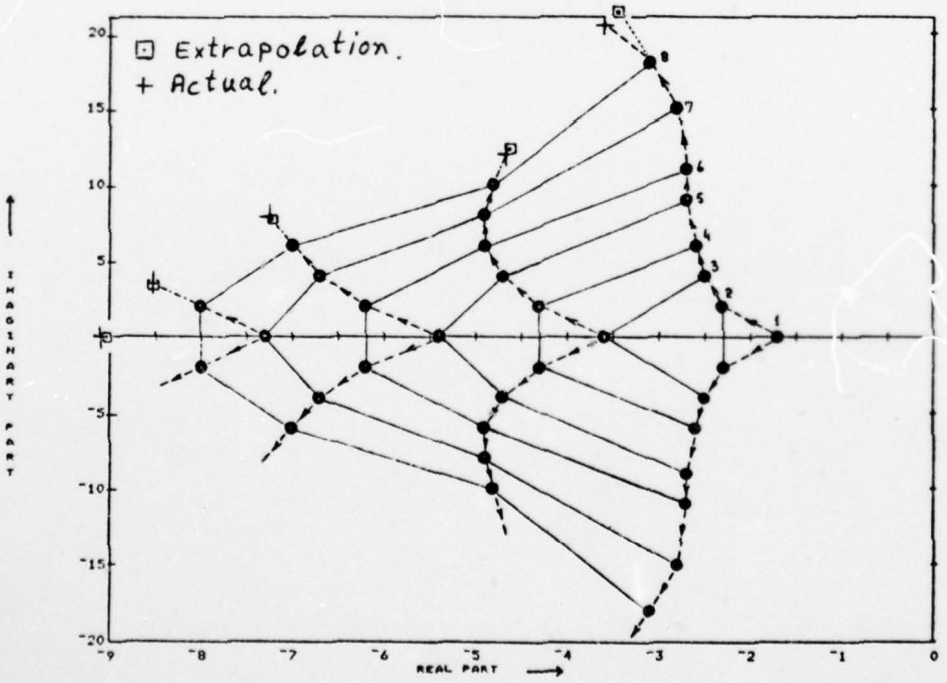

Fig. 3-1-2. SQP tree

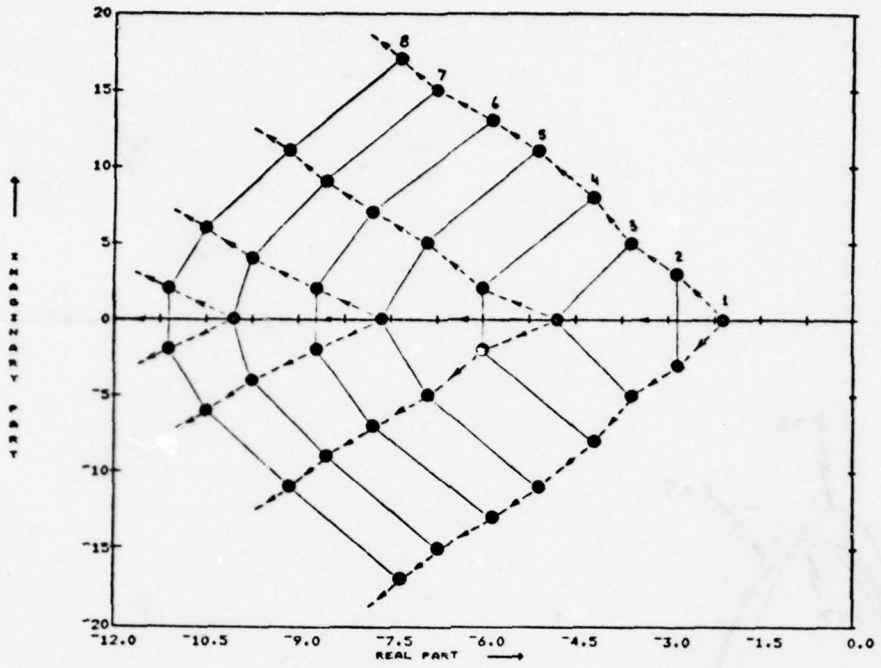

Fig. 3-1-3. GP tree.

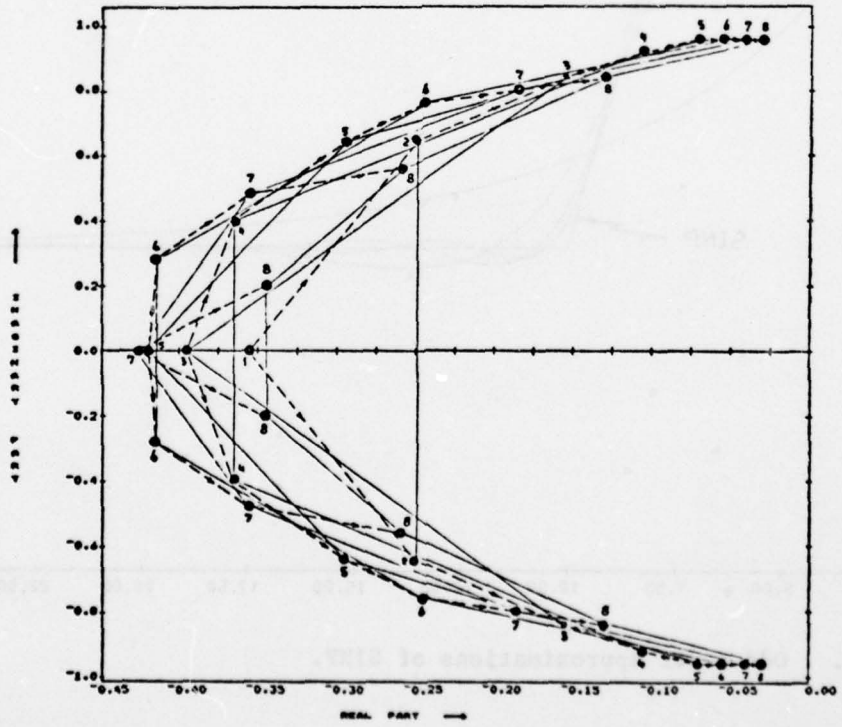

Fig. 3-1-4. SINC tree.

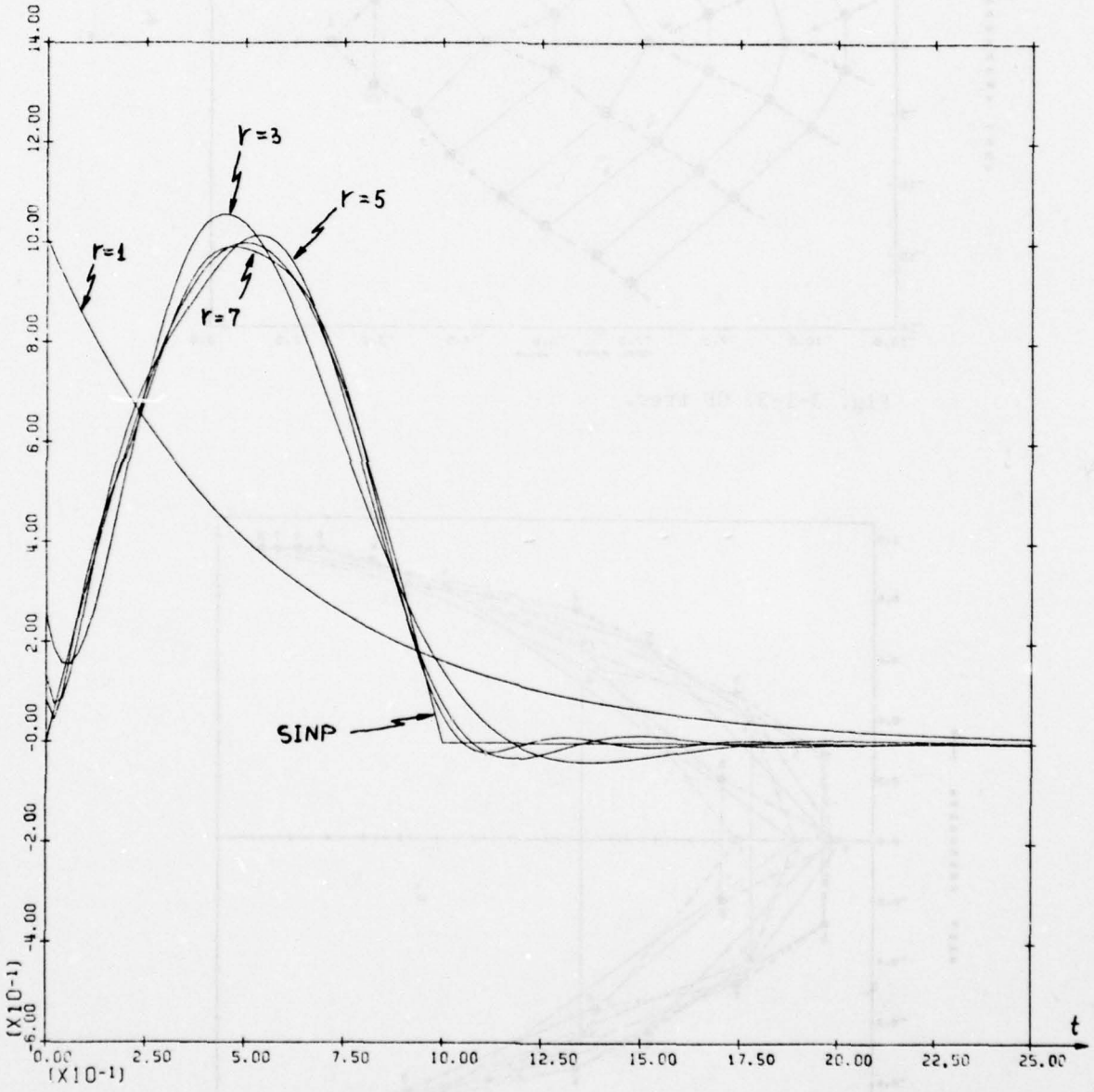

Fig. 3-1-5. Odd order approximations of SINP.

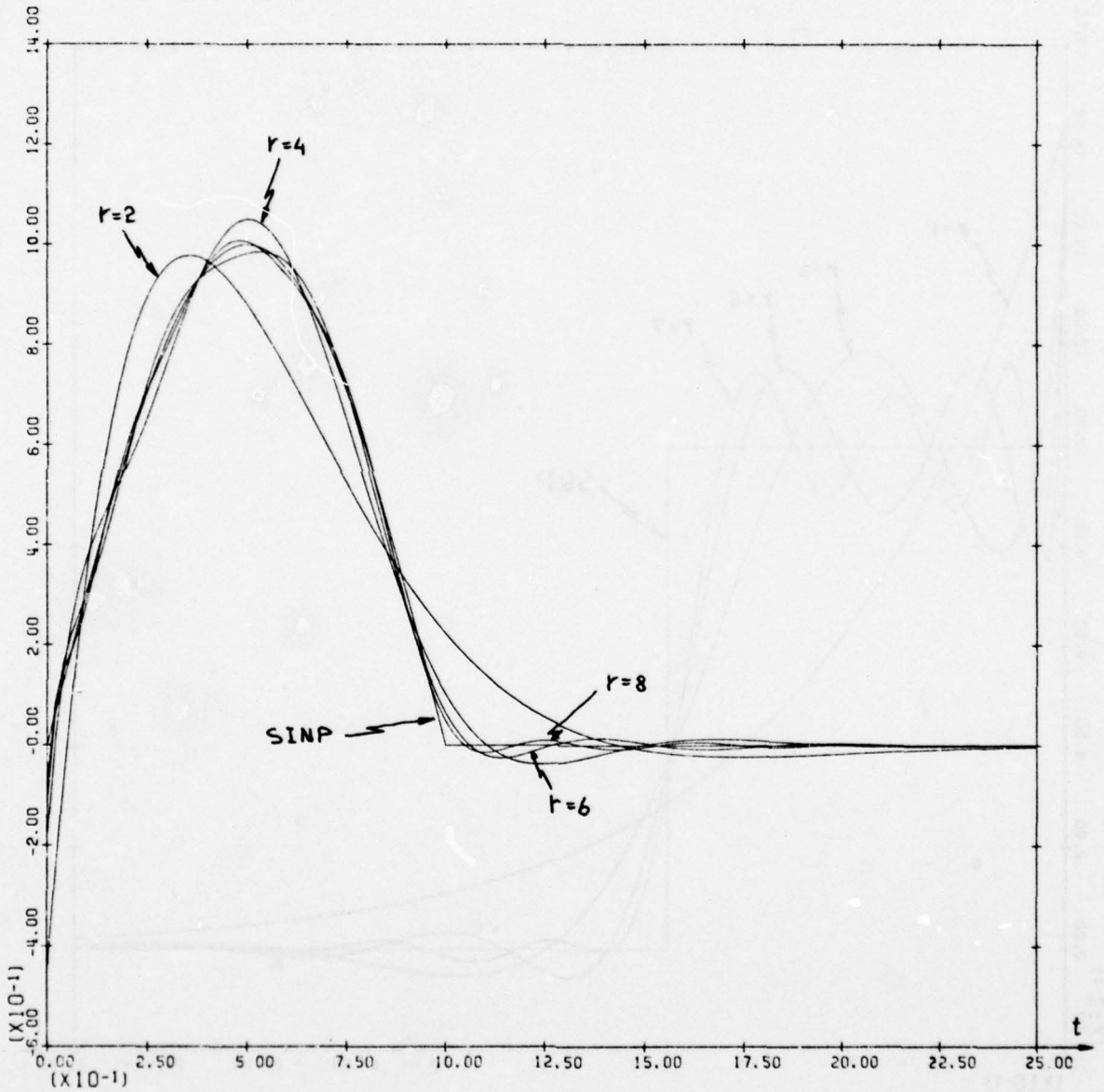

Fig. 3-1-6. Even order approximations of SINP.

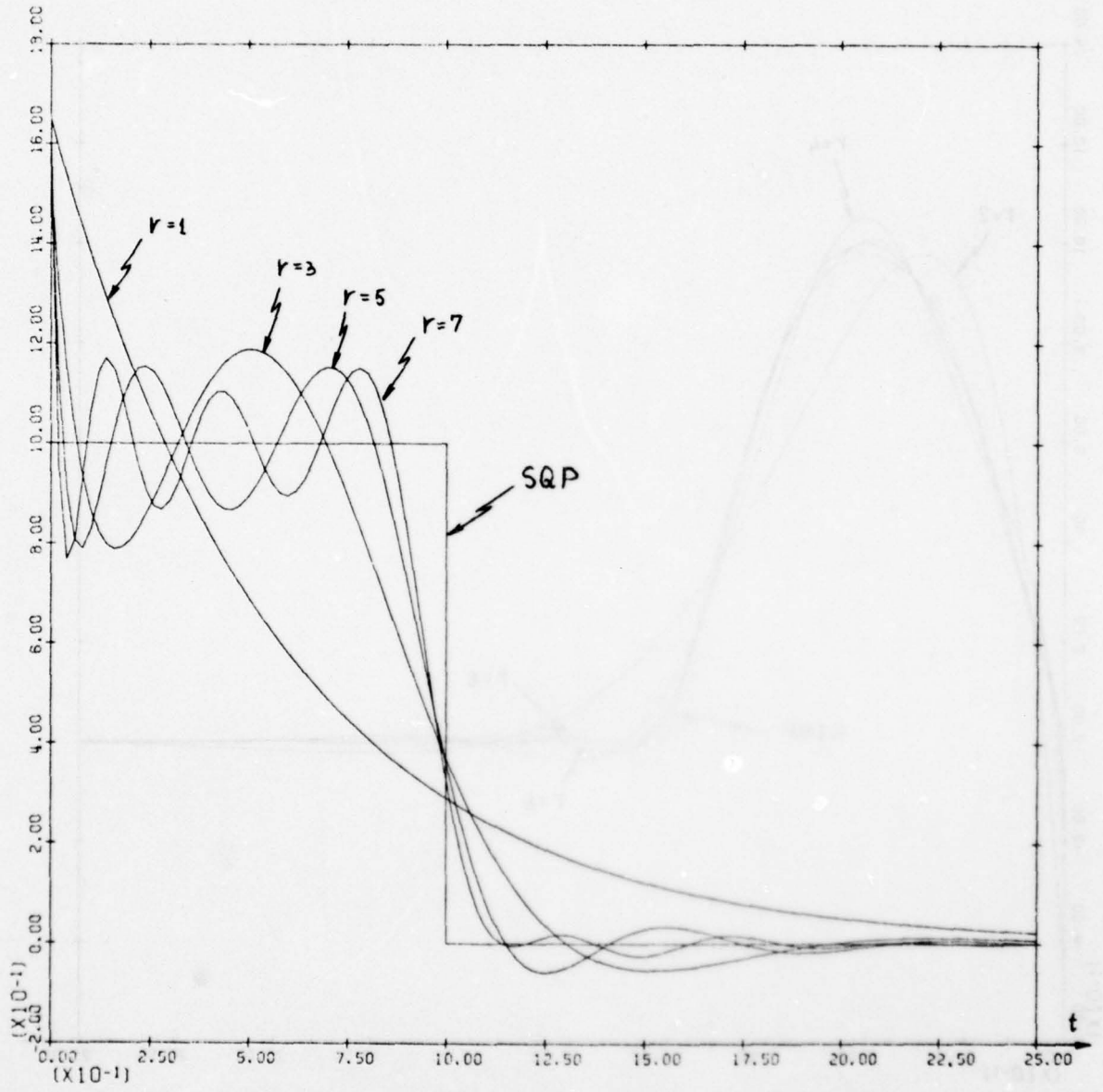

Fig. 3-1-7. Odd order approximations of SQP.

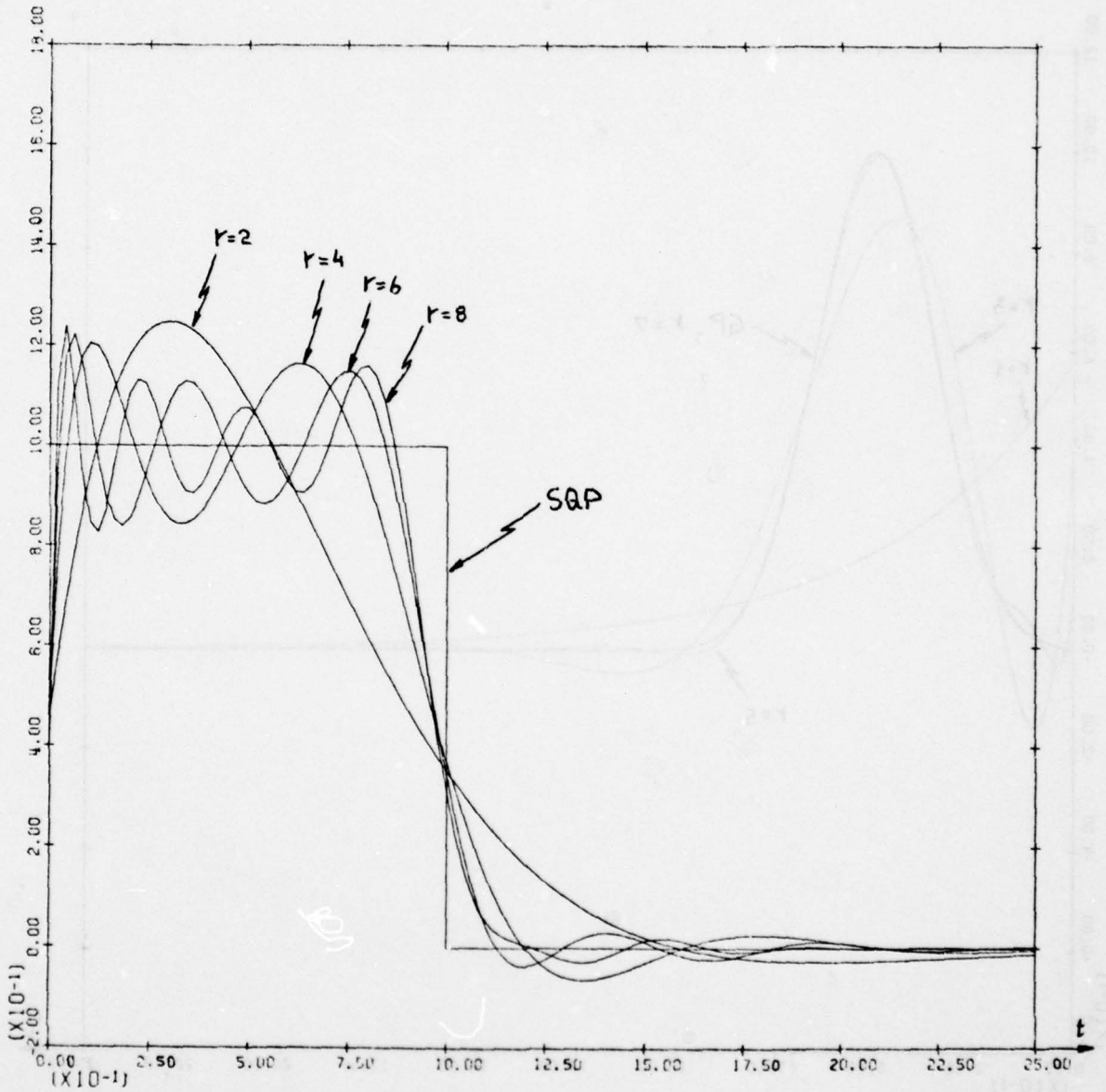

Fig. 3-1-8. Even order Approximations of SQP.

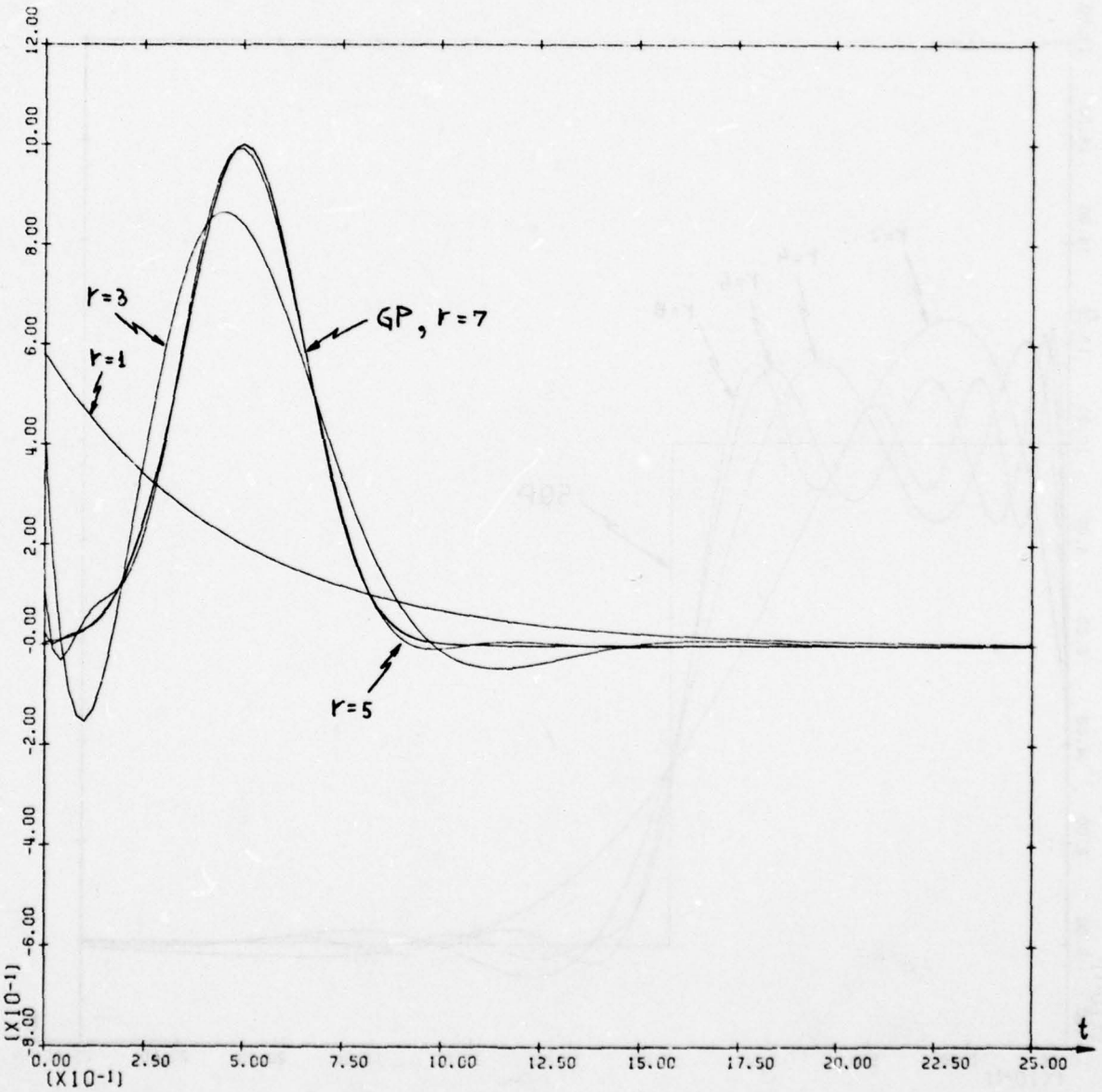

Fig. 3-1-9. Odd order approximations of GP.

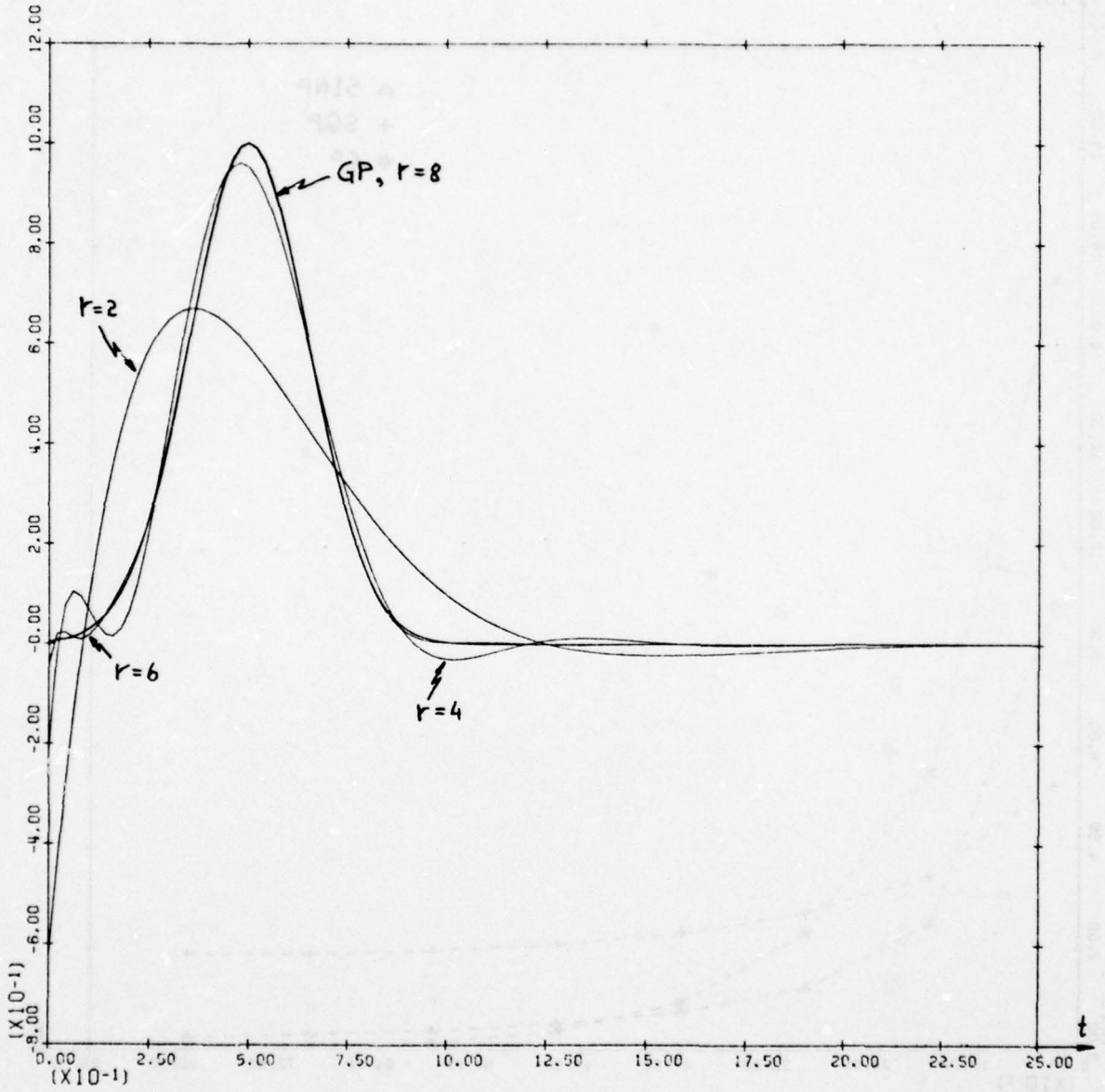

Fig. 3-1-10. Even order approximations of GP.

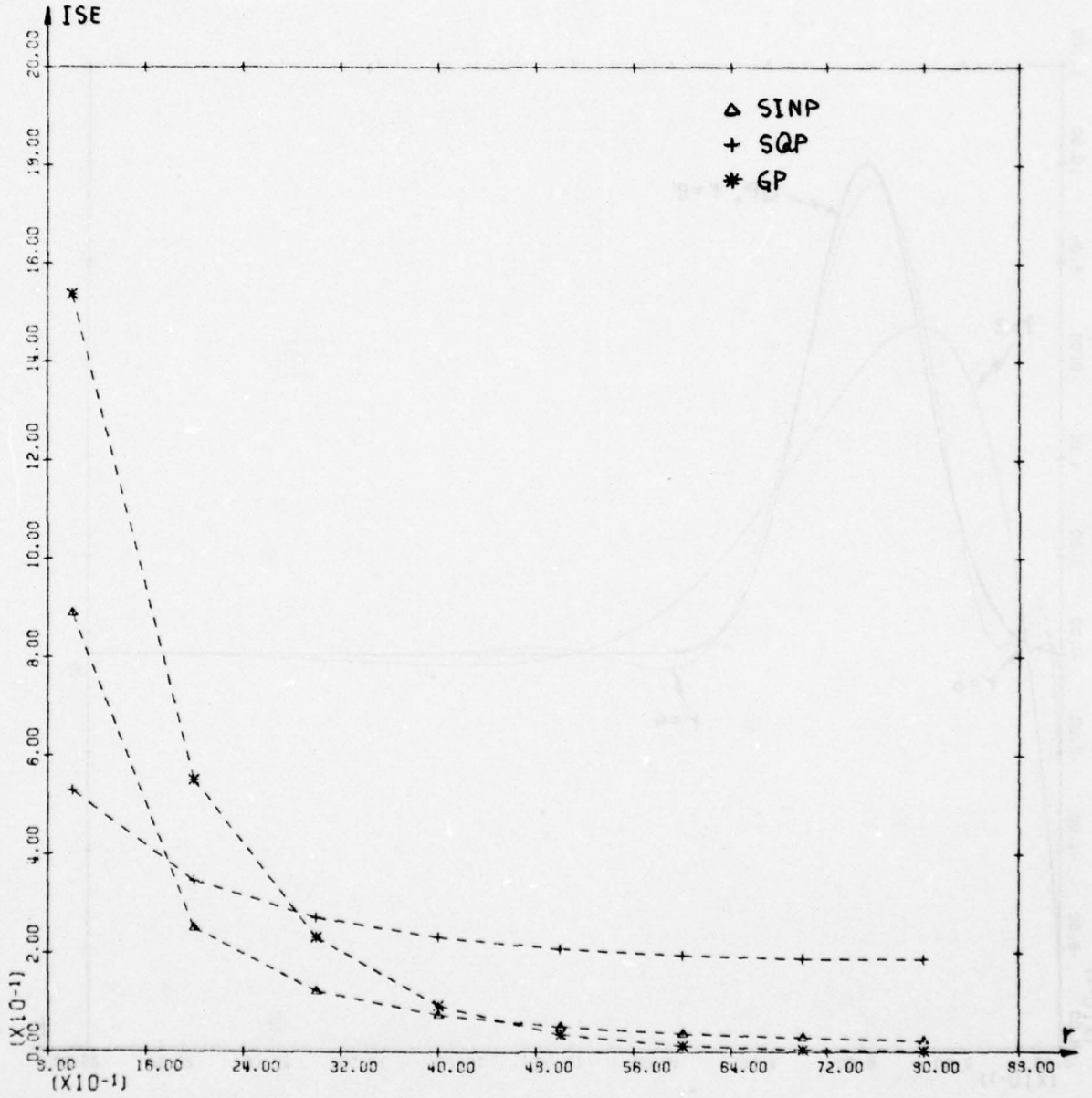

Fig. 3-1-11. The ISE as a function of r for SINP, SQP, and GP.

Although this function exists for all positive time, only that portion over the interval [0, 4π] was approximated (i.e., the integrations in the inner products extended from 0 to 4π). The SINC tree with r = 1, 2, . . ., 8 is presented in Fig. 3-1-4. The SINC function and its approximations for odd and even values of r, respectively, are presented in Figures 3-1-12 and 3-1-13. The integrated squared error, as a function of r, is plotted in Fig. 3-1-14.

Notice that the "time-limited" trees in Figures 3-1-1 through 3-1-3 grow to the left whereas the "nontime-limited" tree in Fig. 3-1-4 grows to the right. The trees demonstrate that a priority exists for the manner in which a waveform is approximated as the number of poles is increased. Given a small value of r, the poles are chosen so as to give a "best" fit to that portion of the waveform where most of the energy is concentrated. Additional poles are then used to refine the approximation to the remaining portion of the signal. For a time-limited signal the additional poles add terms to the approximation which have successively larger rates of decay in an effort to account for the faster-than-exponential decay of the signal at later instants of time. Conversely, for a nontime-limited signal the additional poles add terms to the approximation which have successively slower rates of decay in an effort to account for the slower-than-exponential decay of the signal at later instants of time.

For smooth time functions the tree branches consist of relatively smooth contours which are U-shaped about the real axis. The faster the rate of growth along the real axis, the faster is the decrease in the

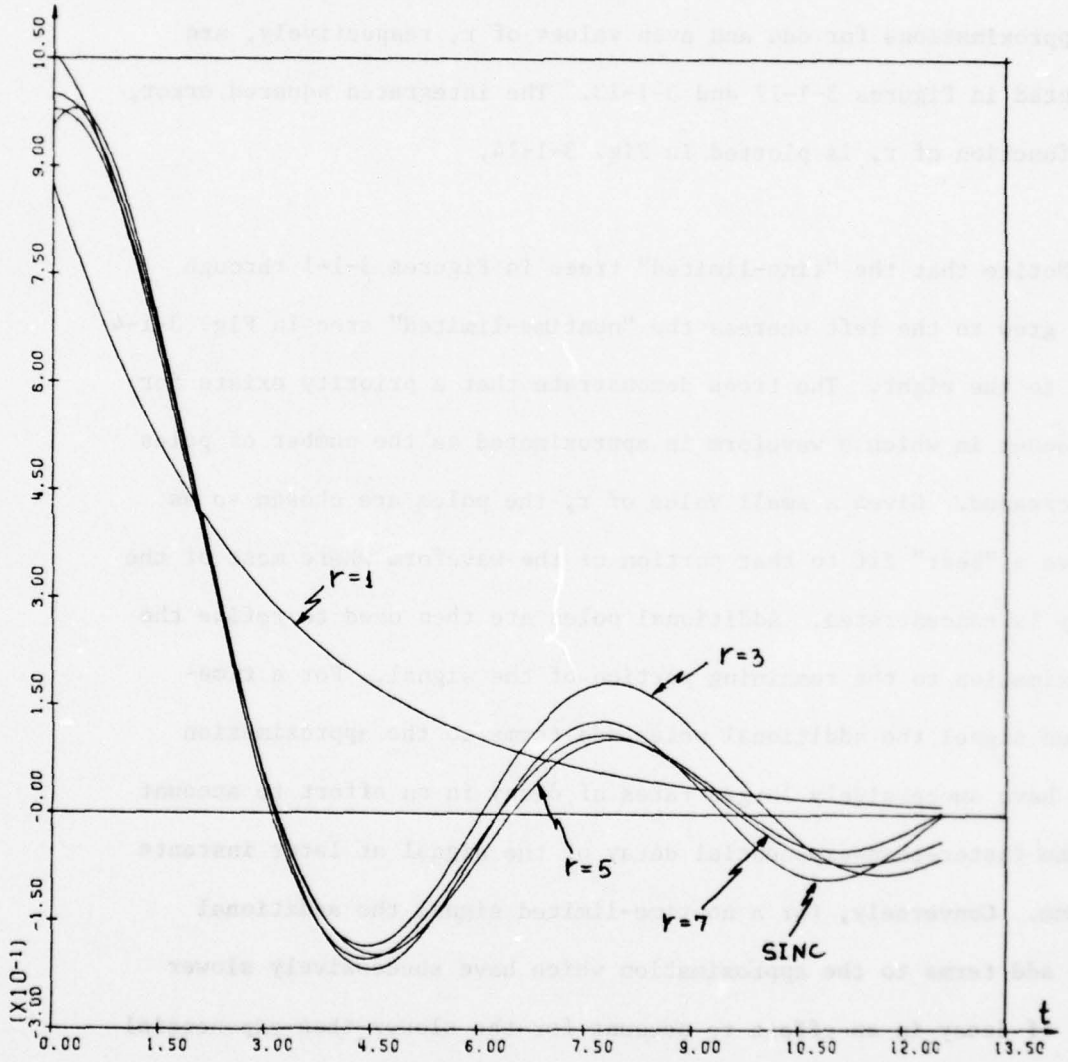

Fig. 3-1-12. Odd order approximations of SINC.

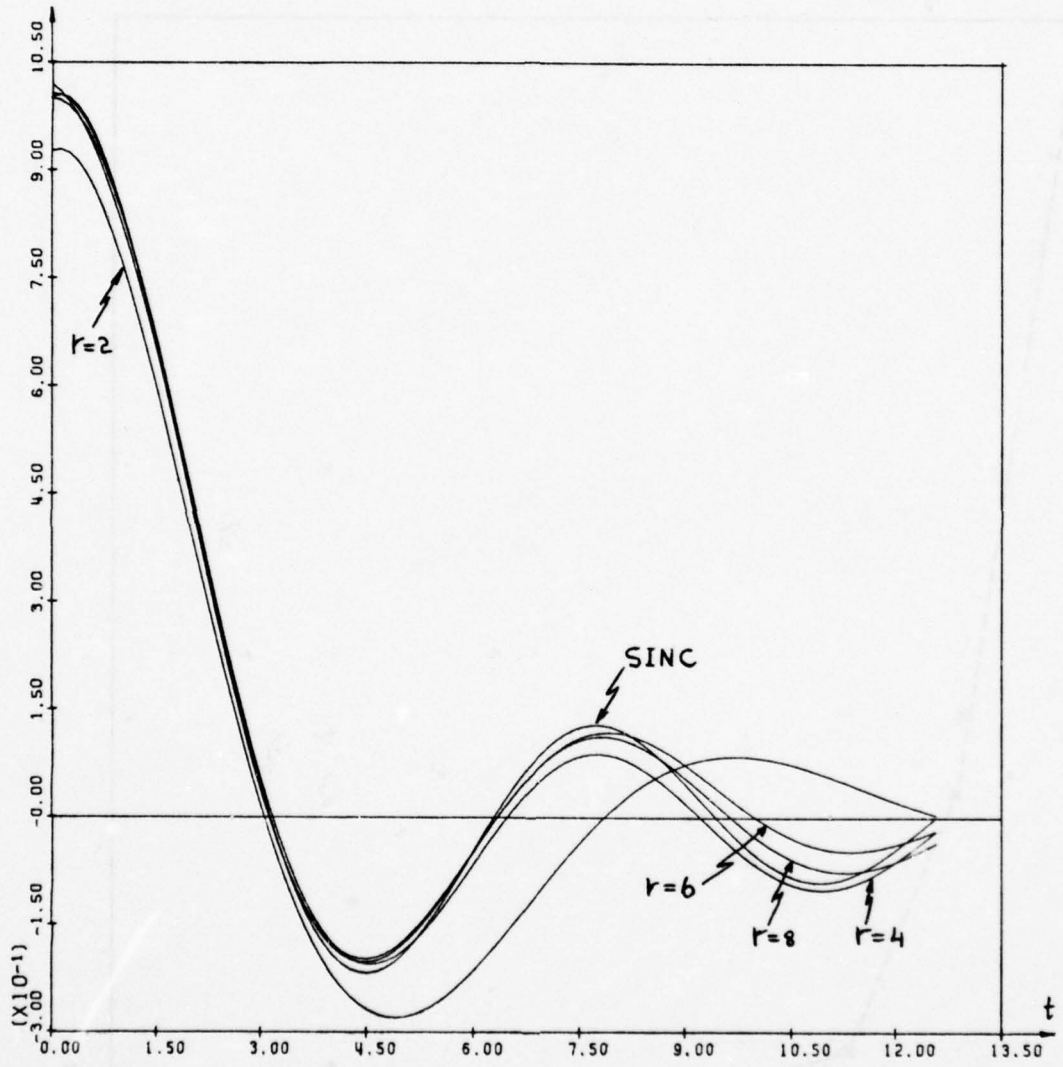

Fig. 3-1-13. Even order approximations of SINC

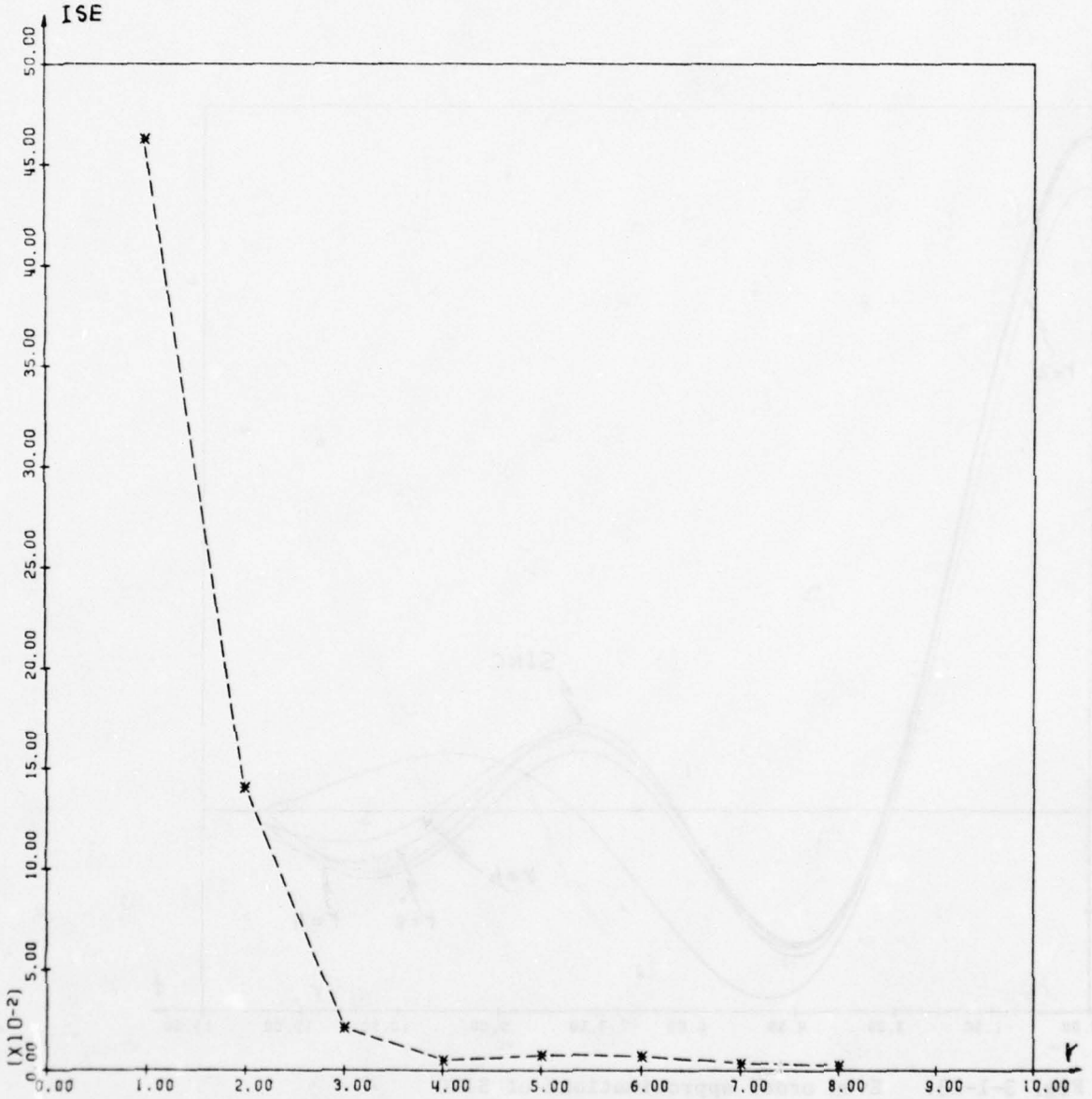

Fig. 3-1-14. The ISE as a function of r for SINC.

ISE. On the other hand, piecewise-continuous functions have tree branches which tend to wiggle to the right and left during the growth of the tree. Since these branches do not progress very rapidly along the real axis, their ISE decreases more slowly. This is illustrated by the ISE curves of Figures 3-1-11 and 3-1-14. This behavior is manifested in the time waveform approximations as a Gibb's phenomenon (see Figures 3-1-5 through 3-1-8).

The growth of the trees is seen to be highly structured. Therefore, given a tree up to order r, it is possible to obtain a reasonably good guess of the $(r + 1)^{th}$ trajectory by simply extrapolating each tree branch. In Fig. 3-1-2 for the SQP tree, the extrapolated pole positions for r = 9 are shown along with the actual approximation.

It is interesting to observe that the r^{th} order trajectory for both time-limited and nontime-limited functions is U-shaped to the right about the real axis. The only difference is that, for time-limited functions, the dominant poles are at the tips of the U while, for nontime-limited functions, the dominant poles are at the base of the U. It is also interesting to note that, although the trees in Figures 3-1-1, 3-1-2, and 3-1-3 are for three different pulses having approximately the same pulse width, the trees span roughly the same region of the S-plane.

The growing tree is a useful tool for discriminating against noise. For a signal composed of n exponentials the tree stops growing at r = n. When noise is present, the tree continues to grow beyond r = n. However, the actual poles tend to be perturbed only slightly while the additional poles, due to the noise, move significantly. This behavior can be used to determine both the system order and system poles under noisy conditions.

3.2 Iterative Optimization Techniques

The approximation/identification technique discussed previously are linear in the sense that a linear set of equations are solved for the numerator and denominator coefficients of the transfer function. These equations are generated by selecting the coefficients to minimize an error criterion such as least squares, integrated squared-error, etc. The system poles and zeros are nonlinearly related to the denominator and numerator coefficients, respectively, by means of polynomial equations. Some approximation/identification techniques solve directly for the poles and residues. The equations are now generated by selecting the poles and residues to minimize some suitable error criterion. These equations are highly nonlinear and are usually solved through some iterative scheme. Different iterative methods, mainly designed for the synthesis problem, are presented in [19], [20], [21], [22], [27], [28]. A good initial guess is highly desirable in order to minimize the number of iterations. In some cases, a good initial guess is required if the correct solution is to be achieved due to the presence of multiple local minima (i.e., the iteration should begin near the correct local minimum). It should be noted that minimizing an error criterion with respect to the transfer function coefficients is not equivalent to minimizing an error criterion with respect to the poles and residues. However, both approaches tend to be equivalent when the errors are small.

Although any one of the identification techniques discussed in chapter 2 could be used to provide the initial guess, not all of the operators and approximation techniques perform the same for a given problem. Hence, the identification technique chosen for a specific problem

should be selected with care. This is illustrated by the example discussed next.

Example 3-2-1

This example is one of the problems given at the RADC Spectral Estimation Workshop held May 24-26, 1978. It is interesting because it involves an FM signal which can be interpreted in terms of a slowly varying linear single-tuned circuit.

This problem concerns identifying emitters by their signal characteristics.

Problem: Determine the instantaneous frequency of the largest amplitude sinusoid within the portion of the spectrum of interest. The instantaneous frequency is defined as

$$\frac{1}{2\pi}\frac{d\phi}{dt}$$

where ϕ = argument of the sinusoid.

It is required to determine the instantaneous frequency every 0.04 sec. from t_1 through t_{16} where

$$t_1 = 0.04 \text{ sec.}$$
$$t_2 = 0.08 \text{ sec.}$$
$$\vdots$$
$$t_{16} = 0.64 \text{ sec.}$$

The data model is

$$x(t) = \sum_{i=1}^{P} A_i \cos(\phi_i) + n(t) \quad (\text{where } P \leq 5)$$

The summation consists of a single large-amplitude sinusoid (the "signal")

plus a number of smaller-amplitude sinusoids (the "interference"). There are "P" sinusoids in all.

The "noise" waveform is n(t). The resulting data waveform, x(t), has been sampled at an 800 samples/sec. rate, and the total duration of the data waveform is 0.64 sec. The sampled noise waveform is actually a sequence of pseudo-uniformly distributed random numbers.

The spectrum of interest is from 130 to 270 Hertz. The sampling rate was chosen to be at least four (4) times greater than the instantaneous frequency of any sinusoid in the summation above.

Some statistics concerning the data are:

1. The rate of frequency drift of any sinusoid is not greater than 190 Hertz/sec.

2. An estimate of the signal-to-noise ratio is:

$$10 \log_{10} \frac{\sum_{i=1}^{N} S_i^2}{\sum_{i=1}^{N} n_i^2} \approx 20 \text{ dB}$$

where N = 512 = the total number of data samples,

S_i denotes the sampled value of the largest amplitude sinusoid, without noise, at the time point t_i

n_i denotes the sampled value, at time point t_i, of the noise waveform, n(t).

3. An estimate of the signal-to-noise-plus-interference ratio is

$$10 \log_{10} \frac{\sum_{i=1}^{N} S_i^2}{\sum_{i=1}^{N} \left(n_i + \sum_{K=1}^{P-1} X_{K_i}\right)^2} \approx 17 \text{ dB}$$

where S_i and n_i have already been defined in (2) and where

$\sum_{K=1}^{P-1} X_{K_i}$ denotes the sum of the sampled values, at time point t_i, of all of the P-1 weaker sinusoids, the "interference".

The first thing to be noted in this problem is the low sampling rate which may produce as few as four samples per cycle. In addition, the frequency drift causes the problem to be time variant. If the problem is to be interpreted in terms of a sequence of time-invariant systems, only a limited number of samples can be used to estimate the frequency drift rate of 190 Hz/sec., the maximum frequency drift in .04 seconds in 7.6 Hz. Since this is less than 6% of the lowest frequency in the spectrum of interest (i.e., 130 Hz), the instantaneous frequency is assumed to be approximately constant over this interval. Hence, 32 samples, spaced about the data point, were used to determine the instantaneous frequency at each instant t_i. The slow sampling rate dictates the use of a discrete time operator for the identification procedure (i.e., it is difficult to visualize the time waveform from the data). In addition, the small number of samples which can be used at a time, discourages the use of a delay operator. Consequently, it was decided to use an overdetermined Prony approach. Because no exponential decays are involved in this problem, ill conditioning due to extremely small sample values is not a concern.

Since complex poles in a real system appear in conjugate pairs, the overdetermined Prony method was used to solve for two poles. (The interference and noise were assumed to be negligible since the signal-to-noise-plus-interference ratio was given to be approximately 17 dB). These poles provided the initial guess for a least squares direct search iterative scheme which varied the poles and residues in a systematic manner in order to minimize the error between the approximation and the sample values in the .04 second interval being considered.

The exact solution to the synthesized problem, as provided by RADC, is presented in Appendix B. The initial guess by means of the Prony technique and the solution obtained via the direct search iteration are shown in Figure 3-2-1 along with the exact solution (solid line). Fig. 3-2-2 is a plot of the instantaneous error for both the initial guess and the direct search. The initial guesses are seen to be quite good. However, the iteration scheme does result in an improvement at 13 of the 16 points. This solution was the best of all those submitted at the workshop and was considerably better than those obtained by conventional spectral estimation techniques such as Burg's maximum entropy, FFT, and ARMA (autoregressive moving average filter) approaches. A technique, based upon zero-crossing FM demodulation [33], provided a solution which was practically as good. Results for this approach are also plotted on Fig. 3-2-1 and compared in Fig. 3-2-3 where the zero-crossing method is seen to provide closer answers in 6 of the 16 points. The sum of squared errors for the iterative approach is 2.34 whereas that for the zero-crossing approach is 4.19.

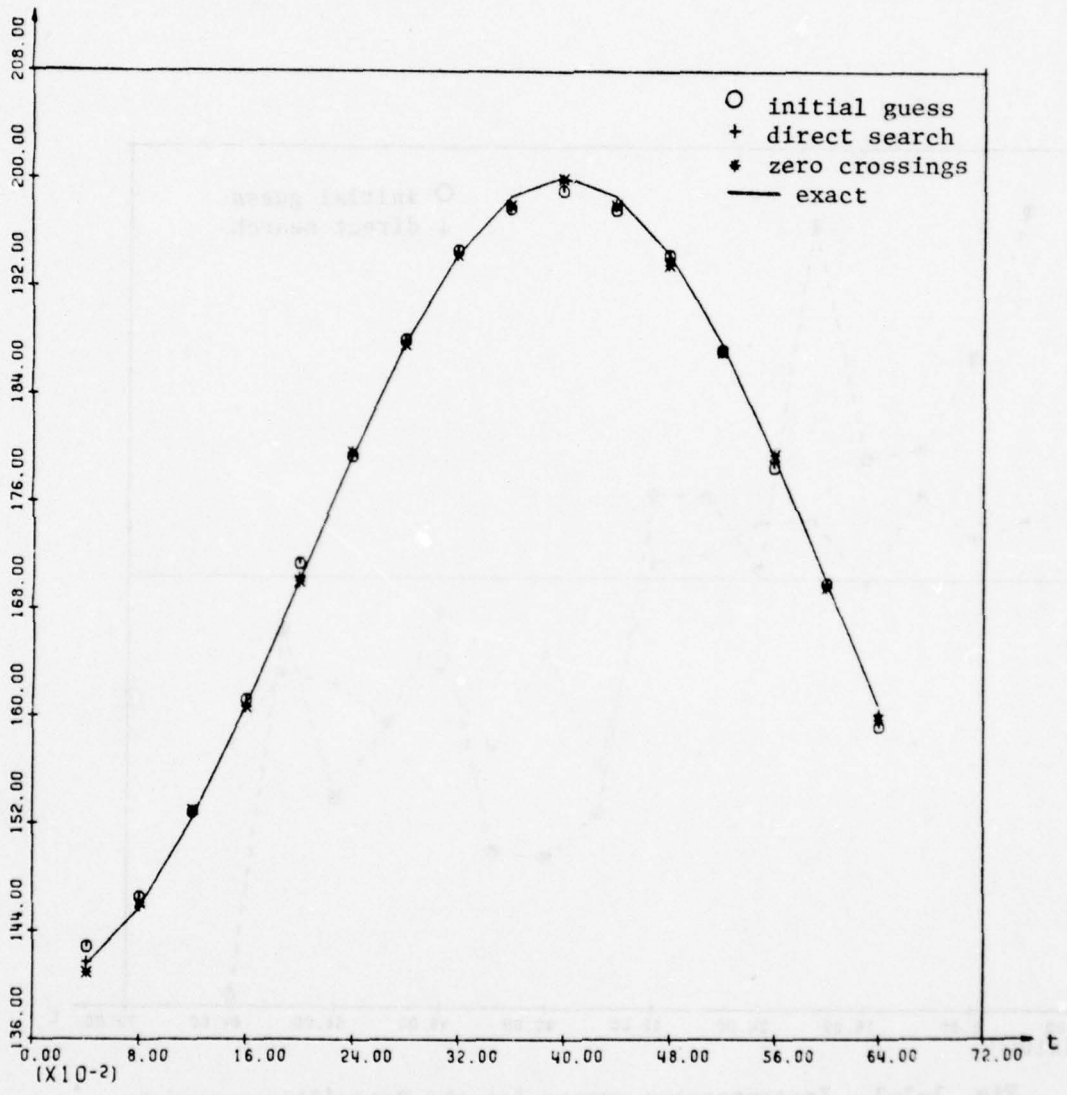

Fig. 3-2-1. Solutions to example 3-2-1.

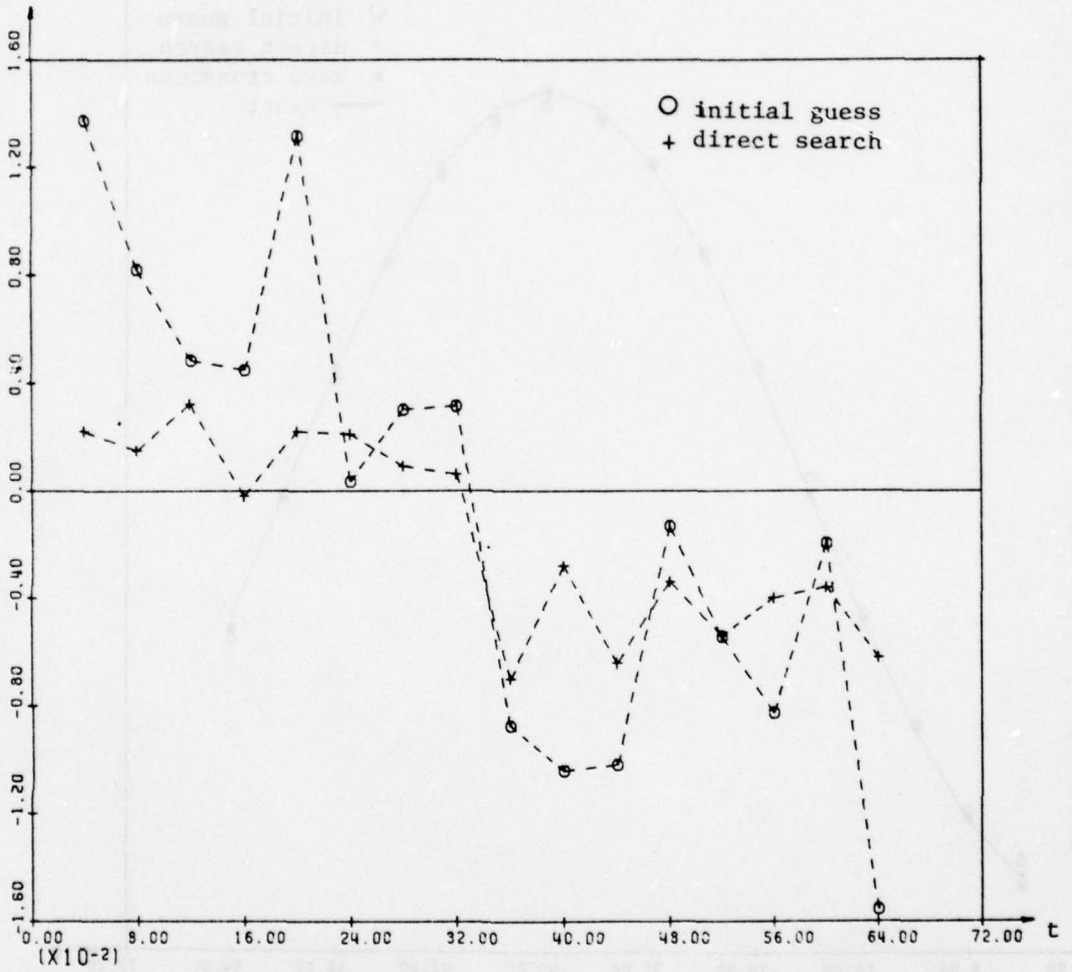

Fig. 3-2-2. Instantanuous errors for the Prony/direct search method.

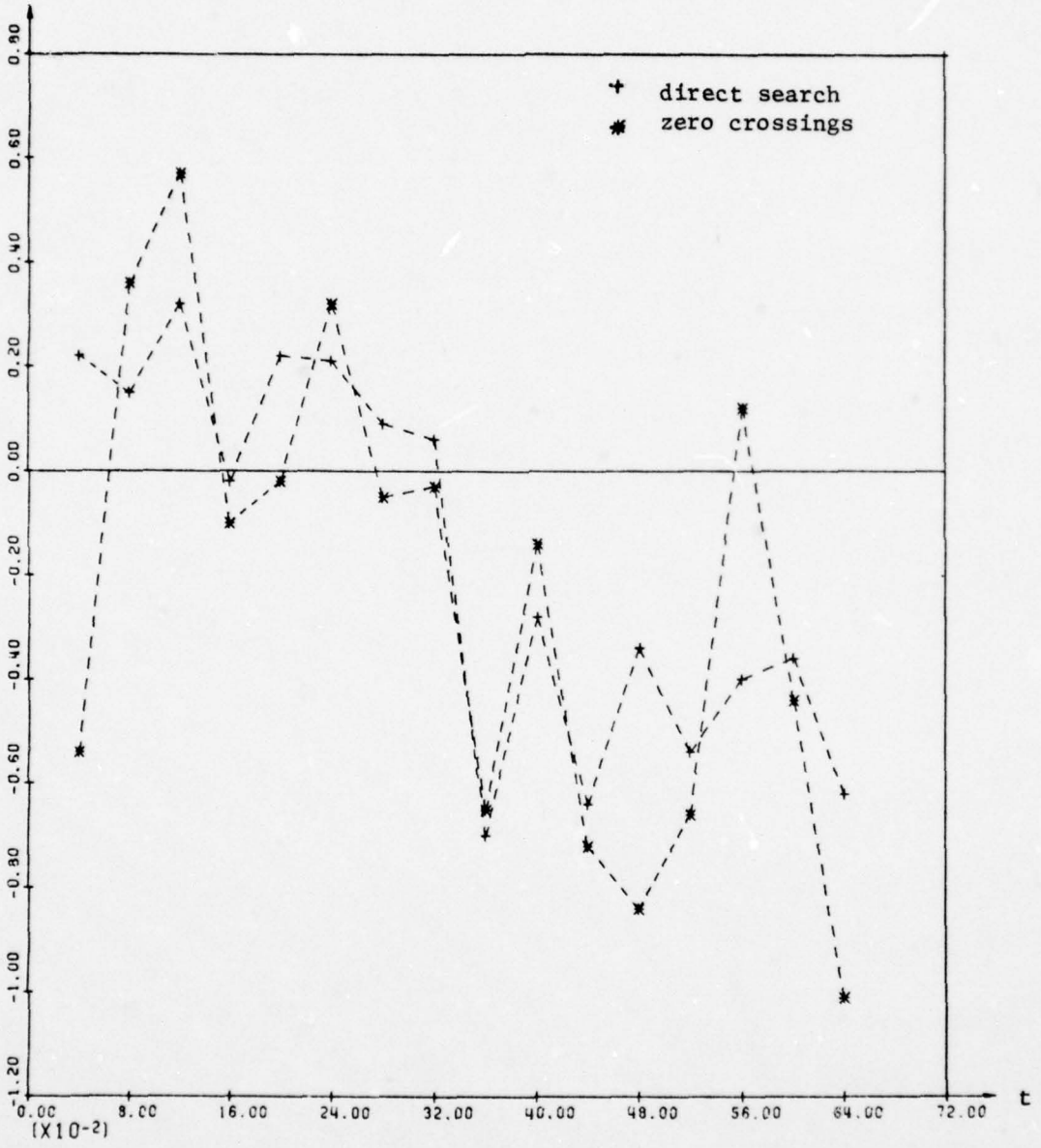

Fig. 3-2-3. Instantanuous errors associated with the direct search and zero crossings techniques.

Chapter 4

IDENTIFICATION OF WEAKLY NONLINEAR SYSTEMS

4.1 Introduction

The Volterra series representation for a weakly nonlinear system was introduced in Chapter 1. The series is most useful in applications where a finite number of terms N is adequate for modeling the system response (see (1-1-6)). It has been shown [34] that the n^{th}-order impulse response $h_n(t_1,\ldots,t_n)$ is a sum of exponentials when the linear impulse response $h_1(t)$ is a sum of exponentials. Also, the natural frequencies of the higher order transfer functions can be determined a priori from the natural frequencies of $h_1(t)$.

In particular, if the linear impulse response is given by

$$h_1(t) = \begin{cases} \sum_{i=1}^{K} R_i e^{\lambda_i t} & ; t \geq 0 \\ 0 & ; t < 0, \end{cases} \tag{4-1-1}$$

then the second-order impulse response is

$$h_2(t_1,t_2) = \begin{cases} \sum_{k_1=1}^{M} \sum_{k_2=1}^{K} A_{k_1k_2} e^{a_{k_1}t_1 + a_{k_2}t_2} & ; t_2 \geq t_1 \\ \sum_{k_1=1}^{M} \sum_{k_2=1}^{K} A_{k_1k_2} e^{a_{k_1}t_2 + a_{k_2}t_1} & ; t_2 \leq t_1 . \end{cases} \tag{4-1-2}$$

The terms for the third-order impulse response are of the same form as in (4-1-2). However, now a triple summation is involved over the indices k_1, k_2, and k_3 and the exponents of each term are of the form $(a_{k_i} \cdot t_1 + a_{k_j} \cdot t_2 + a_{k_\ell} \cdot t_3)$ where i, j, ℓ = 1,2, or 3, $i \neq j \neq \ell$, and there are six terms, one for each condition $t_i \geq t_j \geq t_\ell$ (See (7-5) of [34]).

The relation between the natural frequencies of (4-1-2) and those of (4-1-1) is given by

$$a_{k_1} \in \left\{ \begin{array}{ll} \lambda_i & i = 1,\ldots,K \\ \lambda_i + \lambda_j & i,j = 1,\ldots,K \end{array} \right\} \qquad (4\text{-}1\text{-}3)$$

$$a_{k_2} \in \left\{ \lambda_i \quad i = 1,\ldots,K \right\} .$$

In addition, the parameter M in (4-1-2) is

$$M = K^2 + 1 . \qquad (4\text{-}1\text{-}4)$$

Hence, given $h_1(t)$, the only unknowns in (4-1-2) are the residues $A_{k_1 k_2}$. These are determined using an appropriate sum of exponentials for the input to the weakly nonlinear system. The response is a sum of exponentials. This response is assumed to be the output of an equivalent linear system. The unknowns $A_{k_1 k_2}$ are uniquely related to the residues of the equivalent linear impulse response. Hence, by applying one of the approximation schemes to the equivalent impulse response, a set of linear equations can be written from which the coefficients $A_{k_1 k_2}$ can be determined.

The procedure begins by first determining $h_1(t)$. For this purpose, the input amplitude is maintained small enough such that nonlinear effects are negligible. The next step is to determine $h_2(t_1,t_2)$. The input

amplitude is now chosen such that second-order effects are noticeable but third-and higher-order effects are still negligible. The response due to the second-order portion of the system can be isolated by subtracting out a suitably weighted replica of the linear response. The procedure continues for $h_3(t_1,t_2,t_3)$ and so on. To determine the appropriate signal amplitude at each step, a single sinusoid is used as the input and the harmonic content of the output is checked.

4.2 Identification of a Transistor Amplifier

The identification approach discussed above was applied in [34] to identification of a transistor amplifier. The example is repeated here where the results of this dissertation are utilized to give additional insight into the problem. The amplifier, with the transistor replaced by its nonlinear incremental equivalent circuit, is shown in Fig. 4-2-1.

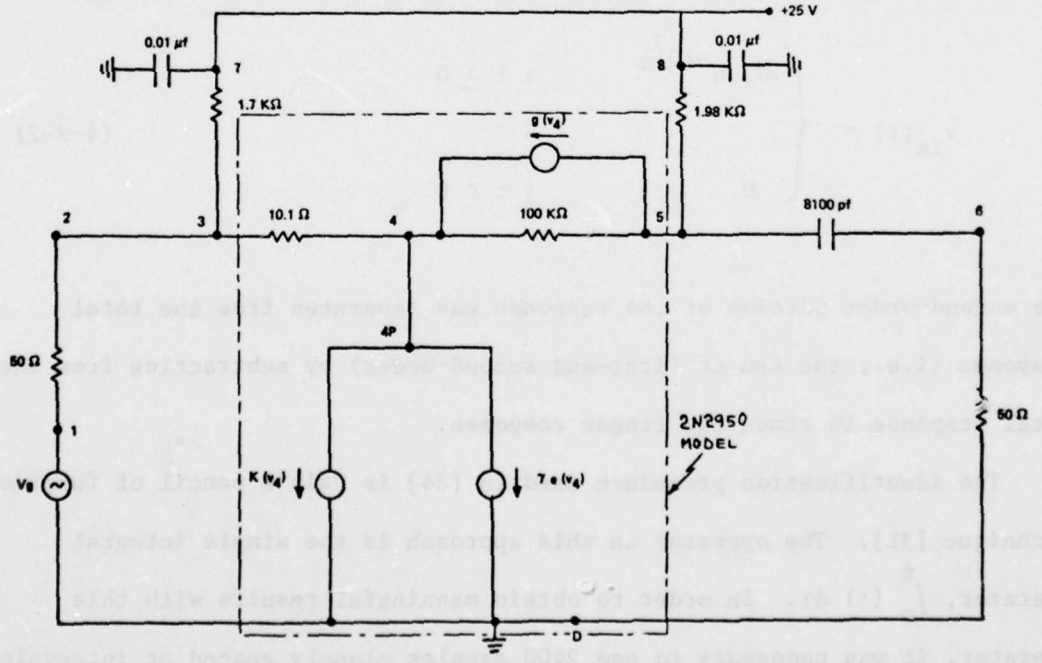

Fig. 4-2-1. Transistor Amplifier

The circuit and model parameters are given in [34] and are not repeated here. From [34] it is known that the system behaves linearly for input amplitudes less than 10^{-3} volts. With an input amplitude of 10^{-2} volts, a second-order response is noted while higher-order responses remain negligible.

In [34] the first-order impulse response was identified using as an input

$$v_{in}(t) = \begin{cases} .001\ e^{-10^7 t} & ;\ t \geq 0 \\ 0 & ;\ t < 0 \end{cases} \quad (4\text{-}2\text{-}1)$$

Identification of the second-order impulse response utilized the input

$$v_{in}(t) = \begin{cases} .01\ e^{-10^7 t} & ;\ t \geq 0 \\ 0 & ;\ t < 0 \end{cases} \quad (4\text{-}2\text{-}2)$$

The second-order portion of the response was separated from the total response (i.e., the sum of first-and second-order) by subtracting from the total response 10 times the linear response.

The identification procedure used in [34] is Jain's pencil of functions technique [31]. The operator in this approach is the simple integral operator, $\int_o^t (\cdot)\, d\tau$. In order to obtain meaningful results with this operator, it was necessary to use 2400 samples closely spaced at intervals of 10^{-9} seconds. The system order was established to be n = 2. (This

value is correct, as is obvious by inspection of Fig. 4-2-1). The poles and residues found in [34] for $h_1(t)$ are given in Table 4-2-1.

Table 4-2-1

Pole	residue
$\lambda_1 = -.011551(2\cdot 10^6\pi)$	$.2807(10^6)$
$\lambda_2 = -10.6169(2\cdot 10^6\pi)$	$273.684(10^6)$

As pointed out in case 5 of example 2-4-1, the simple integral operator is a poor choice because it results in a highly linearly dependent set of basis functions. Consequently, the example was repeated using the advance (negative delay) operator of (2-4-39). Only 151 samples spaced at intervals of 10^{-8} seconds were used (i.e., many fewer samples and a slightly shorter data record than in [34]). The advance T was set equal to 10^{-7} seconds (i.e., every 10 samples). The poles and residues determined in this manner are presented in Table 4-2-2.

Table 4-2-2

pole	residue
$\lambda_1 = -.011454(2\cdot 10^6\pi)$	$.27502(10^6)$
$\lambda_2 = -10.8071(2\cdot 10^6\pi)$	$279.107(10^6)$

Figure 4-2-2 presents the true output and the two responses generated by the poles and residues of Tables 4-2-1 and 4-2-2.

From (4-1-2) notice that $h_2(t_1,t_2)$, evaluated for $t_1 = t_2 = t$, becomes

$$h_2(t,t) = h_1 \text{ equiv. } (t) = \sum_{k_1=1}^{M} \sum_{k_2=1}^{K} A_{k_1 k_2} e^{(a_{k_1} + a_{k_2})t} \qquad (4\text{-}2\text{-}3)$$

From (4-1-4) and table 4-2-1, it follows that

$$M = K^2 + 1 = 2^2 + 1 = 5 \ . \qquad (4\text{-}2\text{-}4)$$

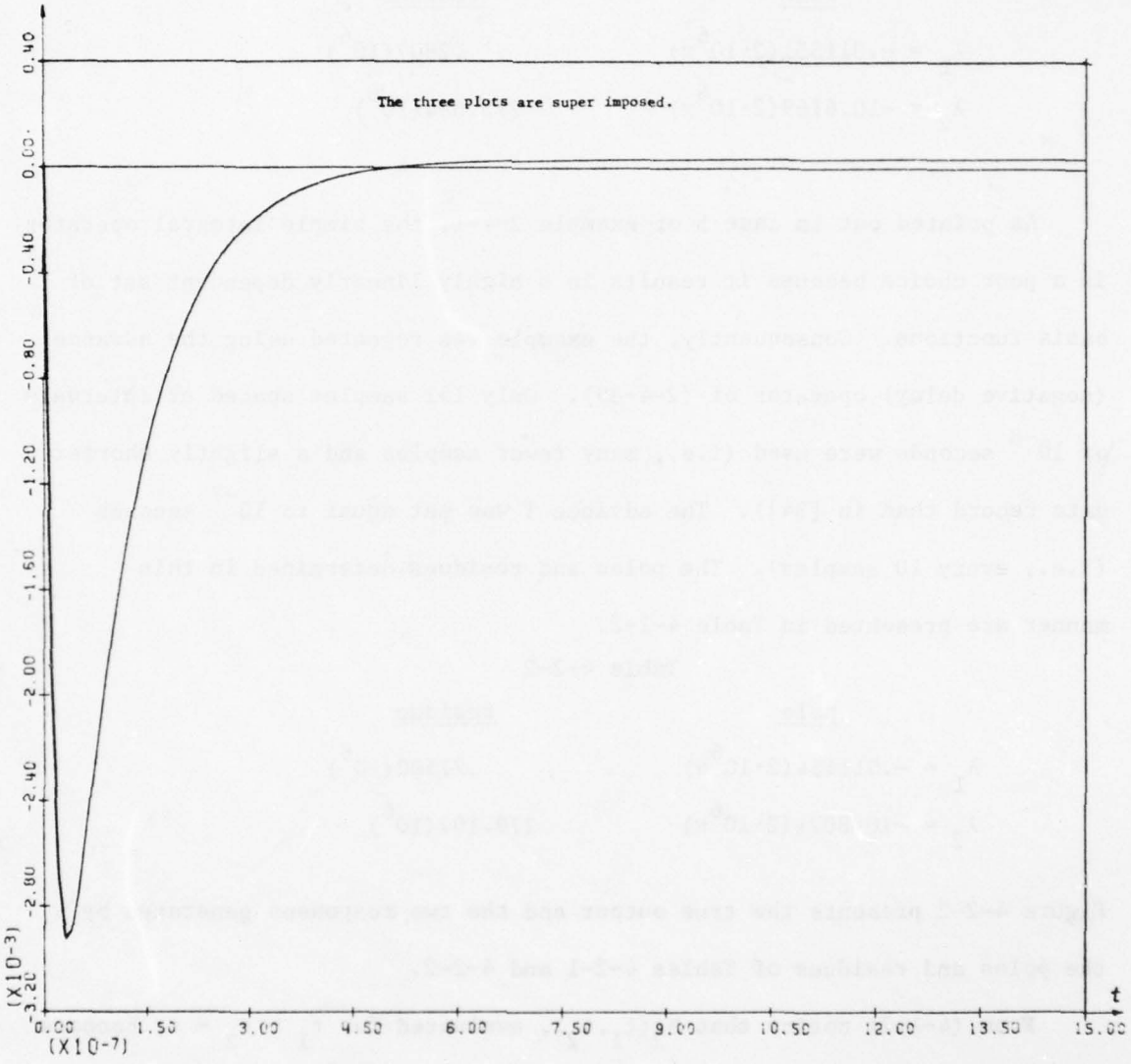

Fig. 4-2-2. True output and responses generated by the identified poles and residues.

Hence, the natural frequencies of (4-2-3) are tabulated in Table 4-2-3.

Table 4-2-3

#	M	K	Natural frequency of (4-2-3)	in terms of λ_1, λ_2	Comments
1	1	1	$a_1 + a_1$	$2\lambda_1$	
2	2	1	$a_2 + a_1$	$\lambda_2 + \lambda_1$	
3	3	1	$a_3 + a_1$	$2\lambda_1 - \lambda_2$	Not allowed
4	4	1	$a_4 + a_1$	λ_2	
5	5	1	$a_5 + a_1$	λ_1	
6	1	2	$a_1 + a_2$	$\lambda_1 + \lambda_2$	Same as 2
7	2	2	$a_2 + a_2$	$2\lambda_2$	
8	3	2	$a_3 + a_2$	λ_1	Same as 5
9	4	2	$a_4 + a_2$	$2\lambda_2 - \lambda_1$	Not allowed
10	5	2	$a_5 + a_2$	λ_2	Same as 4

Therefore, the allowable natural frequencies of (4-2-3) are given by

$$\{\lambda_1, \lambda_2, 2\lambda_1, 2\lambda_2, \lambda_1 + \lambda_2\} . \qquad (4\text{-}2\text{-}5)$$

A procedure for determining the coefficients $A_{k_1 k_2}$ is outlined in [34].

It should be mentioned that the set of equations for $A_{k_1 k_2}$ becomes highly linearly dependent when the dynamic range in the natural frequencies of the linear response is large. For example, if $\lambda_2 >> \lambda_1$, then $\lambda_2 + \lambda_1 \simeq \lambda_2$. The natural frequencies of (4-2-5) then give rise to an almost linearly dependent set of basis functions. In our example,

$$\frac{\lambda_2}{\lambda_1} \simeq 10^3 . \qquad (4\text{-}2\text{-}6)$$

Consequently, the equations in [34] for $A_{k_1 k_2}$ were extremely difficult to solve. A remedy for this situation is to consider $\lambda_2 + \lambda_1$ to be the same natural frequency as λ_2. As a result, the set of (4-2-5) is reduced to

$$\{\lambda_1, \lambda_2, 2\lambda_1, 2\lambda_2\} \qquad (4\text{-}2\text{-}7)$$

Removal of the natural frequency $(\lambda_1 + \lambda_2)$ eliminates the ill-conditioned nature of the equations without severely affecting the identification.

Chapter 5

SUMMARY

5.1 Discussion of Results and Conclusions

A general parametric model for the black box identification of linear time invariant systems, in terms of rational transfer functions, was developed. The parameters obtained from the identification procedure are, in general, the coefficients of the numerator and denominator polynomials of the transfer function transformed to a ν-plane. A transform associated with each operator used was defined such that the transfer function can be transformed back from the ν-plane to the S-plane. From the general class of operators used, two subgroups of operators were emphasized. One group is represented by all the operators preserving the S-plane coefficients. The other is the group of operators defined in the discrete z-domain.

It was demonstrated that parametric techniques from the published literature, are special cases of the general model associated with a particular approximation technique. It is emphasized in this dissertation that there are two separate stages at which the identification is carried out. One is the generation of the basis set via the chosen linear operator. The other is the choice of an approximation scheme.

The use of different operators and different approximation schemes was demonstrated through a variety of examples. It was pointed out that some operators might perform better than others in a given problem. In general, the performance of an operator is dependent upon the data provided, although some operators are shown to be inherently "bad

performers ".

Having in mind line models of spectral estimates, there is a tendency to require very long records of data such that high frequency "resolution" be obtained. This is true for line spectra and is attributed to the Sinc function behavior of the correlation coefficient between two sinusoids (i.e., the correlation function decays as t^{-1}). For decaying signals like exponentials, this conclusion is false. It was shown that for exponentials the correlation coefficient asymptotes to a value defined by the exponentials' parameters. Hence, the magnitude of the correlation coefficient cannot be made arbitrarily small by increasing the record length. A "long-record" was developed based upon the decaying signal parameters. This "long-record" is of finite length and any increase of that record will add negligible improvement to the identification. Also, on the basis of the "long record" a rough estimate for the system's order was developed.

The "growing tree" was introduced as another aid in determining the system's order. The potential benefit of the "growing tree" when applied to time domain synthesis problems was also pointed out.

Application of the identification model to slowly time-variant systems and weakly nonlinear systems was discussed and demonstrated through numerical examples.

5.2 Areas for Future Research

The vast bank of operators should be investigated and classified on the basis of their performance when applied to different types of identification problems.

The applicability of the identification model to the extended class

of slowly time-variant systems and weakly nonlinear systems should be further investigated.

The "growing tree" concept appears to be a promising tool. Its behavior should be analyzed on firmer mathematical grounds. From the different examples worked out, it seems that a signal's rate of decay and its bandwidth are strongly related to the region in the S-plane occupied by the tree. This relation should be examined.

Appendix A

AN INTRODUCTION TO SOME KNOWN APPROXIMATION TECHNIQUES

A-1. Methods Involving a Known Set of Basis Functions

Let $\{g_i(t)\}$, $i = 1,2, \ldots,N$, denote a given set of basis functions. Assume that the real time function $x(t)$ is to be approximated over the closed time interval $[T_1,T_2]$ by the finite sum

$$\hat{x}(t) = \sum_{i=1}^{N} K_i g_i(t). \qquad \text{(A-1-1)}$$

The problem is to determine the N coefficients K_i, $i = 1,2,\ldots,N$, so as to obtain a reasonable approximation. Different approaches to the approximation will, of course, result in different sets of coefficients.

Basically, what is needed is a set of N linearly independent equations involving the N unknown expansion coefficients. One approach is to require the approximation to equal $x(t)$ at N different instants of time t_j, $j = 1,2,\ldots,N$, where $T_1 \leq t_j \leq T_2$. The resulting approximation is written as

$$\hat{x}_I(t) = \sum_{i=1}^{N} D_i g_i(t) \qquad \text{(A-1-2)}$$

where the coefficients are determined from the N linear equations

$$\hat{x}_I(t_j) = x(t_j) \quad , \quad j = 1,2,\ldots,N. \qquad \text{(A-1-3)}$$

The subscript I in (A-1-2) is used to indicate that the approximation can be interpreted as an interpolation scheme for obtaining approximate values of $x(t)$ at instants different from t_j. This approach has the serious disadvantage that all time functions having the same sample

values at the N instants of time result in the same approximation. Therefore, there is no control over the interpolation error at the nonsampling instants.

The approximation may be improved by utilizing M sample points where $M > N$. We can no longer require zero error at the sampling instants. Nevertheless, a "better" overall fit can be obtained according to some specified criterion. Using a least-square approach, we write the approximation as

$$\hat{x}_{LS}(t) = \sum_{i=1}^{N} L_i g_i(t) \qquad \text{(A-1-4)}$$

where the coefficients L_i, $i = 1,2,\ldots,N$ are found by minimizing the sum of the squared errors.

$$\varepsilon_{LS} \triangleq \sum_{j=1}^{M} [x(t_j) - \hat{x}_{LS}(t_j)]^2. \qquad \text{(A-1-5)}$$

Carrying out the minimization with respect to the coefficients results in the N linear equations

$$\frac{\partial \varepsilon_{LS}}{\partial L_k} = -2 \sum_{j=1}^{M} [x(t_j) - \sum_{i=1}^{N} L_i g_i(t_j)] g_k(t_j) = 0, \quad k = 1,2,\ldots,N. \qquad \text{(A-1-6)}$$

Rearranging terms, we obtain

$$\sum_{j=1}^{M} \sum_{i=1}^{N} g_k(t_j) g_i(t_j) L_i = \sum_{j=1}^{M} g_k(t_j) x(t_j), \quad k = 1,2,\ldots,N. \qquad \text{(A-1-7)}$$

When $M = N$, (A-1-7) reduces to (A-1-3).

The sampling ratio is defined to be

$$R = \frac{M}{N}. \tag{A-1-8}$$

When this ratio is greater than unity, the problem is said to be overdetermined. Clearly, the average distance between the sampling instants is reduced by a factor of R in the overdetermined case. In this sense, better control of the interpolated values is obtained due to the higher density of sampling points. However, as before, all time functions having the same sample values at the M time instant result in the same approximation. Ideally, the larger the value of R, the better. On the other hand, the computation becomes excessive when R is made too large. Also, the equations become linearly dependent due to numerical roundoff as the sampling instants become too close.

Instead of restricting attention to discrete instants of time, we now generate approximations by considering the continuous interval $[T_1,T_2]$. The integrated-squared-error is defined to be

$$\varepsilon_{ISE} \triangleq \int_{T_1}^{T_2} [x(t) - \hat{x}_{ISE}(t)]^2 dt \tag{A-1-9}$$

where

$$\hat{x}_{ISE}(t) = \sum_{i=1}^{N} A_i g_i(t) \tag{A-1-10}$$

The coefficients A_i, $i = 1,2,\ldots,N$, are obtained by minimizing ε_{ISE}. The minimization results in

$$\sum_{i=1}^{N} \left[\int_{T_1}^{T_2} g_k(t) g_i(t) dt\right] A_i = \int_{T_1}^{T_2} g_k(t) x(t) dt, \quad k=1,2,\ldots,N \tag{A-1-11}$$

In general, it is not possible to solve for each coefficient individually because (A-1-11) represents N simultaneous linear equations. The situation is greatly simplified when the basis functions are orthonormal.

For emphasis, we denote a set of basis functions which are orthonormal over the interval $[T_1,T_2]$ by $\{\psi_i\}$ and write the approximation as

$$\hat{x}_{OISE}(t) = \sum_{i=1}^{N} \alpha_i \psi_i(t). \qquad \text{(A-1-12)}$$

To simplify matters, the basis functions are assumed to be real. The orthonormal relationship is then written as

$$\langle \psi_i, \psi_j \rangle \triangleq \int_{T_1}^{T_2} \psi_i(t)\psi_j(t)dt = \delta_{ij} \qquad \text{(A-1-13)}$$

where

$$\delta_{ij} = \begin{cases} 1 & i = j \\ 0 & i \neq j \end{cases} \qquad \text{(A-1-14)}$$

Minimizing the integrated-squared-error for the orthonormal basis representation, the equation for the coefficients α_i become

$$\alpha_i = \int_{T_1}^{T_2} \psi_i(t)x(t)dt, \qquad i = 1,2,\ldots,N \qquad \text{(A-1-15)}$$

The solutions for the coefficients are seen to be uncoupled for this special case.

As with the previous methods, several different time functions can result in the same approximation. For example, let n(t) be

orthogonal to $\{g_i\}$ over the interval $[T_1,T_2]$. It then follows that the integrated-squared-error approximations of $x(t)$ and $y(t) = x(t) + n(t)$ are identical. However, the integrated-squared-errors $\varepsilon_{ISE}(x)$ and $\varepsilon_{ISE}(y)$ will be different for the two waveforms.

Another approach to the approximation problem involves consideration of the derivatives and/or integrals of $x(t)$. Let the n^{th} derivative of $x(t)$ be denoted by

$$x^{(n)}(t) = \frac{d^n x(t)}{dt^n} \qquad \text{(A-1-16)}$$

where n is a nonnegative integer. The first N terms of a Taylor series expansion about the point $t = T$ results in the approximation

$$\hat{x}_p(t) = \sum_{\ell=0}^{N-1} x^{(\ell)}(T) \frac{(t - T)^{\ell}}{\ell!} \qquad \text{(A-1-17)}$$

where the subscript p indicates that the basis functions consist of polynomials in t, the error is given by the remainder

$$R_N(t) = x(t) - \hat{x}_p(t) = \frac{1}{(N-1)!} \int_T^t (t-\tau)^{N-1} x^{(N)}(\tau) d\tau \; . \qquad \text{(A-1-18)}$$

Proof of this follows directly by evaluating the integral in (A-1-18) through N successive integrations by parts.

To obtain an accurate approximation of $x(t)$ in the vicinity about $t = T$ when using a general set of basis functions $\{g_i\}$, we require that the approximation and its first N-1 derivatives equal the function and its first N-1 derivatives, respectively, at $t = T$. Denote the approximation by

$$\hat{x}_{ED}(t) = \sum_{i=1}^{N} E_i g_i(t) \qquad \text{(A-1-19)}$$

where the subscript ED represents equality of derivatives at time T. Hence, the N coefficients E_i, i = 1,2,...,N, are determined from the following set of N linear equations:

$$\hat{x}_{ED}^{(\ell)}(T) = x^{(\ell)}(T), \qquad \ell = 0,1,\ldots,N-1 \; . \qquad \text{(A-1-20)}$$

It follows that (A-1-17) may be expressed as

$$\hat{x}_p(t) = \sum_{\ell=0}^{N-1} \hat{x}_{ED}^{(\ell)}(T) \frac{(t-T)^{\ell}}{\ell!} \qquad \text{(A-1-21)}$$

which is recognized as the first N terms in the Taylor series expansion for $\hat{x}_{ED}(t)$. By analogy with (A-1-18),

$$\hat{x}_{ED}(t) - \hat{x}_p(t) = \frac{1}{(N-1)!} \int_T^t (t-\tau)^{N-1} \hat{x}_{ED}^{(N)}(\tau) d\tau \; . \qquad \text{(A-1-22)}$$

Subtraction of (A-1-22) from (A-1-18) yields the instantaneous error expression

$$\varepsilon_E(t) = x(t) - \hat{x}_{ED}(t) = \frac{1}{(N-1)!} \int_T^t (t-\tau)^{N-1} [x^{(N)}(\tau) - \hat{x}_{ED}^{(N)}(\tau)] d\tau \; . \qquad \text{(A-1-23)}$$

Let the interval $[T_3,T_4]$ be contained within the interval $[T_1,T_2]$. An approximation to x(t) can also be obtained by requiring that the approximation and its first (N-1) integrals equal the function and its first (N-1) integrals, respectively, over $[T_3,T_4]$. The n^{th}-order integral of x(t) is given by

$$x^{(-n)}(t) = \underbrace{\int_{T_3}^{t} \cdots \int_{T_3}^{\lambda_3} \int_{T_3}^{\lambda_2}}_{n} x(\lambda_1)d\lambda_1 d\lambda_2 \cdots d\lambda_n \qquad \text{(A-1-24)}$$

$$= \int_{T_3}^{t} \frac{(t-\tau)^{n-1}}{(n-1)!} x(\tau)d\tau.$$

The approximation is denoted by

$$\hat{x}_{EI}(t) = \sum_{i=1}^{N} F_i g_i(t) \qquad \text{(A-1-25)}$$

where the subscript EI indicates equality of integrals over $[T_3,T_4]$. The coefficients F_i, $i = 1,2,\ldots,N$, are determined from the N linear equations

$$\hat{x}_{EI}^{(-\ell)}(T_4) = x^{(-\ell)}(T_4), \qquad \ell = 0,1,\ldots,N-1. \qquad \text{(A-1-26)}$$

The two previous approximations may be combined to yield yet another approximation. This is accomplished by requiring the first K integrals from (A-1-26) and the first N-K derivatives from (A-1-20) to be equal. The approximation is now denoted by

$$\hat{x}_{EID}(t) = \sum_{i=1}^{N} H_i g_i(t) \qquad \text{(A-1-27)}$$

where the subscript EID indicates equality of both integrals and derivatives. For simplicity we set $T_4 = T$. The coefficients H_i, $i = 1,2,\ldots,N$, are then determined from the N linear equations

$$\hat{x}_{EID}^{(\ell)}(T) = x^{(\ell)}(T), \qquad \ell = -K, \ldots,-1,0,1,\ldots,N-K-1 . \qquad \text{(A-1-28)}$$

The approximation in (A-1-27) can be further generalized by overdetermining the problem. Assume the number of sampling points is given by M and that a total of L derivatives and/or integrals of x(t) are to be considered. Let the approximation be expressed as

$$\hat{x}_{GLS}(t) = \sum_{i=1}^{N} Q_i g_i(t) \qquad \text{(A-1-29)}$$

where the subscript GLS indicates that the coefficients Q_i are to be determined from a generalized least-square approach. Taking into consideration the first K integrals and the first L-K derivatives of x(t) (including the zero-order derivative), the sum of the squared errors becomes

$$\varepsilon_{GLS} = \sum_{\ell=-K}^{L-K-1} \sum_{j=1}^{M} [x^{(\ell)}(t_j) - \hat{x}^{(\ell)}_{GLS}(t_j)]^2 \qquad \text{(A-1-30)}$$

where the product of L and M is chosen to be greater than or equal to N. Notice that (A-1-30) reduces to (A-1-5) when L = 1 and K = 0. Also, for L = N and M = 1, the problem is no longer overdetermined and determination of the coefficiencs by the generalized least-squares approach reduces to (A-1-28) with the result that the error ε_{GLS} is identically zero. Minimization of the error in (A-1-30) with respect to the coefficients Q_i, $i = 1,2,\ldots,N$, results in the N linear equations

$$\sum_{\ell=-K}^{L-K-1} \sum_{j=1}^{M} \sum_{i=1}^{N} g_k^{(\ell)}(t_j) g_i^{(\ell)}(t_j) Q_i = \sum_{\ell=-K}^{L-K-1} \sum_{j=1}^{M} g_k^{(\ell)}(t_j) x^{(\ell)}(t_j), \quad k = 1,2,\ldots,N. \qquad \text{(A-1-31)}$$

For L = 1, K = 0 and M = N, the problem becomes the interpolation problem considered in (A-1-2) and (A-1-31) reduces to (A-1-3).

Similarly, the integrated squared error approach can be generalized by involving the first K integrals and L-K derivatives of x(t). The approximation is now denoted by

$$\hat{x}_{GISE}(t) = \sum_{i=1}^{N} B_i g_i(t) \qquad \text{(A-1-32)}$$

where the subscript GISE stands for generalized integrated-squared-error. The generalized integrated-squared-error is defined to be

$$\varepsilon_{GISE} = \sum_{\ell=-K}^{L-K-1} \int_{T_1}^{T_2} [x^{(\ell)}(t) - \hat{x}^{(\ell)}(t)]^2 dt \; . \qquad \text{(A-1-33)}$$

Performing the minimization of (A-1-33) with respect to the coefficients B_i, i = 1,2,...,N, yields the N linear equations

$$\sum_{\ell=-K}^{L-K-1} \sum_{i=1}^{N} \left[\int_{T_1}^{T_2} g_k^{(\ell)}(t) g_i^{(\ell)}(t) dt \right] B_i = \sum_{\ell=-K}^{L-K-1} \int_{T_1}^{T_2} g_k^{(\ell)}(t) x^{(\ell)}(t) dt, \; k = 1,2,\ldots,N \; . \qquad \text{(A-1-34)}$$

The derivatives and/or integrals of x(t) are no longer involved when L = 1, K = 0 and (A-1-34) becomes (A-1-11).

As a final remark, we point out that the sampling instants appearing in the set of N equations of (A-1-20) can be allowed to vary from one equation to another. The same statement applies to the sets of N linear equations appearing in (A-1-26), (A-1-28), and (A-1-31). This allows for greater flexibility in generating the approximations.

At this point we illustrate the previous discussion with a simple example. The objective is to demonstrate the varying amounts of computational effort required and the different waveforms which result using

the various methods of approximation. Following the example, we discuss how the different approximations are related and show that a natural criteria for their comparison is the integrated square error.

Example A-1-1

Given the finite set of basis functions

$$\{g_i\} = \{1, t, t^2\} \tag{A-1-35}$$

approximate the function

$$x(t) = \cos 2\pi t \tag{A-1-36}$$

over the interval $[T_1, T_2] = [0, 1]$.

Case 1 (interpolation scheme)

The approximation is given by (A-1-2) where the coefficients are obtained from (A-1-3). The sampling instants, which are equal in number to the number of coefficients to be determined, are arbitrarily chosen to be $t_j = 0, 1/2, 1$. Sample values of both $x(t)$ and the basis functions are given in Table A-1-1. In matrix form, (A-1-3) becomes

Table A-1-1

t_j	$x(t_j)$	g_1	g_2	g_3
0	1	1	0	0
1/2	-1	1	1/2	1/4
1	1	1	1	1

$$\begin{bmatrix} 1 & 0 & 0 \\ 1 & 1/2 & 1/4 \\ 1 & 1 & 1 \end{bmatrix} \begin{bmatrix} D_1 \\ D_2 \\ D_3 \end{bmatrix} = \begin{bmatrix} 1 \\ -1 \\ 1 \end{bmatrix}. \tag{A-1-37}$$

Solution of (A-1-37) for the coefficients yields the approximation

$$\hat{x}_I(t) = 1 - 8t + 8t^2 \qquad \text{(A-1-38)}$$

$x(t)$ and $\hat{x}_I(t)$ are shown in Fig. A-1-1.

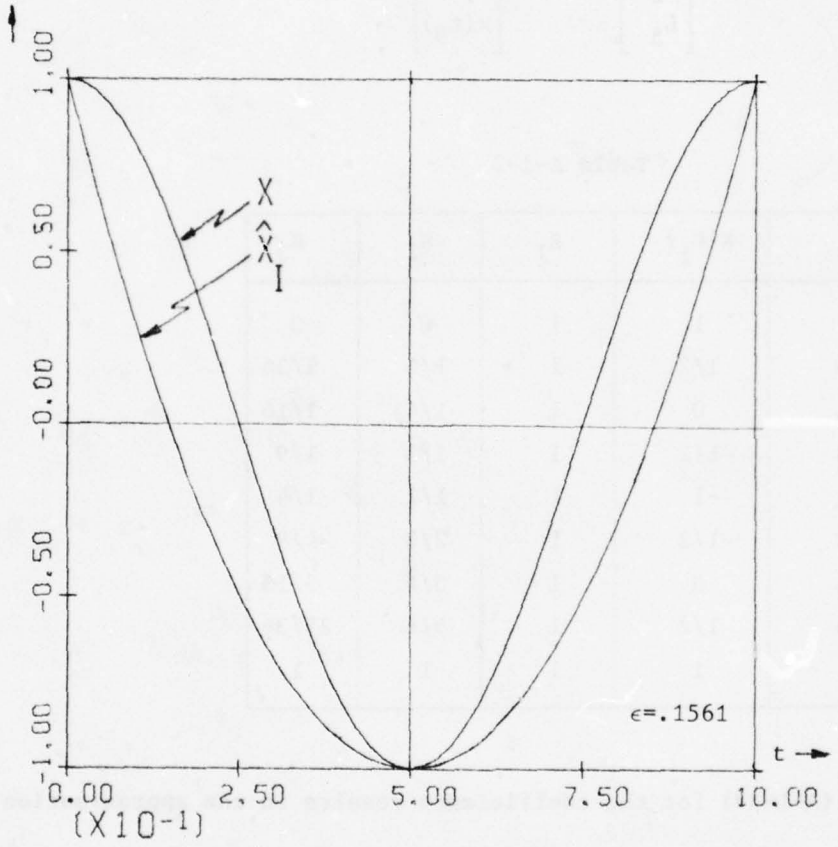

Fig. A-1-1. The function $x(t)$ and its approximation $\hat{x}_I(t)$.

Case 2 (least-squares approach)

The approximation is given by (A-1-4) where the coefficients are determined from (A-1-7). We arbitrarily choose a sampling ratio of 3 so that M = 9 and N = 3. The 9 sampling instants and the corresponding sample values of both $x(t)$ and the basis functions are shown in

Table A-1-2. Let the 9x3 matrix formed from the columns g_i in Table A-1-2 be denoted by [G]. In terms of matrices, (A-1-7) may be expressed as

$$[G]^T [G] \begin{bmatrix} L_1 \\ L_2 \\ L_3 \end{bmatrix} = [G]^T \begin{bmatrix} x(t_1) \\ \vdots \\ x(t_9) \end{bmatrix} . \qquad \text{(A-1-39)}$$

Table A-1-2

t_j	$x(t_j)$	g_1	g_2	g_3
0	1	1	0	0
1/6	1/2	1	1/6	1/36
1/4	0	1	1/4	1/16
1/3	-1/2	1	1/3	1/9
1/2	-1	1	1/2	1/4
2/3	-1/2	1	2/3	4/9
3/4	0	1	3/4	9/16
5/6	1/2	1	5/6	25/36
1	1	1	1	1

Solution of (A-1-39) for the coefficients results in the approximation

$$x_{LS}(t) = 1.1668 - 7.0524t + 7.0524t^2 . \qquad \text{(A-1-40)}$$

$x(t)$ and $\hat{x}_{LS}(t)$ are shown in Fig. A-1-2.

Case 3 (integrated squared error approach)

The set of basis functions $\{g_i\}$, given by (A-1-35), does not constitute an orthonormal set. To simplify evaluation of the coefficients, the Gram-Schmidt orthonormalization procedure was applied to $\{g_i\}$

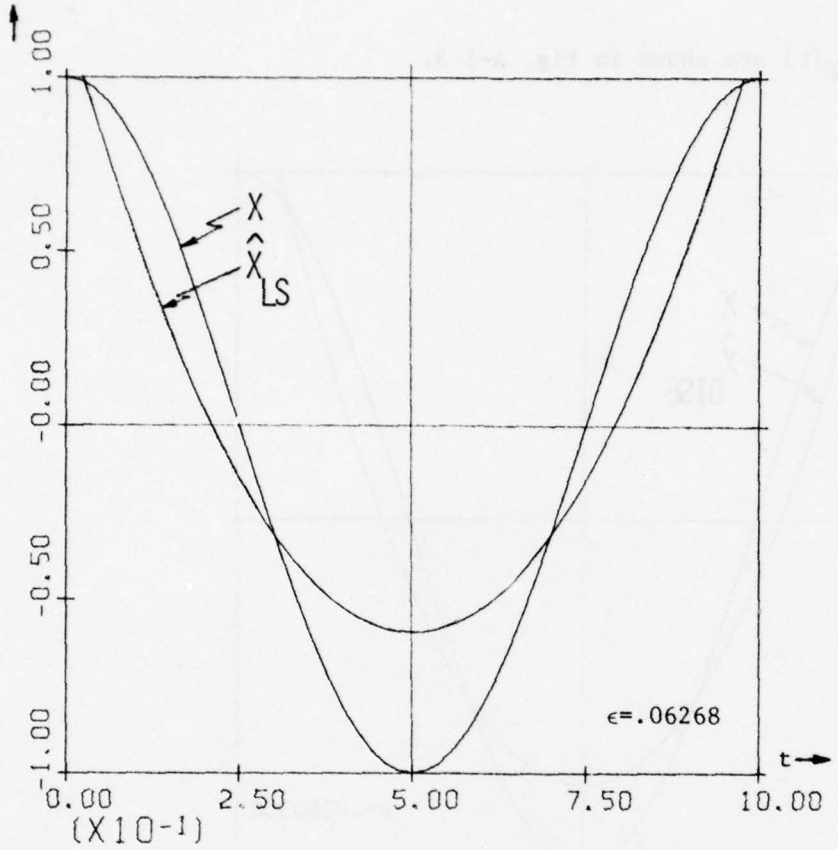

Fig. A-1-2. The function x(t) and its approximation $\hat{x}_{LS}(t)$.

resulting in the orthonormal set $\{\psi_i\}$ where

$$\psi_1(t) = 1$$
$$\psi_2(t) = \sqrt{3}\ (2t - 1) \qquad \text{(A-1-41)}$$
$$\psi_3(t) = \sqrt{5}\ (6t^2 - 6t + 1).$$

The approximation to x(t) is given by (A-1-12) where the coefficients are obtained from (A-1-15). It is found that $\alpha_1 = \alpha_2 = 0$ and $\alpha_3 = 3\sqrt{5}/\pi^2$. Hence,

$$\hat{x}_{OLSE}(t) = 0\psi_1(t) + 0\psi_2(t) + \frac{3\sqrt{5}}{\pi^2}\psi_3(t) = \frac{15}{\pi^2}(6t^2 - 6t + 1). \qquad \text{(A-1-42)}$$

$x(t)$ and $\hat{x}_{OISE}(t)$ are shown in Fig. A-1-3.

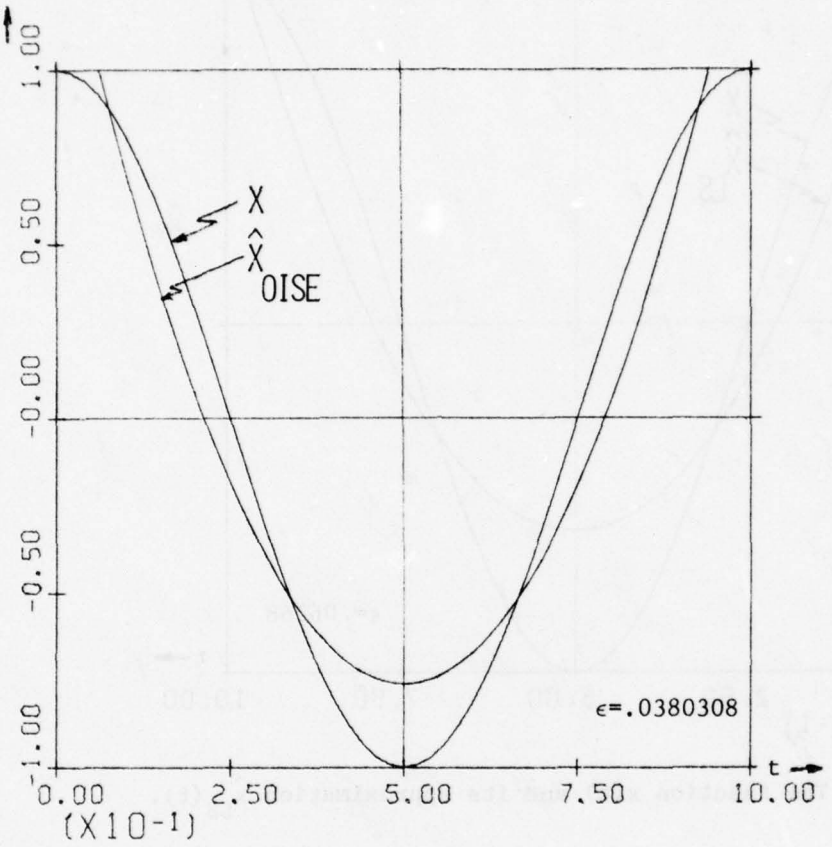

Fig. A-1-3. The function $x(t)$ and its approximation $\hat{x}_{OISE}(t)$.

Case 4 (equality of derivatives approach)

The approximation is given by (A-1-19) where the coefficients are obtained from (A-1-20). As is apparent from (A-1-20), the basis functions and their derivatives are needed for evaluation of the coefficients. Since three basis functions are included in $\{g_i\}$, N=3. Therefore, (A-1-20) consists of three simultaneous equations for which $\ell = 0,1,2$. The corresponding basis functions are given in Table A-1-3.

Table A-1-3

ℓ	$g_1^{(\ell)}$	$g_2^{(\ell)}$	$g_3^{(\ell)}$
0	1	t	t^2
1	0	1	2t
2	0	0	2

In addition, the signal to be approximated and its first two derivatives are

$$x^{(0)}(t) = \cos 2\pi t$$
$$x^{(1)}(t) = -2\pi \sin 2\pi t \qquad \text{(A-1-43)}$$
$$x^{(2)}(t) = -4\pi^2 \cos 2\pi t.$$

Applying (A-1-20) at the time instant $t = T = 1/2$, solving for the coefficients E_i, and substituting into (A-1-19) results in

$$\hat{x}_{ED}(t) = \frac{\pi^2 - 2}{2} - 2\pi^2 t + 2\pi^2 t^2. \qquad \text{(A-1-44)}$$

$x(t)$ and $\hat{x}_{ED}(t)$ are shown in Fig. A-1-4. Note the close fit of $\hat{x}_{ED}(t)$ to $x(t)$ around $t = 1/2$.

Case 5 (equality of integrals approach)

The approximation is now given by (A-1-25) where the coefficients F_i are determined from (A-1-26). As in Case 4, three simultaneous equations are needed since $N = 3$. Integrating over the interval $[1,t]$, the basis functions corresponding to $\ell = 0,1,2$ are shown in Table A-1-4.

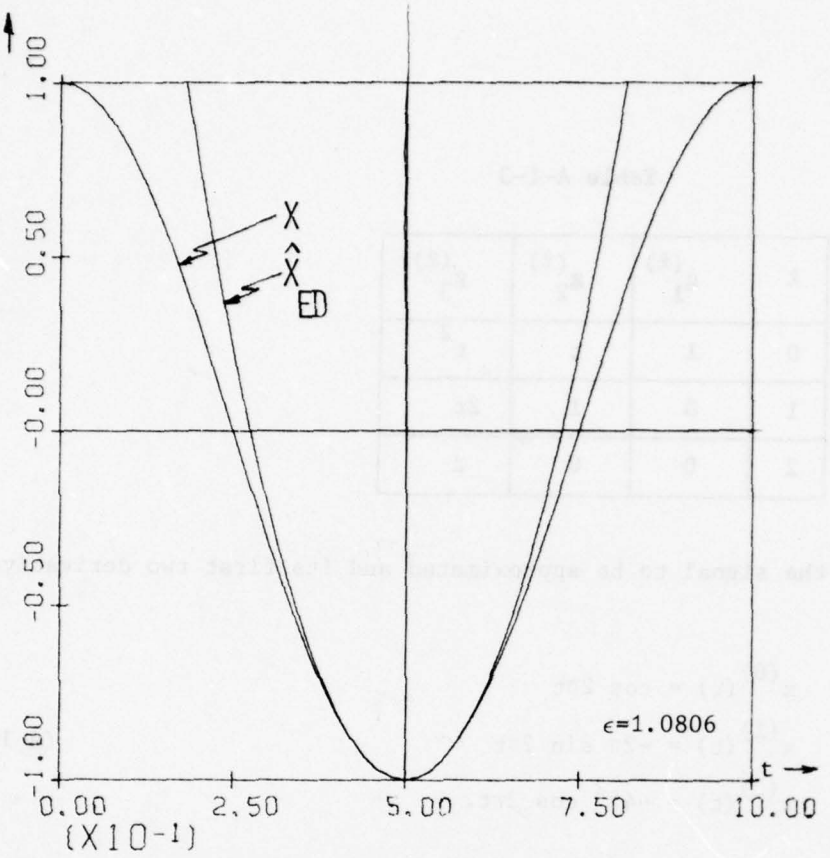

Fig. A-1-4. The function x(t) and its approximation $\hat{x}_{ED}(t)$.

Table A-1-4

ℓ	$g_1^{(-\ell)}$	$g_2^{(-\ell)}$	$g_3^{(-\ell)}$
0	1	t	t^2
1	t-1	$\frac{(t-1)(t+1)}{2}$	$\frac{(t-1)(t^2+t+1)}{3}$
2	$\frac{(t-1)^2}{2}$	$\frac{(t-1)^2(t+2)}{6}$	$\frac{(t-1)^2(t^2+2t+3)}{12}$

Also, the function being approximated and its first two integrals over the interval (1,t) are:

$$x^{(0)}(t) = \cos 2\pi t$$
$$x^{(-1)}(t) = \frac{1}{2\pi} \sin 2\pi t \qquad \text{(A-1-45)}$$
$$x^{(-2)}(t) = \frac{1}{4\pi^2} [1 - \cos 2\pi t] .$$

Solving (A-1-26) with $T_3 = 1$ and $T_4 = 0$, the approximation becomes

$$\hat{x}_{EI}(t) = 1 - 6t + 6t^2. \qquad \text{(A-1-46)}$$

$x(t)$ and $\hat{x}_{EI}(t)$ are shown in Fig. A-1-5.

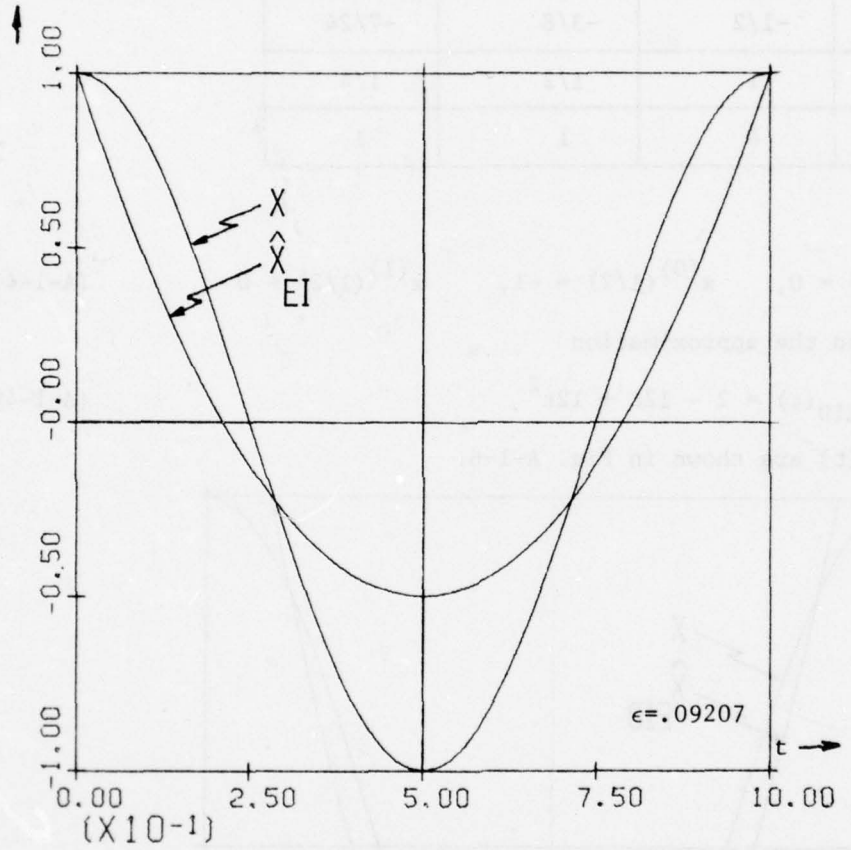

Fig. A-1-5. The function $x(t)$ and its approximation $\hat{x}_{EI}(t)$.

Case 6 (equality of integrals and derivatives approach)

For this case the approximation is given by (A-1-27) where the coefficients are evaluated from (A-1-28). Once again, N = 3. To obtain these three simultaneous equations, we let K = 1 in (A-1-28). Choosing T = 1/2 and evaluating the integral over the interval (1,1/2), the

basis functions evaluated at T = 1/2 are given in Table A-1-5.

Table A-1-5

ℓ	$g_1^{(\ell)}(1/2)$	$g_2^{(\ell)}(1/2)$	$g_3^{(\ell)}(1/2)$
-1	-1/2	-3/8	-7/24
0	1	1/2	1/4
1	0	1	1

Similarly,

$$x^{(-1)}(1/2) = 0, \quad x^{(0)}(1/2) = -1, \quad x^{(1)}(1/2) = 0 \ . \tag{A-1-47}$$

This results in the approximation

$$\hat{x}_{EID}(t) = 2 - 12t + 12t^2 . \tag{A-1-48}$$

x(t) and $\hat{x}_{EID}(t)$ are shown in Fig. A-1-6.

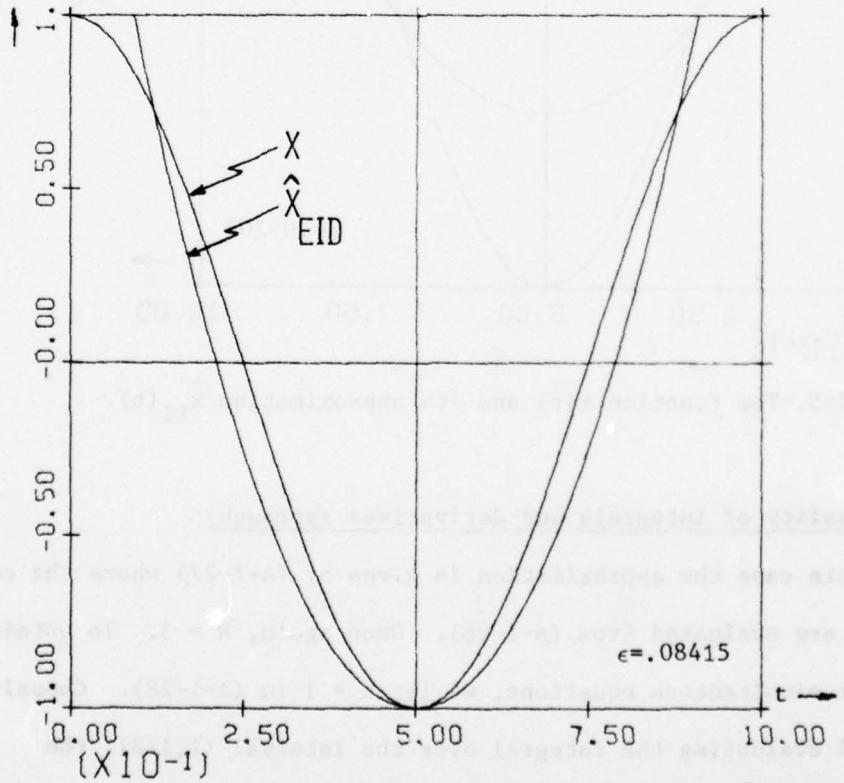

Fig. A-1-6. The function x(t) and its approximation $\hat{x}_{EID}(t)$.

Case 7 (generalized least-square approach)

The approximation to x(t) is given by (A-1-29) where the coefficients Q_i are obtained from (A-1-31). We present two different illustrations. In the first a single sampling point (M= 1) is utilized whereas 9 different sampling points (M= 9) are used in the second. In both illustrations, we consider the function and 4 of its integrals over the interval (1,t).

Part A: In this illustration, N = 3, M = 1, K = 4, and L = 5. The basis functions $g_i^{(\ell)}$ for ℓ = 0,-1,-2 and i = 1,2,3 are given in Table A-1-4. The functions corresponding to ℓ = -3,-4 are listed in Table A-1-6. The function being approximated and its first two integrals are given in

Table A-1-6

ℓ	$g_1^{(\ell)}$	$g_2^{(\ell)}$	$g_3^{(\ell)}$
-3	$\frac{(t-1)^3}{6}$	$\frac{(t-1)^3(t+3)}{24}$	$\frac{(t-1)^3(t^2+3t+6)}{60}$
-4	$\frac{(t-1)^4}{24}$	$\frac{(t-1)^4(t+4)}{120}$	$\frac{(t-1)^4(t^2+4t+10)}{360}$

(A-1-45). In addition, $x^{(-3)}(t)$ and $x^{(-4)}(t)$ are

$$x^{(-3)}(t) = \frac{1}{4\pi^2}(t-1) - \frac{1}{8\pi^3}\sin 2\pi t$$

$$x^{(-4)}(t) = \frac{1}{8\pi^2}(t-1)^2 - \frac{1}{16\pi^4}(1 - \cos 2\pi t)\ . \qquad \text{(A-1-49)}$$

The sampling instant and the corresponding sample values of $x^{(\ell)}(t)$ and $g_i^{(\ell)}(t)$ are shown in Table A-1-7.

Table A-1-7

t_1	$x^{(0)}$	$x^{(-1)}$	$x^{(-2)}$	$x^{(-3)}$	$x^{(-4)}$	$g_1^{(0)}$	$g_2^{(0)}$	$g_3^{(0)}$	$g_1^{(-1)}$	$g_2^{(-1)}$	$g_3^{(-1)}$	$g_1^{(-2)}$	$g_2^{(-2)}$	$g_3^{(-2)}$	$g_1^{(-3)}$	$g_2^{(-3)}$	$g_3^{(-3)}$	$g_1^{(-4)}$	$g_2^{(-4)}$	$g_3^{(-4)}$
0	1	0	0	$\frac{-1}{4\pi^2}$	$\frac{1}{8\pi^2}$	1	0	0	-1	-1/2	-1/3	1/2	1/3	1/4	-1/6	-1/8	-1/10	1/24	1/30	1/36
						$[G^{(0)}]$			$[G^{(-1)}]$			$[G^{(-2)}]$			$[G^{(-3)}]$			$[G^{(-4)}]$		

For a specific value of ℓ, let the 1x3 matrices formed from the columns $g_i^{(\ell)}$ be denoted by $[G^{(\ell)}]$. In terms of matrices, (A-1-31) may be expressed as

$$\{\sum_{\ell=-4}^{0} [G^{(\ell)}]^T [G^{(\ell)}]\} \begin{bmatrix} Q_1 \\ Q_2 \\ Q_3 \end{bmatrix} = \sum_{\ell=-4}^{0} [G^{(\ell)}]^T x^{(\ell)}(t) \quad . \qquad \text{(A-1-50)}$$

Solution of (A-1-50) for the coefficients results in the approximation

$$\hat{x}_{GLS}(t) = 1.00013 - 6.12286t + 6.18055t^2 \quad . \qquad \text{(A-1-51)}$$

$x(t)$ and $\hat{x}_{GLS}(t)$ are shown in Fig. A-1-7.

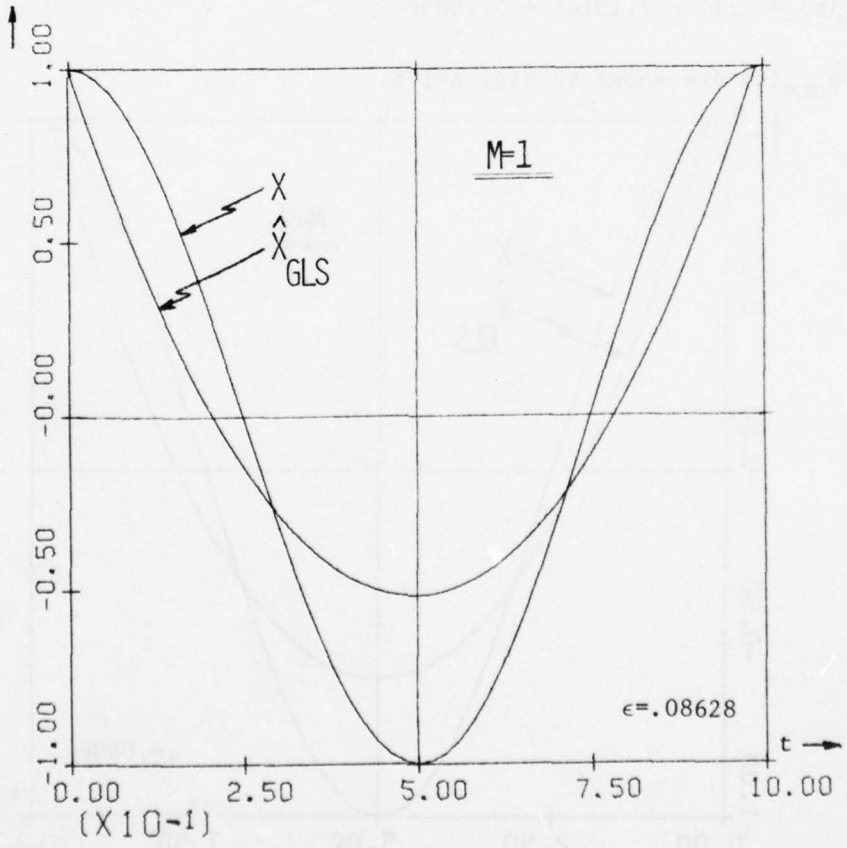

Fig. A-1-7. The function $x(t)$ and its approximation $\hat{x}_{GLS}(t)$, (=1).

Part B: Once again, N = 3, K = 4, and L = 5. However, now $M = 9$ since we sample at 9 different time instants. The sampling instants and the corresponding sample values of $x^{(\ell)}(t)$ and $g_i^{(\ell)}(t)$ are shown in Table A-1-8. For a specific value of ℓ, let the 9x3 matrices formed from the columns $g_i^{(\ell)}$ be denoted by $[G^{(\ell)}]$. In terms of matrices, (A-1-31) becomes

$$\left\{ \sum_{\ell=-4}^{0} [G^{(\ell)}]^T [G^{(\ell)}] \right\} \begin{bmatrix} Q_1 \\ Q_2 \\ Q_3 \end{bmatrix} = \sum_{\ell=-4}^{0} [G^{(\ell)}]^T \begin{bmatrix} x^{(\ell)}(t_1) \\ \vdots \\ x^{(\ell)}(t_9) \end{bmatrix} . \qquad \text{(A-1-52)}$$

Solution of (A-1-52) for the coefficients results in the approximation

$$\hat{x}_{GLS}(t) = 1.17 - 7.1014t + 7.1089t^2 . \qquad \text{(A-1-53)}$$

$x(t)$ and $\hat{x}_{GLS}(t)$ are shown in Fig. A-1-8.

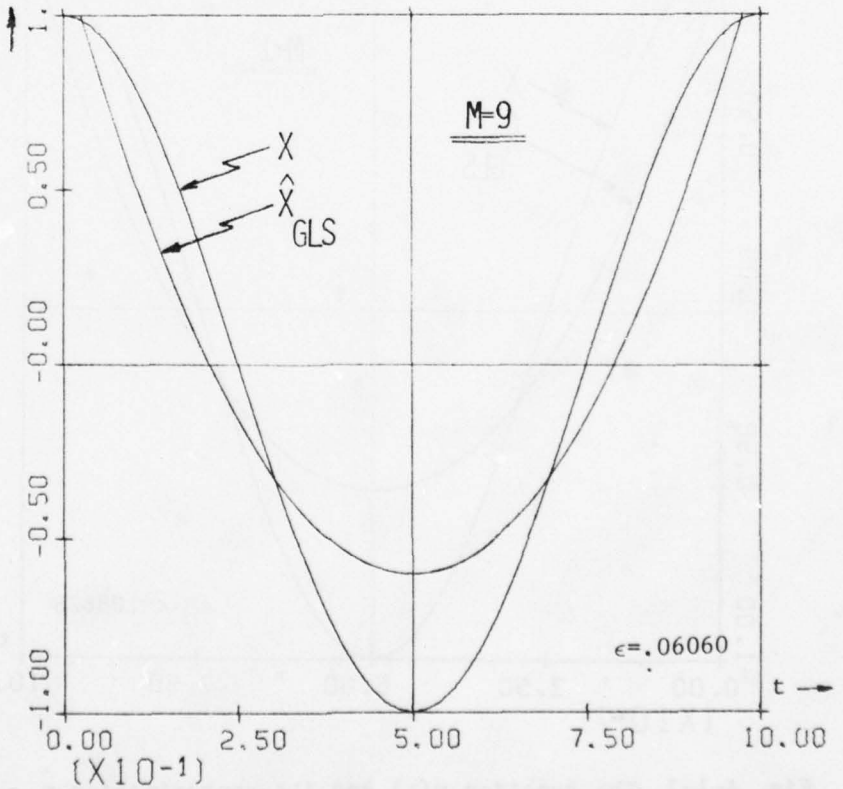

Fig. A-1-8. The function $x(t)$ and its approximation $\hat{x}_{GLS}(t)$, (M=9).

Table A-1-8

j	t_j	$x^{(0)}$	$x^{(-1)}$	$x^{(-2)}$	$x^{(-3)}$	$x^{(-4)}$	$g_1^{(0)}$	$g_2^{(0)}$	$g_3^{(0)}$	$g_1^{(-1)}$	$g_2^{(-1)}$	$g_3^{(-1)}$	$g_1^{(-2)}$	$g_2^{(-2)}$	$g_3^{(-2)}$	$g_1^{(-3)}$	$g_2^{(-3)}$	$g_3^{(-3)}$	$g_1^{(-4)}$	$g_2^{(-4)}$	$g_3^{(-4)}$
1	0	1	0	0	$-\frac{1}{4\pi^2}$	$\frac{1}{8\pi^2}$	1	0	0	-1	$-\frac{1}{2}$	$-\frac{1}{3}$	$\frac{1}{2}$	$\frac{1}{3}$	$\frac{1}{4}$	$-\frac{1}{6}$	$-\frac{1}{8}$	$-\frac{1}{10}$	$\frac{1}{24}$	$\frac{1}{30}$	$\frac{1}{36}$
2	$\frac{1}{6}$	$\frac{1}{2}$	$\frac{\sqrt{3}}{4\pi}$	$\frac{1}{8\pi^2}$	$-\frac{10\pi+3\sqrt{3}}{48\pi^2}$	$\frac{25\pi^2-9}{288\pi^4}$	1	$\frac{1}{6}$	$\frac{1}{36}$	$-\frac{5}{6}$	$-\frac{35}{72}$	$-\frac{215}{648}$	$\frac{25}{72}$	$\frac{325}{1296}$	$\frac{3025}{15552}$	$\frac{-125}{1296}$	$\frac{-2375}{31104}$	$\frac{-5875}{93312}$	$\frac{625}{31104}$	$\frac{3125}{746496}$	$\frac{48125}{3359232}$
3	$\frac{1}{4}$	0	$\frac{1}{2\pi}$	$\frac{1}{4\pi^2}$	$\frac{3\pi-2}{16\pi^3}$	$\frac{9\pi^2-8}{128\pi^4}$	1	$\frac{1}{4}$	$\frac{1}{16}$	$-\frac{3}{4}$	$-\frac{15}{32}$	$-\frac{21}{24}$	$\frac{9}{32}$	$\frac{27}{128}$	$\frac{171}{1024}$	$\frac{-9}{128}$	$\frac{-351}{6144}$	$\frac{-2943}{61440}$	$\frac{27}{2048}$	$\frac{459}{40960}$	$\frac{1593}{163840}$
4	$\frac{1}{3}$	$-\frac{1}{2}$	$\frac{\sqrt{3}}{2\pi}$	$\frac{3}{8\pi^2}$	$-\frac{8\pi+3\sqrt{3}}{48\pi^3}$	$\frac{16\pi^2-27}{288\pi^4}$	1	$\frac{1}{3}$	$\frac{1}{9}$	$-\frac{2}{3}$	$-\frac{4}{9}$	$-\frac{26}{81}$	$\frac{2}{9}$	$\frac{14}{81}$	$\frac{34}{243}$	$\frac{-4}{81}$	$\frac{-80}{1944}$	$\frac{-128}{3645}$	$\frac{2}{243}$	$\frac{26}{3645}$	$\frac{206}{32805}$
5	$\frac{1}{2}$	-1	0	$\frac{1}{2\pi^2}$	$-\frac{1}{8\pi^3}$	$\frac{2-4}{32\pi^4}$	1	$\frac{1}{2}$	$\frac{1}{4}$	$-\frac{1}{2}$	$-\frac{3}{8}$	$-\frac{7}{24}$	$\frac{1}{8}$	$\frac{5}{48}$	$\frac{17}{192}$	$\frac{-1}{48}$	$\frac{-7}{384}$	$\frac{-31}{1920}$	$\frac{1}{384}$	$\frac{3}{1280}$	$\frac{49}{23040}$
6	$\frac{2}{3}$	$-\frac{1}{2}$	$-\frac{\sqrt{3}}{2\pi}$	$\frac{3}{8\pi^2}$	$\frac{3\sqrt{3}-4}{4\pi^3}$	$\frac{4^2-27}{288\pi^4}$	1	$\frac{2}{3}$	$\frac{4}{9}$	$-\frac{1}{3}$	$-\frac{5}{18}$	$-\frac{19}{81}$	$\frac{1}{18}$	$\frac{4}{81}$	$\frac{43}{972}$	$\frac{-1}{162}$	$\frac{-11}{1944}$	$\frac{-19}{3645}$	$\frac{1}{1944}$	$\frac{7}{13580}$	$\frac{29}{65610}$
7	$\frac{3}{4}$	0	$-\frac{1}{2\pi}$	$\frac{1}{4\pi^2}$	$\frac{2-\pi}{16\pi^3}$	$\frac{\pi^2-8}{128\pi^4}$	1	$\frac{3}{4}$	$\frac{9}{16}$	$-\frac{1}{4}$	$-\frac{7}{32}$	$-\frac{37}{192}$	$\frac{1}{32}$	$\frac{11}{384}$	$\frac{27}{1024}$	$\frac{-1}{384}$	$\frac{-13}{6144}$	$\frac{-141}{61440}$	$\frac{1}{6144}$	$\frac{19}{122880}$	$\frac{217}{1474560}$
8	$\frac{5}{6}$	$\frac{1}{2}$	$-\frac{\sqrt{3}}{4\pi}$	$\frac{1}{8\pi^2}$	$\frac{3\sqrt{3}-2\pi}{48\pi^3}$	$\frac{\pi^2-9}{288\pi^4}$	1	$\frac{5}{6}$	$\frac{25}{36}$	$-\frac{1}{6}$	$-\frac{11}{72}$	$\frac{-91}{648}$	$\frac{1}{72}$	$\frac{17}{1296}$	$\frac{193}{15552}$	$\frac{-1}{1296}$	$\frac{-19}{31104}$	$\frac{-331}{466560}$	$\frac{1}{31104}$	$\frac{29}{933120}$	$\frac{101}{3359232}$
9	1	1	0	0	0	0	1	1	1	0	0	0	0	0	0	0	0	0	0	0	0

Case 8 (generalized integrated-squared-error approach)

The approximation to x(t) ig given by (A-1-32) where the coefficients B_i are obtained from (A-1-34). Since the coefficients in the GISE approach are determined by minimizing the sum of errors indicated by (A-1-33), it is of interest to investigate the magnitude of the individual errors in the sum. The values of the coefficients B_i are most influenced by the need to minimize the larger errors.

For this case the approximation is generated by considering the original function, its derivative, and its integral (i.e., L = 3, K = 1). To assess the size of the errors likely to be encountered in (A-1-33), we first carry out ISE approximations to (1) $x^{(-1)}(t)$ in terms of $\{g_i^{(-1)}(t)\}$, (2) x(t) in terms of $\{g_i(t)\}$, and (3) $x^{(1)}(t)$ in terms of $\{g_i^{(1)}(t)\}$. As pointed out earlier, the GISE approach can be specialized to the ISE approach with the proper choice of L and K in (A-1-34).

(1) approximation of $x^{(-1)}(t)$ in terms of $\{g_i^{(-1)}(t)\}$ (L=1, K=1)

The inner product for this case is defined to be

$$\langle y, z\rangle \triangleq \int_0^1 y(t)z(t)dt \,, \qquad \text{(A-1-54)}$$

Hence, the inner products required by (A-1-34) are:

$$[\langle g_k^{(-1)}, g_i^{(-1)}\rangle] = \begin{bmatrix} \langle g_1^{(-1)}, g_1^{(-1)}\rangle & \langle g_1^{(-1)}, g_2^{(-1)}\rangle & \langle g_1^{(-1)}, g_3^{(-1)}\rangle \\ \langle g_2^{(-1)}, g_1^{(-1)}\rangle & \langle g_2^{(-1)}, g_2^{(-1)}\rangle & \langle g_2^{(-1)}, g_3^{(-1)}\rangle \\ \langle g_3^{(-1)}, g_1^{(-1)}\rangle & \langle g_3^{(-1)}, g_2^{(-1)}\rangle & \langle g_3^{(-1)}, g_3^{(-1)}\rangle \end{bmatrix} = \begin{bmatrix} \frac{1}{3} & \frac{5}{24} & \frac{3}{20} \\ \frac{5}{24} & \frac{2}{15} & \frac{7}{72} \\ \frac{3}{20} & \frac{7}{72} & \frac{1}{14} \end{bmatrix}$$

$$[\langle g_k^{(-1)}, x^{(-1)}\rangle] = \begin{bmatrix} \langle g_1^{(-1)}, x^{(-1)}\rangle \\ \langle g_2^{(-1)}, x^{(-1)}\rangle \\ \langle g_3^{(-1)}, x^{(-1)}\rangle \end{bmatrix} = \left(-\frac{1}{4\pi^2}\right) \begin{bmatrix} 1 \\ \frac{1}{2} \\ \frac{4\pi^2-6}{12\pi^2} \end{bmatrix} . \qquad \text{(A-1-55)}$$

In terms of the matrices of (A-1-55), (A-1-34) becomes

$$[<g_k^{(-1)}, g_i^{(-1)}>] \begin{bmatrix} B_1 \\ B_2 \\ B_3 \end{bmatrix} = [<g_k^{(-1)}, x^{(-1)}>] \,. \qquad \text{(A-1-56)}$$

The approximation is given by

$$\hat{x}_{ISE}^{(-1)}(t) = 1.787(t-1) - 10.332[\tfrac{1}{2}(t^2-1)] + 10.211[\tfrac{1}{3}(t^3-1)]$$

$$= -.02427 + 1.787t - 5.166t^2 + 3.404t^3 \,. \qquad \text{(A-1-57)}$$

$x^{(-1)}$ and $\hat{x}_{ISE}^{(-1)}(t)$ are shown in Fig. A-1-9.

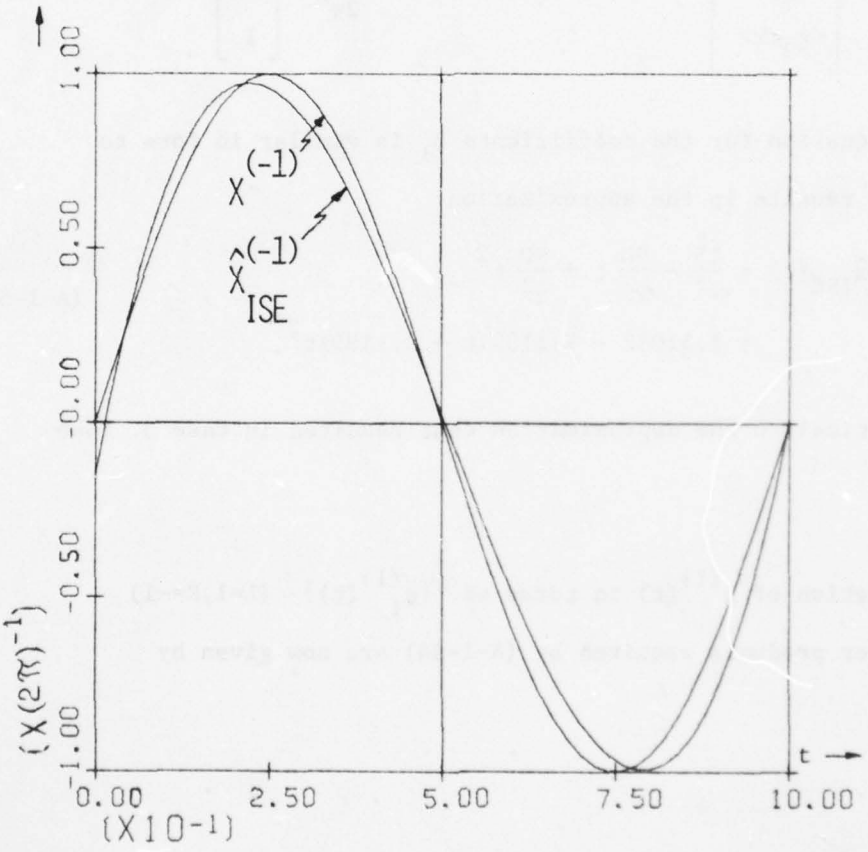

Fig. A-1-9. The function $x^{(-1)}(t)$ and its approximation $\hat{x}_{ISE}^{(-1)}(t)$.

2) approximation of $x(t)$ in terms of $\{g_i(t)\}$ (L=1, K=0)

The inner products required by (A-1-34) are now given by:

$$[\langle g_k, g_i \rangle] = \begin{bmatrix} \langle g_1, g_1 \rangle & \langle g_1, g_2 \rangle & \langle g_1, g_3 \rangle \\ \langle g_2, g_1 \rangle & \langle g_2, g_2 \rangle & \langle g_2, g_3 \rangle \\ \langle g_3, g_1 \rangle & \langle g_3, g_2 \rangle & \langle g_3, g_3 \rangle \end{bmatrix} = \begin{bmatrix} 1 & \frac{1}{2} & \frac{1}{3} \\ \frac{1}{2} & \frac{1}{3} & \frac{1}{4} \\ \frac{1}{3} & \frac{1}{4} & \frac{1}{5} \end{bmatrix} \tag{A-1-57}$$

$$[\langle g_k, x \rangle] = \begin{bmatrix} \langle g_1, x \rangle \\ \langle g_2, x \rangle \\ \langle g_3, x \rangle \end{bmatrix} = \left(\frac{1}{2\pi^2}\right) \begin{bmatrix} 0 \\ 0 \\ 1 \end{bmatrix}.$$

The matrix equation for the coefficients B_i is similar in form to (A-1-56) and results in the approximation

$$\begin{aligned} \hat{x}_{ISE}(t) &= \frac{15}{\pi^2} - \frac{90}{\pi^2} t + \frac{90}{\pi^2} t^2 \\ &= 1.51982 - 9.11891t + 9.11891t^2. \end{aligned} \tag{A-1-58}$$

This is identical to the approximation that resulted in Case 3. (See Fig. A-1-3).

3) approximation of $x^{(1)}(t)$ in terms of $\{g_i^{(1)}(t)\}$ (L=1,K=-1)

The inner products required by (A-1-34) are now given by

$$[\langle g_k^{(1)}, g_i^{(1)} \rangle] = \begin{bmatrix} \langle g_1^{(1)}, g_1^{(1)} \rangle & \langle g_1^{(1)}, g_2^{(1)} \rangle & \langle g_1^{(1)}, g_3^{(1)} \rangle \\ \langle g_2^{(1)}, g_1^{(1)} \rangle & \langle g_2^{(1)}, g_2^{(1)} \rangle & \langle g_2^{(1)}, g_3^{(1)} \rangle \\ \langle g_3^{(1)}, g_1^{(1)} \rangle & \langle g_3^{(1)}, g_2^{(1)} \rangle & \langle g_3^{(1)}, g_3^{(1)} \rangle \end{bmatrix} = \begin{bmatrix} 0 & 0 & 0 \\ 0 & 1 & 1 \\ 0 & 1 & \frac{4}{3} \end{bmatrix} \tag{A-1-59}$$

$$[\langle g_k^{(1)}, x^{(1)} \rangle] = \begin{bmatrix} \langle g_1^{(1)}, x^{(1)} \rangle \\ \langle g_2^{(1)}, x^{(1)} \rangle \\ \langle g_3^{(1)}, x^{(1)} \rangle \end{bmatrix} = \begin{bmatrix} 0 \\ 0 \\ 2 \end{bmatrix} .$$

The matrix equation for the coefficients B_i is similar in form to (A-1-56) and results in the approximation

$$\begin{aligned} \hat{x}_{ISE}^{(1)}(t) &= c(0) - 6(1) + 6(2t) \\ &= -6 + 12t . \end{aligned} \tag{A-1-60}$$

where c is an arbitrary constant. $x^{(1)}(t)$ and $\hat{x}_{ISE}^{(1)}(t)$ are shown in Fig. A-1-10.

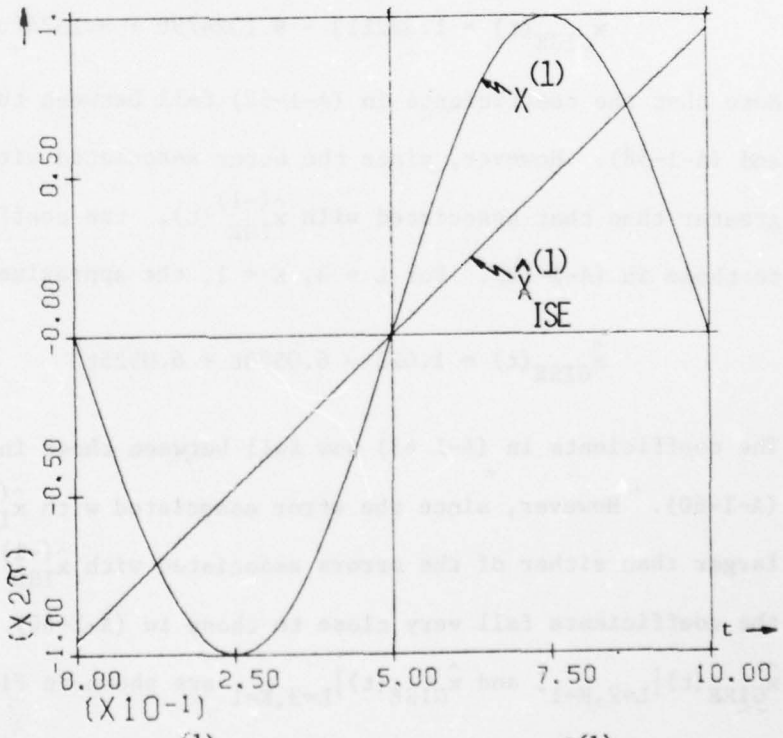

Fig. A-1-10. The function $x^{(1)}(t)$ and its approximation $\hat{x}_{ISE}^{(1)}(t)$.

Having obtained these three approximations, note that the error becomes progressively larger as one proceeds from $\hat{x}_{ISE}^{(-1)}(t)$ to $\hat{x}_{ISE}^{(1)}(t)$.

We now approximate x(t) by means of the GISE approach. However, to emphasize the importance of the various terms in (A-1-33), we first consider the situation for which L = 2, K = 1. With these values of L and K only x(t) and $x^{(-1)}(t)$ are involved in the approximation. We then repeat the procedure for L = 3, K = 1. Then x(t), $x^{(-1)}(t)$, and $x^{(1)}(t)$ are all involved.

Equation (A-1-34) may be expressed in matrix form as

$$\sum_{\ell=-K}^{L-K-1} [\langle g_k^{(\ell)}, g_i^{(\ell)} \rangle] \begin{bmatrix} B_1 \\ B_2 \\ B_3 \end{bmatrix} = \sum_{\ell=-K}^{L-K-1} [\langle g_k^{(\ell)}, x^{(\ell)} \rangle] \quad . \qquad \text{(A-1-61)}$$

For L = 2, K = 1, the approximation is

$$\hat{x}_{GISE}(t) = 1.522113 - 9.132479t + 9.132466t^2 \quad . \qquad \text{(A-1-62)}$$

Note that the coefficients in (A-1-62) fall between those in (A-1-57) and (A-1-58). However, since the error associated with $\hat{x}_{ISE}(t)$ is greater than that associated with $\hat{x}_{ISE}^{(-1)}(t)$, the coefficients fall closer to those in (A-1-58). For L = 3, K = 1, the approximation is

$$\hat{x}_{GISE}(t) = 1.022 - 6.0523t + 6.0525t^2 \quad . \qquad \text{(A-1-63)}$$

The coefficients in (A-1-63) now fall between those in (A-1-57) and (A-1-60). However, since the error associated with $\hat{x}_{ISE}^{(1)}(t)$ is much larger than either of the errors associated with $\hat{x}_{ISE}^{(-1)}(t)$ and $\hat{x}_{ISE}(t)$, the coefficients fall very close to those in (A-1-60). Plots of x(t), $\hat{x}_{GISE}(t)|_{L=2,K=1}$, and $\hat{x}_{GISE}(t)|_{L=3,K=1}$ are shown in Fig. A-1-11.

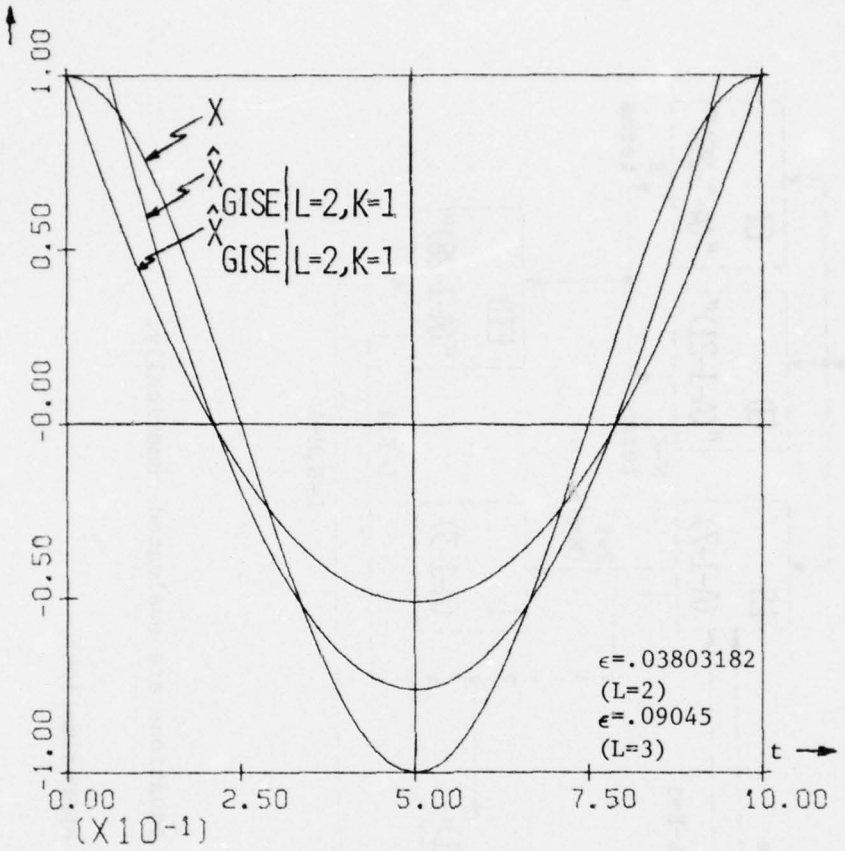

Fig. A-1-11. The function x(t) and its approximations $\hat{x}_{GISE}(t)|_{L=2,K=1}$, $\hat{x}_{GISE}(t)|_{L=3,K=1}$.

The relationships between the various approximations are indicated by the block diagram presented in Fig. A-1-12. The equation used to solve for the coefficients is referred to in each block. The directed paths between the blocks serve to indicate how one approach may be transformed into another.

Note that the block diagram in Fig. A-1-12 subdivides the various approximations into those that process continuous waveforms versus numerical data. In general, as the number of sampling instants is increased (i.e., $R \to \infty$), the solution for the discrete case converges to that of the continuous case. This is illustrated in Fig. A-1-13

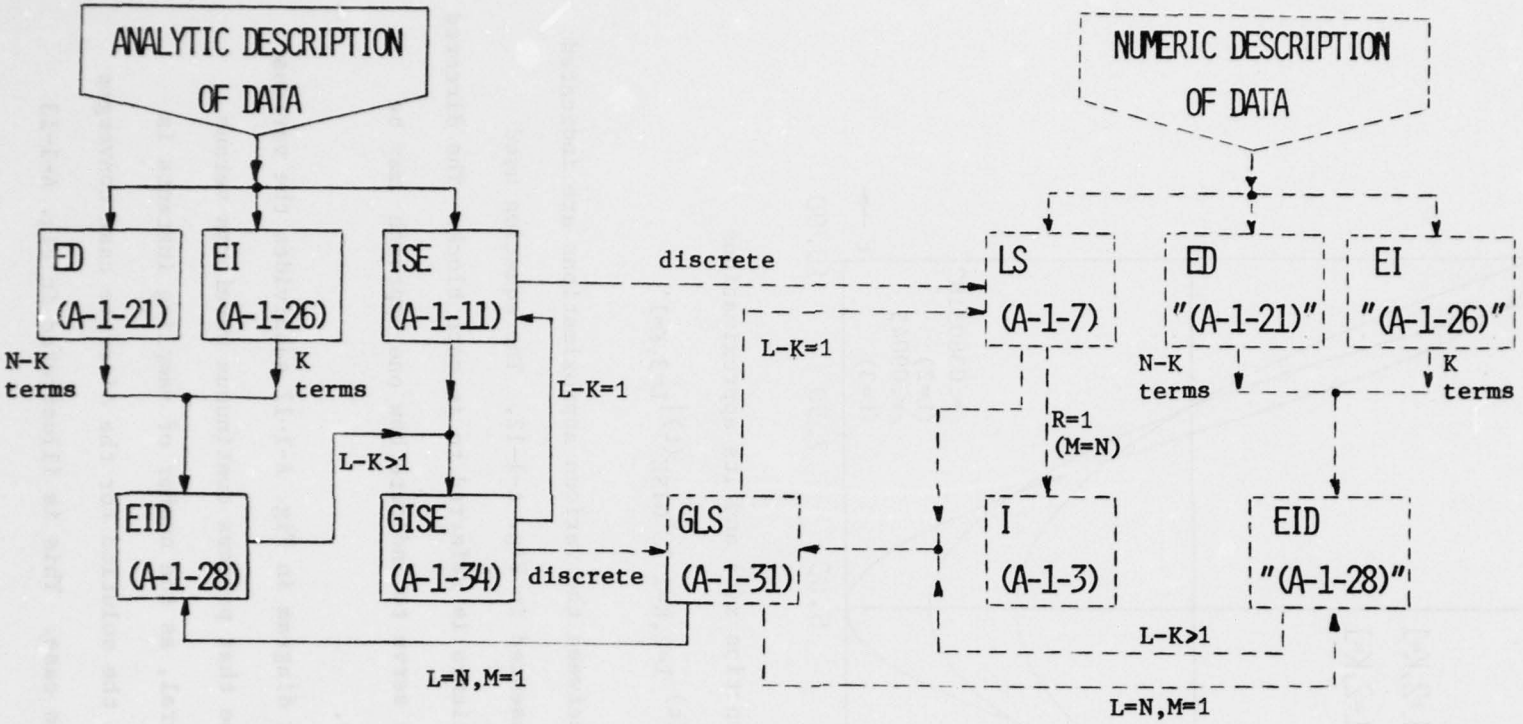

"(A- -)" Integrals and/or derivatives in these equations are evaluated numerically.

Fig. A-1-12. Relations among the different types of approximations.

where $L_i(R)$ denotes the i^{th} least-squares coefficient of (A-1-7) for a specified value of R and A_i denotes the i^{th} integrated-squared-error coefficient of (A-1-11). In our example, as R was increased with a fixed value of N = 3, the smallest magnitudes of the coefficients L_1, L_2, and L_3 all occurred for M = 4. As a result, $L_i(R)$ was normalized by $L_i(4/3)$ in order to compress the plot. The LSE coefficients nicely asymptote to the ISE coefficients. The convergence is even more dramatically illustrated by examining the errors. Because the waveform being approximated is known in our example, it is possible to compute the integrated-squared error for both the discrete and continuous cases. These are shown in Fig. A-1-14. The asymptote is determined from ε_{ISE}, the integrated-squared error for the continuous case. The integrated-squared error for the discrete case, for a specified value of R, is denoted by $\varepsilon_{ISE}^{(R)}$. For convenience, all errors are normalized by that occurring for the interpolation case (i.e., M = N = 3). Note the abrupt convergence. The plot reveals that a value of R equal to 10 is more than adequate for the discrete case to approximate the continuous case.

A summary of the waveforms resulting from the various approximations is given in Fig. A-1-15. The associated integrated-squared error is indicated on each plot. By examination of Case 4, it is obvious that an "interval type" of error criterion, such as ε_{ISE}, is inappropriate for "Taylor type" of approximation.

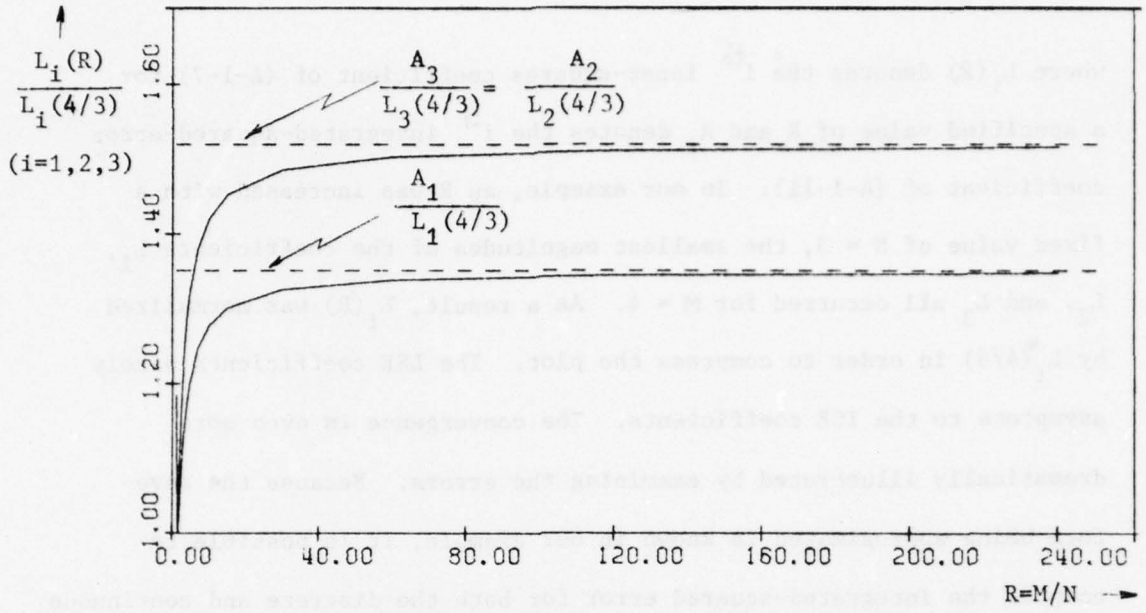

Fig. A-1-13. Normalized approximation coefficients Vs. sampling ratio.

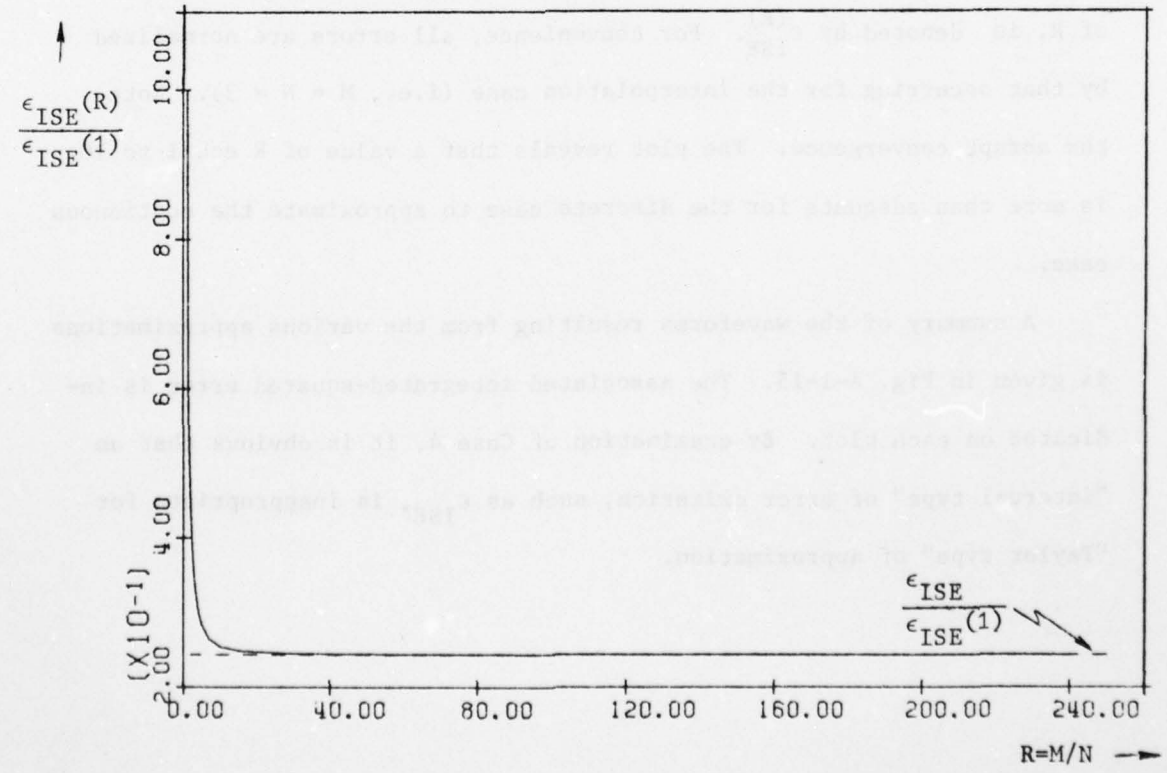

Fig. A-1-14. Normalized integrated squared error Vs. sampling ratio.

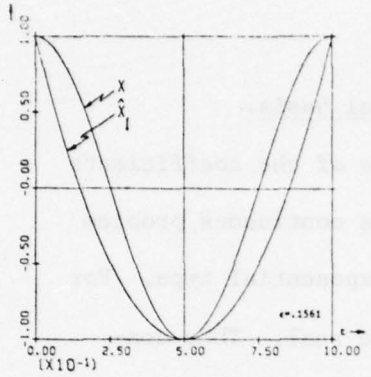

(Case 1 - Fig. 2-1-1)

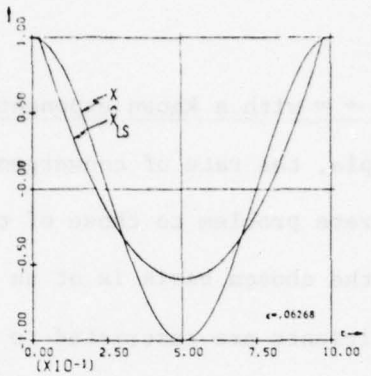

(Case 2 - Fig. 2-1-2)

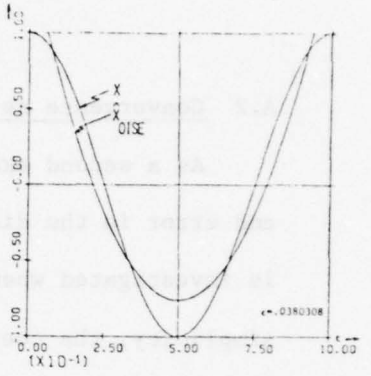

(Case 3 - Fig. 2-1-3)

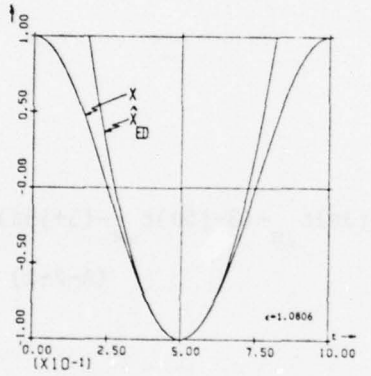

(Case 4 - Fig. 2-1-4)

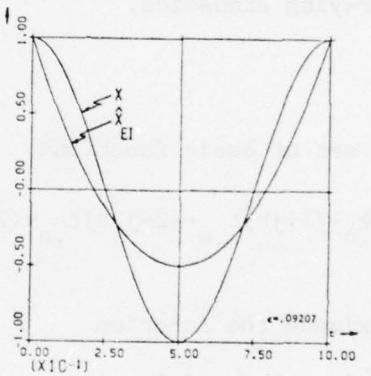

(Case 5 - Fig. 2-1-5)

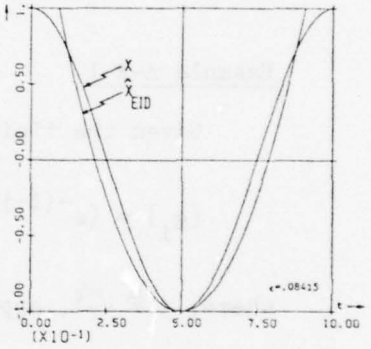

(Case 6 - Fig. 2-1-6)

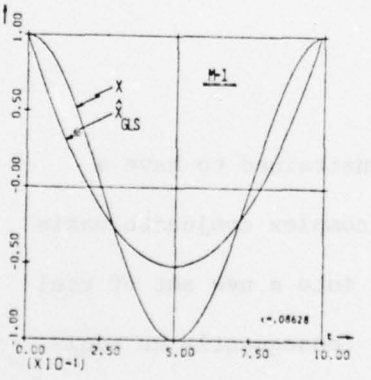

(Case 7 - Fig. 2-1-7)

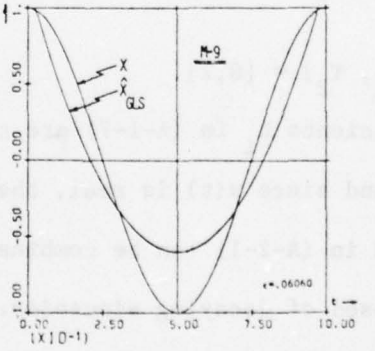

(Case 7 - Fig. 2-1-8)

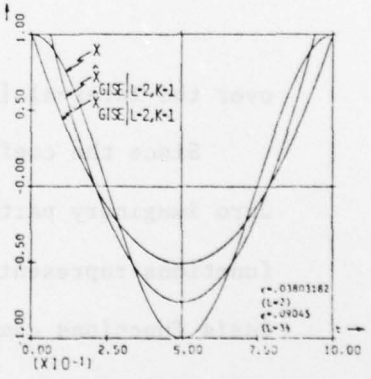

(Case 8 - Fig. 2-1-11)

Fig. A-1-15. Summary of waveforms resulting from example 2-1-1 and their respective Integrated Squared errors (ε).

A.2 Convergence as $R \to \infty$ with a known exponential basis.

As a second example, the rate of convergence of the coefficients and error in the discrete problem to those of the continuous problem is investigated when the chosen basis is of an exponential type. For simplicity, the coefficients are restricted to be real. This constraint is met by combining complex exponentials with their conjugates in order to obtain decaying sinusoids.

Example A-2-1

Given the finite set of basis functions

$$\{g_i\} = \{e^{-(1-j\pi)t}, e^{-(1+j\pi)t}, e^{-(2-j3\pi)t}, e^{-(2+j3\pi)t}, e^{-(3-j5\pi)t}, e^{-(3+j5\pi)t}\} \tag{A-2-1}$$

where, $j \triangleq \sqrt{-1}$, approximate the function

$$x(t) = \begin{cases} 1 \ ; & 0 \leq t \leq 1 \\ 0 \ , & \text{otherwise} \end{cases} \tag{A-2-2}$$

over the interval $[T_1, T_2] = [0,2]$.

Since the coefficients L_i in (A-1-7) are constrained to have a zero imaginary part and since $x(t)$ is real, the complex conjugate basis functions represented in (A-2-1) can be combined into a new set of real basis functions composed of decaying sinusoids. Consequently an equivalent set of basis functions is given by

$$\{g_{S_i}\} = \{e^{-t}\cos \pi t, \ e^{-t}\sin \pi t, \ e^{-2t}\cos 3\pi t, e^{-2t}\sin 3\pi t, e^{-3t} \cos 5\pi t\} \tag{A-2-3}$$

where $e^{-3t}\sin 5\pi t$ has been intentionally omitted in order to increase

the approximation error.

As in example A-1-1, the waveform being approximated is known. Hence, computation of $\varepsilon_{ISE}(R)$ is possible for the discrete case. The normalized least-square coefficients $L_i(R)$, i = 1,2,3,4,5 are plotted in Figures A-2-1 through A-2-5, along with the asymptotes which are given by the integrated-squared-error coefficients A_i. The integrated-squared error for the discrete case, as a function of the sampling ratio, is shown in Fig. A-2-6 where the asymptote is the ISE of the continuous case. As in example A-1-1, notice that R = 10 is more than adequate for the discrete case to approximate the continuous case. Plots of x(t) and its integrated-squared-error approximation are shown in Fig. A-2-7.

To provide additional insight into the convergence of the least-squares approximation of x(t), as given in (A-2-2), the approximation is repeated five times as the number of basis functions is gradually increased from one to five. In particular, the following sets of basis functions were used:

$$\begin{aligned}
&\text{(a) } \{g_{s1}\} \\
&\text{(b) } \{g_{s1}, g_{s2}\} \\
&\text{(c) } \{g_{s1}, g_{s2}, g_{s3}\} \qquad\qquad (A\text{-}2\text{-}4) \\
&\text{(d) } \{g_{s1}, g_{s2}, g_{s3}, g_{s4}\} \\
&\text{(e) } \{g_{si}\} \; ; \; i = 1,2,3,4,5 .
\end{aligned}$$

The corresponding integrated-squared errors versus the sampling ratio are plotted in Fig. A-2-8. Note that the knee occurs for values of R

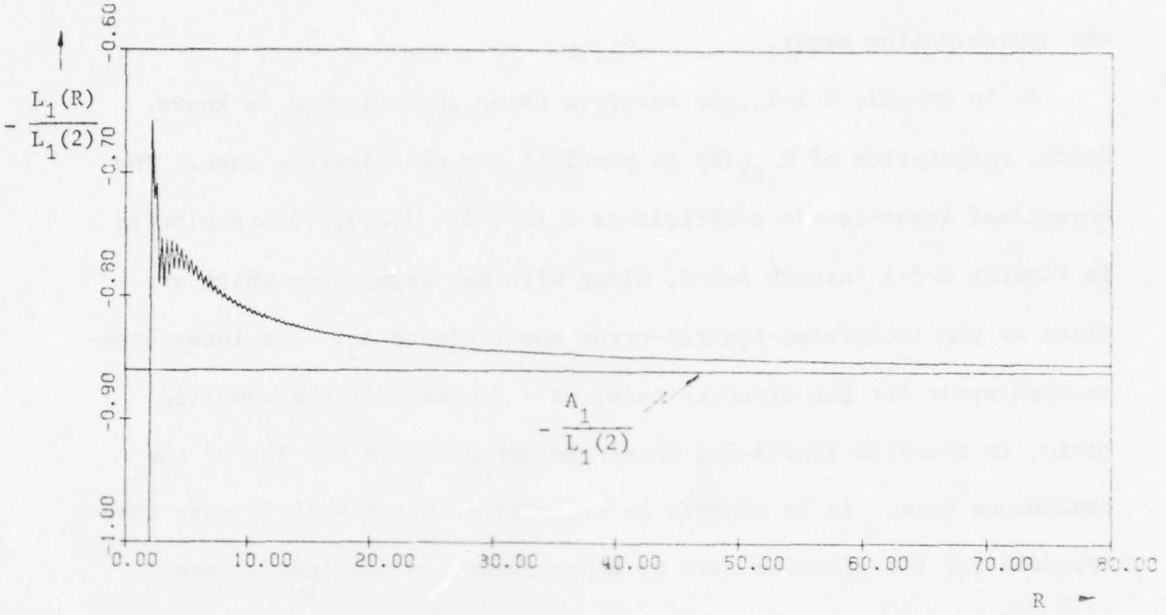

Fig. A-2-1. Normalized L_1 coefficient Vs. sampling ratio.

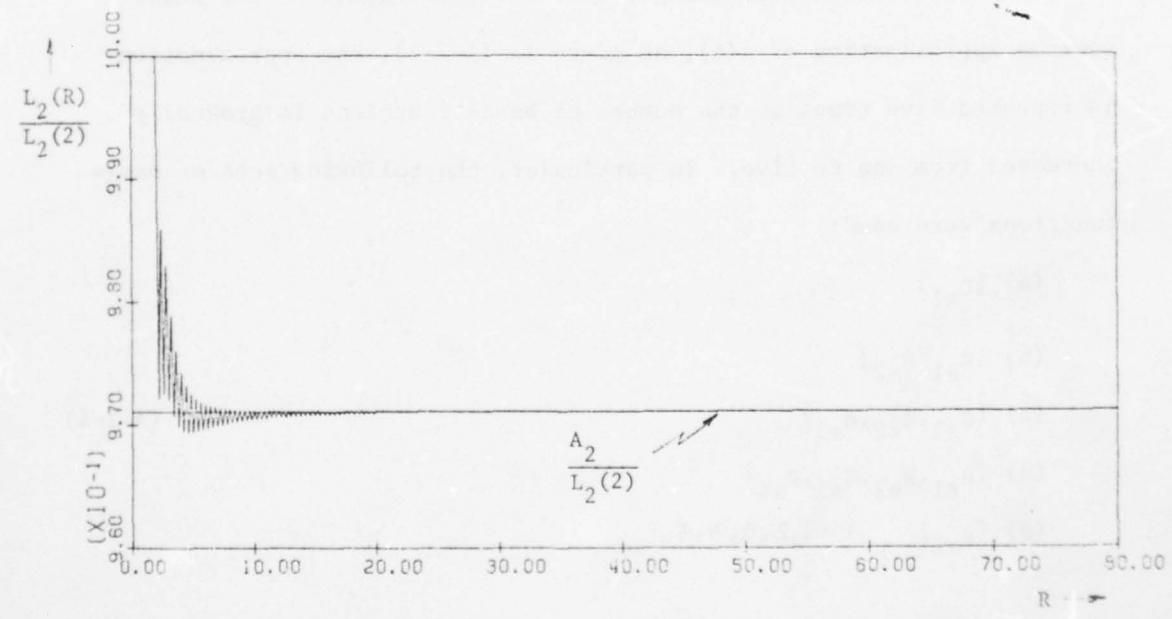

Fig. A-2-2. Normalized L_2 coefficient Vs. sampling ratio.

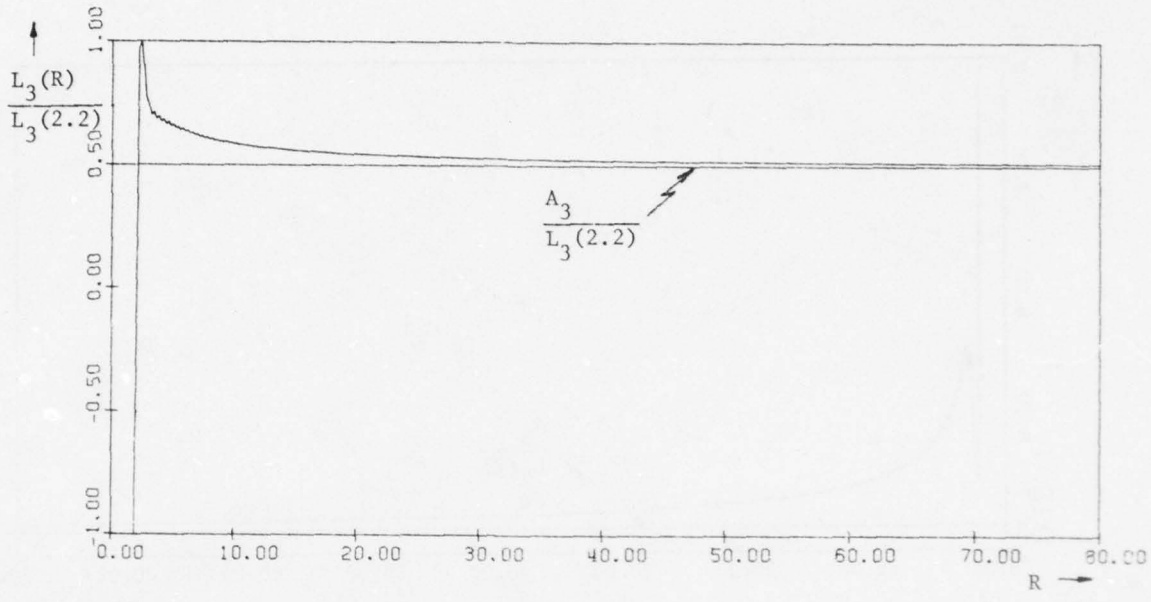

Fig. A-2-3. Normalized L_3 coefficient Vs. sampling ratio.

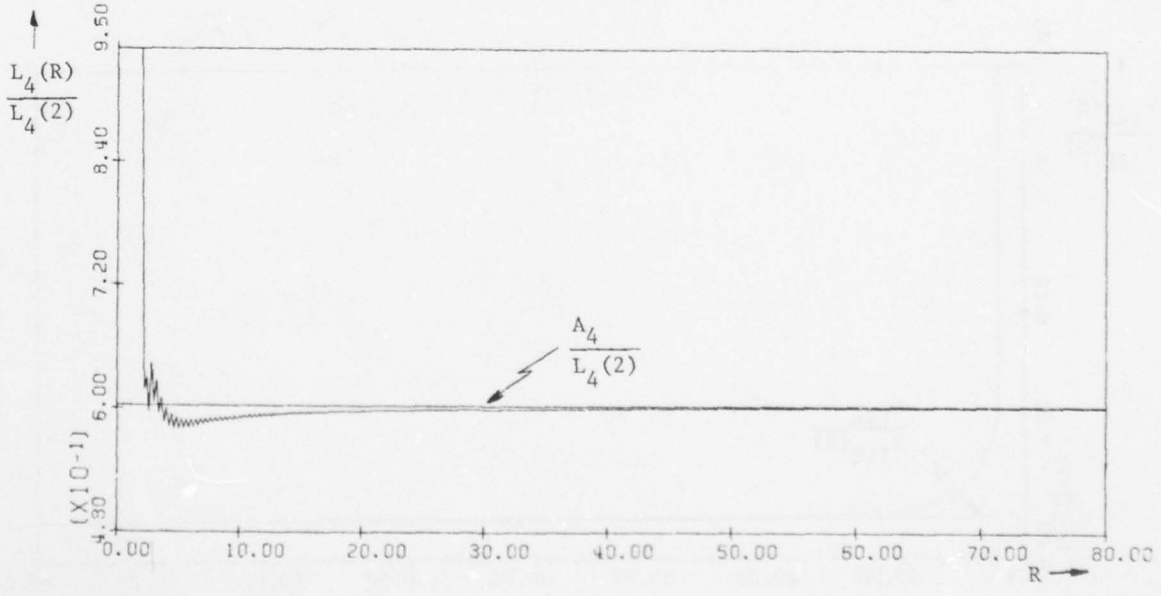

Fig. A-2-4. Normalized L_4 coefficient Vs. sampling ratio.

AD-A061 589 SYRACUSE UNIV N Y F/G 12/2
PARAMETRIC IDENTIFICATION OF SYSTEMS VIA LINEAR OPERATORS.(U)
SEP 78 J NEBAT F30602-75-C-0121
UNCLASSIFIED RADC-TR-78-199 NL

3 OF 3
ADA
061589

END
DATE
FILMED
1 -79
DDC

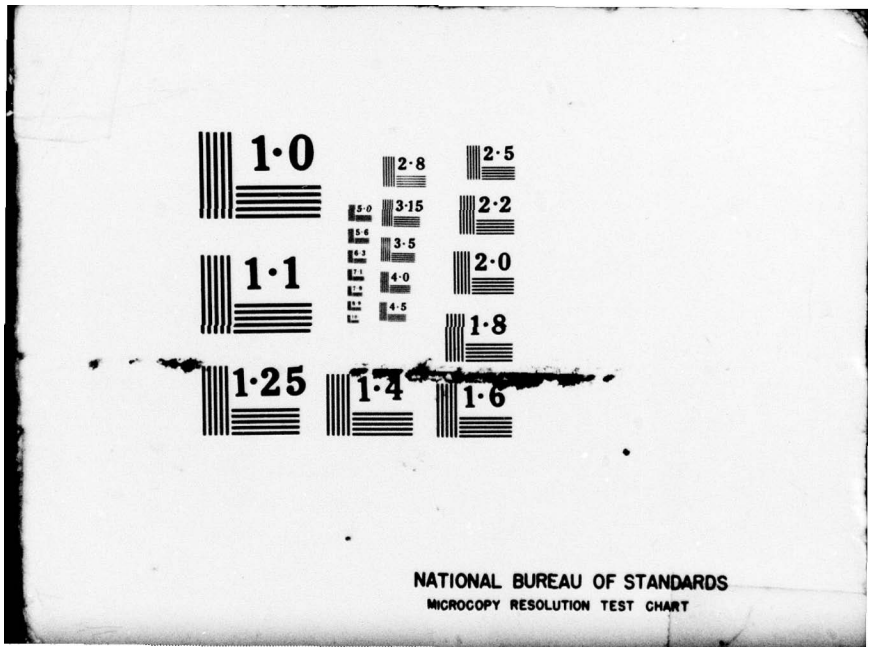
1·0
1·1
1·25
1·4
1·6
1·8
2·0
2·2
2·5
2·8
3·15
3·5
4·0
4·5
NATIONAL BUREAU OF STANDARDS
MICROCOPY RESOLUTION TEST CHART

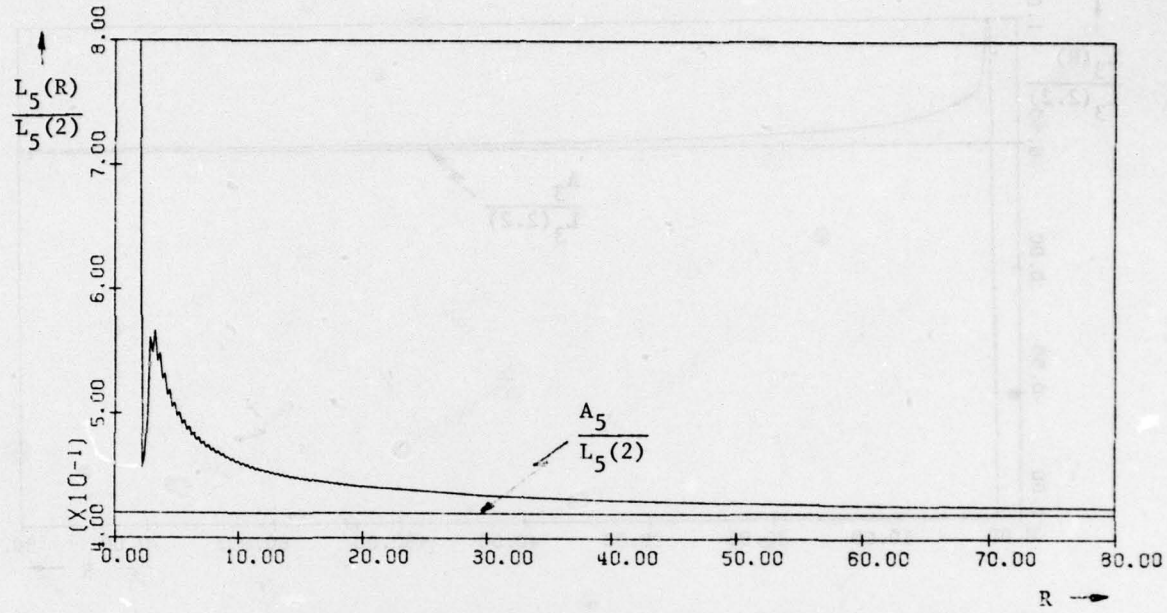

Fig. A-2-5. Normalized L_5 coefficient Vs. sampling ratio.

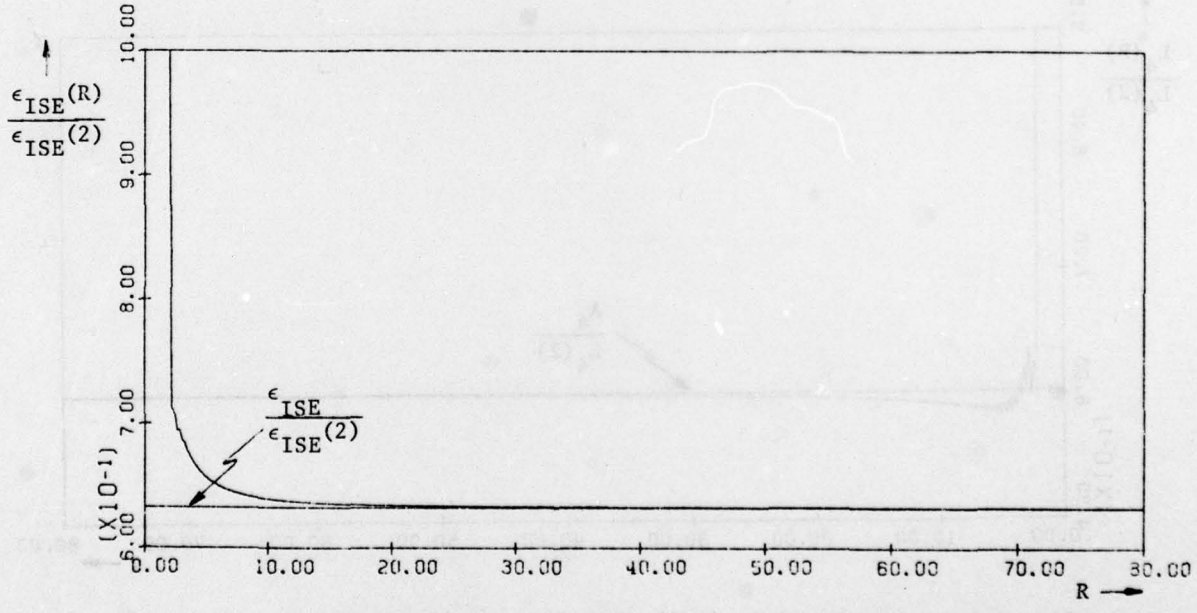

Fig. A-2-6. Normalized integrated squared error Vs. sampling ratio.

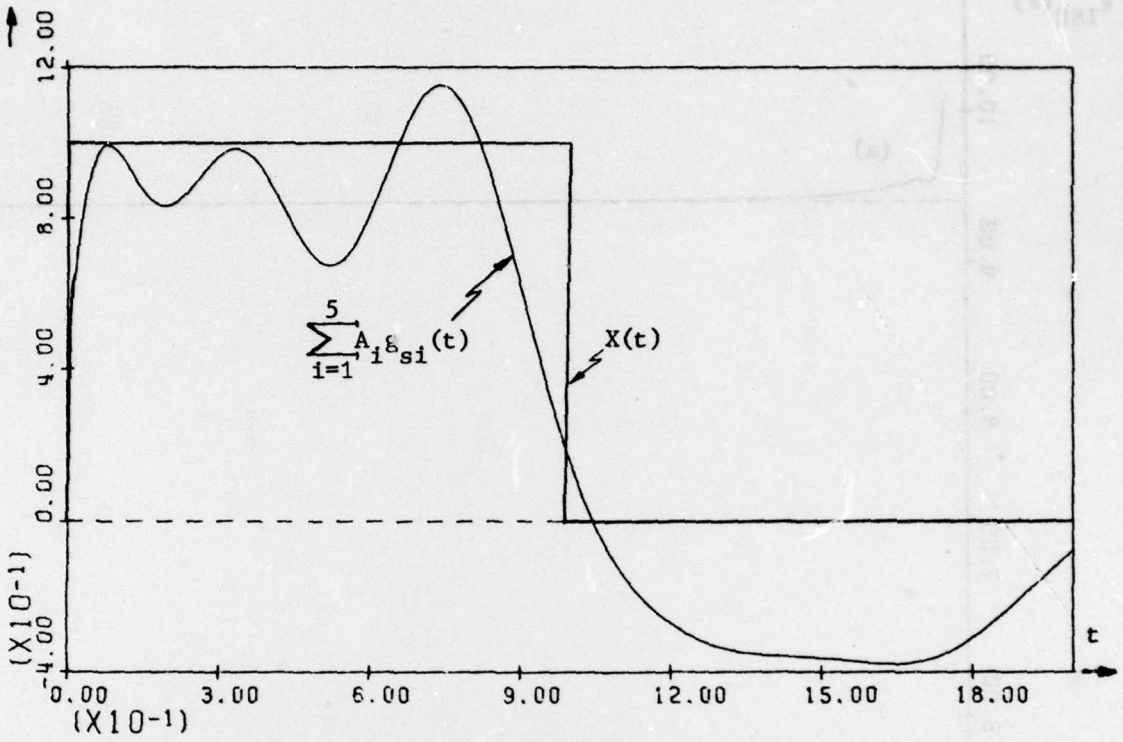

Fig. A-2-7. x(t) and its MISE approximation.

between 3 and 5 and is insensitive to the number of basis functions used (i.e., insensitive to the quality of the approximation).

A.3 General Discussion of Numerical Examples

From the theory of band-limited signals, it is well-known that one has to sample a given signal at least at the Nyquist rate in order to achieve a meaningful reconstruction. If a signal is sampled below this rate, an aliasing error occurs. This type of error can be interpreted in terms of Riemann surfaces. It is clear that a phase variation of larger than π radians between consecutive time samples for any of the complex exponential waveform components will locate the phase of that component on a Riemann surface different from the first. If no information is supplied about the true Riemann surface on which the phase is

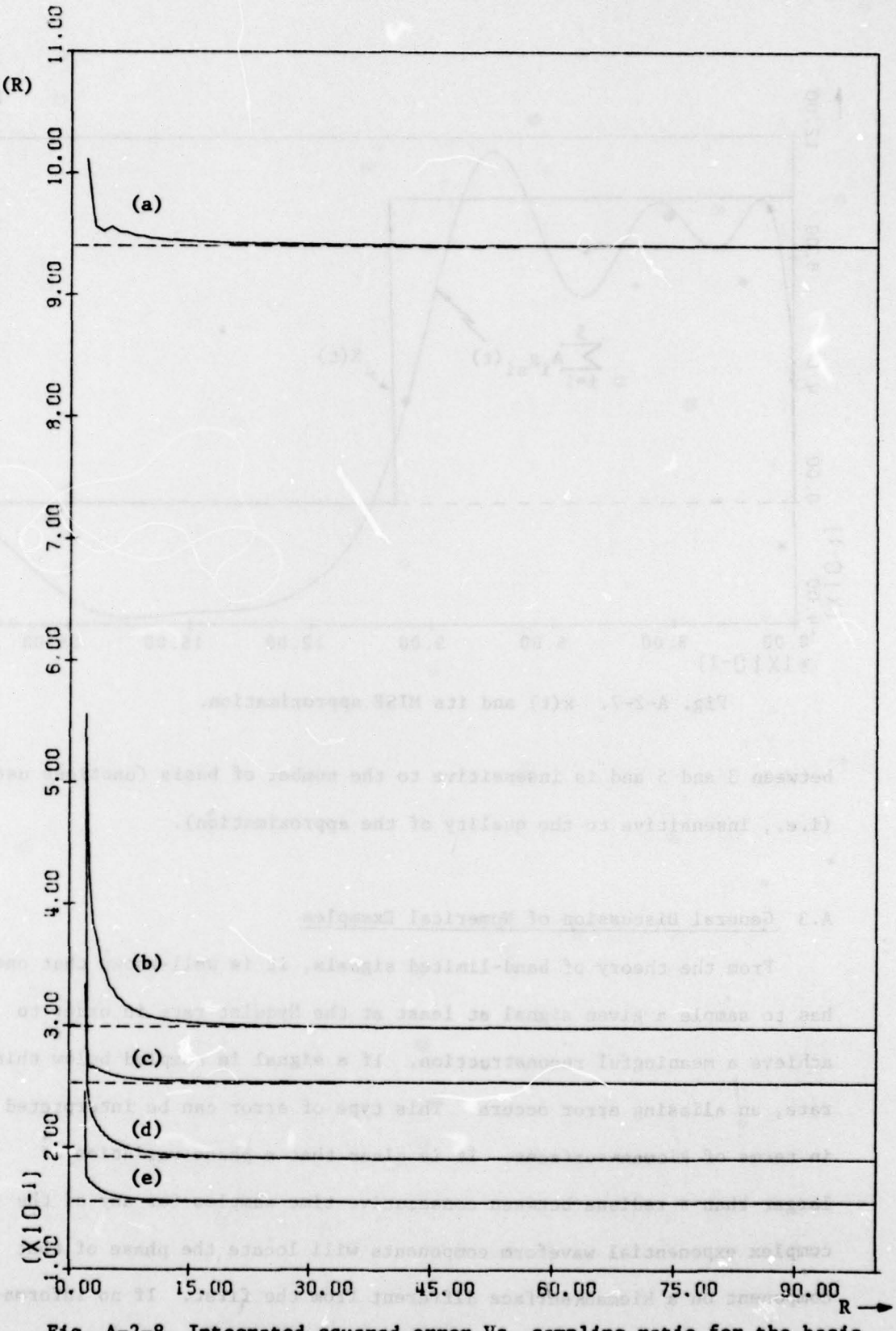

Fig. A-2-8. Integrated squared error Vs. sampling ratio for the basis sets in (A-2-4).

located, then an error will occur in determination of that component's argument. In practise, an aliasing error always occurs since physical signals can never be strictly band limited. For such signals the Nyquist rate is usually determined by specifying a frequency above which the energy content is assumed to be negligible. The aliasing error is then a function of the energy ratio between the in-band and out-of-band components.

Hence, having chosen a suitable set of basis functions, one must assure in the interpolation case that the sampling rate is chosen to be at least the Nyquist rate if a meaningful reconstruction is to be obtained. In the preceding examples, it was shown that a sampling ratio of about 10 yields discrete approximations having an approximation error almost as small as that of the continuous MISE approximation. In the interpolation problem the minimum number of samples required equals the number of known basis functions. For a band-limited signal, the Nyquist rate determines the minimum number of samples over a given interval. This implies that, in general, the minimum number of basis functions for a band-limited signal should equal the Nyquist rate times the length of the sampling interval if a meaningful reconstruction is to be obtained in the interpolation problem. To obtain an ISE(R) error which is close to the MISE with such a set of basis functions, the waveform should be oversampled at 10 times the Nyquist rate. Hence, 20 samples per cycle of the highest frequency component of significance, speaking energywise, are required. If the ratio of highest to lowest frequency is 100 and the approximation is carried over a full cycle of the lowest frequency, 2000 samples are needed. Although this is a

extremely large number of samples, one should remember that such a ratio of frequencies describes a wide band signal. Also, the value of 10 is a conservative choice for R. For such wide-band signals, it may be desirable to pick R as low as 3 to 5 (i.e. 600 to 1000 samples).

Appendix B [32]

Exact solution to the synthesized problem of Example 3-2-1.

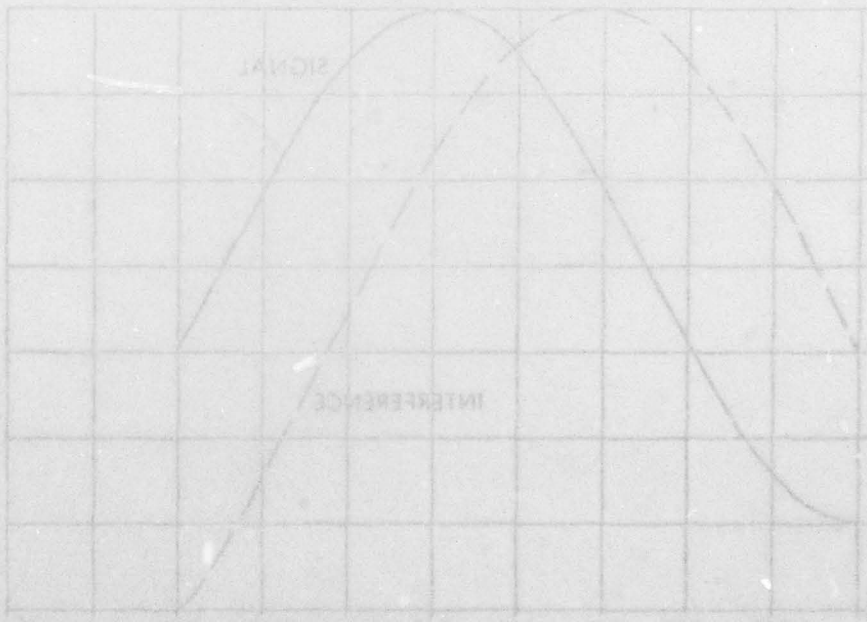

ANSWERS TO INSTANTANEOUS FREQUENCY PROBLEM

DATA: $x(t) = \underbrace{1000 \cos(\theta_1)}_{\text{SIGNAL}} + \underbrace{100 \cos(\theta_2)}_{\text{INTERFERENCE}} + \underbrace{n(t)}_{\text{NOISE}}$

1 SIGNAL: $\theta_1 = 340\pi t - 24 \cos\left(\frac{3\pi}{2} t - \frac{\pi}{2}\right) + 2$

INSTANTANEOUS FREQUENCY $\frac{1}{2\pi}\frac{d\theta_1}{dt} = 170 + 30 \sin\left(\frac{3\pi}{2} t - \frac{\pi}{2}\right)$ (GRAPHED)

2 INTERFERENCE: $\theta_2 = 320\pi t - 40 \cos(2\pi t) - 2$

INSTANTANEOUS FREQUENCY $\frac{1}{2\pi}\frac{d\theta_2}{dt} = 160 + 40 \sin(2\pi t)$ (GRAPHED)

3 NOISE: PSEUDO-UNIFORMLY DESTRIBUTED SEQUENCE OF NUMBERS $n_1, n_2, \ldots, n_{512}$ WITH RANGE $-100 \le n_i \le 100$, THE MULTIPLICATIVE LINEAR CONGRUENTIAL METHOD WAS USED TO GENERATE THE n_i

$n_{i+1} = 200\, F_{i+1} - 100;\ (i = 0, 1, 2, \ldots, 511)$

WHERE F_{i+1} = FRACTIONAL PART OF $(997 \times F_i)$

AND $F_0 = 0.5284163$

INSTANTANEOUS FREQUENCY OF SIGNAL & INTERFERENCE

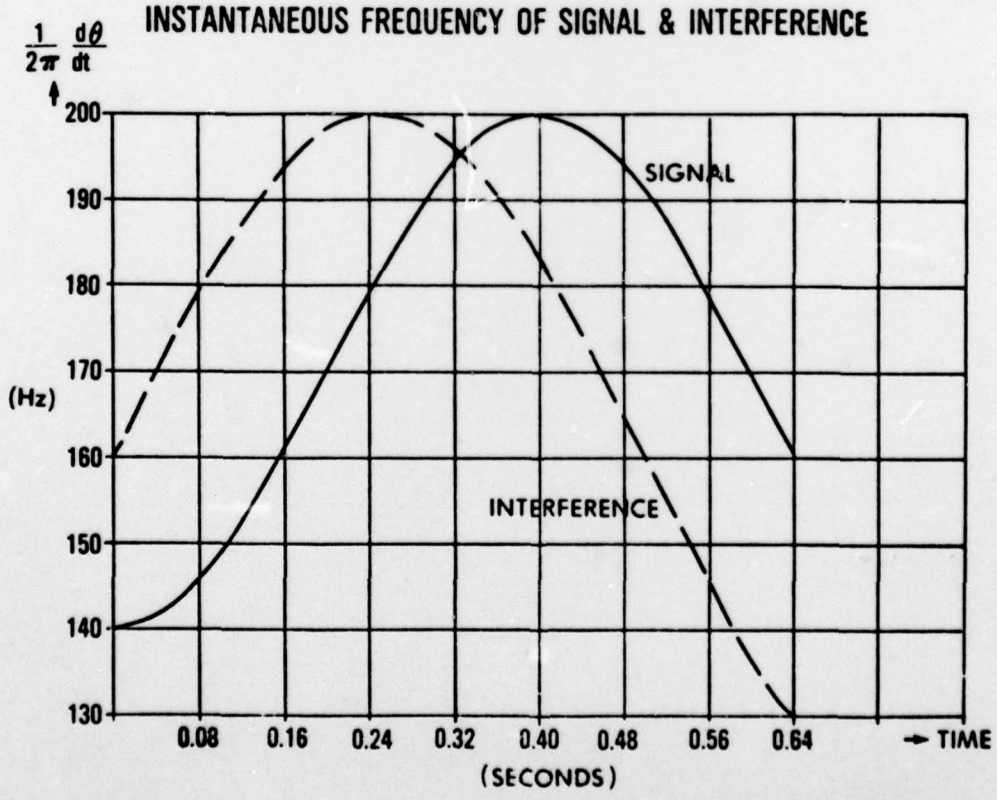

SAMPLE	TIME (SEC)	INSTANTANEOUS FREQ (Hz)
t_1	.04	141.47
t_2	.08	145.73
t_3	.12	152.37
t_4	.16	160.73
t_5	.20	170.00
t_6	.24	179.27
t_7	.28	187.63
t_8	.32	194.27
t_9	.36	198.53
t_{10}	.40	200.00
t_{11}	.44	198.53
t_{12}	.48	194.27
t_{13}	.52	187.63
t_{14}	.56	179.27
t_{15}	.60	170.00
t_{16}	.64	160.73

References

[1] C.T. Chen, Introduction to Linear System Theory. N.Y.: Holt, Rinehart and Winston, Inc., 1970.

[2] V. Volterra, Theory of Functionals of Integral and Integro-differential Equations. N.Y.: Dover, 1959.

[3] N. Wiener, "Response of a Nonlinear Device to Noise," MIT Radiation Laboratory, Report 129, April 1942.

[4] J.W. Graham and L. Ehrman, "Nonlinear System Modeling and Analysis with Applications to Communication Receivers," Signatron, Inc., AD-766278, June 1973.

[5] R.E.A.C. Paley and N. Wiener, "Fourier Transforms in the Complex Domain," Am. Math. Soc. Colloquium Pubs., Vol. XIX, Am. Math. Society, N.Y., N.Y., 1934.

[6] C.A. Desoer, and M. Vidyasagar, Feedback Systems: Input-output Properties. N.Y.: Academic Press, 1975.

[7] L.A. Zadeh, and C.A. Desoer, Linear System Theory. N.Y.: McGraw-Hill, 1963.

[8] K.J. Astrom, and P. Eykhoff, "System Identification - A Survey," Automatica, Vol. 7, pp. 123-162. Pergamon Press, 1971. Great Britain.

[9] L. Kendall Su, Time-Domain Synthesis of Linear Networks. N.J.: Prentice-Hall, Inc., 1971.

[10] William H. Kautz, "Transient Synthesis in the Time Domain," IRE Transactions on Circuit Theory, CT-1, 3, September 1954, pp. 29-39.

[11] W.H. Huggins, "Representation and Analysis of Signals-- Part I. The Use of Orthogonalized Exponentials," Department of Electrical Engineering, The Johns Hopkins University (AFCRC Report TR-57-357), September 30, 1957.

[12] Tzay Y. Young, "Signal Theory and Electrocardiography," Dr. Eng. dissertation, The Johns Hopkins University, 1962.

[13] R. Prony, "Essai experimental et analytique sur les lois de la dilatabilite des fluides elastiques et sur celles de la force expansive de la vapeur de l'eau et de la vapeur de l'alkoal, a differentes temperatures," Journal de l'Ecole Polytechnique (Paris). Vol. 1, Cahier 2, Floreal et Prairial, An. III (1795), pp. 24-76.

[14] F.B. Hildebrand, Introduction to Numerical Analysis. N.Y.: McGraw-Hill, 1956.

[15] J.D. Markel and A.H. Gray, Linear Prediction of Speech. Berlin: Springer-Verlog, 1975.

[16] M.L. Van Blaricum and R. Mittra, "Techniques for Extracting the Complex Resonances of a System Directly from its Transient Response," Electromagnetics Laboratory Scientific Report No. 75-6, University of Illinois at Urbana, December 1975.

[17] L.W. Pearson, M.L. VanBlaricum, and R. Mittra, "A New Method for Radar Target Recognition based on the Singularity Expansion for the Target," Electromagnetics Laboratory, University of Illinois at Urbana.

[18] Lawrence Livermore Laboratory, Livermore, CA 94550, User's Manual for SEMPEX: A Computer Code for Extracting Complex Exponentials from a Time Waveform. Air Force Weapons Laboratory, Kirtland AFB, NM 87117. Report AFWL-TR-76-200, March 1977.

[19] R.N. McDonough, "Representation and Analysis of Signals, Part XV. Matched Exponents for the Representation of Signals," Johns Hopkins University, Baltimore, Maryland, April 30, 1963.

[20] G. Miller, "Representation and Analysis of Signals Part XXVI. Least-Squares Approximation of Functions by Exponentials," Johns Hopkins University, Baltimore, Maryland, June 1969.

[21] R.N. McDonough, and W.H. Huggins, "Best Least-Squares Representation of Signals by Exponentials," IEEE Trans. on Automatic Control, Vol. AC-13, No. 4, August 1968.

[22] A.G. Evans, and R. Fischl, "Optimal Least-Squares Time-Domain Synthesis of Recursive Digital Filters," IEEE Trans. on Audio and Electroacoustics, Vol. AU-21, No. 1, February 1973.

[23] D.F. Tuttle, Jr., "Network Synthesis for Prescribed Transient Response," D. Sc. dissertation, M.I.T., 1948.

[24] W.H. Kautz, "Approximation over a Semi-infinite Interval," M.S. Thesis, M.I.T., 1949.

[25] J.W. Carr,III, "An Analytic Investigation of Transient Synthesis by Exponentials," M.S. Thesis, M.I.T., 1949.

[26] V.K. Jain, "Decoupled Method for Approximation of Signals by Exponentials," IEEE Trans. on Systems Science and Cybernetics, July 1970.

[27] K. Steiglitz, and L.E. McBride, "A Technique for the Identification of Linear Systems," IEEE Trans. on Automatic Control, October 1965.

[28] L.E. McBride, H.W. Schaefgen, and K. Steiglitz, "Time Domain Approximation by Iterative Methods," IEEE Trans. on Circuit Theory, Vol. CT-13, No. 4, December 1966.

[29] V.K. Jain, "On System Identification and Approximation," Engineering Research Report No. SS-II, Florida State University, 1970.

[30] V.K. Jain, "Filter Analysis by Grammian Method," IEEE Trans. on Audio and Electroacoustics, April 1973.

[31] V.K. Jain, "Filter Analysis by Use of Pencil of Functions: Part I," IEEE Trans. on Circuits and Systems, Vol. CAS-21, No. 5, September 1974.

[32] _____ Problems & Solutions to the RADC Spectrum Estimation Workshop, May 1978.

[33] W.R. Carmichael and R.G. Wiley, "Instantaneous Frequency Estimation From sampled Data," Proceedings of the RADC Spectrum Estimation Workshop, pp. 287-300, May 1978.

[34] E.J. Ewen, "Black Box Identification of Nonlinear Volterra Systems," Ph.D. Dissertation, Syracuse University, Syracuse, NY, December 1975.

☆U.S. GOVERNMENT PRINTING OFFICE: 1978-614-023/9

MISSION
of
Rome Air Development Center

RADC plans and conducts research, exploratory and advanced development programs in command, control, and communications (C^3) activities, and in the C^3 areas of information sciences and intelligence. The principal technical mission areas are communications, electromagnetic guidance and control, surveillance of ground and aerospace objects, intelligence data collection and handling, information system technology, ionospheric propagation, solid state sciences, microwave physics and electronic reliability, maintainability and compatibility.